Loss of the *USP22* deubiquitylase confers resistance to chemotherapy in small cell lung cancer

Scott Best

A dissertation

submitted in partial fulfillment of the

requirements for the degree of

Doctor of Philosophy

University of Washington

2025

Reading Committee:

David MacPherson, Chair

Amanda Paulovich

Steve Hahn

Program Authorized to Offer Degree:

Molecular and Cellular Biology

© Copyright 2025

Scott Best

University of Washington

Abstract

Loss of the *USP22* deubiquitylase confers resistance to chemotherapy in small cell lung cancer

Scott Best

Chair of the Supervisory Committee:

David MacPherson

Genome Sciences

Small cell lung cancer (SCLC) responds exceptionally well to cytotoxic chemotherapy. However, relapse with the emergence of chemoresistant disease is rapid and accompanied by poor treatment outcomes. To understand the genetic basis of chemoresistance in SCLC, we applied in vivo CRISPR deletion screening to patient-derived xenograft (PDX) models. Top screen hits included genes encoding components of the transcriptional co-activator SAGA (Spt-Ada-Gcn5 acetyltransferase) complex. We demonstrate that deletion of the SAGA deubiquitylase *USP22* conferred cisplatin/etoposide resistance in two chemosensitive PDX models, and that restoring expression in a PDX model harboring homozygous truncating mutation of *USP22* re-sensitized tumors to chemotherapy. USP22 loss increased gene body histone H2A-

K119 monoubiquitylation in genes encoding key regulators of neuronal differentiation and suppressed neural and neuroendocrine gene expression including targets of ASCL1. Chemoresistance following USP22 loss reflected attenuated DNA damage-driven phosphorylation events and apoptosis, in conjunction with increased expression of glycolysis and hypoxia-related genes. Glycolysis program upregulation may reflect a targetable vulnerability, as inhibition of GLUT1 re-sensitized USP22-null tumors to chemotherapy.

A version of portions of chapters 1, 2, 3, 4 and 5 is currently in preparations as a journal article entitled: Loss of the *USP22* deubiquitylase confers resistance to chemotherapy in small cell lung cancer.

Authors: Scott Best, Daniel S. Hippe, Eli Grunblatt, Pritha Chanana, Feinan Wu, Richard Ivey, Jacob J Kennedy, Ali Ibrahim, Raymond J. Monnat, Jr., Patrick Paddison, Amanda G. Paulovich and David MacPherson.

A version of portions of chapter 2 is published in a journal article entitled: In vivo functional screens reveal KEAP1 loss as a driver of chemoresistance in small cell lung cancer.

Authors: Lauren Brumage[†], Scott Best[†], Daniel S. Hippe, Eli Grunblatt, Pritha Chanana, Feinan Wu, Myung Chang Lee, Zhe Ying, Ali Ibrahim, Jae Heun Chung, Anna Vigil, Jackson Fatherree, Slobodan Beronja, Patrick Paddison, Lucas Sullivan, Barzin Nabet and David MacPherson

[†] These authors contributed equally to this work as co-first authors for this publication.

Acknowledgements

I would like to extend my thanks and sincere gratitude to my graduate adviser David MacPherson for the mentorship and training as a scientist during the past five years. I would also like to thank previous and current members of the MacPherson lab who I have spent considerable time with fostering an environment of camaraderie and support: Lauren Brumage, Eli Grunblatt, Ali Ibrahim, Jackson Fatherree, Justin Norton, Arnaud Augert, Jae Heun Chung, Joe Hiatt, Kelly Heard, Alex Doan, Sheng-You Liao, Holly Sandborg, Henry Arnold. Additionally, I would like to thank the members of my thesis committee for their expertise, support, and guidance during graduate school: Ray Monnat, Amanda Paulovich, Steve Hahn, and Steve Henikoff. I would also like to thank Maia Lowe and the MCB PhD Program for their guidance in helping me navigate through graduate school.

Table of Contents

Chapter 1 – Introduction.....1

Chapter 2 – In vivo CRISPR-Cas9 deletion screens identify drivers of chemoresistance in small cell lung cancer.....7

Chapter 3 – USP22 loss drives chemoresistance in small cell lung cancer.....16

Chapter 4 – Discussion.....45

Chapter 5 – Materials and Methods.....49

References.....66

Appendix.....75

CHAPTER 1: Introduction

Overview of small cell lung cancer

Small cell lung cancer (SCLC) is a highly lethal, neuroendocrine lung carcinoma characterized by early metastatic spread with initial sensitivity to chemotherapy that is typically followed within months by relapse with chemoresistant disease[1, 2].

SCLC comprises 15% of lung cancer cases and accounts for approximately 250,000 new global cases annually[3]. SCLC occurrence is heavily associated with smoking, with over 95% of patients being current or past smokers[4]. SCLC can be classified as limited-stage (LS)-SCLC or extensive-stage (ES)-SCLC, with 70% of patients diagnosed with ES-SCLC that has spread to multiple locations in the body[5]. SCLC prognoses are extremely poor, with approximately 200,000 global deaths annually and a 5-year survival rate of less than 7%, making SCLC one of the deadliest forms of cancer[3, 6, 7]. Limited therapy options and a poor understanding of drug resistance contribute to the significant challenge in the management and treatment of SCLC today.

Molecular and genetic features of small cell lung cancer

With a history of smoking in almost all SCLC patients, SCLC tumors carry a high somatic mutational burden driven by tobacco-induced DNA damage and genetic instability[8]. Inactivation of tumor suppressor genes *TP53* and *RB1* occur in almost all SCLC cases[9, 10, 11]. Additional genetic alterations that commonly occur in SCLC are inactivating mutations of chromatin regulators *CREBBP* (15%), *EP300* (5-13%), and *KMT2D* (8%) as well as amplification of MYC family members *MYC*, *MYCN*, and *MYCL*

in 20% of cases[9, 10, 11, 12, 13]. Inactivating mutations of *PTEN* (13%) and *NOTCH* family genes (25%) frequently occur as well[9, 10, 11].

SCLC is a neuroendocrine malignancy believed to most frequently arise from pulmonary neuroendocrine cells (PNECs), a rare cell population that comprises 0.4% of central airway epithelial cells and 0.01% of all lung cells[14, 15, 16]. PNECs secrete neuropeptides and neurotransmitters in response to environmental stimuli that help regulate various lung processes including oxygen level sensing and lung inflammation[17]. Considerable and ongoing work has been made to define SCLC subtypes based on neuroendocrine status and differential transcription factor or gene expression. While the majority of SCLC commonly express neuroendocrine markers such as chromogranin A (CHGA), synaptophysin (SYP), neural cell adhesion molecule (NCAM), and insulinoma-associated 1 (INSM1), 10-15% of SCLC lack neuroendocrine features and are considered low-neuroendocrine[6, 18, 19, 20]. Neuroendocrine SCLC can be further characterized by differential expression of two basic helix-loop-helix transcription factors *ASCL1* (SCLC-A) or *NEUROD1* (SCLC-N), expressed in ~75% and ~15% of SCLC, respectively, serving as master regulators of neuronal function and differentiation by controlling expression of common and non-overlapping sets of genes[6, 21]. While ASCL1 and NEUROD1 regulate expression of common neuronal markers *INSM1* and *SYT1*, unique targets of ASCL1 include *MYCL1*, *DLL3*, *NFIB*, *SOX2*, and *NKX2-1* whereas the genes *MYC*, *OTX2*, and *SEMA6A* are regulated by NEUROD1[21]. A low-neuroendocrine tuft-cell variant of SCLC expressing the transcription factor *POU2F3* (SCLC-P) with low levels of *ASCL1* and *NEUROD1* has also been characterized[6, 22]. A fourth inflamed low-

neuroendocrine subtype of SCLC (SCLC-I), with low expression of all three transcription factors *ASCL1*, *NEUROD1*, and *POU2F3*, has also recently been described featuring increased inflammatory and epithelial-mesenchymal transition gene signatures that may predict favorable responses to immune checkpoint blockade therapy[23]. Despite these advances in characterizing SCLC subtypes, to this day SCLC is still treated as a homogenous disease in the clinic, highlighting the need to further our understanding of SCLC biology to therapeutically address SCLC subtype heterogeneity.

Current therapies and chemoresistance in small cell lung cancer

Standard of care for extensive stage SCLC is chemotherapy, consisting of a platinum-based agent such as cisplatin or carboplatin administered with a topoisomerase 2 inhibitor such as etoposide, in combination with PD-L1 immune checkpoint blockade (ICB)[24, 25, 26]. While approximately two-thirds of patient tumors respond strongly to chemotherapy, relapse with chemoresistant disease typically occurs within months[27]. This rapid transition to chemoresistant disease leads to extremely poor treatment outcomes. The addition of anti-PDL1 antibodies to platinum/etoposide (cis-eto) chemotherapy in 2019 led to durable responses in only a small subset of patients[25, 26]. A better understanding of the origins of treatment failure and how to improve outcomes has been hampered by few genomic analyses of SCLC following treatment, and few good preclinical models in which to understand the factors that drive relapse and chemoresistance. This unmet need for genomic information from relapsed patients during therapy is just beginning to be addressed[28, 29]. For example, a study of 30 chemo-refractory SCLC patient samples found that recurrent mutations in regulators of

WNT signaling were associated with chemotherapy relapse[29]. SCLC PDX models have been shown to faithfully capture and perpetuate SCLC drug sensitivity and resistance phenotypes observed in patients[7, 8, 9, 10], in contrast to SCLC cell lines derived from chemo-naïve vs relapsed patients[30]. SCLC PDX models have also been used to derive cisplatin-etoposide-resistant derivatives, where the analysis of these chemoresistant PDX variants identified EZH2-mediated epigenetic silencing of *SLFN11*[31] as critical for sensitivity to DNA damaging agents[32, 33]. Our group has shown that overexpression of *MYCN* and *MYCL* could switch highly chemosensitive PDX models of SCLC to therapy resistance[34], while an independent analysis of SCLC PDX models and patient samples found that extra-chromosomal *MYC* family ecDNA amplification arises with the initiation of chemotherapy treatment and contributes to resistance[35]. These observations support the use of PDX models as clinically relevant models in which to investigate mechanisms of SCLC chemoresistance.

Intratumoral heterogeneity and plasticity may contribute to SCLC chemoresistance, as evidenced by increased heterogeneity and enrichment of unique gene expression patterns post-relapse from longitudinal single-cell profiling of SCLC circulating tumor cells taken before and after chemotherapy[36]. SCLC exhibits heterogeneity based on expression of lineage-regulating transcription factors ASCL1, NEUROD1 and POU2F3[6, 9, 10, 11, 22] and a subset of SCLC has been associated with an immune/inflamed tumor phenotype and reduced sensitivity to topotecan chemotherapy[23, 37]. Heterogeneity of expression of neuroendocrine and *MYC* family genes has also been documented[9, 10, 11, 20, 38, 39]. Genetically engineered mouse models of SCLC have further revealed the co-

existence of neuroendocrine cells and chemoresistant non-neuroendocrine NOTCH-expressing cells[38]. These observations provide clues to the origins of chemoresistance in SCLC and emphasize the importance of better understanding the mechanisms responsible in order to improve treatment outcomes for SCLC patients.

CRISPR-Cas9 genetic screens in cancer research

CRISPR-Cas9 screening has become a powerful tool in cancer research. The CRISPR-Cas9 system involves the use a single-guide RNA (sgRNA) designed to bind to a genomic locus of interest, often in the exons of protein coding regions of a gene[40, 41, 42]. The sgRNA directs Cas9, a bacterial endonuclease, to cut DNA at this region inducing double-stranded DNA breaks that can be repaired by non-homologous end joining (NHEJ) in eukaryotic cells. NHEJ repair often involves the insertion or deletion (indels) of nucleotides at break sites, which can result in protein-coding region frameshifts and loss-of-function of the gene target[43].

Researchers can leverage the targeted gene-editing capability of the CRISPR-Cas9 system to systematically interrogate the function of individual genes. In the context of cancer, CRISPR-Cas9 screens have been used to identify genes involved in cancer development, survival, progression, metastasis and drug resistance[44, 45, 46]. In general, CRISPR-Cas9 screening involves the lentiviral transduction of cells with Cas9 cDNA along with a library of sgRNAs targeting the protein coding regions of individual genes. A sgRNA library can have genome-wide coverage, such as the Human GeCKO v2 CRISPR Knockout Pooled Library targeting 19,050 genes with 3-6 sgRNAs per gene[47].

Alternatively, a smaller focused sgRNA library can be used to target a subset of genes of interest allowing for greater statistical power in downstream analyses[48]. Cells are transduced such that each cell receives the Cas9 cDNA and one of the sgRNAs included in the library. Transduced cells then go through a biological assay of interest, such as passaging through a given number of population doublings or subjected to selection pressure, after which genomic DNA from these cells are sequenced to determine the abundance of specific sgRNAs relative to a reference population. In the context of selection pressure, a gene knockout that confers resistance to a given selection pressure may have its corresponding sgRNA enriched in the surviving cell population.

The current study

To further elucidate mechanisms of SCLC chemoresistance, we developed a novel strategy to identify genetic changes that confer SCLC chemoresistance by *in vivo* functional genetic screening of chemosensitive SCLC PDX models[48]. *In vivo* CRISPR-Cas9 deletion screening in two chemosensitive SCLC PDX models confirmed known pathways and revealed novel drivers of SCLC chemoresistance. An important initial hit was *KEAP1*, a master negative regulator of the NRF2 oxidative stress response pathway[49, 50]. We further demonstrated that knockout of *KEAP1* conferred chemoresistance in a chemosensitive PDX model[48]. Here we demonstrate that SAGA complex members identified in CRISPR deletion screens drive SCLC chemoresistance and interrogate mechanisms by which loss of the SAGA complex deubiquitylase USP22 alters SCLC chemotherapeutic response.

CHAPTER 2: In vivo CRISPR-Cas9 deletion screens identify drivers of chemoresistance in small cell lung cancer

2.1 Pilot genome-scale CRISPR deletion screen and design of focused CRISPR deletion gRNA library to identify drivers of chemoresistance in SCLC PDX models

We recently described a custom CRISPR-KO sgRNA library targeting 400 genes with 6 gRNAs/gene and 120 non-targeting control gRNAs to use to identify loss-of-function drivers of SCLC PDX cisplatin-etoposide (cis-eto) resistance[48] (Table 1). The sgRNA library included altered genes identified by SCLC genomic studies[9, 11] or implicated in SCLC chemoresistance such as *SLFN11* and WNT pathway members[29, 31]. We also included genes that displayed sgRNA enrichment after cis-eto chemotherapy selection in a pilot genome-scale CRISPR deletion screen that used the Human CRISPR Knockout Pooled Library (GeCKO v2)[47] in the FHSC14 SCLC PDX model (Fig 2.1a-c) (Table 2). In this pilot screen, FHSC14 tumors were dissociated and transduced with the Human GeCKO v2 library ex vivo for 18 hours (Fig 2.1a). Following this transduction, a subset of cells were left in culture for 72 hours to serve as an initial timepoint (P0), while the rest were injected subcutaneously in the flanks of NSG mice at ~1x10^6 cells per flank. Once tumors reached 150 mm^3, tumors were treated with either saline or 3 weekly cycles of cis-eto. Saline tumors were collected once they reached 1000 mm^3 and cis-eto tumors were collected upon tumor return. In each treatment group, extracted gDNA from each tumor was pooled prior to sequencing at an equimolar ratio to generate a saline (n=9 tumors pooled) pool and a cis-eto (n=11 tumors pooled) pool. We performed MAGeCK[51] analysis on each treatment pool to identify enrichment of sgRNAs relative to P_0 controls. Pilot screen data (Table 2) indicated that a pooled *in*

vivo PDX screen with control and cis-eto-treated arms was feasible, but not well enough powered to identify statistically significant hits despite identifying multiple members of the SAGA complex (Fig. 2.1b). We thus included sgRNAs targeting this complex and 123 additional top-scoring candidate genes (Table 1) in a more focused screen library to identify loss-of-function drivers of cis-eto chemoresistance in SCLC PDX models (Fig. 2.1c).

Figure 2.1

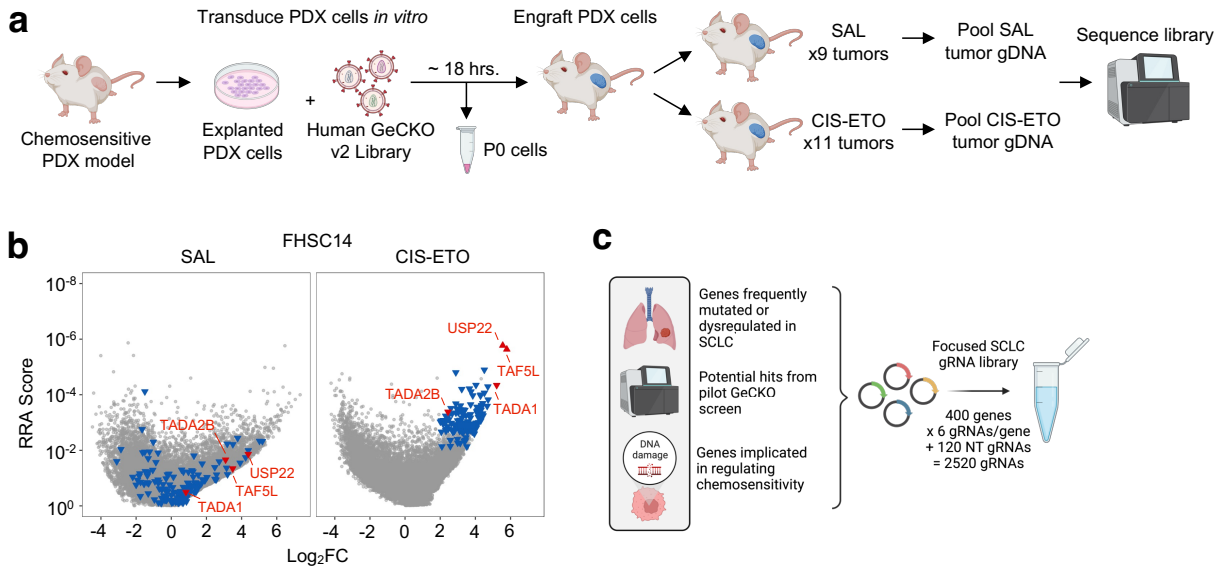

Figure 2.1: In vivo pilot genome-scale CRISPR deletion screen to identify drivers of cisplatin-etoposide resistance in the SCLC PDX models

(**a**) Schematic of the in vivo pilot genome-scale CRISPR deletion screen conducted in the SCLC PDX model FHSC14.

(**b**) Gene-level volcano plots of MAGeCK analyses results from the FHSC14 pilot genome-scale. The positive robust rank aggregation (RRA) score is shown for genes with $Log_2FC > 0$ and the negative RRA is shown for genes with $Log_2FC < 0$ (a smaller

RRA score indicates stronger and more consistent enrichment or depletion of gRNAs for the same gene). Genes displayed in blue or red are 130 genes with $Log_2FC \geq 2$ selected amongst the top enriched genes in the CIS-ETO condition for inclusion in a focused sgRNA library. SAGA complex members amongst these 130 genes are displayed in red. FDR < 0.2 for genes with right-side up triangles, and FDR > 0.2 for genes with upside down triangles.

(**c**) Schematic showing the source of genes that were selected for the focused SCLC CRISPR deletion gRNA library (see Table 1).

2.2 Focused CRISPR deletion gRNA screen in the SCLC PDX model NCI109B

We applied our focused CRISPR deletion gRNA library to PDX models of SCLC to identify loss-of-function drivers of cis-eto resistance (Fig 2.2a). The NCI109B PDX model was chosen initially for exquisite sensitivity to chemotherapy, with two cycles of chemotherapy typically leading to complete tumor regression (Fig. 2.2b). Screens were performed by dissociating NCI109B tumors into single-cell suspensions for transduction with concentrated lentivirus expressing the focused CRISPR-KO sgRNA library (Table 1). After 18 hours *ex vivo*, transduced cells were divided for subcutaneous re-implantation into the flanks of NSG mice ($1x10^6$ cells/injection) or held in culture for 72 hours as a transduced P_0 reference population. Once tumors reached 300 mm^3, mice were randomly assigned to a cis-eto or saline control treatment group. Chemotherapy treatment consisted of two weekly cycles of cis-eto that resulted in complete tumor regression. Tumors that recurred off treatment were collected after re-growth to pre-treatment volume (Fig. 2.2b). A total of 35 saline-treated tumors and 35 cis-eto tumors

were sequenced, where individual tumors in the saline group contained ~50% of all gRNAs present (Fig. 2.2c). In order to identify consistently enriched sgRNAs, we computationally pooled read counts from 7 pooled batches of randomly assigned tumors (5 independent tumors/pool/treatment group) to ensure that > 95% of library gRNAs were present per pool of saline tumors (Fig. 2.2c). These pooled library data were then analyzed using MAGeCK. In cis-eto-treated tumors, *SLFN11*, *USP22*, *TAF5L*, *TADA2B* had at least 3 of 6 of their corresponding gRNAs enriched (Log_2FC > 2, FDR < 0.05) relative to P_0 tumors, with *SLFN11*, *USP22*, and *TADA2B* having a gene-level positive enrichment FDR < 0.05 and *TAF5L* FDR < 0.1 (Fig. 2.2d-e, Tables 3-4). In saline-treated control tumors these genes had ≤ 1 corresponding sgRNAs enriched. Prior reports had demonstrated that epigenetic suppression of *SLFN11* conferred chemoresistance in SCLC PDX models[31], a finding that supports the ability of our screening strategy to identify known drivers of SCLC chemoresistance. The other top screen hits, *USP22*, *TADA2B*, and *TAF5L,* encode members of the SAGA complex, a transcriptional co-activator that regulates gene expression through histone acetyltransferase and deubiquitylase activities[52, 53, 54]. Of note, *USP22* and *TADA1* were the top two hits in our pilot genome-wide study (Fig. 2.1b) though neither had previously been associated with chemoresistance in any cancer type.

Figure 2.2

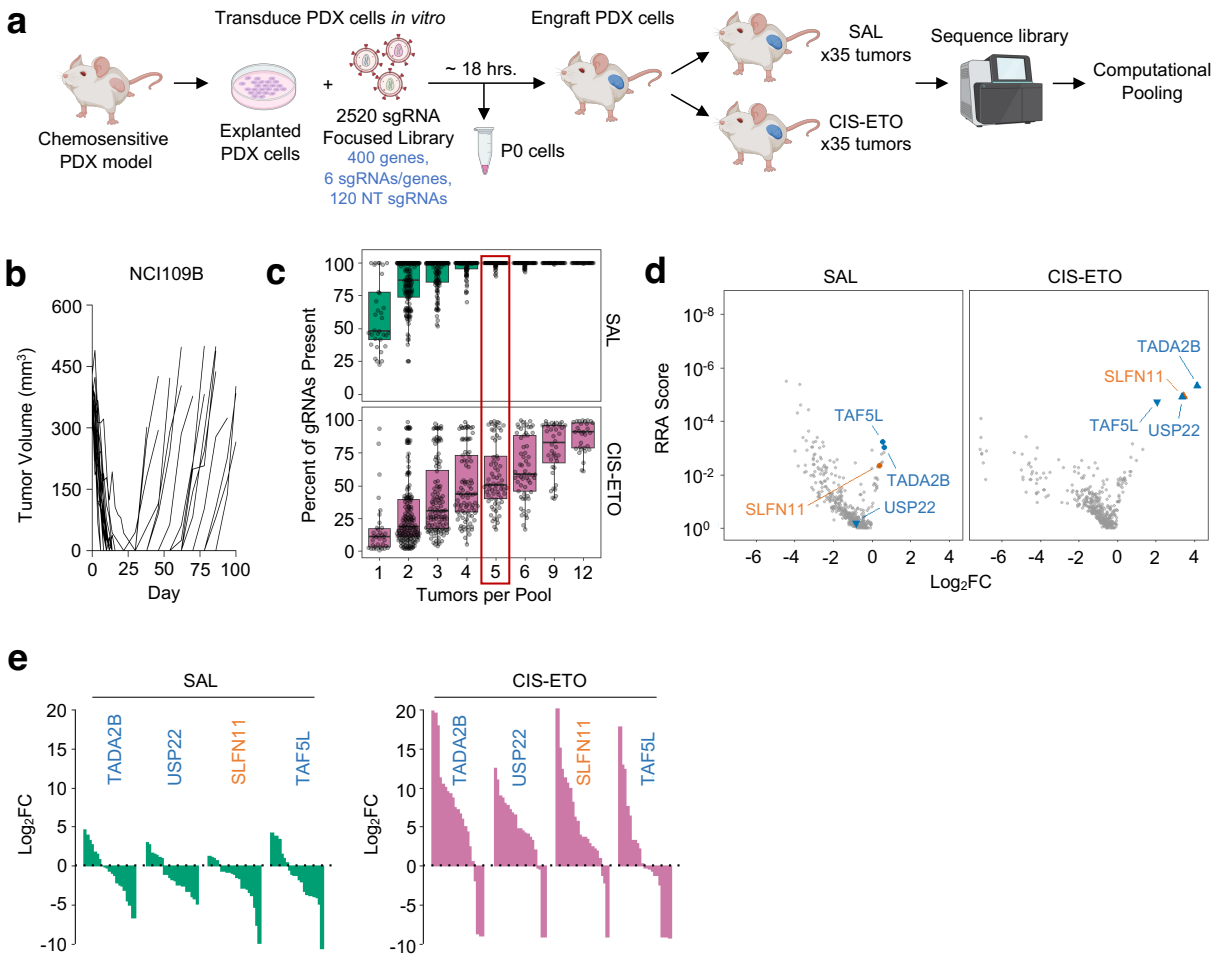

Figure 2.2: *In vivo focused CRISPR-Cas9 deletion screens identify drivers of cisplatin-etoposide resistance in the SCLC PDX model NCI109B*

(**a**) Schematic of the in vivo CRISPR-Cas9 deletion screen conducted using a custom focused 2520 sgRNA focused library to identify loss-of-function drivers of cis-eto resistance in SCLC PDX models.

(**b**) NCI109B PDX models were screened with the focused gRNA library and treated with 2 weekly cycles of saline or cis-eto. The tumor volume kinetics for the largest of two tumors implanted into each mouse is plotted to show tumor regression and relapse in response to cis-eto treatment.

(**c**) Computational pooling of NCI109B tumors screened with the focused gRNA library was performed as previously described[48]. The percentage of focused library sgRNAs present per pool is shown. Five tumors per pool (n=7 pools per treatment condition) was selected for subsequent analyses based on the high sgRNA coverage achieved in the saline group.

(**d**) Volcano plots of MAGeCK analyses results from NCI109B tumors screened with the focused sgRNA library. Genes with FDR < 0.05 or FDR 0.05-0.20 are displayed with right-side up triangles or upside-down triangles, respectively. Genes labelled in blue are SAGA complex members enriched in the CIS-ETO vs P0 condition with at least an FDR < 0.20.

(**e**) Waterfall plots showing treatment vs P0 Log_2FC of the top 3 sgRNAs per gene targeting TADA2B, USP22, SLFN11, and TAF5L for all NCI109B tumor pools. Each vertical bar is one sgRNA from one pooled tumor.

2.3 Focused CRISPR deletion gRNA screen in the SCLC PDX model FHSC14

The recognition of SCLC biological heterogeneity has led to proposed SCLC subtypes based on the activation of key transcription factors such as ASCL1 (SCLC-A) and NEUROD1 (SCLC-N). NCI109B, the PDX model used in this study (Fig 2.2b), expresses high levels of NEUROD1[55]. In order to replicate and extend our functional screening results in NCI109B, we repeated this focused screen in an additional SCLC PDX model FHSC14, the same model used for the pilot whole genome screen, that has distinct biological features including high levels of ASCL1[56]. FHSC14 tumors transduced with our focused gRNA library were treated with 2-3 weekly cycles of saline or cis-eto

until tumors reached <50 mm^3 and then harvested when tumors returned to pre-treatment volume of 250 mm^3 (Fig 2.3a). A total of 27 saline and 48 cis-eto return tumors were sequenced. Using a similar analysis strategy as the NCI109B screen, we applied MAGeCK analyses on computationally pooled tumors (6 tumors per pool) from the saline condition (n=4 pools analyzed) and cis-eto condition (n=8 pools analyzed) (Fig 2.3b-d). The results and figures in Fig 2.3a-c and Tables 5-6 for this focused CRISPR deletion screen experiment in the FHSC14 model are published as shared work in the co-first author publication Brumage, et al., 2025[48]. In the saline condition, three genes *MBOAT4*, *OTOP3*, and *CREBBP* had at least 3 of 6 of their corresponding gRNAs enriched relative to P_0 tumors, with *CREBBP* being a gene mutated in ~9% of SCLC[9, 10, 11] (Fig. 2.3c,d, Tables 5-6). Among the top screen hits in the cis-eto condition was *KEAP1*, a master regulator of the NRF2 anti-oxidative stress response pathway[49, 50] for which we demonstrated that loss-of-function could drive chemoresistance[48]. FHSC14 cis-eto-treated tumors were also enriched in sgRNAs targeting SAGA complex members *USP22*, *TAF5L*, *TADA2B*, *TAF6L*, and *TADA1.* We next compared the results from both focused screens performed in the FHSC14 and NCI109B PDX models. Both FHSC14 and NCI109B cis-eto-treated tumors were enriched for sgRNAs that targeted *USP22*, *TAF5L*, and *TADA2B* (Fig. 2.3e), where NCI109B was lineage transcription factor NEUROD1-active and FHSC14 ASCL1-high[48]. These results suggested the suppression of SAGA components might broadly promote chemoresistance in SCLC across different transcription factor-defined subtypes.

Figure 2.3

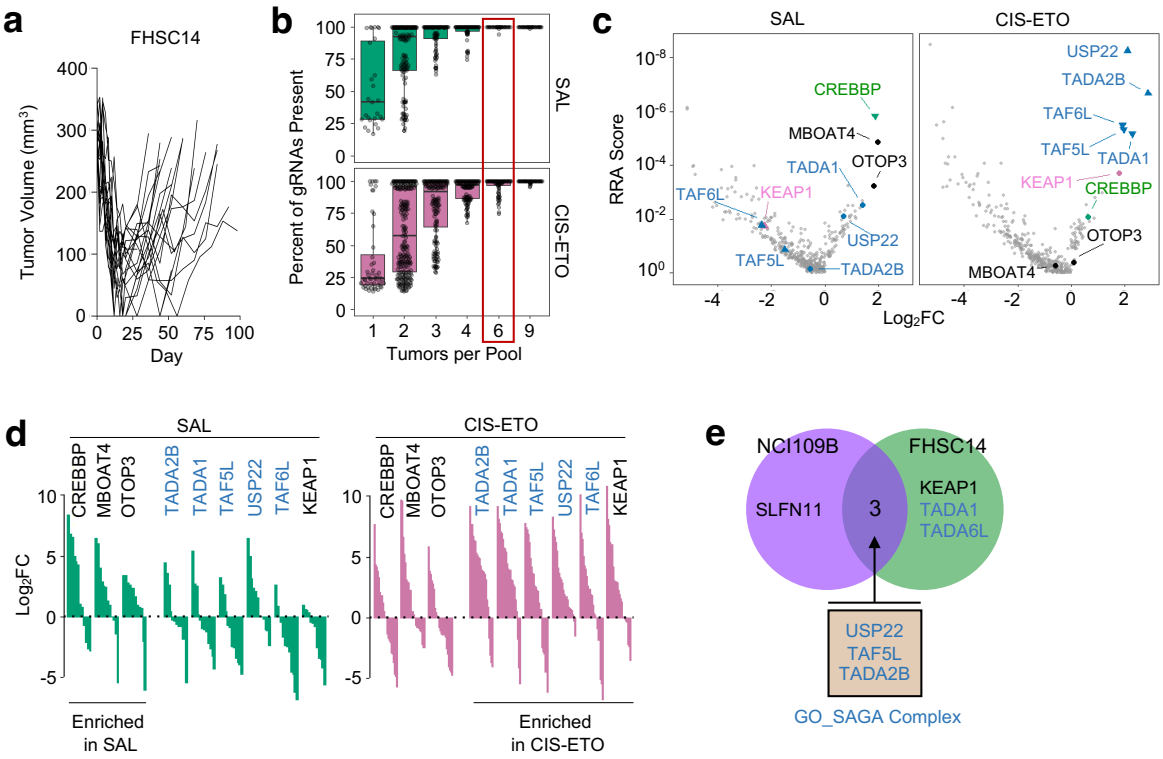

Figure 2.3: *In vivo CRISPR-Cas9 deletion screens identify drivers of cisplatin-etoposide resistance in the SCLC PDX model FHSC14*

(**a**)† FHSC14 PDX models were screened with the focused gRNA library and treated with 2 weekly cycles of saline or cis-eto. The tumor volume kinetics for the largest of two tumors implanted into each mouse is plotted to show tumor regression and relapse in response to cis-eto treatment.

(**b**)† Computational pooling of FHSC14 tumors screened with the focused gRNA library. Six tumors per pool (n=4 pools analyzed for the saline condition and n=8 pool analyzed for the cis-eto condition) was selected for subsequent analyses based on the high sgRNA coverage achieved in the saline group.

(**c**) † Volcano plots of MAGeCK analyses results from FHSC14 tumors screened with the focused sgRNA library. Genes with FDR < 0.05 or FDR 0.05-0.20 are displayed with right-side up triangles or upside-down triangles, respectively. Genes labelled in blue are SAGA complex members enriched in the CIS-ETO vs P0 condition with at least an FDR < 0.20.

(**d**) Waterfall plots showing treatment vs P0 Log_2FC of the top 3 sgRNAs per gene targeting for all genes that had at least 3 out of 6 sgRNAs enriched relative to P_0 tumors for each treatment condition. Each vertical bar is one sgRNA from one pooled tumor.

(**e**) Overlap of genes with at least 3 of their 6 gRNAs enriched ($Log_2FC > 2$, FDR < 0.05) from the NCI109B and FHSC14[48] focused CRISPR-Cas9 deletion screens.

† These figures are from shared work that are published in the co-first author publication Brumage, et al. 2025[48].

CHAPTER 3: USP22 loss drives chemoresistance in small cell lung cancer

3.1 *USP22* deletion confers SCLC PDX model chemoresistance

In order to further investigate the role of SAGA in regulating the response to chemotherapy, we focused first on *USP22,* the top hit from our functional screens. This gene encodes a deubiquitinating subunit of SAGA that catalyzes removal of mono-ubiquitin from histone H2A-K119ub that is associated with Polycomb-mediated gene silencing[57, 58, 59]. USP22 can also deubiquitinate histone H2B-K120ub to promote transcriptional elongation[53, 60, 61, 62], as well as deubiquitinate several other non-histone targets[63, 64, 65]. We generated isogenic FHSC14 PDX models with CRISPR-Cas9 mediated deletion of *USP22* (Fig. 3.1a) by explanting and dissociating tumors prior to *ex vivo* lentivirus transduction to express either of two USP22 gRNAs (USP22-sg1/2) or one of two non-targeting gRNAs (Ctrl-sg1/2). The sgRNAs for these experiments were cloned into a lentiCRISPRv2-ZsGreen vector[66] containing a ZsGreen selection marker (see Table 7 for sgRNA sequences used). Eighteen hours after transduction, cells were re-implanted in the flanks of NSG mice for tumor regrowth after which we used fluorescence-activated cell sorting (FACS) to purify ZsGreen-positive cells: these were re-implanted again to form flank tumors that were > 98% ZsGreen positive (Fig. 3.1a) with *USP22* deletion confirmed by western blotting (Fig. 3.1b).

To determine how *USP22* deletion influenced chemosensitivity, we generated flank tumors by expanding FHSC14 USP22-sg1/2 and sgCtrl cells in NSG mice, then treated mice with tumors that had reached ~250 mm^3 with a 10-day regimen of cis-eto or saline together with daily measurements of tumor volume. Both USP22-sg1 and USP22-sg2 –

expressing tumors were treatment resistant and continued to grow at similar rates, compared to sgCtrl expressing tumors that were growth arrested or regressed in response to cis-eto treatment (Fig. 3.1b). In separate experiments designed to gain additional insight into the effect of *USP22* deletion on the short-term response to cis-eto, we collected FHSC14 Ctrl-sg1/2 and USP22-sg1/2-expressing tumors 48 hours after treatment. In FHSC14 Ctrl-sg1/2 tumors, cis-eto treatment significantly reduced the proportion of mitotic cells while concurrently strongly inducing apoptosis as assessed respectively by phospho-histone H3 S10 (pH3) and cleaved-caspase-3 (CC3) staining (Fig. 3.1c). In contrast, the proportion of pH3 and CC3-positive cells at 48-hours did not change in USP22-sg1/2 tumors treated with cis-eto (pH3 interaction $p < 0.01$, CC3 interaction $p < 0.001$).

To further validate and extend these observations, we deleted *USP22* in PDX model NCI109B where we had identified sgRNAs targeting *USP22* were enriched in functional screens (Fig. 3.1d). Ctrl-sg1/2-expressing NCI109B tumors again decreased in volume more rapidly relative to USP22-sg1/2 tumors after cis-eto treatment (Fig. 3.1d) with reduced cell proliferation and increased apoptosis at 48 hrs in both sgCtrl and sgUSP22-expressing tumors (Fig. 3.1e). Again, larger reductions were observed in sgCtrl versus sgUSP22 tumors (pH3 interaction $p < 0.05$, CC3 interaction $p < 0.05$). These results indicate that USP22 deletion can promote chemotherapy resistance in two independent SCLC PDX models with a stronger effect in FHSC14.

Figure 3.1

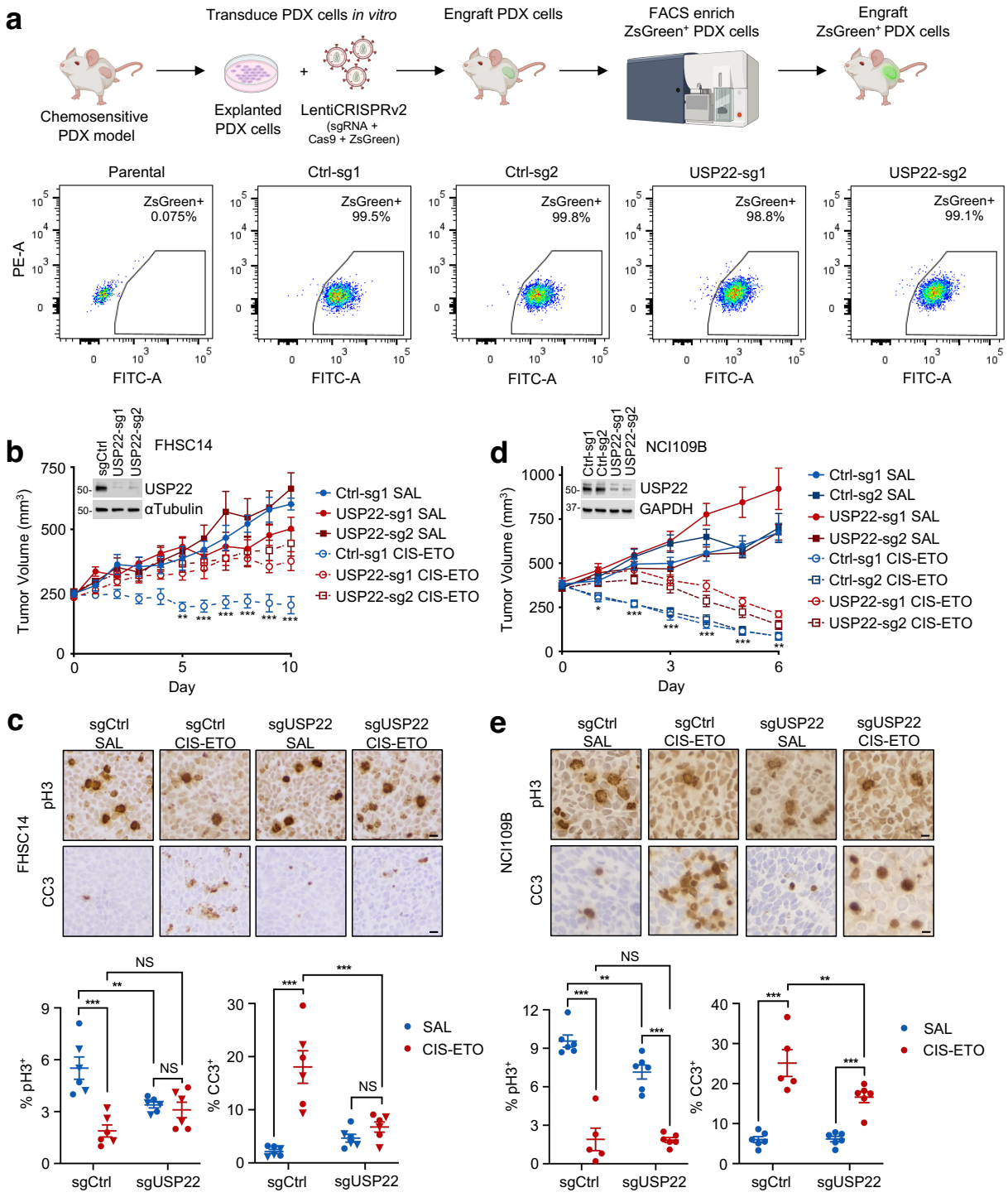
a
Transduce PDX cells *in vitro*
Engraft PDX cells
FACS enrich ZsGreen+ PDX cells
Engraft ZsGreen+ PDX cells
Chemosensitive PDX model
Explanted PDX cells
LentiCRISPRv2 (sgRNA + Cas9 + ZsGreen)
Parental
Ctrl-sg1
Ctrl-sg2
USP22-sg1
USP22-sg2
ZsGreen+ 0.075%
ZsGreen+ 99.5%
ZsGreen+ 99.8%
ZsGreen+ 98.8%
ZsGreen+ 99.1%
PE-A
FITC-A
b
FHSC14
sgCtrl
USP22-sg1
USP22-sg2
USP22
αTubulin
Tumor Volume (mm3)
Day
Ctrl-sg1 SAL
USP22-sg1 SAL
USP22-sg2 SAL
Ctrl-sg1 CIS-ETO
USP22-sg1 CIS-ETO
USP22-sg2 CIS-ETO
d
NCI109B
Ctrl-sg1
Ctrl-sg2
USP22-sg1
USP22-sg2
USP22
GAPDH
Ctrl-sg2 SAL
Ctrl-sg2 CIS-ETO
c
sgCtrl SAL
sgCtrl CIS-ETO
sgUSP22 SAL
sgUSP22 CIS-ETO
pH3
CC3
FHSC14
% pH3+
% CC3+
NS
SAL
CIS-ETO
sgCtrl
sgUSP22
e
NCI109B

Figure 3.1: *Generation of isogenic PDX models reveal USP22 deletion as a driver of chemoresistance in SCLC*

(**a**) Schematic of isogenic PDX model generation with lentiviral CRISPR-Cas9 mediated deletion of *USP22*. FACS plots show purity of transduced FHSC14 cells as assessed by ZsGreen expression relative to parental cells.

(**b**) Tumor volume over time growth curves of isogenic FHSC14 sgCtrl, USP22-sg1, and USP22-sg2 models treated with saline or cis-eto over a 10-day period. Data are means ± SEM; n=5 animals per treatment group. Top-left western blot shows USP22 protein loss in both USP22-sg1 and USP22-sg2 tumors relative to sgCtrl.

(**c**) IHC analyses and representative images for pH3 and CC3 in FHSC14 Ctrl-sg1/2 and USP22-sg1/2 tumors treated for 48 hours with saline or cis-eto. Data are means ± SEM; n=6 tumors per condition. Quantification with triangles depicting data from Ctrl-sg1 and USP22-sg1 while circles depicting Ctrl-sg2 and USP22-sg2. Scale bar, 10 μm.

(**d**) Tumor volume growth curves of isogenic NCI109B Ctrl-sg1, Ctrl-sg2, USP22-sg1, and USP22-sg2 models treated with saline or cis-eto over a 6-day period (n=7 animals per treatment group). Top-left western blot shows USP22 protein loss in USP22-sg1/2 relative to Ctrl-sg1/2 tumors.

(**e**) IHC analyses and representative images for pH3 and CC3 in NCI09B sgCtrl and sgUSP22 tumors treated for 48 hours with saline or cis-eto (n=6 tumors per condition, n=5 tumors for sgCtrl CIS-ETO condition). Scale bar, 10 μm.

Statistical analyses in **b, d,** were performed by 2-way ANOVA with Tukey's multiple comparisons test: adjusted *$p < 0.05$, **$p < 0.01$, ***$p < 0.001$, with asterisks comparing sgUSP22 CIS-ETO vs sgCtrl CIS-ETO treatment groups. Statistical analyses in **c, e,**

were performed by 2-way ANOVA with Fisher's LSD multiple comparisons test: *p < 0.05, **p < 0.01, ***p < 0.001.

3.2 USP22 re-expression chemosensitizes a USP22-null SCLC PDX model

USP22 has not previously been described as a target of inactivating mutations in SCLC; however, genomic whole exome data from a bank of PDX models revealed that SCLC PDX model JHU-LX33 harbors a homozygous E15* nonsense mutation in *USP22* (Fig. 3.2a). Western blot analyses using tissue from this model confirmed loss of USP22 protein (Fig. 3.2a). In contrast to the highly chemosensitive models used for our screens, JHU-LX33 is only modestly sensitive to chemotherapy (Fig. 3.2b). In order the test whether *USP22* inactivation in this PDX contributes to reduced chemotherapy response, we engineered an isogenic JHU-LX33 derivative that re-expressed either a *USP22* cDNA (USP22-PLVX) or an empty vector (Empty-PLVX) expressing a ZsGreen selection marker (Fig. 3.2c). Empty vector JHU-LX33 tumors lacking USP22 were markedly chemoresistant, with robust growth despite a 10-day course of cis-eto treatment (Fig. 3.2b), whereas tumors re-expressing USP22 displayed slower growth together with reduced pH3 and increased CC3 staining in response to cis-eto treatment (Fig. 3.2b,c). In contrast, the same treatment regimen did not cause significant changes in pH3 or CC3 staining in tumors derived from empty vector JHU-LX33 cells (pH3 interaction $p < 0.01$, CC3 interaction $p < 0.01$).

Figure 3.2

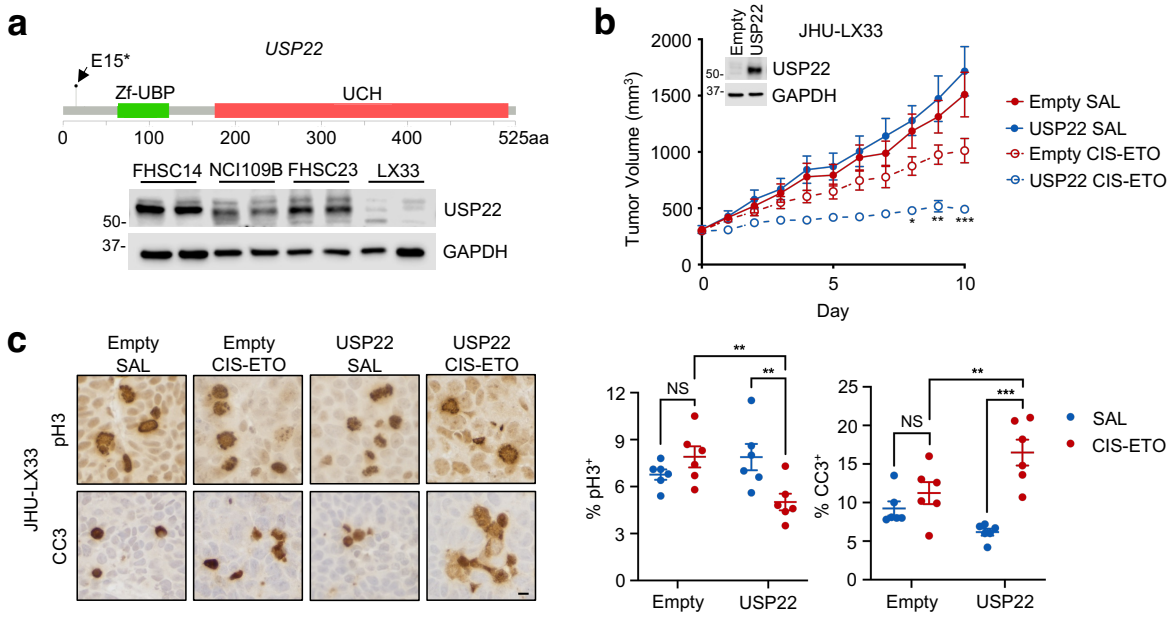

Figure 3.2: *Restoration of USP22 resensitizes a USP22-null PDX model to chemotherapy*

(**a**) Schematic of human USP22 protein showing an E15* truncating mutation present in the JHU-LX33 PDX model. Western blot shows USP22 protein in JHU-LX33 significantly depleted relative to three other SCLC PDX models.

(**b**) Tumor volume growth curves of isogenic JHU-LX33 Empty-PLVX and USP22-PLVX models treated with saline or cis-eto over a 10-day period. Data are means ± SEM; n=8 animals per treatment group. Top-left western blot shows USP22 protein add-back in USP22-PLVX relative to Empty-PLVX tumors.

(**c**) IHC analysis and representative images for pH3 and CC3 in JHU-LX33 Empty-PLVX and USP22-PLVX tumors treated with saline or cis-eto over a course of 10 days. Data are means ± SEM; n=6 tumors per condition.

Statistical analyses in **b**, were performed by 2-way ANOVA with Tukey's multiple comparisons test: adjusted *p < 0.05, **p < 0.01, ***p < 0.001, with asterisks comparing USP22 CIS-ETO vs Empty CIS-ETO treatment groups. Statistical analyses in **c** were performed by 2-way ANOVA with Fisher's LSD multiple comparisons test: *p < 0.05, **p < 0.01, ***p < 0.001.

3.3 USP22 deubiquitylase function is required for chemotherapeutic response

USP22 functions as a deubiquitylase in the SAGA complex. In order to determine whether this catalytic activity is required for SCLC chemotherapeutic response, we extended the engineered JHU-LX33 PDX model to compare the cis-eto sensitivity of tumors that expressed a USP22 catalytic dead mutant, USP22-C185S[67, 68] cDNA, wild-type USP22 cDNA, or the empty vector PLVX-ZsGreen selection marker (Fig. 3.3a). Isogenic JHU-LX33 tumors in NSG mice that re-expressed USP22 grew significantly slower when treated with cis-eto than control empty vector tumors (Fig. 3.3b). In contrast, tumors expressing catalytically dead USP22-C185S were cis-eto-resistant and grew at rates comparable to empty vector control tumors. These results indicate that USP22 is an important determinant of SCLC chemosensitivity, and that loss of USP22 or its deubiquitylase activity promote chemoresistance in three PDX models. These results further support the findings from our initial loss-of-function genetic screens.

Figure 3.3

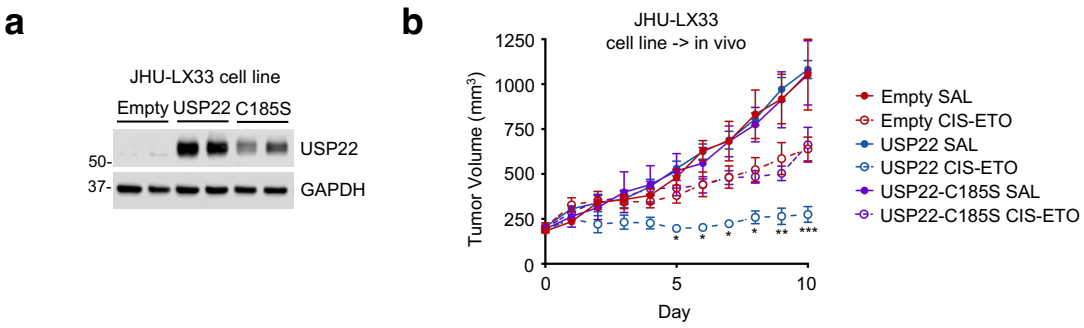

Figure 3.3: *Expression of catalytic dead USP22 fails to resensitize SCLC cell line to chemotherapy*

(**a**) Western blot showing USP22 expression in JHU-LX33 Empty-PLVX, USP22-PLVX, and catalytic dead USP22-C815S-PLVX tumors.

(**b**) Tumor volume growth curves of isogenic JHU-LX33 Empty-PLVX, USP22-PLVX, and USP22-C815S-PLVX models treated with saline or cis-eto over a 10-day period. n=5 animals per treatment group. Statistical analyses in **b**, were performed by 2-way ANOVA with Tukey's multiple comparisons test: adjusted *p < 0.05, **p < 0.01, ***p < 0.001, with asterisks comparing USP22 CIS-ETO vs Empty CIS-ETO treatment groups. Statistical analyses in **c** were performed by 2-way ANOVA with Fisher's LSD multiple comparisons test: *p < 0.05, **p < 0.01, ***p < 0.001.

3.4 Global proteomic analyses reveal USP22 roles in SCLC

In order to gain additional mechanistic insight into USP22 expression and activity as important determinants of SCLC chemosensitivity we performed global proteomic analyses. These compared isogenic FHSC14 USP22-sg1/2 vs sgCtrl-sg1/2 and NCI109B sgUSP22 vs sgCtrl tumors that had been treated for 48 hours with saline or

with cis-eto (Fig. 3.4a-d). Upregulated ($Log_2FC > 0.5$, FDR < 0.05) or downregulated ($Log_2FC < -0.5$, FDR < 0.05) proteins in sgUSP22 tumors from each PDX model were queried for MSigDB Hallmark and GO Biological Process pathway enrichment using Enrichr[69, 70] (Fig 3.4e-j). Top pathways commonly enriched in sgUSP22 relative to sgCtrl tumors in both PDX models included Interferon Alpha Response, Interferon Gamma Response, Myogenesis, and Hypoxia (Fig. 3.4e-h). In *USP22*-deleted FHSC14 tumors, protein sets including interferon response pathways, inflammatory response, regulation of T-cell activation, allograft rejection, and IL2/STAT5 signaling were among the top 10 most significantly enriched Hallmark pathways (Fig. 3.4g). These findings are consistent with multiple studies in human cell lines and mouse models that identified USP22 as a negative regulator of type I-III interferon signaling and interferon-stimulated genes (ISGs) [71, 72, 73, 74, 75]. Pathways commonly depleted in FHSC14 and NCI109B sgUSP22 models included cell-cell junction and cell migration, and neuronal pathways such as Nervous System Development, Central Nervous System and Brain Development (Fig. 3.4e-f). Neuronal gene sets were amongst the top depleted pathways in both *USP22* deletion PDX models (Fig. 3.4i-j) where top downregulated proteins in FHSC14 sgUSP22 tumors included neuronal pathway proteins such as NKX2-2, ROBO1, ROBO2, SEMA6A, FABP7, and PCDHB10 (Fig. 3.4a,c).

Figure 3.4

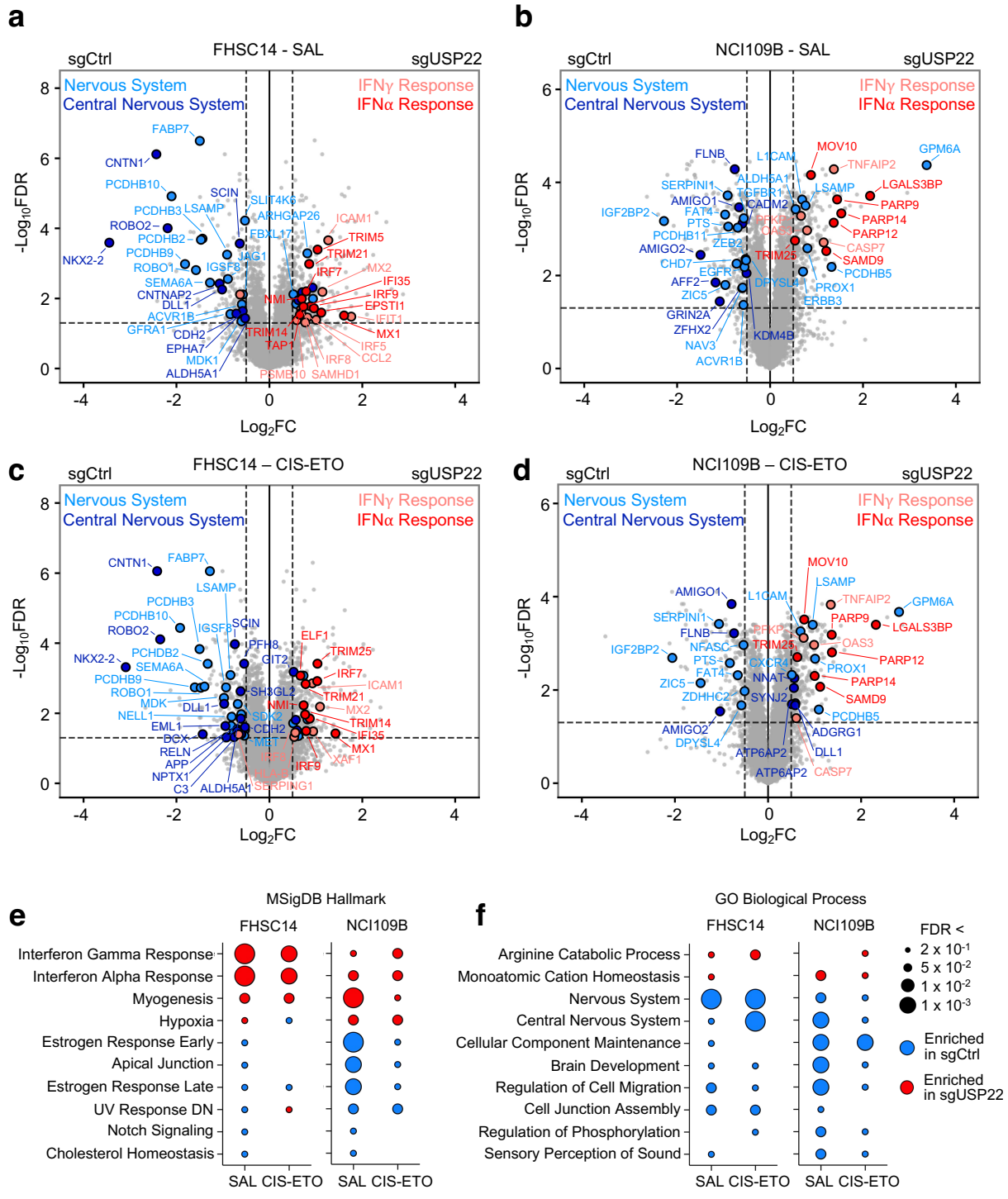
a
FHSC14 - SAL
sgCtrl
sgUSP22
Nervous System
Central Nervous System
IFNγ Response
IFNα Response
-Log10FDR
Log2FC
b
NCI109B - SAL
c
FHSC14 – CIS-ETO
d
NCI109B – CIS-ETO
e
MSigDB Hallmark
FHSC14
NCI109B
Interferon Gamma Response
Interferon Alpha Response
Myogenesis
Hypoxia
Estrogen Response Early
Apical Junction
Estrogen Response Late
UV Response DN
Notch Signaling
Cholesterol Homeostasis
SAL CIS-ETO
f
GO Biological Process
Arginine Catabolic Process
Monoatomic Cation Homeostasis
Nervous System
Central Nervous System
Cellular Component Maintenance
Brain Development
Regulation of Cell Migration
Cell Junction Assembly
Regulation of Phosphorylation
Sensory Perception of Sound
FDR <
2 x 10-1
5 x 10-2
1 x 10-2
1 x 10-3
Enriched in sgCtrl
Enriched in sgUSP22

Figure 3.4 (continued)

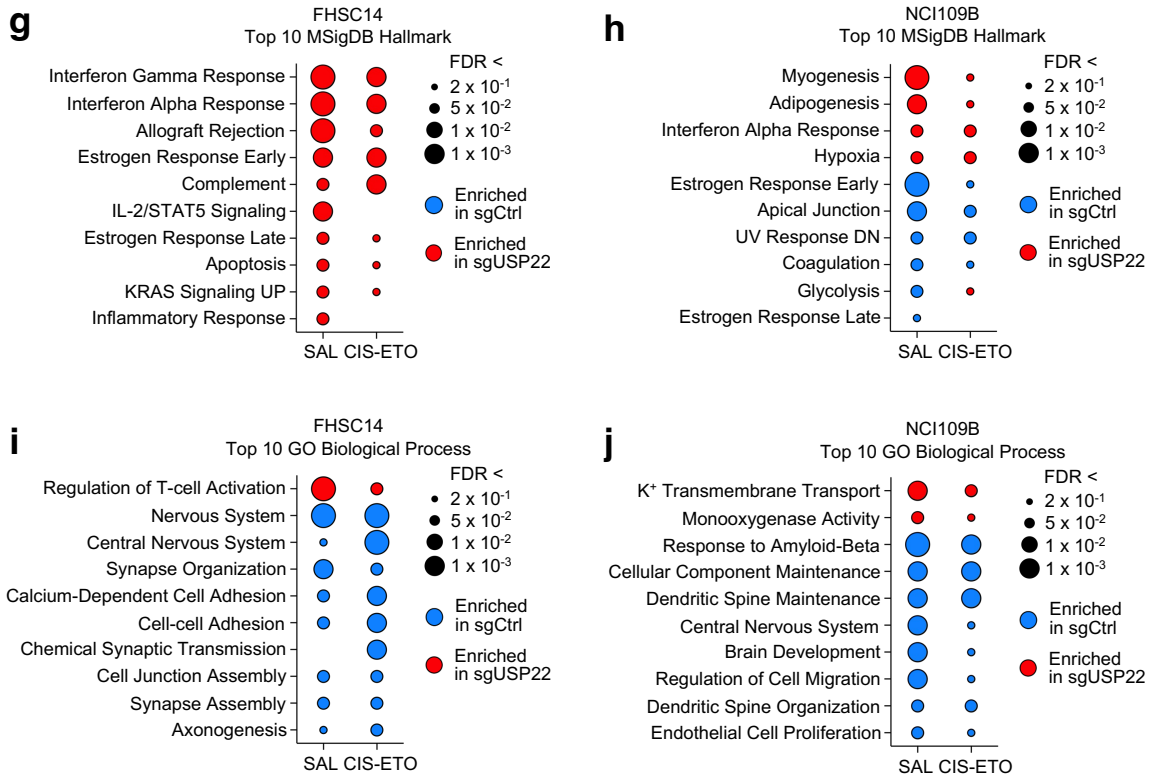

Figure 3.4: *Global proteomic analyses of SCLC PDX models with USP22 deletion*

(**a**-**b**) Volcano plots of global proteomics data from saline-treated FHSC14 USP22-sg1/2 vs Ctrl-sg1/2 tumors (n=2 tumors per sgRNA for a total of n=4 tumors per treatment group) (a) and NCI109B sgUSP22 vs sgCtrl tumors (n=3 tumors per treatment group) (b). Differentially expressed upregulated ($Log_2FC > 0.5$, FDR < 0.05) or downregulated ($Log_2FC < -0.5$, FDR < 0.05) proteins belonging to the indicated Gene Ontology Biological Process 2023 and MSigDB Hallmark 2020 pathways are labelled in blue and red, respectively.

(**c**-**d**) Volcano plots of global proteomics data from 48 hour cis-eto treated FHSC14 USP22-sg1/2 vs Ctrl-sg1/2 tumors (c) and NCI109B sgUSP22 vs sgCtrl tumors (d).

(**e**-**f**) Upregulated or downregulated proteins in FHSC14 and NCI109B sgUSP22 vs sgCtrl tumors treated for 48 hours with saline or cis-eto were independently queried for pathway enrichment using Enrichr. The top commonly enriched or depleted pathways from MSigDB Hallmark (c) and Gene Ontology Biological Process (d) gene set databases from both PDX models with *USP22* deletion are shown. Blue circles indicate pathways enriched in sgCtrl and red circles indicate pathways enriched in sgUSP22 tumors. Point size scaled to FDR.

(**g**-**j**) Upregulated or downregulated proteins in FHSC14 and NCI109B sgUSP22 vs sgCtrl tumors treated for 48 hours with saline or cis-eto were independently queried for pathway enrichment using Enrichr. The top 10 significantly enriched/depleted pathways from MSigDB Hallmark (g-h) and Gene Ontology Biological Process (i-j) gene set databases for each PDX model with *USP22* deletion are shown.

3.5 USP22 regulates transcription of neuronal/neuroendocrine and DNA damage associated genes

The SAGA complex in which USP22 participates plays a key role in gene transcription. We thus complemented our proteomic analyses with RNA-seq analyses of FHSC14 USP22-sg1/2 vs sgCtrl-sg1/2 and NCI109B sgUSP22 vs sgCtrl tumors after 48 hrs of either cis-eto or saline control treatment (Fig. 3.5a-c). In addition, we transcriptionally profiled JHU-LX33 USP22-PLVX vs Empty-PLVX tumors that had been treated for 10 days with either cis-eto or a saline control (Fig. 3.5a,d). Differentially expressed, up- and downregulated genes were identified using Enrichr to identify common pathways altered as a function of *USP22* status in at least 2 out of 3 PDX models tested (FDR < 0.05; Fig.

3.5a). Tables 8-11 provide the complete list of all significantly enriched or depleted pathways. Consistent with our proteomic analyses, the Interferon Gamma Response pathway gene expression was upregulated in FHSC14 and NCI109B sgUSP22 tumors (Fig. 3.5a,c). Gene set enrichment analysis (GSEA)[76] also confirmed strong enrichment of the Interferon Alpha Response (Fig. 3.5e) and Interferon Gamma Response pathways (Fig. 3.5f) in both cis-eto treated PDX models with *USP22* targeting sgRNAs. USP22 loss also increased activation of pathways related to hypoxia and glycolysis (Fig. 3.5a-d) and suppressed expression of DNA-damage response transcripts (Fig. 3.5a,c,g). Multiple pathways related to nervous system development were also consistently suppressed upon USP22 loss (Fig. 3.5a-d).

Among FHSC14 genes downregulated following USP22 loss was *ASCL1*, a transcription factor and master regulator of SCLC neuroendocrine transcriptional programs, together with other regulators of neuronal differentiation and development including *INSM1*, *NXK2-1*, *NKX2-2*, *ROBO2*, and *SEMA6A*[77, 78, 79, 80, 81, 82] (Fig 3.5c). GSEA further confirmed suppression of ASCL1 target genes[21] in FHSC14 sgUSP22 versus sgCtrl tumors, and upregulation of ASCL1 target genes in JHU-LX33 USP22-expressing tumors relative to empty vector control (USP22 null) tumors (Fig. 3.5h). Of note, resistance to platinum-based therapies in SCLC has been associated with reduced ASCL1 expression, enrichment of ASCL1-low cells in relapsed samples, and neuroendocrine to non-neuroendocrine fate switching[23, 29, 36, 38].

Figure 3.5

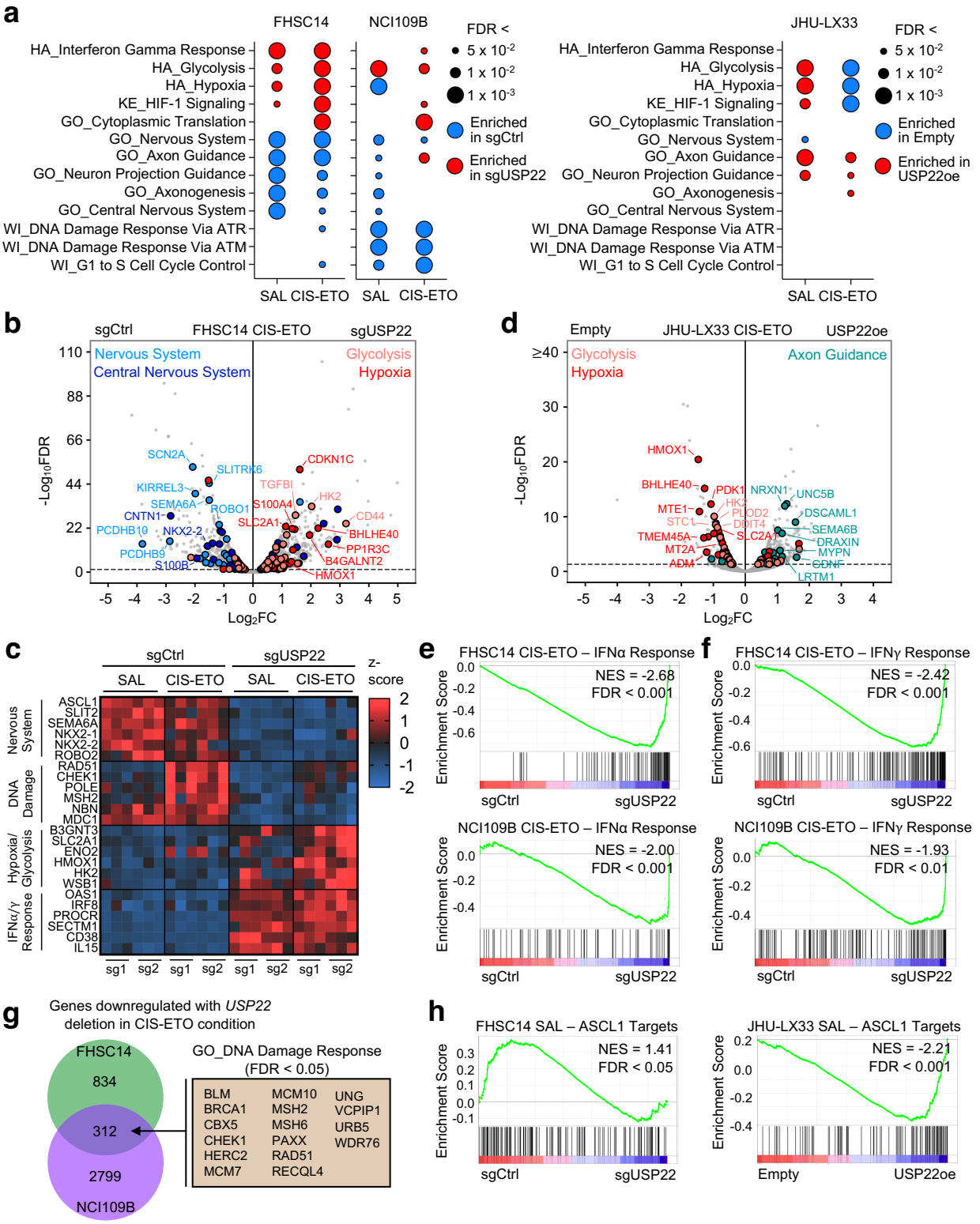
a
FHSC14
NCI109B
JHU-LX33
FDR <
5 x 10-2
1 x 10-2
1 x 10-3
Enriched in sgCtrl
Enriched in sgUSP22
Enriched in Empty
Enriched in USP22oe
HA_Interferon Gamma Response
HA_Glycolysis
HA_Hypoxia
KE_HIF-1 Signaling
GO_Cytoplasmic Translation
GO_Nervous System
GO_Axon Guidance
GO_Neuron Projection Guidance
GO_Axonogenesis
GO_Central Nervous System
WI_DNA Damage Response Via ATR
WI_DNA Damage Response Via ATM
WI_G1 to S Cell Cycle Control
SAL CIS-ETO
b
sgCtrl
FHSC14 CIS-ETO
sgUSP22
Nervous System
Central Nervous System
Glycolysis
Hypoxia
-Log10FDR
Log2FC
d
Empty
JHU-LX33 CIS-ETO
USP22oe
Axon Guidance
c
z-score
Nervous System
DNA Damage
Hypoxia/ Glycolysis
IFNα/γ Response
e
FHSC14 CIS-ETO – IFNα Response
NES = -2.68
FDR < 0.001
NCI109B CIS-ETO – IFNα Response
NES = -2.00
FDR < 0.001
f
FHSC14 CIS-ETO – IFNγ Response
NES = -2.42
FDR < 0.001
NCI109B CIS-ETO – IFNγ Response
NES = -1.93
FDR < 0.01
Enrichment Score
g
Genes downregulated with USP22 deletion in CIS-ETO condition
FHSC14
834
312
2799
NCI109B
GO_DNA Damage Response (FDR < 0.05)
BLM BRCA1 CBX5 CHEK1 HERC2 MCM7
MCM10 MSH2 MSH6 PAXX RAD51 RECQL4
UNG VCPIP1 URB5 WDR76
h
FHSC14 SAL – ASCL1 Targets
NES = 1.41
FDR < 0.05
JHU-LX33 SAL – ASCL1 Targets
NES = -2.21
FDR < 0.001

Figure 3.5: RNA-seq analysis of SCLC PDX models with USP22 perturbation

(**a**) Differentially expressed upregulated or downregulated genes (FDR < 0.05) from RNA-seq data in FHSC14 USP22-sg1/2 vs Ctrl-sg1/2 (n=3 tumors per sgRNA for a total of n=6 tumors per treatment group) and NCI109B sgUSP22 vs sgCtrl tumors models (n=5 tumors per treatment group) treated for 48 hours with saline or cis-eto or JHU-LX33 USP22-PLVX vs Empty-PLVX (n=5 tumors per treatment group) treated for 10 days with saline or cis-eto were independently queried for pathway enrichment using Enrichr. Pathways from Gene Ontology Biological Process 2023 (GO), MSigDB Hallmark 2020 (HA), KEGG 2021 Human (KE), WikiPathways 2024 Human (WI) gene set databases commonly enriched in or depleted in at least 2 out of 3 PDX models with respect to USP22 status are displayed. Point size scaled to FDR.

(**b**) Volcano plot of RNA-seq differential gene expression analysis from 48 hour cis-eto treated FHSC14 USP22-sg1/2 vs Ctrl-sg1/2 models. Significantly changed genes are colored corresponding to the indicated Gene Ontology Biological Process 2023 and MSigDB Hallmark 2020 pathways.

(**c**) Heatmap of RNA-seq data for select FHSC14 USP22-sg1/2 vs Ctrl-sg1/2 differentially expressed genes from the indicated pathways. Each column is a tumor.

(**d**) Volcano plot of RNA-seq differential gene expression analysis from 10 day treated JHU-LX33 USP22-PLVX vs Empty-PLVX. Significantly changed genes are colored corresponding to the indicated Gene Ontology Biological Process 2023 pathways.

(**e**-**f**) GSEA analyses of Hallmark Interferon Alpha Response (d) and Interferon Gamma Response (f) pathways in FHSC14 and NCI109B sgUSP22 vs sgCtrl tumors treated for 48 hours with cis-eto.

(**g**) Enrichr pathway analysis of commonly downregulated genes in both FHSC14 and NCI109B sgUSP22 tumors treated for 48 hours with cis-eto

(**h**) GSEA analysis of custom ASCL1 Targets gene set[21] in FHSC14 sgUSP22 vs sgCtrl and JHU-LX33 USP22-PLVX vs Empty-PLVX.

3.6 USP22 regulates neuronal gene expression by modulating histone H2A ubiquitylation in SCLC

Within SAGA, USP22 is thought to regulate gene expression by deubiquitylation of ub-H2A K119 (H2AK119ub) and ub-H2B K120 (H2BK120ub)[52, 59]. Transcriptional repression of specific genes is mediated through recruitment of Polycomb repressive complexes 1 and 2 (PRC1/2) to deposit H2AK119ub and H3K27me3, respectively[83] where these histone marks overlap at genomic loci due to co-recruitment of PRC1 and PRC2[84, 85]. USP22 can reverse repression of these genes by deubiquitylation of H2AK119ub[52], which displacesPRC2 with the loss of H3K27me3 deposition[86]. Thus, failure to deubiquitinate H2AK119ub may result in improper gene silencing.

To identify molecular mechanisms regulating transcriptional changes upon *USP22* deletion, we performed Cleavage Under Targets and Tagmentation (CUT&Tag)[87] for H2BK119ub and H3K27me3. Following a 48-hour treatment of saline or cis-eto, FHSC14 sgCtrl and sgUSP22 tumors were dissociated, viable cells sorted by FACS then subjected to CUT&Tag processing and sequencing. We performed differential peak analysis comparing H2AK119ub peaks in sgUSP22 tumor cells vs sgCtrl tumor cells in the saline and cis-eto treatment conditions. In saline-treated sgUSP22 tumors,

566 H2AK119ub peaks (324 unique protein-coding genes) were gained while 338 peaks (160 unique protein-coding genes) were lost relative to saline-treated sgCtrl tumors (Fig. 3.6a-b). This increase in H2AK119ub peaks in USP22-null tumors is consistent with USP22 acting as an H2AK119 deubiquitinase. In the cis-eto condition, a total of 1141 H2AK119 peaks 652 unique protein-coding genes) were gained, while 892 peaks (413 unique protein-coding genes) were lost in sgUSP22 tumors relative to sgCtrl tumors (Fig. 3.6c-d). In saline and cis-eto treated sgUSP22 tumors combined, 86 out of 722 unique protein-coding genes with increased H2AK119ub were concurrently transcriptionally downregulated. Of these 86 genes, 16 belonged to the Nervous System Development or Central Nervous System Development pathways (Fig. 3.6e-f, Table 12). Among these 16 neuronal genes in sgUSP22 tumors, H2AK119ub increased and RNA expression decreased for *NXK2-1*, *NKX2-2*, *ZIC5*, *GDNF*, *KIF26A*, and *SEMA6A* (Fig. 3.6g). We also observed increases in H3K27me3 peaks at these loci relative to sgCtrl tumors, consistent with strong epigenetic repression. Western blotting of NKX2-2 and SEMA6A in FHSC14 tumors confirmed protein depletion in sgUSP22 relative to sgCtrl tumors (Fig. 3.6h). In accordance with RNA downregulation of ASCL1 targets in USP22-KO tumors (Fig. 3.5d), we observed a significant decrease in ASCL1 and INSM1 protein levels in FHSC14 sgUSP22 relative to sgCtrl tumors. (Fig. 3.6h). Taken together, these data suggest that USP22 directly regulates the expression of neuronal genes in SCLC at the epigenetic level by removing ubiquitin from H2AK119. Furthermore, deletion of USP22 may result in increased H2AK119ub and H3K27me3 at these genomic loci, resulting in epigenetic and transcriptional repression of neuronal genes in SCLC.

Figure 3.6

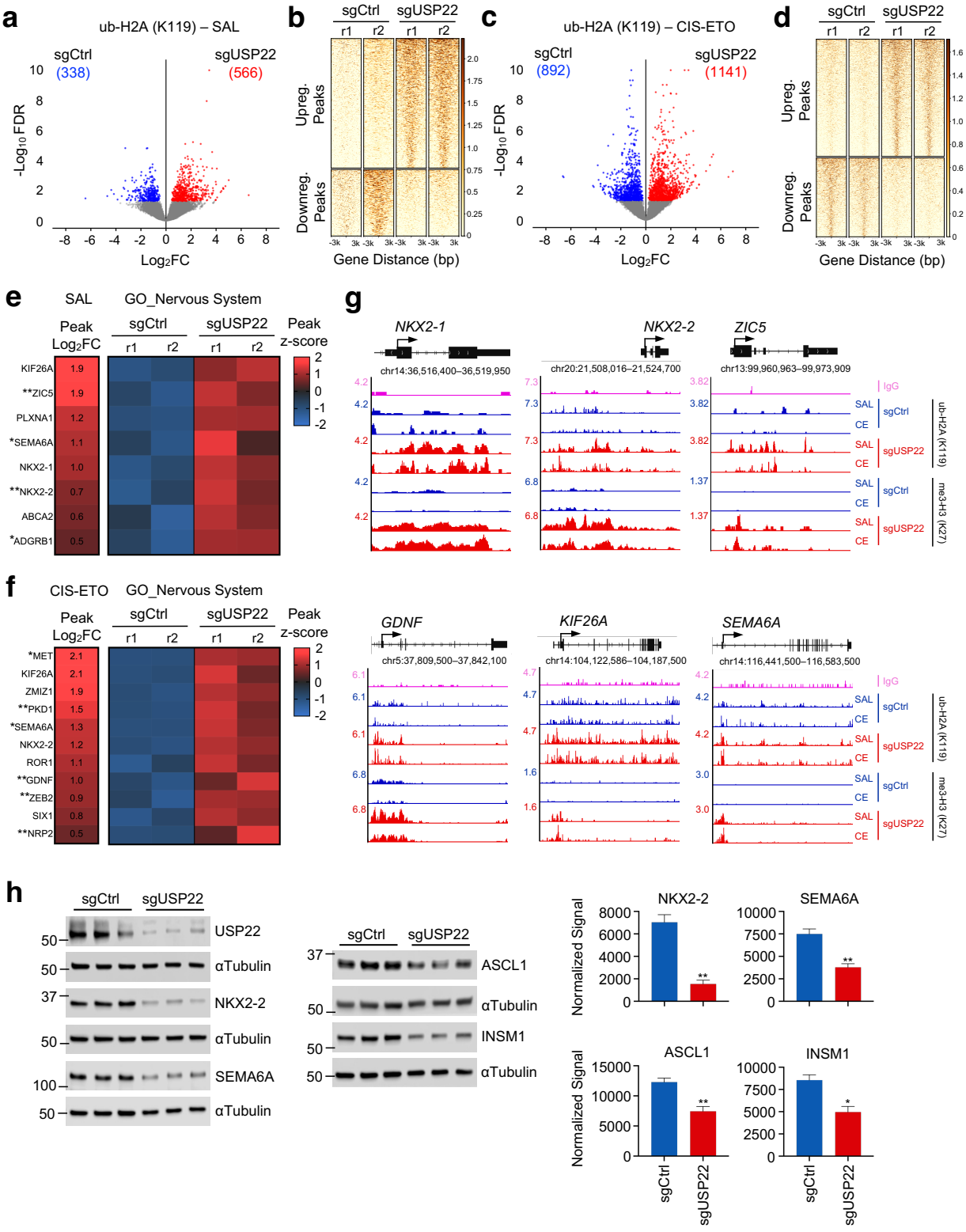
a
ub-H2A (K119) – SAL
sgCtrl
(338)
sgUSP22
(566)
-Log10 FDR
Log2FC
b
sgCtrl
sgUSP22
r1
r2
Upreg. Peaks
Downreg. Peaks
Gene Distance (bp)
c
ub-H2A (K119) – CIS-ETO
sgCtrl
(892)
sgUSP22
(1141)
d
e
SAL
GO_Nervous System
Peak Log2FC
Peak z-score
KIF26A
**ZIC5
PLXNA1
*SEMA6A
NKX2-1
**NKX2-2
ABCA2
*ADGRB1
g
NKX2-1
NKX2-2
ZIC5
chr14:36,516,400–36,519,950
chr20:21,508,016–21,524,700
chr13:99,960,963–99,973,909
IgG
SAL
CE
sgCtrl
sgUSP22
ub-H2A (K119)
me3-H3 (K27)
f
CIS-ETO
GO_Nervous System
*MET
KIF26A
ZMIZ1
**PKD1
*SEMA6A
NKX2-2
ROR1
**GDNF
**ZEB2
SIX1
**NRP2
GDNF
KIF26A
SEMA6A
chr5:37,809,500–37,842,100
chr14:104,122,586–104,187,500
chr14:116,441,500–116,583,500
h
sgCtrl
sgUSP22
USP22
αTubulin
NKX2-2
SEMA6A
ASCL1
INSM1
Normalized Signal

Figure 3.6: USP22 regulates histone H2A ubiquitylation at neuronal genes in SCLC

(**a**-**b**) Volcano plot showing ub-H2A (K119) differential peak analyses results of CUT&Tag data from FHSC14 sgUSP22 vs sgCtrl models treated for 48 hours with saline (n=2 tumors per treatment group). The number of differentially enriched or depleted peaks (FDR < 0.05) in sgUSP22 tumors (red) compared to sgCtrl tumors (blue) is shown (a). Heatmaps depicting significantly (FDR < 0.05) upregulated and downregulated ub-H2A (K119) peaks in sgUSP22 tumors. Heatmaps show data 3 kb upstream and downstream of peak center (b). (**c**-**d**) Volcano plot of CUT&Tag data for ub-H2A (K119) differential peak calling data in FHSC14 sgUSP22 vs sgCtrl models treated for 48 hours with cis-eto (c) Heatmaps depicting significantly (FDR < 0.05) upregulated and downregulated ub-H2A (K119) peaks (d). (**e**-**f**) Heatmaps of FHSC14 sgUSP22 vs sgCtrl ub-H2A (K119) peak Log_2FC and z-scores for genes with enriched ub-H2A (K119) peaks and concurrent downregulation at the RNA level (RNA-seq, USP22-sg1/2 vs Ctrl-sg1/2, FDR < 0.05) within the GO Nervous System Development (no asterisk), GO Nervous System Development (*) or both pathways (**). (**g**) IGV images of CUT&Tag data displaying ub-H2A (K119) and me3-H3 (K27) peaks from select GO Central Nervous System Development and GO Nervous System Development genes in **e** and **f**. (**h**) Western blot analyses of FHSC14 sgUSP22 vs sgCtrl tumors (n=3 per group). Quantification of protein signal normalized to loading control is shown for each genotype. Statistical analyses in **h** were performed by unpaired student's two-tailed t-test: *p < 0.05, **p < 0.01, ***p < 0.001.

3.7 SCLC PDX models with *USP22* deletion exhibit blunted DNA damage signaling in response to chemotherapy

In our RNA-seq analyses, we observed suppression of multiple DNA damage response pathways in FHSC14 and NCI109B sgUSP22 tumors prior to or after 48 hours of cis-eto treatment relative to control sgCtrl tumors (Fig. 3.5a,c,g). Among the differentially expressed genes identified were identified 312 genes downregulated upon USP22 deletion that were shared between cis-eto treated FHSC14 and NCI109B (Fig. 3.5g). Pathway analysis on these genes revealed the DNA IR Damage and Cellular Response via ATR (WikiPathway, WP4016) transcripts, such as *CHEK1*, *RAD51*, *BRCA1*, *MSH2*, that were suppressed in both USP22 KO FHSC14 and NCI109B (Fig. 3.5g). In FHSC14 control tumors, transcript levels of multiple DNA damage response genes increased robustly upon cis-eto treatment versus suppressed expression of these DNA damage response genes after treatment in FHSC14 sgUSP22 tumors (Fig. 3.5c).

Activation and maintenance of the DNA damage response (DDR) is mediated through rapid and dynamic phosphorylation cascades involving DNA damage sensors, signal transducers, repair machinery and cell cycle checkpoint kinases[88]. Both FHSC14 and NCI109B sgUSP22 models exhibited reduced expression of DDR genes relative to sgCtrl models treated with cis-eto (Fig. 3.5a,c,g). Phosphorylation events are critical for DDR signaling. Thus, we next performed phospho-proteomics profiling of tumors after 48 hrs of cis-eto or control treatment of FHSC14 USP22-sg1/2 vs Ctrl-sg1/2, NCI109B sgUSP22 vs sgCtrl and JHU-LX33 USP22-PLVX vs Empty-PLVX. Genes whose phosphorylation sites were enriched ($Log_2FC > 0.5$, FDR < 0.05) or depleted ($Log_2FC <$

-0.5, FDR < 0.05) in cis-eto treated sgUSP22 vs sgCtrl tumors were queried for pathway enrichment using Enrichr. After cis-eto treatment multiple DDR pathways were depleted in USP22-deleted FHSC14 and NCI109B models (Fig. 3.7a-b). DNA damage-related pathways were conversely enriched in upon USP22 restoration in JHU-LX33 (Fig. 3.7c). Phosphosite-specific signature enrichment analysis (PTM-SEA)[89] of all three models allowed the identification of specific kinases on substrate phosphorylation. In the cis-eto treated samples of FHSC14 and NCI109B both ATM and ATR exhibited reduced activity upon USP22 loss (Fig. 3.7d-f), with increased activity following USP22 addback to JHU-LX33 (Fig. 3.7d,g). These data indicate that USP22 loss can reduce DNA damage response phospho-signaling upon cis-eto treatment.

H2AX is phosphorylated at Serine 139 (γH2AX) at DNA break sites by ATM and ATR, serving to recruit DNA repair factors[90, 91, 92]. We performed γH2AX IHC analyses on FHSC14 USP22-sg1/2 vs Ctrl-sg1/2 treated for 48 hours with cis-eto or saline as well as JHU-LX33 USP22 add-back vs empty vector control treated under 10 days of treatment. While cis-eto increased the number of $\gamma H2AX^+$ cells in Ctrl-sg1/2 tumors, the impact of cis-eto on $\gamma H2AX^+$ cells was significantly reduced in USP22-sg1/2 FHSC14 (interaction $p < 0.01$) (Fig. 3.7h). In the JHU-LX33 model, both empty vector control and USP22 add-back tumors exhibited an increase in $\gamma H2AX^+$ cells in response to cis-eto; however, this increase was reduced in the empty vector control tumors relative to the USP22 add-back tumors (interaction $p < 0.001$) (Fig. 3.7i). To further assess the impact of USP22 loss on γH2AX foci formation, we performed immunofluorescence analysis on FHSC14 sgCtrl and sgUSP22 tumors cells treated *in vivo* with saline or cis-eto for 48 hours. In

sgCtrl tumors, cis-eto led to a robust increase in number of γH2AX puncta per cell, puncta MFI and total MFI per cell relative to saline treatment (Fig. 3.7j). The impact of cis-eto on γH2AX was significantly reduced in sgUSP22 tumors. In line with decreased formation of cis-eto induced γH2AX puncta, western blot analyses in FHSC14 reveal decreased phosphorylation of downstream ATM/ATR kinase DDR targets, including phospho-RAD50 (S635), phospho-MRE11 (S676), and phospho-Chk1 (S345) in cis-eto sgUSP22 tumors relative to cis-eto treated sgCtrl tumors (Fig. 3.7k). Basal protein levels of RAD50, MRE11, and Chk1 remain unchanged across genotypes and treatment conditions. Again, adding back USP22 in JHU-LX33 increased the abundance of cis-eto induced phosphorylation of these 3 DDR proteins (Fig. 3.7l). Taken together, these data show USP22-null SCLC tumors exhibit a strikingly reduced DNA damage responses to chemotherapy.

Figure 3.7

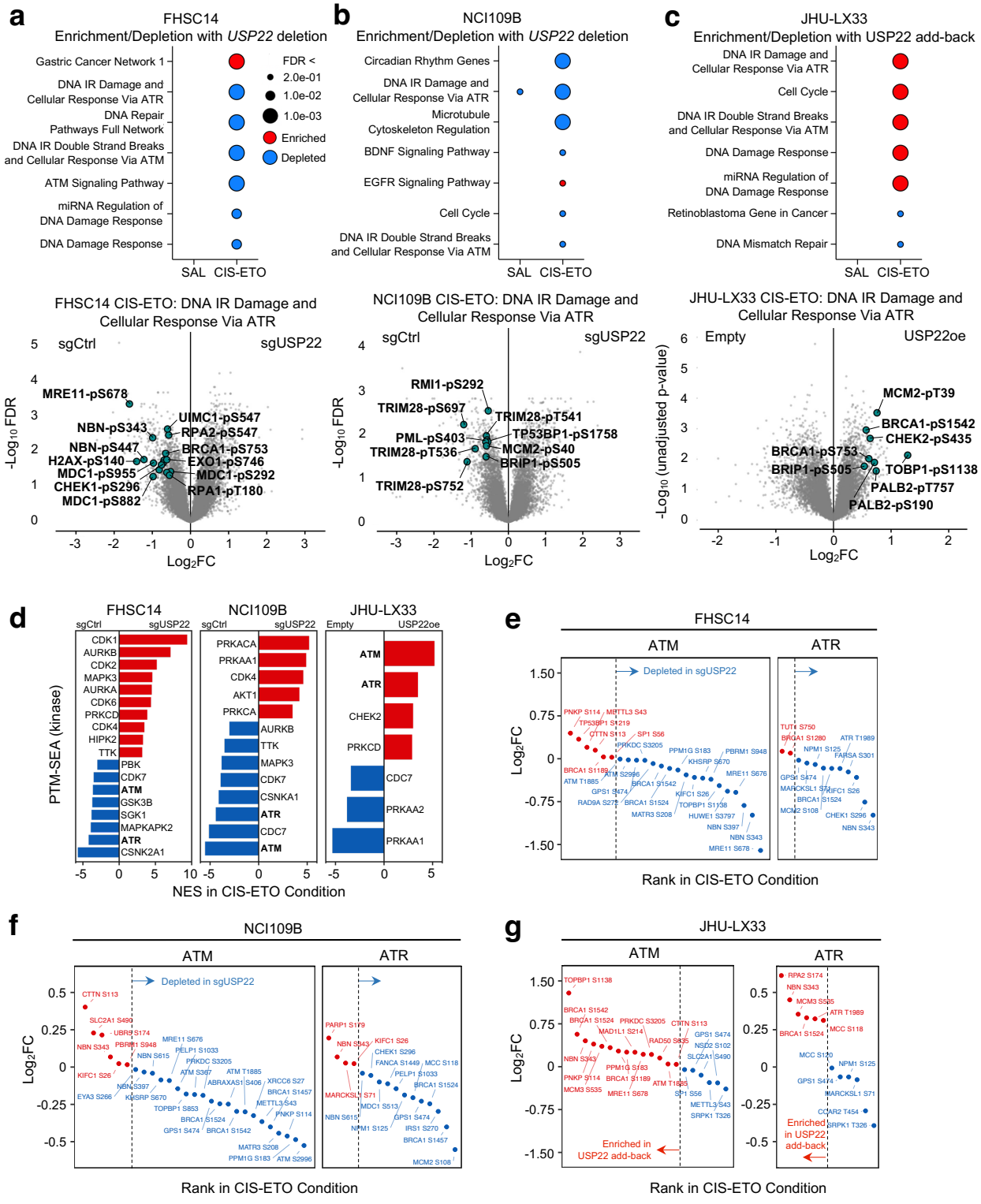
a
FHSC14
Enrichment/Depletion with USP22 deletion
Gastric Cancer Network 1
DNA IR Damage and Cellular Response Via ATR
DNA Repair Pathways Full Network
DNA IR Double Strand Breaks and Cellular Response Via ATM
ATM Signaling Pathway
miRNA Regulation of DNA Damage Response
DNA Damage Response
FDR <
2.0e-01
1.0e-02
1.0e-03
Enriched
Depleted
SAL CIS-ETO
b
NCI109B
Enrichment/Depletion with USP22 deletion
Circadian Rhythm Genes
DNA IR Damage and Cellular Response Via ATR
Microtubule Cytoskeleton Regulation
BDNF Signaling Pathway
EGFR Signaling Pathway
Cell Cycle
DNA IR Double Strand Breaks and Cellular Response Via ATM
SAL CIS-ETO
c
JHU-LX33
Enrichment/Depletion with USP22 add-back
DNA IR Damage and Cellular Response Via ATR
Cell Cycle
DNA IR Double Strand Breaks and Cellular Response Via ATM
DNA Damage Response
miRNA Regulation of DNA Damage Response
Retinoblastoma Gene in Cancer
DNA Mismatch Repair
SAL CIS-ETO
FHSC14 CIS-ETO: DNA IR Damage and Cellular Response Via ATR
sgCtrl
sgUSP22
MRE11-pS678
NBN-pS343
NBN-pS447
H2AX-pS140
MDC1-pS955
CHEK1-pS296
MDC1-pS882
UIMC1-pS547
RPA2-pS547
BRCA1-pS753
EXO1-pS746
MDC1-pS292
RPA1-pT180
-Log10 FDR
Log2FC
NCI109B CIS-ETO: DNA IR Damage and Cellular Response Via ATR
sgCtrl
sgUSP22
RMI1-pS292
TRIM28-pS697
PML-pS403
TRIM28-pT536
TRIM28-pS752
TRIM28-pT541
TP53BP1-pS1758
MCM2-pS40
BRIP1-pS505
-Log10 FDR
Log2FC
JHU-LX33 CIS-ETO: DNA IR Damage and Cellular Response Via ATR
Empty
USP22oe
MCM2-pT39
BRCA1-pS1542
CHEK2-pS435
BRCA1-pS753
BRIP1-pS505
TOBP1-pS1138
PALB2-pT757
PALB2-pS190
-Log10 (unadjusted p-value)
Log2FC
d
FHSC14
NCI109B
JHU-LX33
sgCtrl
sgUSP22
Empty
USP22oe
PTM-SEA (kinase)
CDK1
AURKB
CDK2
MAPK3
AURKA
CDK6
PRKCD
CDK4
HIPK2
TTK
PBK
CDK7
ATM
GSK3B
SGK1
MAPKAPK2
ATR
CSNK2A1
PRKACA
PRKAA1
CDK4
AKT1
PRKCA
AURKB
TTK
MAPK3
CDK7
CSNKA1
ATR
CDC7
ATM
ATM
ATR
CHEK2
PRKCD
CDC7
PRKAA2
PRKAA1
NES in CIS-ETO Condition
e
FHSC14
ATM
ATR
Depleted in sgUSP22
Log2FC
Rank in CIS-ETO Condition
f
NCI109B
ATM
ATR
Depleted in sgUSP22
Log2FC
Rank in CIS-ETO Condition
g
JHU-LX33
ATM
ATR
Enriched in USP22 add-back
Enriched in USP22 add-back
Log2FC
Rank in CIS-ETO Condition

Figure 3.7 (continued)

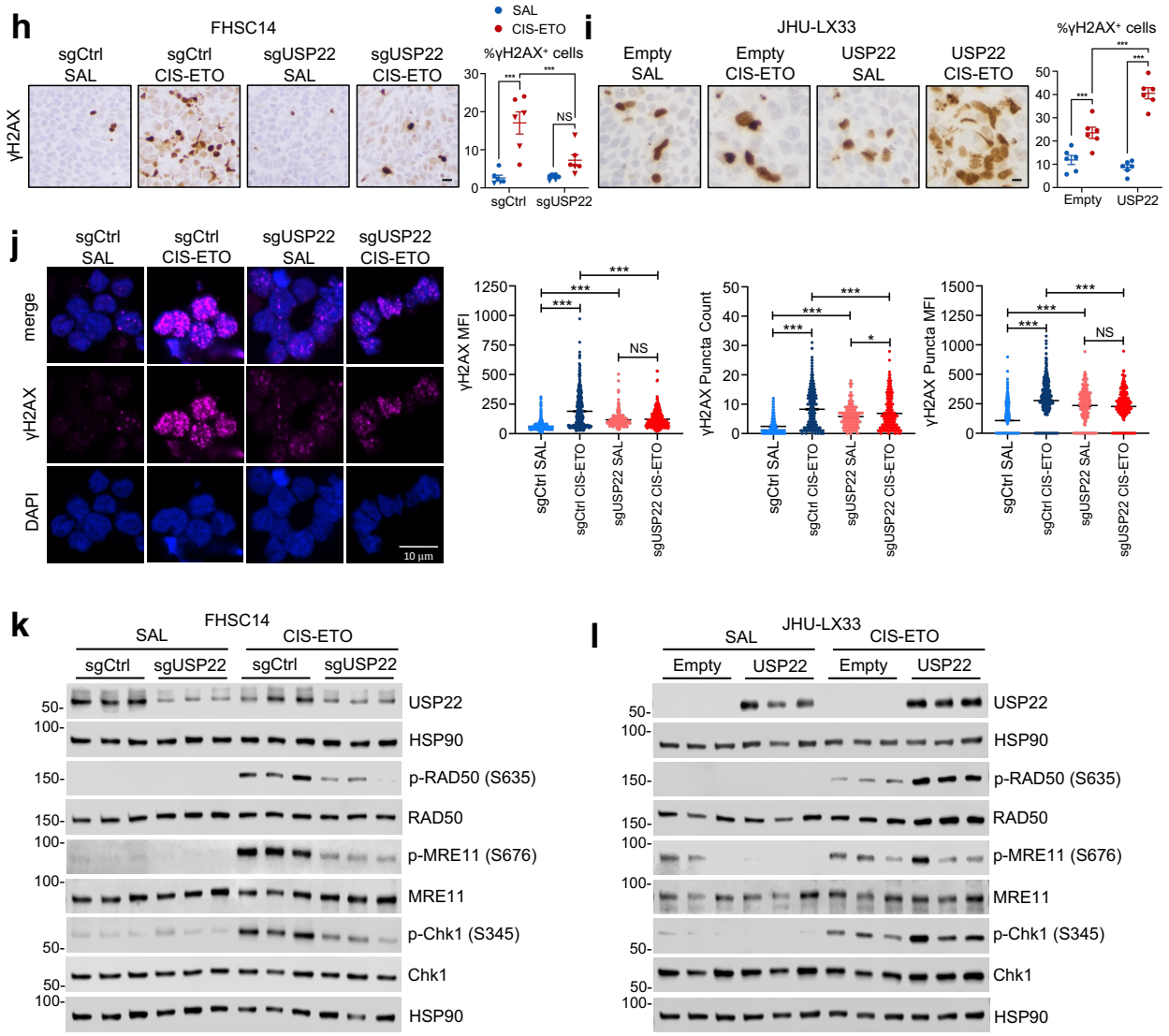

Figure 3.7: USP22 loss results in blunted cis-eto induced DNA damage signaling in SCLC PDX models

(**a**-**c**) Phospho-proteomics analysis of FHSC14 USP22-sg1/2 vs Ctrl-sg1/2 (n=2 tumors per sgRNA, n=4 tumors per condition), NCI109B sgUSP22 vs sgCtrl (n=3 tumors per condition), and JHU-LX33 USP22-PLVX vs Empty-PLVX models (n=4 tumors per condition) treated for 48 hours with cis-eto. Genes whose corresponding phospho-sites were enriched (Log2FC > 0.5, FDR < 0.05) or depleted (Log2FC < -0.5, FDR < 0.05) in

FHSC14 USP22-sg1/2 vs Ctrl-sg1/2 (a), NCI109B sgUSP22 vs sgCtrl (b), and JHU-LX33 USP22 add-back vs Empty vector control (c) treated for 48 hours with saline or cis-eto were independently queried for pathway enrichment using Enrichr. The Top 7 most significant pathways are displayed for each PDX model. For a-c, point size is scaled to FDR, and Volcano plots show all significant phospho-sites (depleted in FHSC14 and NCI109B sgUSP22 vs sgCtrl, enriched in JHU-LX33 USP22 vs Empty vector control) whose respective genes were in the WikiPathway DNA IR Damage and Cellular Response Via ATR pathway.

(**d**) PTM signature enrichment analysis (PTM-SEA) of phospho-proteomics data from FHSC14 USP22-sg1/2 vs Ctrl-sg1/2, NCI109B sgUSP22 vs sgCtrl, and JHU-LX33 USP22-PLVX vs Empty-PLVX models treated for 48 hours with cis-eto. Shown are significant kinase signatures (FDR < 0.05) in the cis-eto condition comparing control to USP22-perturbed for each model.

(**e**-**g**) PTM-SEA analysis ATM and ATR kinase signatures of phospho-proteomics data from FHSC14 USP22-sg1/2 vs Ctrl-sg1/2 (e), NCI109B sgUSP22 vs sgCtrl (f), and JHU-LX33 USP22-PLVX vs Empty-PLVX models treated for 48 hours with cis-eto.

(**h**-**i**) IHC analyses and representative images for γH2AX in 48 hour cis-eto treated FHSC14 Ctrl-sg1/2 and USP22-sg1/2 (h) or 10 day cis-eto treated JHU-LX33 Empty-PLVX and USP22-PLVX tumors (i) (n=6 tumors per treatment group). In **h**, triangles depict data from FHSC14 Ctrl-sg1 and USP22-sg1 while circles depict data from FHSC14 Ctrl-sg2 and USP22-sg2. Scale bar, 10 μm.

(**j**) Immunofluorescence quantification and representative images for γH2AX and DAPI for explanted cells from FHSC14 sgCtrl vs sgUSP22 tumors treated in vivo for 48 hours

with saline or cis-eto. Data are means ± SEM. Each circle is an individual cell, and all cells from each treatment condition (at least 188 cells compiled from n=3 tumor biological replicates were analyzed per treatment condition) are displayed. Scale bar, 10 μm.

(**k**-**l**) Western blot analysis of FHSC14 sgUSP22 vs sgCtrl tumors (k) or JHU-LX33 USP22-PLVX vs Empty-PLVX tumors (l).

Statistical analyses in **h**, **i** were performed by 2-way ANOVA with Fisher's LSD multiple comparisons test: *p < 0.05, **p < 0.01, ***p < 0.001. Statistical analyses in **j** were performed by unpaired student's two-tailed t-test: *p < 0.05, **p < 0.01, ***p < 0.001.

3.8 Treatment-dependent upregulation of glycolytic gene expression in response to USP22 loss: a targetable therapeutic vulnerability

Gene expression analyses of the USP22-deleted PDX models FHSC14 and NCI109B identified upregulation of glycolysis and hypoxia/HIF-1 pathways upon cis-eto treatment, and the absence of these responses in USP22-expressing JHU-LX33 tumors (Fig. 3.5a-e). GSEA further revealed enrichment of Glycolysis and Hypoxia Hallmark pathways in cis-eto treated FHSC14 sgUSP22 and JHU-LX33 empty vector control (USP22-null) tumors relative to USP22-expressing tumors (Fig. 3.8a). Pathway analysis on 77 common genes upregulated in cis-eto treated FHSC14 sgUSP22 and JHU-LX33 Empty-PLVX (USP22-null) models further revealed strong enrichment of Glycolysis and Hypoxia-related transcripts (Fig. 3.8b). Key genes upregulated upon USP22 loss in FHSC14 and JHU-LX33 models included the GLUT1 glucose transporter encoded by

SLC2A1, and hexokinase 2 encoded by HK2 encoded by HK2 that catalyzes the conversion of glucose to glucose-6-phosphate (Fig. 3.5c-e, Fig. 3.8b).

Given the role for glycolysis in driving platinum resistance in other tumor types[93, 94, 95, 96, 97, 98, 99], we determined whether inhibiting glycolysis would re-sensitize USP22 deleted SCLC tumors to cis-eto chemotherapy. To test this hypothesis, we generated FHSC14 sgCtrl and sgUSP22 tumors in parallel cohorts of NSG mice, then treated the cohorts with saline, cis-eto, the GLUT1 inhibitor BAY-876[100] or combinations over the 3 week time course (Fig. 3.8c). Both FHSC14 sgCtrl and sgUSP22 tumors grew at comparable rates after saline or BAY-876 treatment. Cis-eto treatment led to near complete ablation of saline control tumor, while sgUSP22-deleted tumors exhibited partial cis-eto resistance and continued to grow for 10 days with continued growth up to 20 days. In contrast, BAY-876 treatment restored cis-eto sensitivity to sgUSP22 tumors, where tumor volume significantly decreased with tumor growth rates closely mimicking sgCtrl control tumors treated with cis-eto alone (Fig. 3.8c). These results suggest that inhibiting glycolytic metabolism may represent a targetable vulnerability in USP22-deleted PDX models leading to the restoration of chemotherapeutic sensitivity.

The results from this study collectively show that loss of the USP22 deubiquitylase profoundly alters transcription and protein phosphorylation across PDX models of SCLC, with suppression of neuronal/neuroendocrine programs, activation of glycolytic programs and the suppression of DNA damage-driven protein phosphorylation responses leading to continued tumor growth through chemotherapy (Fig. 3.9).

Figure 3.8

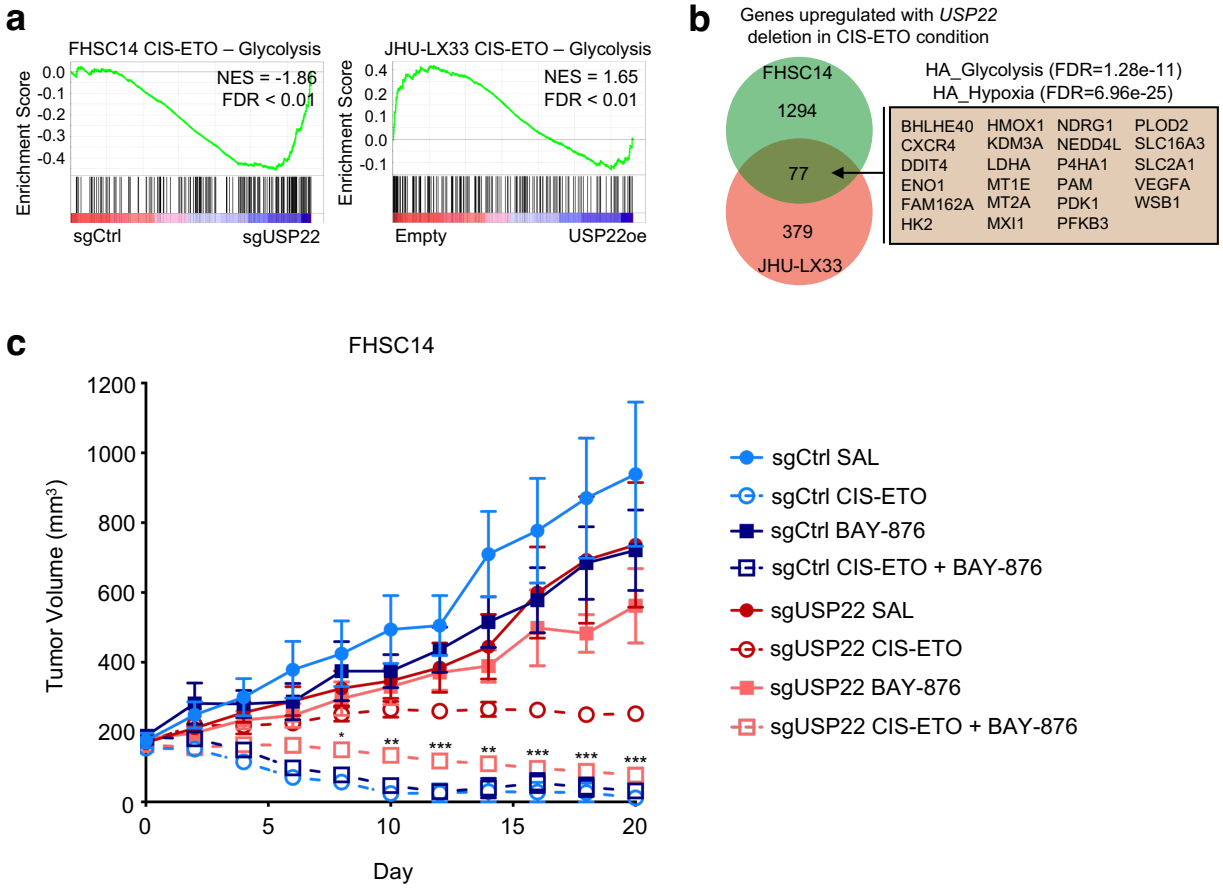

Figure 3.8: Glycolytic gene expression upregulated in response to cis-eto treatment in PDX models with USP22 deletion: a targetable therapeutic vulnerability

(**a**) GSEA analyses of Hallmark Glycolysis gene set in FHSC14 USP22-sg1/2 vs Ctrl-sg1/2 treated for 48 hours with cis-eto and JHU-LX33 USP22-PLVX vs Empty-PLVX tumors treated for 10 days with cis-eto.

(**b**) Enrichr pathway analysis of commonly upregulated genes with respect to *USP22* deletion in FHSC14 USP22-sg1/2 vs Ctrl-sg1/2 treated for 48 hours with cis-eto and JHU-LX33 USP22-PLVX vs Empty-PLVX tumors treated for 10 days with cis-eto.

(**c**) Tumor volume over time growth curves of isogenic FHSC14 sgCtrl and sgUSP22 models treated with saline, cis-eto, GLUT1 inhibitor BAY-876, or combination over a 20-day period. Data are means ± SEM; n=6 animals per treatment group. Statistical analyses in **c** were performed by 2-way ANOVA with Tukey's multiple comparisons test: adjusted *p < 0.05, **p < 0.01, ***p < 0.001, with asterisks comparing sgUSP22 CIS-ETO vs sgUSP22 CIS-ETO + BAY-876 treatment groups.

Figure 3.9

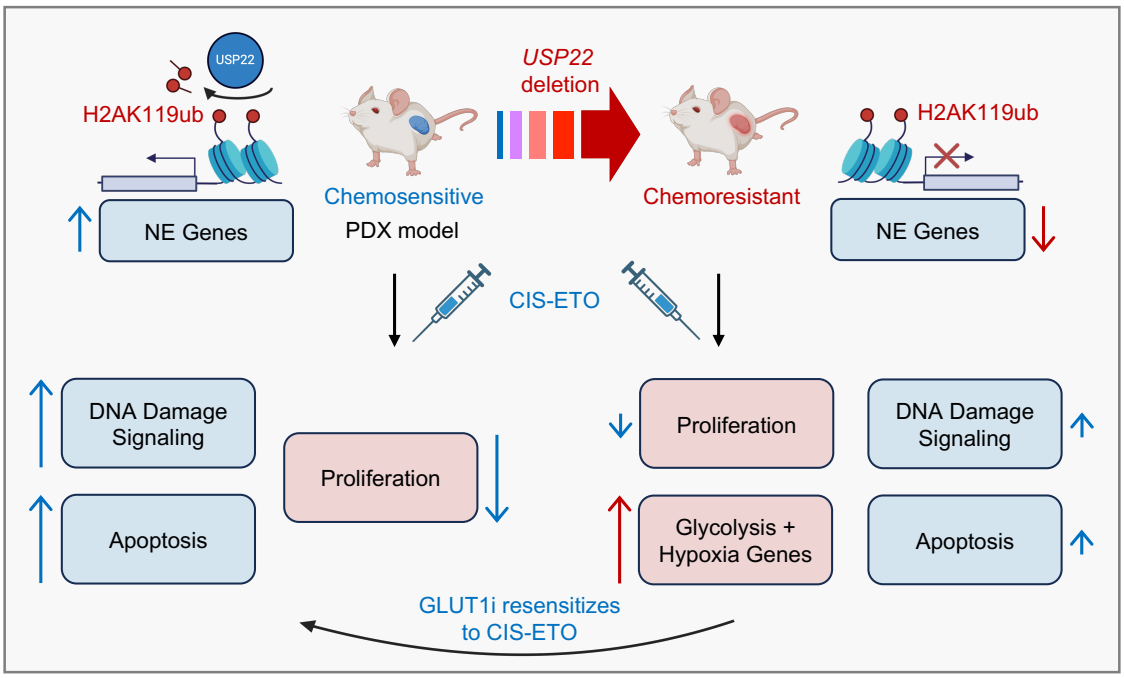

Figure 3.9: Schematic diagram showing the effects of USP22 loss on the cellular response to CIS-ETO treatment in SCLC PDX models

CHAPTER 4: Discussion

We have developed and used *in vivo* CRISPR-Cas9-based functional deletion screens in chemosensitive SCLC PDX models to identify genes that govern the response to the SCLC standard-of-care chemotherapy. The reproducible enrichment of sgRNAs targeting multiple members of the SAGA complex in cis-eto-treated SCLC PDX tumors led us to investigate the importance of the SAGA complex USP22 deubiquitylase in SCLC chemoresistance. We perturbed USP22 expression in three SCLC PDX models where deletion of *USP22* switched chemosensitive FHSC14 and NCI109B PDX models to become chemoresistant. In contrast, re-expressing USP22 in the USP22-null, chemoresistant JHU-LX33 PDX model partially re-sensitized the tumors to chemotherapy. Of note, a point mutant of USP22 that abolished deubiquitylase activity failed to re-sensitize USP22-null, chemoresistant JHU-LX33 PDX tumors.

Subsequent functional analyses of USP22 further supported the notion that USP22 deubiquitylation activity within SAGA is an important determinant of SCLC chemotherapeutic response in major transcriptional subsets of SCLC represented by ASCL1-active (FHSC14) and NEUROD1-active (NCI109B and JHU-LX33) PDX models. Other mouse models support the role of USP22 tumor suppressor activity in different tumor types, where deletion of *Usp22* sensitized models of colon cancer[101] and myeloid leukemia[102] with accelerated tumorigenesis. While we did not find evidence of a growth advantage in the absence of chemotherapy upon USP22 deletion, the observation of a homozygous USP22 inactivating mutation in the PDX model JHU-LX33 could have tumor suppressor function even in the absence of chemotherapy. More detailed

genomic analyses of SCLC post-treatment patient samples will be important to determine if mutations or deletion of *USP22* or other SAGA components are enriched in chemotherapy-relapsed SCLC.

Our results provide clues to the mechanisms by which USP22 as a SAGA complex deubiquitylase modulates gene and protein expression, tumor growth and therapeutic response. SAGA is known to have modular activities that regulate gene activation and transcription. For example, USP22 removes ubiquitin at the histone site H2A-K119[52], a repressive mark deposited by PRC1 that is often co-localized with H3K27me3 to promote gene silencing[83, 84, 85, 86] USP22 can also remove ubiquitin from H2B-K120[59] to promote transcription elongation [53, 62]. In addition to PDX model NCI109B, SAGA complex members including *USP22* were top hits in functional screens in the ASCL1-high expressing model FHSC14[48]. Thus, USP22 appears to be able to contribute to chemoresistance across different SCLC subtypes.

Several consequences of *USP22* deletion in SCLC PDX models may contribute to an impaired response to chemotherapy. For example, deleting *USP22* in FHSC14 and NCI109B PDX models suppressed cis-eto-induced apoptosis, an effect that could be reversed by re-expressing USP22 in the USP22-null JHU-LX33 PDX model. *USP22* loss also reduced the transcriptional upregulation of DDR repair genes in response to chemotherapy and the phosphorylation of canonical ATM/ATR kinase targets. Activation of ATM and ATR can induce cell death through p53-dependent and p53-independent

mechanisms: suppression of these downstream pathways upon USP22 loss may reduce cis-eto-induced tumor cell death as we observed in treated PDX models.

SCLC exhibit differing levels of activation of neuroendocrine transcriptional programs. In murine SCLC GEMM models and cell lines, low-neuroendocrine cells generated through constitutive NOTCH activation were less sensitive to platinum chemotherapy relative to neuroendocrine cells[38]. In circulating tumor cell-derived xenograft models of SCLC, development of platinum resistance correlated with a decrease in ASCL1-expressing cells[36]. Further, studies of tumor samples taken from relapsed SCLC patients show reduced ASCL1 expression and enrichment of ASCL1-low expression subtypes relative to treatment-naïve samples[23, 29]. In our study, RNA and protein levels for ASCL1 and INSM1, markers of neuroendocrine differentiation were reduced by USP22 deletion in FHSC14, and ASCL1-target gene sets were depleted in USP22-deleted FHSC14 and JHU-LX33 models. Reduced expression of neuronal genes at the transcriptomic and proteomic level was associated with USP22 loss in one ASCL1-high PDX model FHSC14 and two NEUROD1-high models NCI109B and JHU-LX33. A mechanistic explanation for these effects is provided by the observation that *USP22* deletion increased H2A-K119ub levels in association with increased H3K27me3 deposition in gene bodies, leading to the decreased expression of neuronal and neuroendocrine differentiation programs. One additional intriguing finding was increased expression of glycolysis and hypoxia-related genes, where activation of these metabolic programs has been linked to platinum resistance in multiple tumor types[93, 94, 95, 96, 97, 98, 99]. Prior work had revealed that inhibition of glycolysis with 2-deoxy-D-glycose in

combination cisplatin could overcame platinum resistance in head and neck cancer cells[96], gastric cancer cells[94], and neuroblastoma cells[103]. We found that activation of glycolytic programs at the transcriptional level in chemoresistant SCLC USP22-null models was a targetable vulnerability, where inhibition of GLUT1 re-sensitized tumors to cis-eto treatment. Further work to identify the precise mechanisms by which USP22 regulates glycolysis will be important to further develop this potential new therapeutic opportunity.

Our results identify the SAGA complex USP22 deubiquitylase as an important determinant of chemotherapy responsiveness in SCLC. Our global proteomic, phospho-proteomic, transcriptomic and histone modification analyses further reveal multiple histone and non-histone targets for the USP22 deubiquitylase, and detail pleiotropic consequences that follow USP22 deletion. These include upregulation of interferon and glycolytic pathways, suppression of neuronal and ASCL1 targets, and suppressed DNA damage responses and apoptosis. We found further glycolytic program activation was functionally important and may provide a therapeutic opportunity in SCLC: GLUT1 inhibition was able to resensitize USP22-deleted SCLC PDX tumors to cis-eto chemotherapy.

Our results thus provide a rich data set and useful PDX models for further investigating the functional roles and mechanistic pathways that regulate chemotherapeutic response in SCLC. Furthermore, our results provide the first evidence for loss of USP22 function conferring resistance to chemotherapy in any cancer type. Extending beyond the

current studies, our in vivo functional genetic screening platform in PDX models can be used by others as a powerful strategy to elucidate novel determinants of drug resistance across multiple tumor types.

CHAPTER 5: Materials and Methods

Mice

Male and female NOD *scid* gamma mice (NSG, JAX strain 005557) immunodeficient mice were obtained from Translational Research Model Services at Fred Hutch Cancer Center (FHCC). All procedures were approved by the Institutional Animal Care and Use Committee (IUCUC) at FHCC (protocol #50783).

Patient Derived Xenograft (PDX) models

The following PDX models were used in this study: FHSC14, NCI109B, and JHU-LX33. NCI109B was obtained from the NCI Patient-Derived Models Repository (distribution lot 594431-109-B). JHU-LX33 was provided by Dr. Charles Rudin (Memorial Sloan Kettering). All PDX models were propagated by mixing cells with Matrigel at a 1:1 v/v ratio and injected subcutaneously in the flanks of NSG mice. To generate single-gene perturbed PDX models, tumors were dissociated into single-cell suspensions, digested in 1 mg/mL collagenase type IV at 37°C for 30 minutes, cleared of red blood cells using ACK Lysing Buffer (ThermoFisher, A1049201), and infected ex vivo with concentrated lentivirus containing lentiCRISPRv2-ZsGreen vectors with Ctrl-sg1, Ctrl-sg2, USP22-sg1, or USP22-sg2 gRNAs (see Table SX for sgRNA sequences) or lentivirus containing Empty, USP22, or USP22-C185S PLVX ZsGreen vectors in the presence of

4 μg/mL polybrene. PDX models were cultured in DMEM-F12 (Gibco, 11320-033) with 10% FBS, 1% Pen-Strep (Gibco, 15140-122), and 1% Insulin-Transferring Selenium (Gibco, 41400-045). No more than 18 hours after infection, cells were washed and injected into NSG mice flanks. Once regrown, tumors were again dissociated into single-cell suspension and successfully transduced ZsGreen^{+} cells were purified via FACS and re-implanted into mice. *USP22* deletion in FHSC14, NCI109B or USP22 overexpression in JHU-LX33 was confirmed by western blot analysis.

Drug treatments

For mouse drug treatment experiments, flank tumor dimensions were measured with calipers daily or every other day and tumor volume was calculated by volume = major axis × (minor axis^2)/2104. Saline (VetOne, 510224) was administered by intraperitoneal (IP) injection once a week. Cisplatin (5 mg/kg, Millipore Sigma, 479306) + etoposide (10 mg/kg, Millipore Sigma, E1383) treatments were administered by IP injections on a weekly cycle with the following schedule: Day 1 = cisplatin + etoposide, Day 2 = etoposide, Day 3 = etoposide, Days 4-7 = drug holiday. BAY-876 (3 mg/kg, MedChemExpress, HY-100017) was administered by oral gavage daily.

Cell lines

293TN producer cells (System Bioscience, LV900A-1) were used for lentivirus production. Cells were cultured in DMEM containing 10% FBS and 1% Pen-Strep (DMEM-10) a humidified incubator at 37°C, 95% air, and 5% CO_2.

Lentivirus production and concentration

To produce concentrated lentivirus, 293TN cells were seeded onto 0.01% poly-L-lysine (Sigma Aldrich, P4832) coated 500 cm^2 plates (Corning, 431111) at a density of $15x10^6$ cells per plate. A transfection mix containing 137.5 µg transfer vector, 137.5 µg psPAX2 (Addgene, 12260), and 90 µg pMD2.G (Addgene, 12259), 1.14 mL 2M $CaCl_2$ (Quality Biological, 351-130-721), and 4.75 mL 2X HBS buffer in 90 mL DMEM-10 was applied to cells once reaching 75% confluency. 16 hours post-transfection, media was changed to Viral Producing Media (VPM): DMEM, 1% FBS, 1% Pen-Strep, 1% 100 mM Sodium Pyruvate (Gibco, 11360-070), 1% Sodium Bicarbonate 7.5% solution (Corning, 25-035-CI), 1% 0.5 M Sodium Butyrate solution, and 2 µg/mL insulin human recombinant zinc (Gibco 12585-014). 64 hours post-transfection, lentivirus-containing supernatant was filtered through 0.45 µm Millipore low-protein binding filter units (Millipore Sigma, S2HVU02RE) and concentrated via centrifugation at 3300 x g for 30-45 minutes at 4°C using Millipore Centricon 70 Plus cartridges (ThermoFisher, UFC710008).

Western blot analysis

Protein was extracted from snap-frozen tumor tissue by mechanical disruption and homogenization using the Agile Tissue Grinder (Thomas Scientific, ACT-AG3080) in RIPA buffer (Cell Signaling, 9806S) supplemented with Halt Protease and Phosphatase Inhibitor Cocktail (ThermoFisher, 78444). Protein lysates were cleared by centrifugation and quantification was performed using Pierce BCA Protein Assay Kit (ThermoFisher, 23227). Western blotting was performed by loading 10 µg protein western mix in 4-20% Mini-PROTEAN TGX Precast Protein Gels (BioRad, 4561096). Protein was transferred

onto nitrocellulose membranes (GE Healthcare Life Sciences, 10600002), blocked in 5% NFDM in TBS with 0.1% Tween-20 (Millipore Sigma, 655206), and incubated at 4°C overnight in primary antibody. The next morning, membranes were incubated in anti-rabbit IgG HRP-linked (Cell Signaling, 7074) or anti-mouse IgG HRP-linked (Cell Signaling, 7076) and imaged on a LI-COR Odyssey Fc. The following antibodies were used for western blotting: anti-USP22 (Novus, NBP1-49644), anti-NKX-2 (Proteintech, 13013-1-AP), anti-ASCL1 (BD Biosciences, 556604), anti-INSM1 (Santa Cruz, sc-271408), anti-phospho-RAD50 S635 (Cell Signaling, 14223), anti-RAD50 (Cell Signaling, 3427), anti-phospho-MRE11 S676 (Cell Signaling, 4859), anti-MRE11 (Cell Signaling, 4847), anti-phospho-Chk1 S345 (Cell Signaling, 2348), anti-Chk1 (Cell Signaling, 2360), anti-HSP90 (Santa Cruz, sc-13119), anti-GAPDH (Santi Cruz, sc-32233), anti-alpha-Tubulin (Cell Signaling, 3873).

Immunohistochemistry (IHC)

PDX tumors were fixed in 10% neutral-buffered formalin for 72 hours and sectioned at 4 μM thickness into paraffin blocks and slides. Slides were deparaffinized in xylene and tissue sections were hydrated in an ethanol-water series. Antigen retrieval was performed in pre-heated citrate buffer (10 mM citric acid, 0.1% Tween-20, pH 6.0) and tissue sections were blocked first in 3.5% hydrogen peroxide and 10% methanol and then in 5% goat serum. Tissue sections incubated in primary antibody overnight at 4°C in a humidified chamber. The next morning, tissue sections were incubated in biotinylated goat anti-rabbit IgG secondary antibody (Vector Laboratories, BP-9100-50) and then in VectaStain ABC kit (Vector Laboratories, PK-4000) reagents. Tissue

sections were developed using DAB Substrate Kit Peroxidase (Vector Laboratories, SK-4100) and subjected to dehydration, clearing, and mounting. At least two images were captured per tissue section using a Nikon Ni-UI microscope and quantified manually at 400X magnification using ImageJ (Fiji). The following antibodies were used for IHC: 1:200 anti-phospho-histone H3 S10 (Millipore, 06-570), 1:100 anti-cleaved caspase-3 N175 (Cell Signaling, 9661), and 1:100 anti-phospho-histone H2A.X S139 (Cell Signaling, 9718).

Immunofluorescence

Following 48 hours of saline or cis-eto treatment, PDX tumors were dissociated into single-cell suspensions and incubated on 0.01% poly-L-lysine coated coverslips for 4 hours at 37°C. Cells adhered to coverslips were washed, fixed in 4% paraformaldehyde for 10 minutes at room temperature, permeabilized with 0.2% Triton X-100 for 10 minutes, and blocked with 1% BSA with 22.52 mg/mL glycine for 30 minutes. Cells were co-incubated with 1:200 anti-phospho-histone H2A.X S139 (Cell Signaling, 80312) and 1:200 53BP1 (ThermoFisher, PA1-16565) overnight at 4°C in humidified chamber. Cells were washed and co-incubated with 1:1000 anti-mouse AlexaFluor 647 (ThermoFisher, A-31571) and 1:1000 anti-rabbit AlexaFluor 568 (ThermoFisher, A-11011) for 1 hour at room temperature. Cells were washed and counterstained with 1 µg/mL DAPI (Invitrogen, 62248) for 5 minutes at room temperature. Cells on coverslips were washed a final time, mounted onto slides with Fluoromount-G (Invitrogen, 00-4958-02), and sealed with Prolong Coverslip Sealant (Invitrogen, P56128). Slides were imaged using a Andor Spinning Disk Dragonfly confocal microscope at 630X magnification under oil

immersion. At least 5-10 images (single z-plane images) were captured per slide depending on cell density. Images were analyzed using automated Image J software designed to quantify γH2AX cell MFI, γH2AX puncta count, and γH2AX MFI within puncta on a per basis in nuclei (DAPI). γH2AX raw signal was pseudocolored to magenta for visualization.

CRISPR knockout screening in vivo

Tumor processing, library transduction, and drug treatment

PDX tumors were dissociated into single-cell suspensions and transduced with concentrated lentivirus containing a custom focused 2520 sgRNA CRISPR knockout library or the Human CRISPR Knockout Pooled Library (GeCKO v2)[47] in the presence of 4 μg/mL polybrene. Eighteen hours after transduction, a subset of cells was saved as an initial timepoint (PO) comparator while the rest were washed and injected subcutaneously in both flanks of NSG mice at $1x10^6$ cells per flank. When tumors reached 300-350 mm^3, mice were assigned to SAL or CIS-ETO treatment groups, where SAL tumors were immediately harvested, and CIS-ETO tumors were treated with 2 weekly cycles of cis-eto for the NCI109B PDX model until tumor ablation or 3 weekly cycles of cis-eto for FHSC14 and harvested upon regrowth to initial pre-treatment size. Harvested tumors were snap-frozen using dry ice and stored at -80°C.

CRISPRko screen library preparation and sequencing

Genomic DNA was isolated from snap-frozen PDX tumors as previously described[46]. CRISPR libraries were prepared as previously described[66] and pilot whole genome

screen[44]) and were sequenced on an Illumina HiSeq2500 high throughput flow cell at 11.5 pM with 57 base pair single-end reads.

RNA-seq

RNA was isolated from snap-frozen PDX tumors by mechanical dissociation and homogenization in TRIzol reagent (ThermoFisher, 15596026) and mRNA was enriched using the NEBNext Poly (A) mRNA Magnetic Isolation Module (New England Biolabs, E7490) kit. RNA libraries were prepared using the NEBNext Ultra II RNA Library Prep Kit for Illumina (New England BioLabs, E7770) and sequenced on an Illumina NextSeq P3 with 50 base pair single-end reads. Reads were aligned to human genome assembly hg38 and GENCODE gene annotation v38 as well as mouse genome assembly mm10 and GENCODE gene annotation vM23 using STAR v2.7.7a[105] with 2-pass mapping. Reads of mouse origin were removed using R package XenofilteR[106]. Gene expression quantification was performed using FeatureCounts in Subread 2.0.0 and genes with low expression were excluded using edgeR function filterByExpr with min.count = 10 and min.total.count = 15. Following TMM normalization[107], differentially expressed genes between sample groups were identified using Bioconductor package edgeR 3.34.1[108] and were subjected to significance testing using GLM LRT method and Benjamini-Hochberg p-value correction. Up- or downregulated protein-coding genes with FDR < 0.05 were queried for pathway enrichment analysis using Enrichr[69, 70] (see Supplemental Tables 8-11 for all significantly enriched or depleted pathways). Gene Set Enrichment Analysis (GSEA)[76] was performed using version 4.3.3. The ASCL1 Targets

gene set comprised a list of 141 ASCL1 target genes that were shared between mouse and human chromatin occupancy analyses[21].

CUT&Tag

Viable cells from dissociated FHSC14 PDX tumors treated for 48 hours with cis-eto or vehicle were enriched by FACS. 50,000 cells per reaction were processed for CUT&Tag[87] and sequenced on an Illumina NextSeq P3 with 50/50 base pair paired-end reads. The following antibodies were used for CUT&Tag: ubiquityl-histone H2A K119 (Cell Signaling, 8240), tri-methyl-histone H3 K27 (Cell Signaling, 9733), normal Rabbit IgG (Cell Signaling, 2729). The nf-core cutandrun pipeline[109] was followed for quality trimming using TrimGalore and alignment to GRCh38 reference genome using Bowtie2. MACS2[110, 111] was used to call broad peaks with and without IgG controls and an intersection of the two was considered the final peak set for each sample. For quality control, a combination of Samtools[112] and the bedtools suite[113] was used to calculate fragment length and number of reads in peaks. Peak annotation generated using Homer[114] and Gencode v38 annotations. Read counts for each peak were generated using Subread featureCounts[115], tabulated and passed to Bioconductor edgeR for differential peaks (FDR < 0.05) expressed between groups of interest (Supplemental Table 12). Heatmaps illustrating significantly up and down-regulated peaks were generated using deepTools[116]. Peak gene tracks for were viewed using Integrative Genomics Viewer (IGV) version 2.18.4[117].

Global Proteomics and phospho-proteomics mass spectrometry and data analysis.

Protein lysate preparation

Frozen tumors (mean mass = 117 mg, range = 78-135 mg) were cryo-pulverized with a Covaris cryoPREP CP02 Impactor, and protein was solubilized in 1 mL urea lysis buffer (6 M urea, 25 mM Tris, pH 8.0, 1 mM EDTA, 1 mM EGTA, 1% Sigma Phosphatase Cocktail 2, 1% Sigma Phosphatase Cocktail 3, and 1% Sigma Protease Inhibitor Cocktail). Samples were vortexed at maximum speed for 15 seconds, and lysates were transferred to 1.7 mL screw-top microfuge tubes. Samples were subjected to 5 minutes of sonication using Qsonica Q800R3 sonicator. Samples were then cleared by centrifugation (20,000 RCR, 10 minutes at 4°C) and transferred to cryovials (NUNC, Cat. #363401) for storage in the vapor phase in an LN2 tank. Protein concentrations of the clarified lysates were measured by Micro BCA assay (ThermoFisher Scientific, Cat. #23235).

Protein digestion

Lysates were diluted to 2.0 mg/mL using lysis buffer and 125 µL of lysate (250 µg of protein) was reduced with the addition of 8 µL of 500 mM TCEP (ThermoFisher) for 30 minutes at 37°C with shaking, followed by alkylation with the addition of 18 µL of 500 mM iodoacetamide (Sigma) in the dark at room temperature for 30 minutes. Lysates were then diluted with 0.85 mL 200mM Tris (pH 8.0). Lys-C (Wako) was dissolved in 25 mM Tris (pH 8.0) at 400 µg/mL and added to lysates at 1:50 (enzyme:protein) ratio by mass and incubated for 2 hours at 37°C with shaking. Trypsin was then added at a 1:100 trypsin:protein ratio and incubated overnight at 37°C with shaking. After 16 hours, the

reaction was quenched with formic acid to a final concentration 1% by volume. Samples were desalted using Oasis HLB 96-well plates (Waters) and a positive pressure manifold (Waters). The plate wells were washed with 3 x 400 µL of 50% MeCN/0.1% FA and then equilibrated with 4 x 400 µL of 0.1% FA. The digests were applied to the wells, then washed with 4 x 400 µL 0.1% FA before being eluted drop by drop with 3 x 400 µL of 50% MeCN/0.1% FA. The eluates were lyophilized, followed by storage at -80°C until use.

Isobaric labeling

Individual trypsin digestion samples were labeled with the TMTpro™ 16plex isobaric label reagent set (TMT; ThermoFisher Scientific, Cat. #A44520, Lot #YA357799). Desalted peptides were resuspended in 500 µL of 100 mM HEPES (pH 8.5). TMT reagents were resuspended in 200 µL MeCN and 100 µL was transferred to the peptide sample. Samples were incubated at room temperature for 1 hour with mixing. Labeling reactions were quenched by the addition of 50µL of hydroxylamine (Sigma, Cat. # 438227) diluted to 5% in H2O and incubated for 15 minutes at room temperature with mixing. The independent labeling reactions were then pooled together and lyophilized. The labeled peptides were desalted as above and then lyophilized and stored at -80°C.

Basic (high pH) reverse phase (RP) liquid chromatography

The labeled, pooled and desalted tryptic digests were fractionated by high-pH reverse phase (RP) liquid chromatography on an LC system consisting of an Agilent 1200 HPLC (Agilent, Santa Clara, CA) with mobile phases of 5 mM NH_4HCO_3, pH 10 (A) and 5 mM NH_4HCO_3 in 90% MeCN, pH 10 (B). The peptides were separated by a 4.6 mm x 250 mm

Zorbax Extend- C18, 3.5 µm, column (Agilent Cat. #770953-902) over 96 minutes at a flow rate of 1.0 mL/min by the following timetable: hold 0% B for 9 minutes, gradient from 0 to 10% B for 4 minutes, 10 to 28.5% B for 50 minutes, 28.5 to 34% B for 5.5 minutes, 34 to 60% B for 13 minutes, hold at 60% B for 8.5 minutes, 60 to 0% B for 1 minute, re-equilibrate at 0% B for 5 minutes. 1-minute fractions were collected from 0 – 96 minutes by the shortest path by row in a 1 mL deep well plate (Thermo Cat. #95040450). The high pH RP fractions were concatenated into 24 samples by every other plate column (e.g.: sample 1 contained fractions from wells A1, C1, E1, etc.). 95% of every 12th fraction of the 24 samples was combined (1,13; 2,14; ...) to generate 12 samples, which were dried down and stored at −80°C prior to phosphopeptide enrichment. The remaining 5% was dried down, re-suspended in 0.1% FA, 3% MeCN and frozen at -80°C until analysis.

Immobilized metal affinity chromatography (IMAC)

For discovery LC-MS/MS analysis, fractionated samples were enriched for phosphopeptides by immobilized metal affinity chromatography (IMAC). Enrichment was performed using Ni-NTA-agarose beads (Qiagen, Cat. #36113) stripped with EDTA and incubated in a 10 mM FeCl3 solution to prepare Fe3+-NTA-agarose beads. Peptide samples were reconstituted in 200 µL of 0.1% TFA in 80% MeCN and incubated for 30 minutes with 100µL of the 5% bead suspension, mixing at 1400 rpm at room temperature. After incubation, the beads were washed 3 times with 300µL of 0.1% TFA in 80% MeCN. Phosphorylated peptides were eluted from the beads using 200 µL of 70% MeCN, 1% ammonium hydroxide for 1 minute with agitation at room temperature (do not exceed 5min). Samples were transferred into a fresh tube containing 60 µL of 10% FA, dried

down and re-suspended in 0.1% FA, 3% MeCN. The samples were frozen at -80°C until analysis.

Nano-liquid chromatography-tandem mass spectrometry

Fractionated samples (both global proteome samples and phosphopeptide-enriched samples were analyzed by LC-MS/MS on an Easy-nLC 1000 (Thermo Scientific) coupled to an Orbitrap™ Eclipse™ Tribrid™ mass spectrometer (Thermo Scientific) operated in positive ion mode with a FAIMS Pro™ Interface. The LC system consisted of a fused-silica nanospray needle (PicoTip™ emitter, 50 µm ID x 27 cm, New Objective) packed in-house with ReproSil-Pur 120 C18-AQ (Dr. Maisch) and a trap (IntegraFrit™ Capillary, 100 µm ID x 2 cm, New Objective) packed in-house with Magic C18-AQ with mobile phases of 0.1% FA in water (A) and 0.1% FA in 80% MeCN (B). The peptide sample was diluted in 20 µL of 0.1% FA, 2% MeCN and 8.5 µL was loaded onto the column and separated over 150 minutes at a flow rate of 300 nL/min with a gradient from 4 to 9% B for 2 min, 9 to 25% B for 80 min, 25 to 44% B for 60 min, 44 to 63% B for 8 min, hold 63% B for 1 min, 63 to 90% B for 11 min, hold 90% B for 1 min. A spray voltage of 2300 V was applied to the nanospray tip. FAIMS MS/MS analysis occurred over a 3 second cycle time consisting of 1 full scan MS from 400-1600 m/z at resolution 120,000 followed by data dependent MS/MS scans cycling through FAIMS CV of -40, -60 and -80 using HCD activation at resolution 50,000 with 38% normalized collision energy of the most abundant ions. Selected ions were dynamically excluded for 60 seconds after a repeat count of 1.

Shotgun mass spectrometry data analysis

Raw MS/MS spectra from the analysis were searched twice using MSFragger v3.8[118] first against the reviewed Human Universal Protein Resource (UniProt) sequence database downloaded on 11/1/2023 and then against a database combining both Human and Mouse UniProt sequence databases (both downloaded on 11/1/2023). Both databases were appended with reverse sequences and common contaminants. MS and MS/MS mass calibration, MS/MS spectral deisotoping, and parameter optimization were enabled[119]. For the analysis of whole proteome data, cysteine carbamidomethylation (+57.0215), TMT labeling (+304.20715) of lysine and the peptide N-terminal were specified as fixed modifications and methionine oxidation (+15.9949) was specified as a variable modification. For phosphopeptide enriched data, phosphorylation (+79.9663) of serine, threonine, and tyrosine residues also included were specified as a variable modification. The search was restricted to tryptic peptides, allowing up to two missed cleavage sites. The post-processing of the search results was done using the Philosopher toolkit version v5.0.0. MSFragger output files (in pepXML format) were processed using PeptideProphet[120] (with the high–mass accuracy binning and semi-parametric mixture modeling options) to compute the posterior probability of correct identification for each peptide to spectrum match (PSM). In the phosphopeptide-enriched dataset, PeptideProphet files were additionally processed using PTMProphet[121] to localize the phosphorylation sites. The resulting pepXML files from PeptideProphet (or PTMProphet) were then processed together to assemble peptides into proteins (protein inference) and to create a combined file (in protXML format) of high confidence protein groups. The combined protXML file were further processed using the Philosopher filter command as

follows. Each peptide was assigned either as a unique peptide to a particular protein group or set as a razor peptide to a single protein group with the most peptide evidence. The protein groups assembled by ProteinProphet[122] were filtered to 1% protein-level False Discovery Rate (FDR) using the best peptide approach (allowing both unique and razor peptides) and applying the picked FDR target-decoy strategy. The PSM lists were filtered using a sequential FDR strategy, retaining only those PSMs with PeptideProphet probability of 0.9 or higher (which in these data corresponded to less than 1% PSM-level FDR) and mapped to proteins that also passed the global 1% protein-level FDR filter. For each PSM that passed these filters, the corresponding precursor ion MS1 intensity was extracted using the Philosopher label-free quantification module, using 10 ppm mass tolerance and 0.4 min retention time window for extracted ion chromatogram peak tracing. For all PSMs corresponding to a TMT-labeled peptide, 16 TMT reporter ion intensities were extracted from the MS/MS scans (using 0.002 Da window). The precursor ion purity scores were calculated using the intensity of the sequenced precursor ion and that of other interfering ions observed in MS1 data (within a 0.7 Da isolation window). All supporting information for each PSM, including the accession numbers and names of the protein/gene selected based on the protein inference approach with razor peptide assignment and quantification information (MS1 precursor-ion intensity and the TMT reporter ion intensities), was summarized in the output PSM.tsv files. To generate summary reports on different levels (gene, peptide, and protein for global and phosphopeptide enriched data; additional modification site report for phosphopeptide data), all PSM.tsv files were processed together using TMT-Integrator[123] using default parameters described previously[124]. In generating the site-level reports (phosphopeptide-

enriched data), sites with PTMProphet computed localization probability equal or greater than 0.75 were considered as confidently localized.

STATISTICAL ANALYSIS

All statistical tests and number of biological replicates per condition are included in the figure legends. Data are presented as mean ± standard error of measure (SEM) or median ± interquartile range (IQ) where indicated. Statistical analyses were performed using GraphPad Prism software. Statistical tests were performed by unpaired two-tail student's t test or 2-way ANOVA followed by Tukey's multiple comparison test or uncorrected Fisher's LSD multiple comparisons test when indicated.

CRISPRko Screen Analyses

Differential abundance analysis between treatment groups and the P0 group in pilot and focused CRISPR knockout screens was performed using MAGeCK[51] version 0.5.7 (pilot genome scale screen) and version 0.5.9 (focused library screen). Samples underwent pooling to increase the number of gRNAs present and overall gRNA coverage per sample. In the pilot genome scale screen, DNA from 11 cis-eto- and 9 saline-treated tumors were pooled into a single DNA pool per group prior to library preparation and sequencing. In the focused library screen, individual tumors underwent computational pooling by randomly assigned tumors to pools and tumors for each computational pool were treated as technical replicates. gRNA counts were median normalized after pooling. Gene-level robust rank aggregation (RRA) scores were generated by

MAGeCK. Gene-level and sgRNA-level p-values were corrected using Benjamini-Hochberg FDR procedure.

Global proteomics and phospho-proteomics analyses

The proteins and phospho-sites that were quantified in at least 50% of samples were included in the analysis for each PDX model. The tandem mass tags (TMT) values were median-normalized and log2-transformed before analysis. Missing values were imputed using the DreamAI algorithm, which is an ensemble of six commonly used imputation methods that was optimized specifically for proteomics datasets[125]. Log2-transformed relative abundances were compared between treatment groups (cis-eto vs saline) and genotype (sgCtrl vs sgUSP22 for FHSC14 and NCI109B tumors and Empty-PLVX vs USP22-PLVX for JHU-LX33 tumors) using linear regression models with treatment group, genotype, and treatment x genotype interaction terms. Multiple testing was accounted for using the Benjamini-Hochberg FDR procedure.

PTM signature enrichment analysis

Post-translational modification signature enrichment analysis (PTM-SEA) was conducted using ssGSEA2.0 as implemented in the ssGSEA2 R package[89]. The PTMsigDB version 2.0.0 database[89] was used to map phospho-sites to kinases. The relative abundances of each phosphorylated protein were compared between cis-eto and saline groups as described in the Phospho-proteomics Analysis section, the results of which were used for PTM-SEA calculations. Specifically, the ranking metric for each phospho-site was calculated as $-10\log_{10}$(p-value) multiplied by the sign of the log2-fold

change estimate. Kinases in the PTMsigDB under the KINASE-PSP category with at least 5 phospho-sites that overlapped with the phospho-proteomics results were included in the analysis. Kinase-level enrichment was quantified using a normalized enrichment score (NES) and the corresponding p-value was calculated using permutation tests (1,000 permutations). Kinase-level p-values were adjusted using the Benjamini-Hochberg FDR procedure. The specific parameters used for the ssGSEA2 package were: statistic = “area.under.RES”, correl.type = “rank”, sample.norm.type = “none”, weight = 0.75, nperm = 1000, and min.overlap = 5.

REFERENCES

1. Sen T*, et al.* Pulmonary neuroendocrine neoplasms: the molecular landscape, therapeutic challenges, and diagnosis and management strategies. *Lancet Oncol* **26**, e13-e33 (2025).

2. Redin E, Quintanal-Villalonga A, Rudin CM. Small cell lung cancer profiling: an updated synthesis of subtypes, vulnerabilities, and plasticity. *Trends Cancer* **10**, 935-946 (2024).

3. Rudin CM, Brambilla E, Faivre-Finn C, Sage J. Small-cell lung cancer. *Nat Rev Dis Primers* **7**, 3 (2021).

4. Wang Q*, et al.* SCLC: Epidemiology, Risk Factors, Genetic Susceptibility, Molecular Pathology, Screening, and Early Detection. *J Thorac Oncol* **18**, 31-46 (2023).

5. Sabari JK, Lok BH, Laird JH, Poirier JT, Rudin CM. Unravelling the biology of SCLC: implications for therapy. *Nat Rev Clin Oncol* **14**, 549-561 (2017).

6. Rudin CM*, et al.* Molecular subtypes of small cell lung cancer: a synthesis of human and mouse model data. *Nat Rev Cancer* **19**, 289-297 (2019).

7. Cittolin-Santos GF*, et al.* The changing landscape of small cell lung cancer. *Cancer* **130**, 2453-2461 (2024).

8. Pleasance ED*, et al.* A small-cell lung cancer genome with complex signatures of tobacco exposure. *Nature* **463**, 184-190 (2010).

9. Rudin CM*, et al.* Comprehensive genomic analysis identifies SOX2 as a frequently amplified gene in small-cell lung cancer. *Nat Genet* **44**, 1111-1116 (2012).

10. Peifer M*, et al.* Integrative genome analyses identify key somatic driver mutations of small-cell lung cancer. *Nat Genet* **44**, 1104-1110 (2012).

11. George J*, et al.* Comprehensive genomic profiles of small cell lung cancer. *Nature* **524**, 47-53 (2015).

12. Augert A*, et al.* Small Cell Lung Cancer Exhibits Frequent Inactivating Mutations in the Histone Methyltransferase KMT2D/MLL2: CALGB 151111 (Alliance). *J Thorac Oncol* **12**, 704-713 (2017).

13. Iwakawa R*, et al.* Genome-wide identification of genes with amplification and/or fusion in small cell lung cancer. *Genes Chromosomes Cancer* **52**, 802-816 (2013).

14. Park KS*, et al.* Characterization of the cell of origin for small cell lung cancer. *Cell Cycle* **10**, 2806-2815 (2011).

15. Sutherland KD, Proost N, Brouns I, Adriaensen D, Song JY, Berns A. Cell of origin of small cell lung cancer: inactivation of Trp53 and Rb1 in distinct cell types of adult mouse lung. *Cancer Cell* **19**, 754-764 (2011).

16. Kuo CS*, et al.* Neuroendocrinology of the lung revealed by single-cell RNA sequencing. *Elife* **11**, (2022).

17. Noguchi M, Furukawa KT, Morimoto M. Pulmonary neuroendocrine cells: physiology, tissue homeostasis and disease. *Dis Model Mech* **13**, (2020).

18. Carney DN*, et al.* Establishment and identification of small cell lung cancer cell lines having classic and variant features. *Cancer Res* **45**, 2913-2923 (1985).

19. Gazdar AF, Carney DN, Nau MM, Minna JD. Characterization of variant subclasses of cell lines derived from small cell lung cancer having distinctive biochemical, morphological, and growth properties. *Cancer Res* **45**, 2924-2930 (1985).

20. Zhang W*, et al.* Small cell lung cancer tumors and preclinical models display heterogeneity of neuroendocrine phenotypes. *Transl Lung Cancer Res* **7**, 32-49 (2018).

21. Borromeo MD*, et al.* ASCL1 and NEUROD1 Reveal Heterogeneity in Pulmonary Neuroendocrine Tumors and Regulate Distinct Genetic Programs. *Cell Rep* **16**, 1259-1272 (2016).

22. Huang YH*, et al.* POU2F3 is a master regulator of a tuft cell-like variant of small cell lung cancer. *Genes Dev* **32**, 915-928 (2018).

23. Gay CM*, et al.* Patterns of transcription factor programs and immune pathway activation define four major subtypes of SCLC with distinct therapeutic vulnerabilities. *Cancer Cell* **39**, 346-360 e347 (2021).

24. Poirier JT*, et al.* New Approaches to SCLC Therapy: From the Laboratory to the Clinic. *J Thorac Oncol* **15**, 520-540 (2020).

25. Horn L, Liu SV. Atezolizumab plus Chemotherapy in Small-Cell Lung Cancer. Reply. *N Engl J Med* **380**, 889-890 (2019).

26. Paz-Ares L*, et al.* Durvalumab plus platinum-etoposide versus platinum-etoposide in first-line treatment of extensive-stage small-cell lung cancer (CASPIAN): a randomised, controlled, open-label, phase 3 trial. *Lancet* **394**, 1929-1939 (2019).

27. Rossi A*, et al.* Carboplatin- or cisplatin-based chemotherapy in first-line treatment of small-cell lung cancer: the COCIS meta-analysis of individual patient data. *J Clin Oncol* **30**, 1692-1698 (2012).

28. George J*, et al.* Evolutionary trajectories of small cell lung cancer under therapy. *Nature* **627**, 880-889 (2024).

29. Wagner AH*, et al.* Recurrent WNT pathway alterations are frequent in relapsed small cell lung cancer. *Nature communications* **9**, 3787 (2018).

30. Polley E*, et al.* Small Cell Lung Cancer Screen of Oncology Drugs, Investigational Agents, and Gene and microRNA Expression. *J Natl Cancer Inst* **108**, (2016).

31. Gardner EE*, et al.* Chemosensitive Relapse in Small Cell Lung Cancer Proceeds through an EZH2-SLFN11 Axis. *Cancer Cell* **31**, 286-299 (2017).

32. Zoppoli G*, et al.* Putative DNA/RNA helicase Schlafen-11 (SLFN11) sensitizes cancer cells to DNA-damaging agents. *Proc Natl Acad Sci U S A* **109**, 15030-15035 (2012).

33. Lok BH*, et al.* PARP Inhibitor Activity Correlates with SLFN11 Expression and Demonstrates Synergy with Temozolomide in Small Cell Lung Cancer. *Clin Cancer Res* **23**, 523-535 (2017).

34. Grunblatt E*, et al.* MYCN drives chemoresistance in small cell lung cancer while USP7 inhibition can restore chemosensitivity. *Genes Dev* **34**, 1210-1226 (2020).

35. Pal Choudhuri S*, et al.* Acquired Cross-Resistance in Small Cell Lung Cancer due to Extrachromosomal DNA Amplification of MYC Paralogs. *Cancer Discov* **14**, 804-827 (2024).

36. Stewart CA*, et al.* Single-cell analyses reveal increased intratumoral heterogeneity after the onset of therapy resistance in small-cell lung cancer. *Nat Cancer* **1**, 423-436 (2020).

37. Thomas A*, et al.* Therapeutic targeting of ATR yields durable regressions in small cell lung cancers with high replication stress. *Cancer Cell* **39**, 566-579 e567 (2021).

38. Lim JS*, et al.* Intratumoural heterogeneity generated by Notch signalling promotes small-cell lung cancer. *Nature* **545**, 360-364 (2017).

39. Zhou H*, et al.* Multi-region exome sequencing reveals the intratumoral heterogeneity of surgically resected small cell lung cancer. *Nat Commun* **12**, 5431 (2021).

40. Jinek M, Chylinski K, Fonfara I, Hauer M, Doudna JA, Charpentier E. A programmable dual-RNA-guided DNA endonuclease in adaptive bacterial immunity. *Science* **337**, 816-821 (2012).

41. Cong L*, et al.* Multiplex genome engineering using CRISPR/Cas systems. *Science* **339**, 819-823 (2013).

42. Mali P*, et al.* RNA-guided human genome engineering via Cas9. *Science* **339**, 823-826 (2013).

43. Lieber MR. The mechanism of human nonhomologous DNA end joining. *J Biol Chem* **283**, 1-5 (2008).

44. Shalem O*, et al.* Genome-scale CRISPR-Cas9 knockout screening in human cells. *Science* **343**, 84-87 (2014).

45. Wang T, Wei JJ, Sabatini DM, Lander ES. Genetic screens in human cells using the CRISPR-Cas9 system. *Science* **343**, 80-84 (2014).

46. Augert A*, et al.* MAX Functions as a Tumor Suppressor and Rewires Metabolism in Small Cell Lung Cancer. *Cancer Cell* **38**, 97-114 e117 (2020).

47. Sanjana NE, Shalem O, Zhang F. Improved vectors and genome-wide libraries for CRISPR screening. *Nat Methods* **11**, 783-784 (2014).

48. Brumage L*, et al.* In vivo functional screens reveal KEAP1 loss as a driver of chemoresistance in small cell lung cancer. *Sci Adv* **11**, eadq7084 (2025).

49. Romero R*, et al.* Keap1 loss promotes Kras-driven lung cancer and results in dependence on glutaminolysis. *Nat Med* **23**, 1362-1368 (2017).

50. Jeong Y*, et al.* Role of KEAP1/NRF2 and TP53 Mutations in Lung Squamous Cell Carcinoma Development and Radiation Resistance. *Cancer Discov* **7**, 86-101 (2017).

51. Li W*, et al.* MAGeCK enables robust identification of essential genes from genome-scale CRISPR/Cas9 knockout screens. *Genome Biol* **15**, 554 (2014).

52. Zhang XY, Pfeiffer HK, Thorne AW, McMahon SB. USP22, an hSAGA subunit and potential cancer stem cell marker, reverses the polycomb-catalyzed ubiquitylation of histone H2A. *Cell Cycle* **7**, 1522-1524 (2008).

53. Wyce A*, et al.* H2B ubiquitylation acts as a barrier to Ctk1 nucleosomal recruitment prior to removal by Ubp8 within a SAGA-related complex. *Mol Cell* **27**, 275-288 (2007).

54. Wang L, Dent SY. Functions of SAGA in development and disease. *Epigenomics* **6**, 329-339 (2014).

55. Hiatt JB*, et al.* Molecular phenotyping of small cell lung cancer using targeted cfDNA profiling of transcriptional regulatory regions. *Sci Adv* **10**, eadk2082 (2024).

56. Augert A*, et al.* Targeting NOTCH activation in small cell lung cancer through LSD1 inhibition. *Sci Signal* **12**, (2019).

57. Zhang XY*, et al.* The putative cancer stem cell marker USP22 is a subunit of the human SAGA complex required for activated transcription and cell-cycle progression. *Mol Cell* **29**, 102-111 (2008).

58. Ramachandran S*, et al.* The SAGA Deubiquitination Module Promotes DNA Repair and Class Switch Recombination through ATM and DNAPK-Mediated gammaH2AX Formation. *Cell Rep* **15**, 1554-1565 (2016).

59. Zhao Y*, et al.* A TFTC/STAGA module mediates histone H2A and H2B deubiquitination, coactivates nuclear receptors, and counteracts heterochromatin silencing. *Mol Cell* **29**, 92-101 (2008).

60. Koutelou E, Hirsch CL, Dent SY. Multiple faces of the SAGA complex. *Curr Opin Cell Biol* **22**, 374-382 (2010).

61. Soffers JHM, Workman JL. The SAGA chromatin-modifying complex: the sum of its parts is greater than the whole. *Genes Dev* **34**, 1287-1303 (2020).

62. Henry KW*, et al.* Transcriptional activation via sequential histone H2B ubiquitylation and deubiquitylation, mediated by SAGA-associated Ubp8. *Genes Dev* **17**, 2648-2663 (2003).

63. Wang A*, et al.* USP22 Induces Cisplatin Resistance in Lung Adenocarcinoma by Regulating gammaH2AX-Mediated DNA Damage Repair and Ku70/Bax-Mediated Apoptosis. *Front Pharmacol* **8**, 274 (2017).

64. Li C*, et al.* The H2B deubiquitinase Usp22 promotes antibody class switch recombination by facilitating non-homologous end joining. *Nat Commun* **9**, 1006 (2018).

65. McCann JJ*, et al.* USP22 Functions as an Oncogenic Driver in Prostate Cancer by Regulating Cell Proliferation and DNA Repair. *Cancer Res* **80**, 430-443 (2020).

66. Doench JG*, et al.* Optimized sgRNA design to maximize activity and minimize off-target effects of CRISPR-Cas9. *Nat Biotechnol* **34**, 184-191 (2016).

67. Quesada V, Diaz-Perales A, Gutierrez-Fernandez A, Garabaya C, Cal S, Lopez-Otin C. Cloning and enzymatic analysis of 22 novel human ubiquitin-specific proteases. *Biochem Biophys Res Commun* **314**, 54-62 (2004).

68. Liu YL*, et al.* The deubiquitinating enzyme activity of USP22 is necessary for regulating HeLa cell growth. *Gene* **572**, 49-56 (2015).

69. Chen EY*, et al.* Enrichr: interactive and collaborative HTML5 gene list enrichment analysis tool. *BMC Bioinformatics* **14**, 128 (2013).

70. Kuleshov MV*, et al.* Enrichr: a comprehensive gene set enrichment analysis web server 2016 update. *Nucleic Acids Res* **44**, W90-97 (2016).

71. Cai Z*, et al.* USP22 promotes IRF3 nuclear translocation and antiviral responses by deubiquitinating the importin protein KPNA2. *J Exp Med* **217**, (2020).

72. Liu Q*, et al.* Broad and diverse mechanisms used by deubiquitinase family members in regulating the type I interferon signaling pathway during antiviral responses. *Sci Adv* **4**, eaar2824 (2018).

73. Dietlein N*, et al.* Usp22 is an intracellular regulator of systemic emergency hematopoiesis. *Sci Immunol* **7**, eabq2061 (2022).

74. Hong A, Lee JE, Chung KC. Ubiquitin-specific protease 22 (USP22) positively regulates RCAN1 protein levels through RCAN1 de-ubiquitination. *J Cell Physiol* **230**, 1651-1660 (2015).

75. Karlowitz R*, et al.* USP22 controls type III interferon signaling and SARS-CoV-2 infection through activation of STING. *Cell Death Dis* **13**, 684 (2022).

76. Subramanian A*, et al.* Gene set enrichment analysis: a knowledge-based approach for interpreting genome-wide expression profiles. *Proc Natl Acad Sci U S A* **102**, 15545-15550 (2005).

77. Sussel L, Marin O, Kimura S, Rubenstein JL. Loss of Nkx2.1 homeobox gene function results in a ventral to dorsal molecular respecification within the basal telencephalon: evidence for a transformation of the pallidum into the striatum. *Development* **126**, 3359-3370 (1999).

78. Briscoe J*, et al.* Homeobox gene Nkx2.2 and specification of neuronal identity by graded Sonic hedgehog signalling. *Nature* **398**, 622-627 (1999).

79. Brose K*, et al.* Slit proteins bind Robo receptors and have an evolutionarily conserved role in repulsive axon guidance. *Cell* **96**, 795-806 (1999).

80. Blockus H*, et al.* Synaptogenic activity of the axon guidance molecule Robo2 underlies hippocampal circuit function. *Cell Rep* **37**, 109828 (2021).

81. Kerjan G*, et al.* The transmembrane semaphorin Sema6A controls cerebellar granule cell migration. *Nat Neurosci* **8**, 1516-1524 (2005).

82. Xu XM*, et al.* The transmembrane protein semaphorin 6A repels embryonic sympathetic axons. *J Neurosci* **20**, 2638-2648 (2000).

83. Wang H*, et al.* Role of histone H2A ubiquitination in Polycomb silencing. *Nature* **431**, 873-878 (2004).

84. Blackledge NP*, et al.* Variant PRC1 complex-dependent H2A ubiquitylation drives PRC2 recruitment and polycomb domain formation. *Cell* **157**, 1445-1459 (2014).

85. Cooper S*, et al.* Targeting polycomb to pericentric heterochromatin in embryonic stem cells reveals a role for H2AK119u1 in PRC2 recruitment. *Cell Rep* **7**, 1456-1470 (2014).

86. Tamburri S*, et al.* Histone H2AK119 Mono-Ubiquitination Is Essential for Polycomb-Mediated Transcriptional Repression. *Mol Cell* **77**, 840-856 e845 (2020).

87. Kaya-Okur HS*, et al.* CUT&Tag for efficient epigenomic profiling of small samples and single cells. *Nat Commun* **10**, 1930 (2019).

88. Jackson SP, Bartek J. The DNA-damage response in human biology and disease. *Nature* **461**, 1071-1078 (2009).

89. Krug K*, et al.* A Curated Resource for Phosphosite-specific Signature Analysis. *Mol Cell Proteomics* **18**, 576-593 (2019).

90. Chatterjee N, Walker GC. Mechanisms of DNA damage, repair, and mutagenesis. *Environ Mol Mutagen* **58**, 235-263 (2017).

91. Kuo LJ, Yang LX. Gamma-H2AX - a novel biomarker for DNA double-strand breaks. *In Vivo* **22**, 305-309 (2008).

92. Mah LJ, El-Osta A, Karagiannis TC. gammaH2AX: a sensitive molecular marker of DNA damage and repair. *Leukemia* **24**, 679-686 (2010).

93. Zhang XY*, et al.* Hexokinase 2 confers resistance to cisplatin in ovarian cancer cells by enhancing cisplatin-induced autophagy. *Int J Biochem Cell Biol* **95**, 9-16 (2018).

94. Qian X*, et al.* Enolase 1 stimulates glycolysis to promote chemoresistance in gastric cancer. *Oncotarget* **8**, 47691-47708 (2017).

95. Varghese E, Samuel SM, Liskova A, Samec M, Kubatka P, Busselberg D. Targeting Glucose Metabolism to Overcome Resistance to Anticancer Chemotherapy in Breast Cancer. *Cancers (Basel)* **12**, (2020).

96. Simons AL, Ahmad IM, Mattson DM, Dornfeld KJ, Spitz DR. 2-Deoxy-D-glucose combined with cisplatin enhances cytotoxicity via metabolic oxidative stress in human head and neck cancer cells. *Cancer Res* **67**, 3364-3370 (2007).

97. Guo Q, Lan F, Yan X, Xiao Z, Wu Y, Zhang Q. Hypoxia exposure induced cisplatin resistance partially via activating p53 and hypoxia inducible factor-1alpha in non-small cell lung cancer A549 cells. *Oncol Lett* **16**, 801-808 (2018).

98. Chakraborty PK*, et al.* MICU1 drives glycolysis and chemoresistance in ovarian cancer. *Nat Commun* **8**, 14634 (2017).

99. Wu HM, Jiang ZF, Ding PS, Shao LJ, Liu RY. Hypoxia-induced autophagy mediates cisplatin resistance in lung cancer cells. *Sci Rep* **5**, 12291 (2015).

100. Siebeneicher H*, et al.* Identification and Optimization of the First Highly Selective GLUT1 Inhibitor BAY-876. *ChemMedChem* **11**, 2261-2271 (2016).

101. Kosinsky RL*, et al.* USP22 exerts tumor-suppressive functions in colorectal cancer by decreasing mTOR activity. *Cell Death Differ* **27**, 1328-1340 (2020).

102. Melo-Cardenas J*, et al.* USP22 deficiency leads to myeloid leukemia upon oncogenic Kras activation through a PU.1-dependent mechanism. *Blood* **132**, 423-434 (2018).

103. Chuang JH*, et al.* 2-Deoxyglucose treatment complements the cisplatin- or BH3-only mimetic-induced suppression of neuroblastoma cell growth. *Int J Biochem Cell Biol* **45**, 944-951 (2013).

104. Hodgkinson CL*, et al.* Tumorigenicity and genetic profiling of circulating tumor cells in small-cell lung cancer. *Nat Med* **20**, 897-903 (2014).

105. Dobin A*, et al.* STAR: ultrafast universal RNA-seq aligner. *Bioinformatics* **29**, 15-21 (2013).

106. Kluin RJC*, et al.* XenofilteR: computational deconvolution of mouse and human reads in tumor xenograft sequence data. *BMC Bioinformatics* **19**, 366 (2018).

107. Robinson MD, Oshlack A. A scaling normalization method for differential expression analysis of RNA-seq data. *Genome Biol* **11**, R25 (2010).

108. Robinson MD, McCarthy DJ, Smyth GK. edgeR: a Bioconductor package for differential expression analysis of digital gene expression data. *Bioinformatics* **26**, 139-140 (2010).

109. Ewels PA*, et al.* The nf-core framework for community-curated bioinformatics pipelines. *Nat Biotechnol* **38**, 276-278 (2020).

110. Zhang Y*, et al.* Model-based analysis of ChIP-Seq (MACS). *Genome Biol* **9**, R137 (2008).

111. Feng J, Liu T, Qin B, Zhang Y, Liu XS. Identifying ChIP-seq enrichment using MACS. *Nat Protoc* **7**, 1728-1740 (2012).

112. Danecek P*, et al.* Twelve years of SAMtools and BCFtools. *Gigascience* **10**, (2021).

113. Quinlan AR, Hall IM. BEDTools: a flexible suite of utilities for comparing genomic features. *Bioinformatics* **26**, 841-842 (2010).

114. Heinz S*, et al.* Simple combinations of lineage-determining transcription factors prime cis-regulatory elements required for macrophage and B cell identities. *Mol Cell* **38**, 576-589 (2010).

115. Liao Y, Smyth GK, Shi W. featureCounts: an efficient general purpose program for assigning sequence reads to genomic features. *Bioinformatics* **30**, 923-930 (2014).

116. Ramirez F, Dundar F, Diehl S, Gruning BA, Manke T. deepTools: a flexible platform for exploring deep-sequencing data. *Nucleic Acids Res* **42**, W187-191 (2014).

117. Robinson JT*, et al.* Integrative genomics viewer. *Nat Biotechnol* **29**, 24-26 (2011).

118. Kong AT, Leprevost FV, Avtonomov DM, Mellacheruvu D, Nesvizhskii AI. MSFragger: ultrafast and comprehensive peptide identification in mass spectrometry-based proteomics. *Nat Methods* **14**, 513-520 (2017).

119. Yu F*, et al.* Identification of modified peptides using localization-aware open search. *Nat Commun* **11**, 4065 (2020).

120. Keller A, Nesvizhskii AI, Kolker E, Aebersold R. Empirical statistical model to estimate the accuracy of peptide identifications made by MS/MS and database search. *Anal Chem* **74**, 5383-5392 (2002).

121. Shteynberg DD*, et al.* PTMProphet: Fast and Accurate Mass Modification Localization for the Trans-Proteomic Pipeline. *J Proteome Res* **18**, 4262-4272 (2019).

122. Nesvizhskii AI, Keller A, Kolker E, Aebersold R. A statistical model for identifying proteins by tandem mass spectrometry. *Anal Chem* **75**, 4646-4658 (2003).

123. Djomehri SI*, et al.* Quantitative proteomic landscape of metaplastic breast carcinoma pathological subtypes and their relationship to triple-negative tumors. *Nat Commun* **11**, 1723 (2020).

124. Clark DJ*, et al.* Integrated Proteogenomic Characterization of Clear Cell Renal Cell Carcinoma. *Cell* **179**, 964-983.e931 (2019).

125. Ma W*, et al.* DreamAI: algorithm for the imputation of proteomics data. *bioRxiv*, (2021).

APPENDIX

Table 1: Focused CRISPR deletion gRNA library composition

Gene	Sequence	Gene	Sequence	Gene	Sequence	Gene	Sequence
AKT3	TTATAATCAGATGTCTCCAG	EPHA5	TGTTATGAAACTGAATACAG	MAP2K4	TGGATAAGGAAATCGGCCTG	RPL22L1	AAGGTCCAAATTAAACCTCC
AKT3	ATTTCATGTAGATACTCCAG	EPHA5	ATACAGTTCAATGGACGCTG	MAP2K4	CAACTAACACAAGTCGTGAA	RPL22L1	CGGGAGAAGGTTAAAGTCAA
AKT3	TGGACTGCATGGACAATGAG	EPHA5	ATCAGTAGGTGAATGGCTAG	MAP2K4	TCCTCAGAATTACTCAGCTG	RPL22L1	GGAGCAATTTCTACGGGAGA
AKT3	ACTGCATGGACAATGAGAGG	EPHA5	TCAGAATGGGAGAAACATCA	MAP2K4	GACCCAAGCGCATCACGACA	RPL22L1	CTTACTCATCCAGTAGAAGA
AKT3	TAGGAAAATTGAGGGAAATG	EPHA5	TCTGGGGCCTACAGATCAGT	MAP2K4	CTGTCCAGAAGAATATTGGA	RPL22L1	CATCTTCTACTGGATGAGTA
AKT3	TCTCTATAACAGTAGTCCAC	EPHA5	ATACCAAGTATGCAAAGTGA	MAP2K4	TTACGAAGGATGAATCCAAA	RPL22L1	AATGGCAAAACTGGAAATCT
ALDH3A1	CCAGTCCCCGGTGATGCAAG	EPHA7	TGGTTTCAGATTATTAATGG	MAP2K7	CATTCTGGGCAAGATGACAG	RPTOR	TCATGAGCTCAGGAGACGTG
ALDH3A1	TTAGTGCCCGGCACTTCCAG	EPHA7	AATCCAACATTAGCTGGTGA	MAP2K7	GCACGATGTAGGGGCAGTCG	RPTOR	AACAACATCAAGTACTACGA
ALDH3A1	CGTGTGCGTGCGCAGCCTGG	EPHA7	TTATCGTTTACCAGCACCCA	MAP2K7	CCAGGCTCCATACGTCGGCC	RPTOR	CGTCTCCTGAGCTCATGAGG
ALDH3A1	TTGCACTCTCTGCCCTTCGG	EPHA7	TCCATTAATAATCTGAAACC	MAP2K7	AATGCGGCGCTCCGGGAACA	RPTOR	TTCCCACCGCTCACTCATCG
ALDH3A1	GATGTGGACGATGACATCGT	EPHA7	CCTTTTGTTCAGTTGGAGAA	MAP2K7	CATCCTCATGGACCTGGATG	RPTOR	ATGCGATCAGGTCCGCCTGG
ALDH3A1	ACTGGGGGTCCACGTCCGTG	EPHA7	AATGTTGGATTGTTGGCAAA	MAP2K7	CCGGATGTCATAGTCCGGCT	RPTOR	GGCCAGCCACGATGAGTGAG
ALDOA	CATTGGCACCGAGAACACCG	EPHB1	GCTGAGCCAGTCATCCACGG	MAP3K1	TGGCTTGTGCAAAACCACCA	RUNX1	CACTTCGACCGACAAACCTG
ALDOA	CAAGTTATCAAATCCAAGGG	EPHB1	AGGCAAGAGGGAAATCTACG	MAP3K1	TGTTTTTCTGCATTCCATGG	RUNX1	GAGTGGTTCAGGGAGGCACG
ALDOA	CCCCAATGCAGGGGTTCACG	EPHB1	GATCTGAGGTGTCATCCTGG	MAP3K1	GTAATTGCTCTTCTCACACG	RUNX1	GGAGCTTGTCCTTTTCCGAG
ALDOA	AGGTGCCTTCCAGGTAGATG	EPHB1	TGTGAGATGGACAGCTCCAG	MAP3K1	TAAGAGGTCAACAGTATGGA	RUNX1	AGCTGCGGCGCACAGCCATG
ALDOA	CGCCATTTGTCCCTGCCAGG	EPHB1	GCGTCGGGACTTTCTGAGTG	MAP3K1	TGGCTGAAAGGTCAACAGAT	RUNX1	TGCCATCTGGAACATCCCCT
ALDOA	TGACAGCGGGGGGCACTGTG	EPHB1	CATACCCACAAGCTGGATCA	MAP3K1	TGATGTTTGGATGATTCAGA	RUNX1	GGTCATTAAATCTTGCAACC
ALK	TGGTTCCTGAGGTCATGCAG	ERBB3	TGATCCAGCAGAGAACCCAG	MAP3K11	CTACGCCATAGGCCACAGCA	S100G	GAGTACTAAAAAGTCTCCTG
ALK	TGTCCCATTCCAACAAGTGA	ERBB3	ATCATGTGAGACAACACCGG	MAP3K11	ACTGCCCTTAGAGAAGGTGG	S100G	AGTCTCCTGAGGAACTGAAG
ALK	ACCCCACACTCCTCAATGGC	ERBB3	AAAGTCATTGAGGACAAGAG	MAP3K11	ACCGGGGAGGTGCCATACCG	S100G	TGATCCAGACCAGTTGTCAA
ALK	GCAGGCCTGTGACTTCCACC	ERBB3	AGTCTGCATTAAAGTCATTG	MAP3K11	GCCCGCGGCACTCATTTGTG	S100G	GTTCTTGAAAGAGATCATCT
ALK	AGGGTCCTGACCTGCCATTG	ERBB3	GTCCCAGCAGCCTTACAATG	MAP3K11	CATCCAGGCGTAGGTGCCCG	S100G	TTTCAAGAACTGGACAAGAA
ALK	AACTTTGAAGATGGCTTCTG	ERBB3	GGCCGGTGATCAGAAAGTCC	MAP3K11	AGGCAGTCAATGCCACGGTA	S100G	ATATCTTTTTTACTAATACT
ALOX12B	ACACCGCCAAGCTGTCATCG	ERBB4	CTGTTGCTTGAGGATAAGCA	MAP3K13	ACGGAAGAAAATGAATTCAG	SCML1	GTTTCCATGCGAGATCCCTG
ALOX12B	TGGGAAGTTGGGCATCCAGG	ERBB4	ATTGTGCTCCAGTTGAAAGG	MAP3K13	TGTAGGTCTGAGTCATCCCT	SCML1	ATTATGCTCAGAGAAATCTG
ALOX12B	GTCCATGAAGGTCTCCAGAG	ERBB4	CAGGGACTGGAACTGTAGAG	MAP3K13	CATCCCAGACTCAATATGCA	SCML1	TAAGCACCCTTCAACCTGGT
ALOX12B	ATATCGGATCAGCTCAGGCA	ERBB4	TGCATGAATTTCAATGACAG	MAP3K13	GTCTGCATCCCAGATTTGTG	SCML1	ACAAGAGGGCATAATGCAAG
ALOX12B	TTACCCGAGTGACGCAGCCG	ERBB4	TGGCAGCAGTCACTGACGTA	MAP3K13	TATCATCCATCCCAATGCCA	SCML1	GATGCACTGGACTCGGAGTG
ALOX12B	GCGATGACAGCTTGGCGGTG	ERBB4	GGTGGTTGGATTGTAGACAA	MAP3K13	GGGTGTCGTTTGTAGGTCCC	SCML1	GACCACTGCTTCCACCGACC
AMER1	GGCCTGTGAGAAACTCACAG	ERCC4	TGAAGTGGAGCCAAGATACG	MAX	GGTGTAGAGGCTGTTGTCTG	SEMA6C	AGGCATCAATCTCTTCCAGG
AMER1	CTCGGGGTAGACAATCCCTG	ERCC4	AAGCCCGTTCTTTGTTTTGG	MAX	GGTAGCTTGAAATGAAGGTG	SEMA6C	AGGTCAGGACATCATCAGGG
AMER1	GCAGTCCCAAGTATCGAGGG	ERCC4	TTTCGCCAGAAAAACAAACG	MAX	ATGCACTGGAACGAAAACGT	SEMA6C	GGACAGCCCAAACAGCACGA
AMER1	AAGCTGAGGTAATTCCCCGG	ERCC4	AGACTATATCACTCTTGGAG	MAX	TCCGTGCACTGGAGAAGGCG	SEMA6C	TGATGTCCTGACCTTCATCA
AMER1	TAAAGGCAGTCATCTCCAGG	ERCC4	AGAAAGCAACCCAAAGTGGG	MAX	AAGCAGGAAGAAGCTCCGGA	SEMA6C	CTGCTAGTGAGAGTGAGTAG
AMER1	TCCCCGGTGGGAAATCTGAG	ERCC4	TTGTGAGGAAACTGTATCTG	MAX	GACTCAGTCCCATCACTCCA	SEMA6C	CCTACTGACCCAAGTAGCTG
ANKRD11	CCCACCGTTTATGACCCCGG	ESR1	GGGATACGAAAAGACCGAAG	MBOAT4	GAAAGCAGAAGGTCCACCTG	SENP2	TATCCTAAATTAAAGTCTGG
ANKRD11	CGGCTCCTCAGCCACTACGG	ESR1	GCACCATTGATAAAAACAGG	MBOAT4	GTGCAGACCTAGGTGACACA	SENP2	TTTTTACATGAATCTTCTGG
ANKRD11	ATCTTGCGTGGAGTCCACTG	ESR1	CAAGGCACTGACCATCTGGT	MBOAT4	AGCAGGGGTGAAGACGAGCA	SENP2	TTCAAATTGCGAATTACTCG
ANKRD11	GCGGAAGCTGCCCTTCACCG	ESR1	GAAGGTGGACCTGATCATGG	MBOAT4	CAAAGGGAAATGCAGCCCCC	SENP2	AGACATTAAAGAACTATCAC
ANKRD11	AAGACCCCAAAACTGGAGCG	ESR1	CGGGGGCTCAGCATCCAACA	MBOAT4	TCCTATATCGTTTTACCAGG	SENP2	GCAGTGAAACGATGGACCAA
ANKRD11	TTAAGAAGGAGCCTGTCACC	ESR1	GCTCCGTAAATGCTACGAAG	MBOAT4	ATAATTGAAGAGAAGTGCAA	SENP2	GTGATCTGAATCTTTTAGAG
ANKS1A	TTGCCATGTGTTCAGCACCG	ESRP2	GTAGTTCAGGTAGAGTTGAG	MCM2	CGAGTCCATGATCCGCATGG	SETD2	CGAGCTGTCTTCCAGTTGGG
ANKS1A	ATGCTGATCAAAGATCTGCG	ESRP2	AGACATCCTGAGCTTTCTGG	MCM2	GGACAGAACCAGCATCCATG	SETD2	CCTGGGCTTTCCCAAGTAGG
ANKS1A	GATCCGGAACATTTCCTGTG	ESRP2	TCAATTGTTTTCGAAGCCCG	MCM2	CGTGCAGCGAGCCTGCAGGG	SETD2	CCGGAAACCTGACTGCAAAG
ANKS1A	TGAACACATGGCAATAGTGG	ESRP2	GATGAAGGAGCGCTACGTGG	MCM2	GATGATCACTAGCCTCTCCA	SETD2	CCATTGTCTTACCTCCCAAC
ANKS1A	GTATGTGATGGACAGGATGA	ESRP2	TGGTGTAGGTAGGTGGTGAG	MCM2	CATCGAGTCCATGATCCGCA	SETD2	CTCAGTGGGATCCTCCTACT
ANKS1A	CTTGGCACAGGCGTCTTGCG	ESRP2	GCTCAGGATGTCTTCAATGG	MCM2	ACAGAGCATCTCCATCTCGA	SETD2	TAGTAATAAATCTTCCCTTC
APC	CCGGCTCACATGATGCTGAG	ETV1	TACAGGGTTCAGAAAGCTGG	MDC1	ACAGGAACTTGACTGTCCGG	SF3B1	AAAACTGTACCACAGATCTG
APC	AGGAGTGGGAGAAATCAACA	ETV1	GGGAAGGACCCACATACCAA	MDC1	GTGGTCAGAGCAAAACACTG	SF3B1	ATAACCAAATGTGTTGACTG
APC	CAGCTTGATAGCTACAAATG	ETV1	GTATGGACTGCGATGGAGGG	MDC1	GTCACCACATATTCATCCGG	SF3B1	AGACCTTGTACACAGACAGA
APC	GCTACTAGAACTCAAAACAC	ETV1	GCTGAAGTGATCCTCGCCGT	MDC1	AACCGGCATAGCTCTTACTG	SF3B1	ATAACTGCCTGAAATCTTCG
APC	ATGTGCTGACAAATTCCATA	ETV1	GGTTCCTGTTTAATCATCAG	MDC1	AGGAGATTGGAATTCAGGGG	SF3B1	CAGACAGACGGCTAGTGCAG
APC	AAAGCGTATTGAGTGCCTTA	ETV1	AACATCCCCTTCCCACCACA	MDC1	GTAAGAAGAAACCAGCCTTG	SF3B1	AATATGTATCTGCAAGAGAG
APMAP	CCTGGTGGCAGAAACAACCA	ETV3	ATCGTGGAAAAGCCAGAAGG	MDM2	AATTGCTCTCCTTCTAGATG	SFN	TATTGAGCAGAAAGCAACG
APMAP	TTACAGTCACTCAGGATGGG	ETV3	GAAAGCCGGCTGTAGCATCG	MDM2	AACAGGTGTCACCTTGAAGG	SFN	AGCCCGGTCAGCCTACCAGG
APMAP	AAGTTTTATTGGACCAGCTG	ETV3	GTGGAAAAGCCAGAAGGAGG	MDM2	GTACATCTGTGAGTGAGAAC	SFN	TGATCTGCACACCCTCAGCG
APMAP	TGGCAGAAACAACCATGGCC	ETV3	TTCATCAACATTCGGTCAAG	MDM2	GTTCTTGTCCTTCTTCACTA	SFN	GGCCAAGACCACTTTCGACG
APMAP	GAATGATCTTACAGTCACTC	ETV3	TAAATTTAACTTCAACAAGC	MDM2	CAGAGCCAGGCTTTCATCAA	SFN	AGTAGCCTATAAGAACGTGG
APMAP	GTGATGGAGGGCACAGATGA	ETV3	TTTTCCCTTTTGTTTTATGA	MDM2	CTTCCTGAAGCTCTTGTACA	SFN	AGACAACCTGACACTGTGGA
AQP9	GATTATGAGGAGTATCATGG	FAH	CAAATGTGTAGGGCTCGTCA	MDM4	AACAGATACAGAAAACATGG	SFRP5	TGGAGCACATCTGCTCCATG
AQP9	AGAAACTTGGGAGCCCCCAG	FAH	GAGGTTGATGTCAAATGTGT	MDM4	TATGGCAGTGATATCAGACG	SFRP5	CGGTGGGCTACAAGCGCATG
AQP9	GCCACTGTTCAGTCCCAGGG	FAH	ACTTGCATATGGTAGCCGCC	MDM4	AAGTTTCCTAAAAACCACCA	SFRP5	AAGCCGTAGGCCTCCATGAG
AQP9	GCGTTCGCCAGAGATAGATA	FAH	CGTCATGGCACAGATACGGC	MDM4	GGGAAAAAATGATGACCTGG	SFRP5	TAGCCCACCGTGTGGCAGAG
AQP9	GACGGTTGCAGCCCCCACAA	FAH	CTTAAAATTGGACTTGCATA	MDM4	TGTGAGAAAAGACCACGAGA	SFRP5	GAGATGGAGCACAGTGCTGA
AQP9	CACATTGCTAAAGACACAGC	FAH	AACATGGAGCCGAAGTTTTC	MDM4	GAACAAACAAGTGAAGAAGT	SFRP5	CACTGTGCTCCATCTCACAC
AR	ACATCCGGGACTTGTGCATG	FAM90A1	GCTCAAGTGCAAAAACTGTG	MED12	TTGCTGCTGCCGGTACACAG	SFXN2	CCATTGCAGGTCATGCTGAG
AR	GCCATCCAAACTCTTGAGAG	FAM90A1	CAGATAATCAGAAGATTCCG	MED12	CTACCCGCCACCTGCAACAG	SFXN2	CCTCATCTTCATGGTGCCAG
AR	ACAGCCAGTGTGTCCGAATG	FAM90A1	GTTTCCTGGAAAATATGTGG	MED12	GCATTGGTAAGCGCACAGGA	SFXN2	CACTGCCAGAAGATCACCGC
AR	ACTTCGAATGAACTACATCA	FAM90A1	ACCTGGTACTTCTGGCCGTG	MED12	CACCTGCAACAGCGGCCCAG	SFXN2	TGCTGCCAGTCATCATGGAA
AR	GGTCGTCCACGTGTAAGTTG	FAM90A1	GGAAGGAAAACCTGAAACCA	MED12	GGACGGTATGGGTCCACACG	SFXN2	GGGGGAAGCCGCATTCCTGT
AR	GCACTATTGATAAATTCCGA	FAM90A1	TTTGGCAGCGGCTTCTCTGG	MED12	GAGTAGGATTGGTAGAAGGG	SFXN2	GGGAAAAGCCCACACGCCAC
ARAF	CATGGTCCAGCTCATCGACG	FANCA	TATGAAGTCGACCATCAGGG	MED16	CATGATCAACCTCAAGACGG	SHC2	AAGGTTGCTCTTGCCCAGGA
ARAF	TGTGTGATGATGGCAAATCC	FANCA	CTGCCGCAGAGGACAGACGA	MED16	AGCCCAAGATCGACCACCTG	SHC2	TGGTGACGCTGTCTCGCACA
ARAF	GGCCGACACACGCTTCGACA	FANCA	CTGCCTTCGTCTGTCCTCTG	MED16	CATGCTTCGGGAATTGATGG	SHC2	CGGCCGGATGAGCCGCCGGG
ARAF	TTGGCACCGTGTTTCGAGGG	FANCA	CCATCTCAGAGTTGACCAAG	MED16	TTCCCGAAGCATGCCCAGCG	SHC2	GGCGCGTGGCAGGCACGGAG
ARAF	ATGCCACCGCCCTCGAAACA	FANCA	TGCAGAAGCTACAAGAAGGC	MED16	GCTGTCCTGGGTATCCGAGG	SHC2	GAGGACATACTGCCCGGGGT
ARAF	GTGAGGTGCAGCTGCTGAAG	FANCA	TCCGCAGACAGGCGTTCAGG	MED16	CAAGGTGCAGCCTCCGCAGG	SHC2	TGCTCATGCCGGCAAAGCGA
ARID1A	GTGGCTTCAACAGAGCCAGG	FAS	AAGTGGAAATAAACTGCACC	MED23	TCACTTAGACACCAGCCCTG	SHQ1	AGATCATTCAGTATGTACGC
ARID1A	CATATGGCCCTCCTGCCAAG	FAS	AGATGTAGATTGTGTGATGA	MED23	GTTTTCGTTTGAGAAATGCG	SHQ1	ACATCTCAGACTACTGTGTG
ARID1A	GAATGGAGACTTGCTAGGAG	FAS	GTTTGGTTTACATCTGCACT	MED23	ATGCGCTATGAATGCACGAG	SHQ1	TATCTTTATAGTGTCCCTGT
ARID1A	GAGTTAACTTTACATCCCCA	FAS	GACTGCGTGCCCTGCCAAGA	MED23	GTGATAGAGGAAGTCACAGA	SHQ1	TTTCATAGCAATATGCCAGA
ARID1A	GGCAATCAGTTCTCCACCCA	FAS	GTAGAGTTACAAAAAAAGTT	MED23	AATTTAAATGGGTGCTACAC	SHQ1	TATGAAACCCGTGTCACTGA
ARID1A	CTGCCAGGAGACCAGACTTG	FAS	GTACTCCTTCCCTTCTTGGC	MED23	GTAAAAATGGTCCAACAAGA	SHQ1	ACTGTAGCACACTTGACGAC
ARID1B	GATGCTTCTACTGAGCCAGG	FAT1	CTGCAGTACAAGTTTGACTG	MED24	TGTGGGAGGAGTAGGAACTG	SKOR1	GGAAATCCTATCCAGACCAA
ARID1B	GTACCATCATATCGTCTGTG	FAT1	AGTGACGTCCCCTGTACTCG	MED24	GGAGGGAAACTTGATCTGCG	SKOR1	ATTCCCGTTCCAGCTTCTTG
ARID1B	CCCAACAAGGACCCCTTTGG	FAT1	AGCCGTGCGTGTTCTCACAG	MED24	GTAGGGCATTGTGTCCACCC	SKOR1	TGTCACAGGAACTCATTTGG
ARID1B	GATGCCCTATGAGCCCAACA	FAT1	CATGGAAGAAGTCCTCAAGT	MED24	GGGCATTGTGTCCACCCCGG	SKOR1	CCGCCGATGATTTGGAAACG
ARID1B	GGATAAATCATGAGAGCCAG	FAT1	GCCCTCTGTGAGAACACGCA	MED24	ACTGCACGAACTGGGTGTGG	SKOR1	GGGCTTACCTTGGATGTCAC
ARID1B	CAGGTTAGACATTGCTCCGG	FAT1	ACATCCGTCAGCAGGGAACA	MED24	GGAACTGAGGGCACACCACA	SKOR1	CCTCGTTTCCAAATCATCGG
ARID2	CATGCAGCAACTGAACATGG	FBXW7	AAGATGCATACAACGCACAG	MET	ATGTATGGTAGGACCACCAG	SLC25A33	CGTTACGTTTACCAGACCGA
ARID2	GTGCTGCACTTATGGCTCTG	FBXW7	ACATTAGTGGGACATACAGG	MET	AGTTTCCCAATTTCTGACCG	SLC25A33	GGTAAACGTAACGAGCACAC
ARID2	ACTTGTACAGCTGGTGAAGG	FBXW7	CAGATCGGACACTCAAAGTG	MET	TTTGGTCTTCAAGTAGCCAA	SLC25A33	CACTAGAAGTCATTAAGACA
ARID2	AGCACTGGGATGATTCACAA	FBXW7	GGGCACCAGTCGTTAACAAG	MET	AAGTGAAGGGTCTCCGCTGG	SLC25A33	TTCGGAAATTCCAGCATACG
ARID2	GGATTAAAACAAGATGAACC	FBXW7	AATATCCCAAACCCTAAGAG	MET	GGATGAAAAATTCACAGTCA	SLC25A33	CTGAAAGAGTCCAGGTGTCA
ARID2	GACAGAACTTCATGTGTCTG	FBXW7	CCATCAAAACATGTAAACAC	MET	AAAGTTTGTCCACAGAGACT	SLC25A33	TTCAGAACCTGAAAGAGTCC
ARID5B	ATAATGTCTGCGGGTACAAG	FGFR1	CCAGAGTGAAGATCTCCCAC	METTL14	CAGAGAAAAATAAATGATCG	SLC2A5	CTGGCTCTCCAACTTCACCG
ARID5B	AGATGAACAAGCCTTCTTGG	FGFR1	CAACATCTTCACAGCCACTT	METTL14	CAGTTCCTTTGATCCCCATG	SLC2A5	GAGGGCATGTCCTATGACGT
ARID5B	CATATTTATGATGAATTAGG	FGFR1	ACTGGTCTTAGGCAAACCCC	METTL14	GACTAAGACTTTAGATCCAA	SLC2A5	AATGATAAGCTCAAATGATG

ARID5B	CATAAATATGTTTCCACTGA	FGFR1	ACCCAACCGTGTGACCAAAG	METTL14	ACTGTGAAGCGTAGCACAGA	SLC2A5	TGAGCACGCAGCAGGCTATG
ARID5B	TAATAAATCTTTCATATGGT	FGFR1	CCCATACCCCGGTGTGCCTG	METTL14	CTGTAATATTCTTCTAAAGG	SLC2A5	CCCCCCACCATGAAGGCAGA
ARID5B	TTTATAAAGTGCCACCAAGA	FGFR1	AAGTTCCTCCACAGGCACAC	METTL14	TATCTCTTCCAAATAGATGA	SLC2A5	TGGTGGAGCTCCTGGGTCGG
ARNT2	GCAAACATTTCAGCAAACCG	FGFR3	TGGACGTCACGGTAAGGACA	METTL3	GAGTTGATTGAGGTAAAGCG	SLC30A9	ACACAGAAGCACTCTTAGGG
ARNT2	GTAGGCATTCCCACTTGGCG	FGFR3	CAGGTCGTGTGTGCAGTTGG	METTL3	CTGTGACTATGGAACCAAGG	SLC30A9	TGCCCACACCCAAAGAACCT
ARNT2	ACCCAGCAGATCTACTCCCA	FGFR3	CGACACCTGCAAGCCGCCCG	METTL3	ATGTTAAGGCCAGATCAGAG	SLC30A9	TCCAGCCAGAACAAGTACAA
ARNT2	GAAATCGATACATGACCGAC	FGFR3	TCGAAGGAGTAGTCCAGGCC	METTL3	TCCATGTGAATATCCCAGGG	SLC30A9	AGAAGTAAGGCCCATGCAAG
ARNT2	GGAATGTGAAGCTGCTGGTG	FGFR3	CTGGGAGATCTTCACGCTGG	METTL3	CCCACCCTGGGATATTCACA	SLC30A9	TTTACCTAATCCCAGATCTG
ARNT2	ATTCTGGAATGTGAAGCTGC	FGFR3	CCTGTGCCTACCAGGTGGCC	METTL3	ATACCCGTACTACAGGATGA	SLC30A9	TACAAATGTGATATTATTGG
ARPC5L	ATTCGTCGATGTCCACCCGG	FGFR4	GCAGGAGACCAGGACTGGGA	MGA	CACACACTGCCAATGAGCGG	SLC35E1	CTGAAGCGAGAAGCACAGCG
ARPC5L	GCAGCGCAGTGTTACTCCAG	FGFR4	CGACGGTCCTCGGAGCAGTG	MGA	GGACACACACTGCCAATGAG	SLC35E1	AAGCGAGAAGCACAGCGTGG
ARPC5L	GTTGACGGGAGAGTTCCGCA	FGFR4	GCATGCAGTATCTGGAGTCC	MGA	ACAAGGTTGGCAGAGGTGTG	SLC35E1	TCACTCATCCCCATCATCAG
ARPC5L	AGGCCCGGACCCGAGCGAGG	FGFR4	CTCCCCGTATCCTGGCATCC	MGA	TCAAGTTGCCGGTAGTGCTG	SLC35E1	TCATAATGATCCGGGACAGG
ARPC5L	GTCCACCCGGCGGAAGCGCG	FGFR4	GTATCCTGGCATCCCGGTGG	MGA	AGAATTAGCAAACAGCAGGA	SLC35E1	GGCCACCATGCCCATCTGGG
ARPC5L	GGGCATTCCATGCAGCCTTG	FGFR4	GCTGCGGGAGGGACATCGGA	MGA	ACACTGCCAATGAGCGGCGG	SLC35E1	GAGGACCACCCAGATGGGCA
ASXL1	GAATCAGTGCGTATACAGCG	FHL3	GTAGGGATCTTCATCCCGGG	MGAT5	TGTTGACCTCAACAATCAGG	SLC46A2	ACTGATCAGGATCCAGAGTG
ASXL1	TAGCCTGCCTCAGGAAACTG	FHL3	ACAAAAGAACGGGAGCCCAG	MGAT5	AGGTCAACAGTCCACACATG	SLC46A2	TCTCTTTCACAAAAGCCAAG
ASXL1	ATAGCATTGAGGCATGCGAG	FHL3	CATGACAGTCTCCCCACAAG	MGAT5	ACGCTGAAGTTTTCATCGGG	SLC46A2	CGTAGGACGCCTTCACCACG
ASXL1	GAGGAGGCTGAAATCAAAAG	FHL3	GGATGAAGATCCCTACTGTG	MGAT5	GTCCCTTGTGTATGGCAAAG	SLC46A2	GATGAGAGCAAACAGCATGA
ASXL1	TAACGAGTTTTTTACCCATG	FHL3	AGCAGCCCTCGTGGAAATGG	MGAT5	GCTTGACCTGTAGGGCGCTG	SLC46A2	TTTGGACATAGCTGATCGGA
ASXL1	ATGCTACATTCCAATTCAAG	FHL3	TGACATACCGTGATCAGCCG	MGAT5	GTGGCCACATCACTTGCCCA	SLC46A2	TGAGTTTGGACATAGCTGAT
ATM	TTCATGGTCCAGTCAAAGAG	FLCN	TCACGCCATTCCTACACCAG	MID1	CTCCGATGATGAGTTCAGCG	SLFN11	GACCTGATCTCAGAGCACAG
ATM	CTCACCAGAGATATTGTGGA	FLCN	TGACAAGTGATGACAACCTG	MID1	CACGCTGAACTCATCATCGG	SLFN11	GTATATCGCAAATATCCTGG
ATM	GAACTGTCTCAGGAGTAGGA	FLCN	GATGCCCACAGCGTGCTCAG	MID1	ATGACACCATCACTGTGCAT	SLFN11	TGTCAGCTGAGTCTATCTAG
ATM	AGTTTTCCGTTACTTCTGCA	FLCN	GTGGCTGACGTATTTAATGG	MID1	TGACCACTTCCCAATAATGC	SLFN11	GTCCCTGCATTTGCAAACAC
ATM	TATTTGGTTTGAGAAGCGAT	FLCN	GGAAGGGCCAGGAGTTGATG	MID1	TGGCCGGCATTATTGGGAAG	SLFN11	TTGACCCTGACTCTTTGAGA
ATM	GGAAGTGATGAGAAACTCTC	FLCN	GGCTCCGGACACAGGCCTGG	MID1	ATGTGTTTATTGATAGTGGC	SLFN11	ATTCACAATTTTGAGTGTGA
ATP6V1G3	ACGGGCCAAGGACAAGCTAG	FLT1	TCTAGAGTCAGCCACAACCA	MITF	CAACTTTCGGATATAGTCCA	SLPI	AGATGTTGTCCTGACACTTG
ATP6V1G3	AAAGCGATTGAAGCAAGCCA	FLT1	AGGTTGAGGGATACCATATG	MITF	AACCATCTTAAAAGCATCCG	SLPI	GGGGGTTAAGCATCAAACAT
ATP6V1G3	GCGATTGAAGCAAGCCAAGG	FLT1	TAACTTGGAAAAAATGCCGA	MITF	ATTGATCTTTATGGAAACCA	SLPI	GCGTGACTTGAAGTGTTGCA
ATP6V1G3	TCAGGCAGAAAAACGGGCCA	FLT1	ACGTTACTTGGATTTTACTG	MITF	AAGTACCTAGTTCTTTAATG	SLPI	ACTTCAAGTCACGCTTGCAC
ATP6V1G3	TTTTCCTAAAACGAAGAGAC	FLT1	CGGGTCTGGAAACGATGACA	MITF	GGCCAAAGAGAGGCAGAAAA	SLPI	TGCCAGTCACTCTGGCACTC
ATP6V1G3	TATCTCTCTGCATTCTGTAC	FLT1	AGGATTTGTCTGCTGCCCAG	MITF	GTCCACGGATGCTTTTAAGA	SLPI	CTGGACACTGCCAGTCACTC
ATR	GAGCATGTGAAGTTACAATG	FLT3	GGTCATATGGAATATTACTG	MMP14	GGGATCCCTGAGTCTCCCAG	SLX4	CCTGCACTATCTCTACACTG
ATR	TTGACATTACTGCAGTGGAA	FLT3	GCCTTCAAACAGGCTTTCGG	MMP14	CCATCAACACTGCCTACGAG	SLX4	ATAGTGCAGGAACGTGCGGG
ATR	AATGGGTCCTATGGGAACAG	FLT3	TTTGCATATCAAGTTGCCAA	MMP14	GCAGCATCAATCTTGTCGGT	SLX4	GCTGGGTGACGTGAGCACCG
ATR	CTGACTTTGGTAGCATACAC	FLT3	AAACGAAGTCAAATTAGGGA	MMP14	TAGGCAGTGTTGATGGACGC	SLX4	TCTGAAACTGGACATCACTC
ATR	AACCACTCATGAAAAATAGG	FLT3	GAAGTCAAATTAGGGAAGGA	MMP14	GATGGATACCCAATGCCCAT	SLX4	GTTTCAGACGGACAGCGGGG
ATR	AAAAGACCCTCTGTTCCCAT	FLT3	ATATCAAGTTGCCAAAGGAA	MMP14	GCTCTCTTCTGGATGCCCAA	SLX4	GAGTGATGTCCAGTTTCAGA
ATRX	CAAACAGTGTGACAGCAGTG	FLT4	TATCTGCTCAAACTCCTCCG	MMP26	ATATATACTGTCTTTCACTG	SMAD3	CAAAAATAGCGCTGTCACTG
ATRX	TGAGAGTTGAAACTGACAGG	FLT4	AGCAGGCATAGACAAGAAAG	MMP26	TGTGTCTCCTGGGTAAGGAG	SMAD3	CTCGCAGCCATCCATGACTG
ATRX	AGTGAGGATTCAACCTCTTG	FLT4	TCTGAGCTCTGAGAGCTGCG	MMP26	TCTCGCCAGGAAGATGCAAG	SMAD3	GTGCGGCTCTACTACATCGG
ATRX	GGGGGTAAATTGGTCCCAGT	FLT4	ACCAGCAGTTCAGCATGATG	MMP26	GGAGTCGCCACTCCTTACCC	SMAD3	GCTCTACTACATCGGAGGGG
ATRX	GCTGAAATTATATCCTCAAG	FLT4	CTGCTGGTCCGGAGACCCCA	MMP26	GAATGGAGATGCAGACATCA	SMAD3	GTAGGAGATGGAGCACCAGA
ATRX	AGTTGGTATGTTGAAACGCA	FLT4	ACCTGCATTCTCGGAGCTGG	MMP26	GCGGATGGCTTCATATCATG	SMAD3	GGTTGACCGACTGGGCCAGG
ATXN7	TGTCCGGTGAGGAATACGTG	FOXF2	CACTTCCGCCTGAAGCCGCG	MRM1	GGAGAGTAGGCCGTTCCCAG	SMARCA4	CAGTGGACGTCAGCTCAGCG
ATXN7	AATGCCAGTAGCAGTACCAG	FOXF2	AAATCTTTTCTGTCACACAC	MRM1	GGTGGGCTGCCCAAGCACAG	SMARCA4	GAAGACCGACTGCAAGACGA
ATXN7	GTTACCGTTGAGGGGTAGGG	FOXF2	ATAATACGACCCGCTAGCTG	MRM1	GGGCTCAGGTCTATCCCAGG	SMARCA4	CGAGCTCATCCGCAAGCCCG
ATXN7	CAAATCGTTTTCTTCTACCC	FOXF2	TCGTTCCGCCGCCGGCCGCG	MRM1	TGAGTCCTTGAACGTCTCTG	SMARCA4	CGTTGAGGCTGCGGTACTTG
ATXN7	CACATTCCTTAACCCAGCGC	FOXF2	GAGTAGAGTGATGCTGGTAA	MRM1	TTCAAGGACTCAAGTCCAGG	SMARCA4	CATCCAGCTGCCCTCGCGAA
ATXN7	CCGAGCACAAAAACAAAACC	FOXF2	AGAAGGGGAAGCGCGCCTGC	MRM1	TTGCTGACTACTGGAGTGAG	SMARCA4	TCTCTAGGTCGTTGAGGCTG
ATXN7L3	CACAGCACACAGATGAGCAG	FOXH1	CTTGCGGAAGCATCGGTTGG	MRPL14	CAGATTCGACTCCAACAACG	SMC1A	GAGATTCGTAAGAAACTCGG
ATXN7L3	CAGATGGGGAGCAAAGCGGG	FOXH1	GATCATGGCCAAGTAGGTGT	MRPL14	TTATAGACATGGATGCAGCG	SMC1A	CTCATCCAGGACGAAGAAGG
ATXN7L3	TCTCCAGATGGGGAGCAAAG	FOXH1	GGCCAGCTTCAGTCTGCGGG	MRPL14	GTTGTTGGAGTCGAATCTGG	SMC1A	GAAGATCATAGATGAGACCA
ATXN7L3	AGAAGTGCCTGGGAATGGGT	FOXH1	GGAAGCATCGGTTGGAGGAA	MRPL14	GCTCAGCACTCTGCTTACAC	SMC1A	ATAGACTCCAATGAGGCTCT
ATXN7L3	CCCGAGAAAATAAATCCGTA	FOXH1	ATCGGTTGGAGGAAAGGTTG	MRPL14	CACTCTGCTTACACAGGTGA	SMC1A	TCAGCATCTGGCCAAGAAGT
ATXN7L3	ATGAGCAGAGGCGAACCGTA	FOXH1	CAAGCCCCCCTACACCTACT	MRPL14	TGGCTTTCTTTACTGGGCTC	SMC1A	AGGTCTCCTGGAACTTGTCT
AURKB	CAAGTCCCAGATAGAGAAGG	FOXJ1	TTGACCCCGAGTACGCGGAG	MSH2	GTCAGCAGAAGTGTCCATTG	SMG9	GCAGAACAAAGCTCGCCGAG
AURKB	ACAATGAGAAGGTGGATCTG	FOXJ1	AGCGTGGCATACGAGTAGGG	MSH2	CATAGTTAAGGTCTCTTCAG	SMG9	TGGGGAAGGTTGTACTCTGG
AURKB	TCTCTATCTGGGACTTGAAG	FOXJ1	GCGCATTGACCCCCAGTACG	MSH2	AGAGGAACTTCTACCTACGA	SMG9	CCTGCATTTCAACGTAAGTG
AURKB	GGGGGCGCATGCACAATGAGA	FOXJ1	TACGCGGAGCGGCTACTGAG	MSH2	TGCTAACCCAAATCCATCGT	SMG9	ACTTCTGTCCTCGGAAGCTG
AURKB	CCATTTCATCGTGGCGCTCA	FOXJ1	GCCAGGTGGGATCTGCGTGG	MSH2	AACTGGGGTGATAGTACTCA	SMG9	TCCGAGGACAGAAGTCCTCT
AURKB	GATGCTCTAATGTACTGCCA	FOXJ1	CCCTGTCGGCCATCTACAAG	MSH2	GACTGCATCTTAGCCCGAGT	SMG9	CCGATGAGCTGCTGGACTCG
BAP1	CAGCAATGAGAGTACAGACA	FOXO1	GGGTGACAGCAACAGCTCGG	MSH6	TGACATTCTAATAGGCTGTG	SMYD3	GGTCCGAGTACCATAGAACA
BAP1	AAGCACCTTGGAGATGTGGG	FOXO1	GGTGGCGCAAACGAGTAGCA	MSH6	TCCTTTAAGCTCTAAGAAGG	SMYD3	AGTCACATTCAAAGCAGTAC
BAP1	CTGCTAGTCTTGATGGACAG	FOXO1	GCCATTGCAGCTGCTCACGG	MSH6	AGAATTACTGGGCGACACAT	SMYD3	TCATAAGCAGCAATTCTGAA
BAP1	ATATGCGATTGGCAATGCCC	FOXO1	TAAGGGTGACAGCAACAGCT	MSH6	TGTTGCATGCATGAGTATGC	SMYD3	GGCAAACTGCAGCTACATCA
BAP1	GATTGGCAATGCCCCGGAGT	FOXO1	CGGGACGAGCTGCTCTTGCG	MSH6	TACTGCAACATTTGATGGGA	SMYD3	CAGCATATCCAGGTAGCAGA
BAP1	CAATGCCCCGGAGTTGGCCA	FOXO1	CACGAATGAACTTGCTGTGT	MSH6	ACGTCCCTGCTGAAGTGTGC	SMYD3	CACTGGTCATCAGCATATCC
BAX	GGGGGAGTCTGTGTCCACGG	FOXP1	TCCGACGCAACGCGGCCACG	MST1R	CGAGTCATTCACAGTCAAGG	SPEN	CCCCACTAAGGATCGCCCAG
BAX	CTCGGAAAAAAGACCTCTCGG	FOXP1	TGCTTACTTCCGACGCAACG	MST1R	TAAGGTCAAAAGGGTCAATG	SPEN	TCACAACATCCTCTTGGTCA
BAX	GGACACAGACTCCCCCCGAG	FOXP1	TGCATTGAGAGGTGTGCAGT	MST1R	GGTCAAAAGGGTCAATGTGG	SPEN	GCCCTGTGGCCGTGACCAAG
BAX	TTCTTGGTGGACGCATCCTG	FOXP1	TCCACGTGGCCGCGTTGCGT	MST1R	ACATGGGGCGATCCTTAGTGG	SPEN	CTCTGGGCGATCCTTAGTGG
BAX	AGCGAGTGTCTCAAGCGCAT	FOXP1	TGCATGTTTTTAATAAGGGA	MST1R	TGAGAGCCAGCACATTCGGG	SPEN	GCAACAACGTCCTGGCCCAT
BAX	CAAGCGCATCGGGGACGAAC	FOXP1	ATTAAAGATGCATATGTAAA	MST1R	GGACGAGTCATTCACAGTCA	SPEN	TCTGGCTCACAACATCCTCT
BBC3	ACCTCAACGCACAGTACGAG	FRAT1	GCCCACAGTCTCCGCCAACG	MTOR	ATGAATAGATTCTGGCACTG	SRSF4	CAATTACTCGCTCACCACAA
BBC3	TCCGCGGGGAGGAGGAACAG	FRAT1	TCGCGAATGAAGCCTTCGCA	MTOR	AGACGGTTTGGTGAAACCAG	SRSF4	TTGTGGAGAATTTGTCAAGT
BBC3	GCCGCTCGTACTGTGCGTTG	FRAT1	TCATCAAGGAGGCCGTCGCA	MTOR	GCAACAAGCGATCCCGAACG	SRSF4	GATGCTGTTTATGAACTGAA
BBC3	CAGCTCCCCGGAGCCCGTAG	FRAT1	CCATCAAGGTCGGCCTGAGG	MTOR	ATGAGCAGCTCAACTTGCGT	SRSF4	AGAGCTTTGGAAAAGTTGGA
BBC3	CATGGCCCGCGCACGCCAGG	FRAT1	TCATGCACCGGGGCCGACAG	MTOR	CTTCTCTCATGATGACACTT	SRSF4	CTGAATGGCAAAGACCTTTG
BBC3	TGCGGGGACCCCCAGGCCAG	FRAT1	TGCGAAGGCTTCATTCGCGA	MTOR	AGCACTGGCAGAGGTTTTCA	SRSF4	ATTTGTCAAGTCGGTGCAGC
BBS4	AGAGCTTGATTAGAGCCCAG	FTSJ3	AGAAGCCGTGGTGAACACAG	MUC1	GGGTGGTAGGAGTATCAGAG	SSR4	TGAGGTTAGATTCTTCGACG
BBS4	CCTGAAACGAGCCAACTACT	FTSJ3	GATGTCCACTGTGTTCACCA	MUC1	GCTTCTACTCTGGTGCACAA	SSR4	TAACCTCATAGGTGCCTGCG
BBS4	ATCAAAGGGTGCCAAGTAGT	FTSJ3	GTTGCCTGTTGGTAAGAAGG	MUC1	CTGTGATTGGAGGAGGTGAG	SSR4	CGCCCACGCAGGCACCTATG
BBS4	ATACAGAATCTTCCAATCAA	FTSJ3	TGCACGTCCCATCAAGAAGG	MUC1	TGAACTGTGTCTCCACGTCG	SSR4	ATGGCGGCGATGGCATCTCT
BBS4	CAGAAGGCATTTGAACATCT	FTSJ3	CATCTCAGAACGAGAGAAAG	MUC1	CAAGGCAATGAGATAGACAA	SSR4	GATGGCATCTCTCGGCGCCC
BBS4	CAAGATGTTCAAATGCCTTC	FTSJ3	AACCCGTCATCATCTGACTT	MUC1	GATCGTCAGGTTATATCGAG	SSR4	AGCGGGAGAGGCTGGACAGC
BCAR1	CAAAGCGCTCTATGACAATG	FZD1	GTGTAATGACAAGTTCGCCG	NBN	TCTGATCCTCCAATGATGTG	STAG2	TTAGTGGAATCAGCAGCCGG
BCAR1	TGGGCAGTACGAGAACAGCG	FZD1	CAGGAAGAACTTGAGCTCAG	NBN	AAACTTCCACACATCATTGG	STAG2	GATTCCACTAATGACTGACA
BCAR1	CATGGACACACGCAGCTGGG	FZD1	GTGGACGGCGATGTGCTGAG	NBN	TGGGAAGAAACGTGAACTCA	STAG2	GAATTTCGGTAAGACATCAG
BCAR1	GGCACATCATAGATGTCCTG	FZD1	CTTCGTGGGGCTTAACAACG	NBN	AACTCAAGGAAGACTCACTA	STAG2	GCCCAAAAGATTACGGCCTG
BCAR1	GTTGGAGTTTGCCCGCAGCG	FZD1	GCAAGACCCTCAACTCCTGG	NBN	AGAGTGGCTAAGGCAGGAAA	STAG2	ATAATAGTGGAGGTGAGTTG
BCAR1	CCGCAAGGGTGACATCATGA	FZD1	ACTTGTCATTACACACCACT	NBN	TCTACTTCCAGAAATCCATC	STAG2	GTAGTAGTAGTGACAGTATG
BCL2L11	AGGTAGACAATTGCAGCCTG	FZD3	AGTTAAAAAAGTAAACAATG	NCOR1	ATCCCCTTCTGAATGTACAG	STAT5B	CCGAATGGAGAAGTCTCTGG
BCL2L11	TTGTGGCTCTGTCTGTAGGG	FZD3	GGGGCATCTGGGAAACAACG	NCOR1	ATCAGAGTCACCTCCAACGG	STAT5B	ATTCAAGTCTCCCAAGCGGT
BCL2L11	AGTTCTGAGTGTGACCGAGA	FZD3	TCAATGCATCAACATCGTAG	NCOR1	AAGGCTACTTAGGAACGGAA	STAT5B	GCGGTCGGCTAGGGACCGAA
BCL2L11	TATGGATCGCCCAAGAGTTG	FZD3	AATCCAGATTCACCATAGGG	NCOR1	TTCTGGAATGTAGAAGTAGG	STAT5B	GCATCTGCAGATGCCGGGGG
BCL2L11	AGTTTAACGCTTACTATGCA	FZD3	GAACAATCCAGATTCACCAT	NCOR1	ACCATAGGCAGACGCCAGGG	STAT5B	GTACGTGGCGCTGCCGCCCC
BCL2L11	TGCAGGTTCAGCCTGCCTCA	FZD3	CTTGTGAACCTATTACCTTG	NCOR1	CTTTGGTATCTACACCTGTG	STAT5B	GGTACATGTTATAGTGAGCC
BCOR	GGGGTGGAGCCACTCTACAG	FZD7	GAGAACGGTAAAGAGCGTCG	NDUFV3	GTAGCTAGTCCCAGTCCCAG	STIP1	GCTTTGGAGGAGAAGAACAA
BCOR	ATTGCAGCGAAATATGCGGG	FZD7	GGACGATGGCTACCGCACGG	NDUFV3	GTTCCTGTTGAGAATAACCA	STIP1	CTTCAAAGAAGAAAAGTACA
BCOR	TTATAACATCCAAGTATCTG	FZD7	GTCGGGCTGCTACTTCATGG	NDUFV3	GGATCAGTAATGTCCACATG	STIP1	CAAACTCCTGGAGTTCCAGC
BCOR	TCTACCTGAGTACGTAGCCA	FZD7	GATAGTGATGGTCTTGACGG	NDUFV3	AAGCAAGTCCTCGAAACACC	STIP1	AGACTTGTTATAGAAATGGA
BCOR	TTATGGTGCTGACCCCACCT	FZD7	TGTACTTTAAGGAGGAGGAG	NDUFV3	GCCCCGTGTTTGCTGCGGCA	STIP1	GTACTTTTCTTCTTTGAAGT
BCOR	CACCATAAGAGAGAAGTAGT	FZD7	ACATGGAGCATAAGAAAAAG	NDUFV3	GGAATCAGGGAAGAGTGAAA	STIP1	AAACCCCGACCTGGCTTTGG
BLM	CAAACTGGAAAAATATGGTG	GAB4	AACACAGACTCAGAAGACAG	NEGR1	GGAAGGCTCTGGTTTCCCAG	SUMO1	GGAGGCAAAACCTTCAACTG
BLM	TGCAAGCTTCTTGAGAGTGA	GAB4	CACTGGTAACATCCACTACG	NEGR1	CAAACAAGTAAGAGTGACGT	SUMO1	ACCTTCAACTGAGGACTTGG
BLM	AGTGTCTCAGAGGGAAGAGA	GAB4	ACTCAGAAGACAGTGGAGAG	NEGR1	GGGAGGTGATAAGTGGTCAG	SUMO1	GTGTTCCAATGAATTCACTC

BLM	TCAATTTGAAGCAAAACCTC	GAB4	TGCATAGAAAGCTCTGTGAG	NEGR1	CATCTACATTCTGTATCTGG	SUMO1	TATATTAAACTCAAAGTCAT
BLM	TATTACAGAAATACTCTGAA	GAB4	CCAGCAGTTCAGCCCCGCCG	NEGR1	AGTGGCCTGATAAGATGTGA	SUMO1	AGAAACCTGAGTGAATTCAT
BLM	GAGATGGTTAAAAAATGTCT	GAB4	CTGTTGTTTCTCAGGTTGGG	NEGR1	TTGTACCATTCAAAGGCTGG	SUMO1	TTCACTCAGGTTTCTCTTTG
BRAF	GAACAGTCTACAAGGGAAAG	GATA3	CGAGGAGGCTCCACCCAGGG	NELFB	TCCTGCACATCACCAAGCAG	TADA1	AGATCGTACATGTTCACCGG
BRAF	GGCAGGAAGACTCTAACGAT	GATA3	CCACCACAACCACACTCTGG	NELFB	GGAAGGACATGAGCATCGGG	TADA1	AACGCGTGAGAATGGCCAGG
BRAF	TCCTGATGGGCAGATTACAG	GATA3	GGGCAACCTCGACCCCACTG	NELFB	AGTGTAGTCATCCACCAGGA	TADA1	GGGTTTTCCAGGTTTTGCTG
BRAF	CTCCAGATCTCAGTAAGGTA	GATA3	CCTCCAGAGTGTGGTTGTGG	NELFB	GTGGAGGAAGATGTCGCCAA	TADA1	TGACGTCAGTTGTGTCAAGA
BRAF	CCTTACTGAGATCTGGAGAC	GATA3	ACTGTGGCGGCGAGATGGCA	NELFB	TGAAAGTGTAGTCATCCACC	TADA1	TCTACCTGCATCTTTGCCTC
BRAF	CCTGTCTCCAGATCTCAGTA	GATA3	TCGCCGCCACAGTGGGGTCG	NELFB	GCCAAAGGCCAAGTCGCCAA	TADA1	AAAGCTTATCGGTTACGAGA
BRCA2	GTACAAATGGGACTAACAGG	GLI1	CCGTATGTATGTAAGCTCCC	NELL1	CAATGGGAAGCCAAGGACAG	TADA2B	GAGTCCGGGAAGCACCAACG
BRCA2	TTGCTGCAAGCAACCTCCAG	GLI1	GACGCACCTGCGGTCACACA	NELL1	AGAGGCACTTCCTTACCGCA	TADA2B	TGCTTCCCGGACTCCCCAAG
BRCA2	AGAAGGCATTTCAGCCACCA	GLI1	CCAGGGAGCTTACATACATA	NELL1	ACCGCATGGCAGATGGACAA	TADA2B	GGGCGGCTGGACCAGTCGCG
BRCA2	CATCTGGGCTGAGACAGGTG	GLI1	TCGGTCACTGGCATTGCTGA	NELL1	CCAGATACCAACCTTCCCCC	TADA2B	TCCGAAGCCGAACTGCTCGA
BRCA2	TGCATGCAAATGATCCCAAG	GLI1	GCTAGGATCTGTATAGCGTT	NELL1	ATTGATTCCTGGGGGAAGGT	TADA2B	GCGACTGGTCCAGCCGCCCT
BRCA2	CTGAAGTGAAGGGGCTCCCG	GLI1	CGAGGCGTGAGTATGACTTC	NELL1	ATAAATTGATTCCTGGGGGA	TADA2B	CGTAATGCTCCATCACCTCT
BRD9	CTCCTGGACCAGATCACAGG	GOT1	ACAGGCGTGGAGGACAACAA	NF1	ACCACTGGCCACTGTAACAG	TAF5L	AAACAGTCCGAAGAGCACAG
BRD9	CGCCTGTGATCTGGTCCAGG	GOT1	AATGTCTTTAAAACCAGCAG	NF1	TCGTTGATCAAACTCATCTG	TAF5L	AAGTACAGTTTGGACGACTG
BRD9	GAGCTGCTCTACTCAGCCTA	GOT1	TACTGGGATGCAGAGAAGAG	NF1	GAGTTCGTCCACTGTTACAG	TAF5L	ATTCCTAGATAACAAGTACG
BRD9	GAAGCACAGGCGGAGCGCGG	GOT1	GACAGGTAATGTGAAGACAA	NF1	TCCACTGTTACAGTGGCCAG	TAF5L	GGTAGACAAAGAGAGGATAG
BRD9	AGTATTTGGCGACTTGAAGT	GOT1	AGGACAACAATGGAGAACTC	NF1	ATGTGGGTGCTGTTGTGATG	TAF5L	AGTGTCTGCAGCCCCTTGCC
BRD9	CCCTGTCCAACGCCTCCGAG	GOT1	GATCATTCAGGAAGCCCTGG	NF1	GACTTTGGGAAACACAACAC	TAF5L	AGGGGCTGCAGACACTATGT
C2CD4A	AGTACTGTCCGGGAACCGGG	GP6	ACGGTGACCGCCGCCCACAG	NFE2L2	CACATCCAGTCAGAAACCAG	TAF6L	GCTCCATAGTGGCAGCAGAG
C2CD4A	GAGCACATTTGCGCACGCGG	GP6	TAACCCTACAGTGTCAGACT	NFE2L2	TAATTCGGGATATACGTAGG	TAF6L	GTGGCTCCAGGACACAGTAG
C2CD4A	GAAGGCACTCAGGACCCAAG	GP6	GGAGAAGCTGTAGCATCGGT	NFE2L2	TATTTGACTTCAGTCAGCGA	TAF6L	GAGTCCAGTGGTCATTCAGG
C2CD4A	AGTGCTGCATTGCCGAAGCG	GP6	TACCGCTGCTCCTACCAGAA	NFE2L2	GGACATTGAGCAAGTTTGGG	TAF6L	AAGAGCATGCAGCCCCACCA
C2CD4A	CAGGTGCGGCAGTGACAGCG	GP6	GAGTATCACCGCCAGTCCAA	NFE2L2	CATTAATTCGGGATATACGT	TAF6L	TGAATGACCACTGGACTCTG
C2CD4A	GTGCGCAAATGTGCTCACTC	GP6	CCAGAGGCTTCCGTTCTGGT	NFE2L2	TAGGAGGGGTAAGAATAAAG	TAF6L	ATAGCAGGATATGCTGATAG
CACNA1H	GCTGTTCCGCGTGTCCACGG	GPX3	ATACGTCCTCTTTGTCAACG	NKX3-1	GGTCGTTCTGCGCCCCGGCG	TBX3	TGTCATTGGCTCTTACAATG
CACNA1H	GCTGCGCGAGTGCTCCCGTG	GPX3	TTAGGGACAAAGCCTCCACC	NKX3-1	GATCACCTGAGTGTGGGAGA	TBX3	AAAGAGGATGTACATTCACC
CACNA1H	CTACTTCGTGACCTTCGTGC	GPX3	CCCAGAATGACCAGACCGAA	NKX3-1	TCCTGCGGGACGGCGCGCAG	TBX3	CCGACCCCGAAATGCCAAAG
CACNA1H	GGCCATGCCGAAGTTGCTGA	GPX3	AGCCCTCACCATTGATGGGG	NKX3-1	GCTGTCTCTGGCTGCTCGTG	TBX3	CATCCACTGTTCCCCAGTAG
CACNA1H	TCAGGCAGTGCTTGTCCTCA	GPX3	GGCCAGCTACTGAGGCCTGA	NKX3-1	CCACACTCAGGTGATCGAGT	TBX3	AGGGAGTTTCAAGATGTCAT
CACNA1H	TACGGGCATGCGCGCCCTGC	GPX3	AGAGCTTGCACCATTCGGTC	NKX3-1	CCAACTCGATCACCTGAGTG	TBX3	TTCGGCCATTTCCAGTGTCC
CACNG8	GAAGATCAATCATTTCCCGG	GRHL1	CGGGCCAGCTTGGTAGAAGG	NME6	AGTGTTCCGAGCACGCCATG	TCF25	CGGCTTCCTTGATCTCAGAG
CACNG8	CTTGGACTTGTAGACGCGGG	GRHL1	AAGTCATCTTCTGTGCCGTA	NME6	CAGTGAGGCCGAAACTCCCA	TCF25	AAACCCCATCACAGACTGCG
CACNG8	CCCGCGTCTACAAGTCCAAG	GRHL1	CGCTTGTGAGAGGGAAGCAG	NME6	AGGATGCCATCCAGCTCTGG	TCF25	GAGTAGATTGTGTCCGAAGG
CACNG8	TCCTCTTGGACTTGTAGACG	GRHL1	GATATCCATTCGCTTGTGAG	NME6	TTTTTTCTATCAGAGGCTGG	TCF25	TAGGAGTAGATTGTGTCCGA
CACNG8	CGTGAAGATCAATCATTTCC	GRHL1	ATGAGTGCCCCGCTGCAAGT	NME6	CATGCTCTCGGTAAAACCTC	TCF25	TGATCTCAGAGAGGATCACA
CACNG8	TGGTCGTAGTCCGTGTCCTC	GRHL1	GTCTTGAAAAGGGGGCCGTA	NME6	GCGTTTTTTCTATCAGAGGC	TCF25	CAGAGAGGATCACATGGCGG
CADM1	CGATATCCAGAAAGACACTG	GRIN2A	CAGCTTCGTCAAGACCACAG	NOP10	TCATCTGGGGAGAACCGAGC	TCF7	TGTGCACTCTGCAATGACCT
CADM1	CTATGTTTGAAGCTTCACAG	GRIN2A	GATGAGGCTAAGGGCCATGG	NOP10	CTCGATCTCCCTGCTCGTTG	TCF7	CTGCACATGCAGCTATACCC
CADM1	AGCCAGCCACGACTATCAGG	GRIN2A	AACTGGAAGAAGGTAGACGT	NOP10	CCAGTATTACCTCAACGAGC	TCF7	ATGAGCTGGCCCGCAAGGAG
CADM1	TTTGAACCACCTGATAGTCG	GRIN2A	GCTCTACTGTTCCAAAGACG	NOP10	CTGGGGAGAACCGAGCAGGA	TCF7	TGTACAGCATGAAGGCATTG
CADM1	GTGGTGTAACTTTCCTGTGG	GRIN2A	GGCGGGCGTATTCTACATGC	NOP10	CACCATCAAGAAACGCTTCA	TCF7	GAGAGGTCAGGGGTCTGCAG
CADM1	ATGGTGGTGTAACTTTCCTG	GRIN2A	GGCAGATCCCAGTGAGCCAC	NOP10	CCTGCTCGTTGAGGTAATAC	TCF7	GAGCTGCCCCATGCTGCCTG
CAMK2D	AGTTTGTTGAAGAAACCAGA	GSG1L	TGTGGGCGACCATTCCCAGG	NOTCH1	GTTCTTCAGGAGCACAACTG	TERT	CCCCCAGGACAGGCTCACGG
CAMK2D	GAGTTCAAATACAACAATTG	GSG1L	CTTGGTGTAGGAGTTGAGCG	NOTCH1	ATCAGAGCGTGAGTAGCGGG	TERT	TGACCCCAGGAGTGGCACGT
CAMK2D	CTGATCGAAGCTATCAACAA	GSG1L	GGGCAGGGTATCTCTCGTGG	NOTCH1	GGCATCCACATTGTTCACGG	TERT	TTGACAAAGTACAGCTCAGG
CAMK2D	TGCTTCCATGATGCACAGAC	GSG1L	CCCATTCCTGGGACTACGGG	NOTCH1	CCTGGAGACGGGCAACAGCG	TERT	GAACAGTGCCTTCACCCTCG
CAMK2D	GCTTTGGGTAATTTAGTGGA	GSG1L	CGCCCACATGATGTACACGC	NOTCH1	CGTCGGCGTGTGAGTTGATG	TERT	GGAGTGGCACGTAGGTGACA
CAMK2D	TGGTTTCTTCAACAAACTCT	GSG1L	GAAGAGGGACGGGAGCGAGG	NOTCH1	ATGAAGTCGGAGATGACGGC	TERT	ATCGTCCAGGCCCAGCACAG
CAMSAP3	TCCCCACCTCAGAACAACAG	GSK3B	GAATGTGCACAAGCTTCCAG	NOTCH2	AGAACTGATCAACTGCCAAG	TET1	CCATCACAGCAGTTGGACAG
CAMSAP3	ACGTGGGCCTCTTCACCCCG	GSK3B	CCGACCCCGAACTCCACCGG	NOTCH2	CCAAGCGGATGTGAATGCAG	TET1	GAGGAATAACACCCAAAGAG
CAMSAP3	AGCAGTGTGATAGGGCATTG	GSK3B	TTGGTGTATACTCCAGCAGA	NOTCH2	CCACTGCATTCACATCCGCT	TET1	GAGCTCTGTGTATAGCCGGT
CAMSAP3	CCTATCACACTGCTGCCTGG	GSK3B	TGGAAATGGATCATTTGGTG	NOTCH2	GGCAGCTGCTGTCAATAATG	TET1	TCATGTTGTGAATGTCCCTG
CAMSAP3	GTGGGCCTCGTTGGCCACAG	GSK3B	TATACAGACACTAAAGTGAT	NOTCH2	GTTGTCCTGCATGTCTCGGT	TET1	GATCAAATCTGGGGCCATCG
CAMSAP3	GCTGTTGTTCTGAGGTGGGG	GSK3B	GCTCCCTTGTTGGAGTTCCC	NOTCH2	TGGGGCCAACCGAGACATGC	TET1	GCTTATAAAGAGGTAGCACA
CARM1	CAACCTGACGGACCGCATCG	GSTM5	CTGTGTATTCCAGGAGCAAG	NOTCH3	GGTTGCTGCTGACATCCGCG	TET2	GGGCTGGATCCAGAAACCTG
CARM1	AGGGGTTTTTCAGATCCAGG	GSTM5	TGTGGAAAAGAAGTACACGC	NOTCH3	CTCAACGGCACTGATCCTGG	TET2	AGAATTTGGAGGAAAACCTG
CARM1	GGTGAAGAGTAACAACCTGA	GSTM5	CTTCATGTCAAGGACATCAT	NOTCH3	AGCCCCCTGGCAGATCAGGT	TET2	TTTATACAAAGTCTCTGACG
CARM1	AGCACCTACAACCTCAGCAG	GSTM5	GAAGTCCTTCAAGTTTAGGA	NOTCH3	CCCGTGCTGATGCAGCCAAG	TET2	CAGGAGGAGAAAAAACGGAG
CARM1	CTCCCACTACACATCTCCCT	GSTM5	CAAATATACGCTTCATGTCA	NOTCH3	CCGCATGGCAGATGGCTCAA	TET2	GACTTGCACAACATGCAGAA
CARM1	CGTGGTCATCCCGGGCAAGG	GSTM5	CCACGCCATCCGCTTGCTCC	NOTCH3	ACCAATGCCCAGGACCACTC	TET2	ATATGTTGGTGCCATAAGAG
CASP14	GTGAGCCATGAGTACCACGA	HAGH	TCGGGACTGAAGGTGTACGG	NOTCH4	CCGGGTGGTCAGGGCCACAG	TFAP2B	CATGTCTGTCAACACCGGCG
CASP14	CACACAGTATTAGGGCCAGG	HAGH	GATGTGTAAAGCTCTGCTGG	NOTCH4	GGTGTGGATTTGTCCCGCTG	TFAP2B	CCGAGTGGTAGTCCCTCCGG
CASP14	GACCCCGGTGAAACAGTAGG	HAGH	GAAGTTCTATGAAGGGACTG	NOTCH4	TGCAGCCCAAGCAGACGTGG	TFAP2B	TTCGAAGTACAAAGTAACTG
CASP14	AGGTGGAGATGAGATTGTGA	HAGH	AACAAATGTGTCCTGAAGTG	NOTCH4	TGAGGGTGGACAGCCAGCAG	TFAP2B	CGCCGAGGAGAGATGCATTG
CASP14	AGGGACCCCGGTGAAACAGT	HAGH	ATGTGTCCTGAAGTGTGGCA	NOTCH4	GACATCCCAACCATGCCCCT	TFAP2B	TCTCGGGCCTTGACCCCCGG
CASP14	TGGTACTCATGGCTCACGGG	HAGH	CCCGCAGCCAGCCACAAACA	NOTCH4	CCACTGCAGTTTGTCTGCTA	TFAP2B	GCAGCAGCACGTCCGGCCGG
CASP3	TGTGGCATTGAGACAGACAG	HEATR1	CTCGGAAAGTTTGACAACCA	NPM1	GCAGAGGCAATGAATTACGA	TFAP4	AGATCGCCAACAGCAACGAG
CASP3	CGTGGTACAGAACTGGACTG	HEATR1	AGGCGGTTAGCTGAGACTGA	NPM1	CAGTCCAATTAAAGTAACAC	TFAP4	GCTTCTCTCCGTCTGTGTGG
CASP3	GGCGTGTCATAAAATACCAG	HEATR1	CATTGACTGTCTAGTAGCCA	NPM1	CAGTTTAGGGGCTGGTGCAA	TFAP4	ACCCTCATCCCCCACACAGA
CASP3	AGTTTCTGAATGTTTCCCTG	HEATR1	TAAAATGCTGGGTATCAAAA	NPM1	CAAAGATTATCACTTTAAGG	TFAP4	AGCCGAGTACATCTTCTCCC
CASP3	AAAATAACAAACTTTTTCAG	HEATR1	TCTGGAGGAAGTTGGAAAAA	NPM1	GCACAAAAGTCAAATCAGAA	TFAP4	AGATGTACTCGGCTGTCTGC
CASP3	GAAACTTGAAATATGAAGTC	HEATR1	TCTCTTTACTTATAAAATGC	NPM1	GACTTTTGTGCATTTTTGGC	TFAP4	CTCGGCTGTCTGCTGGAGAA
CASP6	AGTACAAAATGGACCACAGG	HECW1	GGATCACAAGATGCCCATCG	NQO1	TCGTACTGGCTCACTCAGAG	TGFB1	GCTGTACATTGACTTCCGCA
CASP6	ACTTAACACTGCCAGAAAGG	HECW1	GCTTCTGCATAGAGAAATGG	NQO1	GAATGACATTCATGTCCCCG	TGFB1	CGGAGAAGAACTGCTGCGTG
CASP6	CAAAGCAATCGGCATCTGCG	HECW1	CCACCGCAGCCCAGAACCAG	NQO1	TTTGAAGAAGAAAGGATGGG	TGFB1	GTTAAAAGTGGAGCAGCACG
CASP6	GTCTTCCTGAGCCATGGCGA	HECW1	TGACCTGGAATATTTGGATG	NQO1	CATGGAGCCACTGCCACCAG	TGFB1	CAGGGATAACACACTGCAAG
CASP6	AAAAGTACAAAATGGACCAC	HECW1	CCAGAGTTTGCAGTGGATGA	NQO1	GGACTCCAAACCACTGCAGG	TGFB1	GGGTTCACTACCGGCCGCCG
CASP6	AAATGTGATTGCCTTCGCCA	HECW1	CCGGGGCTGGGAGATCAAAA	NQO1	CTGGAATATCACAAGGTCTG	TGFB1	GCTGAGGCTCAAGTTAAAAG
CASP7	TCCTCGATACAAGATCCCAG	HESX1	CATGTCCCAAATCCTCCCAG	NSD1	TCAGATTGAGACAGTCTGCG	TGFBR2	CACATGGAGTGTGATCACTG
CASP7	GAACCGTGGAATAGGCGAAG	HESX1	AGCTCAAAAATTGAATCTAG	NSD1	CCCAACCCCGCTGTAATGTG	TGFBR2	CAGAGCCATGGAGTAGACAT
CASP7	GAAGCACTTGAAGAGCGCCT	HESX1	TCTTCTCTAATATCGATACC	NSD1	GTCCCAAAGGAAACTATGCT	TGFBR2	GGGAAAGCCCAAAGTCACAC
CASP7	AGACAATCACGTCAAAACCC	HESX1	TTTTGAGTAAAAGCAGTTCT	NSD1	TTAGTGCAAAAAGGCCTACA	TGFBR2	ATGGAGTGTGATCACTGTGG
CASP7	TCCACTGGGATCTTGTATCG	HESX1	TAAAAGCAGTTCTTGGTCTT	NSD1	ATCATTGATGCTGGTCCCAA	TGFBR2	CGCACCTTGGAACCAAATGG
CASP7	TCCATGGCTTAAGAGGATGC	HESX1	TTTAGAGTAAACTGCTATCC	NSD1	ACATTCTAGGTTGTAGTTGA	TGFBR2	CCCCTGTGTCGAAAGCATGA
CBFB	GAGAGACAGATTGGTTCCTG	HEXA	TATACGGTTCAGGTACCAGG	NTRK1	CTGGTACCAGCTCTCCAACA	TJP1	GGCATATTTAACAGCAATGG
CBFB	GGAGTCTGTGTTATCTGGAA	HEXA	GAGGAAGAAAGGCTTCGGTG	NTRK1	GCCCACTAGACAGTTGCGTG	TJP1	CCTCAAGGAGCCATTCCCGA
CBFB	AAGTCGACATACTCTCGGCT	HEXA	CACAGCACAGGATGTGAAGG	NTRK1	TCGGCAGGACTCCAGCGTG	TJP1	TGGGGACCACACATCACCAA
CBFB	GTCTCATCGGGAGGAAATGG	HEXA	CTGGTCCCCAGGACAAAGTG	NTRK1	TCTAGTGGGCCAGGGACTGG	TJP1	CTGAGTCCTTTGGTGATGTG
CBFB	CGATTTCCGAGCGGCCGTCG	HEXA	AGGAGGTCATTGAATACGCA	NTRK1	CGCAGCGACCTGGCTAGCCA	TJP1	CCTTTCTCTTTATCTAAAGG
CBFB	AGCACAACAGGCCTTTGAAG	HEXA	ACTGGGATTCACTGGTCCAA	NTRK1	CTTACGGTACAGGATGCTCT	TJP1	TTGGTGATGTGTGGTCCCCA
CBL	GCAGCCATGAGTCTCCAAGG	HGF	TAATTGCACAGTACTCCCAG	NTRK3	GCTGGTGAATGTGACGAGTG	TLE2	GTGGTTTGTGAGCACCGGGA
CBL	AGATATCTGAGAGAGTTCGG	HGF	GGGATCATCAGACACCACAC	NTRK3	AATGTGACGAGTGAGGACAA	TLE2	GCTGGTATTTCTCCGGCTTG
CBL	ATCCAGAGACAACCAGCCAA	HGF	CTATGATGGCCTATTACGAG	NTRK3	TCATGCCATCAACTTGACGC	TLE2	ATATTTCCGATTACGGCACT
CBL	GATTACTAAAGCAGATGCTG	HGF	AAATGCAGCCAGCATCATCG	NTRK3	CTATCCAGTCCACATCAGGA	TLE2	GGACGGTGGTTTGTGAGCAC
CBL	AGATGAGGGACAGTTTGGTT	HGF	TTTCAGGCAAGAATTTGTGC	NTRK3	AACGCTGTTATCACTTGCAA	TLE2	GGAGAAGCAAACCTTGGCGT
CBL	TCTCCCTGAAAGAGTCCACT	HGF	CCCTTCAATAGCATGTCAAG	NTRK3	TGGATCACCCCTTCCTGATG	TLE2	CCGATTACGGCACTCGGCTC
CBX3	ACGTGTAGTGAATGGGAAAG	HHIPL2	GTGGGGAAGTCAGTCACTGG	OPN4	TGTGGCGTCCAAGAGGCGTG	TLE3	CCCATGATGGCACCAAACTG
CBX3	ATTGGTGCCACAGACAGCAG	HHIPL2	CCTATGGGATCAGGAACATG	OPN4	AGGGCAATGGCGAGTCCCTG	TLE3	TCCTCCAAGACCAAAGACCT
CBX3	CAATTCTCCACTGCTGTCTG	HHIPL2	ACTGGAGGTTATGTCTATCG	OPN4	AGATGATGATAAGCAGAGGG	TLE3	TGCATAGACATCTCCCATGA
CBX3	TCTTTCAGGATCAAGACCTC	HHIPL2	GGGCAGGCTCACATGGCAAG	OPN4	CCTTTGGTGTGGCGTCCAAG	TLE3	GGAAGGTGTGCTACTGGAAG
CBX3	CTAGATCGACGTGTAGTGAA	HHIPL2	AAACTATGGCTGGAGAGCAA	OPN4	TGCGAGTTCTATGCCTTCTG	TLE3	TTGTCCAGCCCATTTTCAGG
CBX3	GGAATATTTCCTGAAGTGGA	HHIPL2	TGACTGACTTCCCCACTGCA	OPN4	CTGGGCTCCCTATTCCGCTG	TLE3	ATGGGAGATGTCTATGCAGC
CCDC170	GCAGAAAATAGCCCAGCTGG	HIST1H3A	CTCCTGCAGAGCCATCACAG	OTC	TCGATCACTAGTGTTCCCAG	TMEM50A	GTATCGAATGGACAAGTCCG
CCDC170	GTTGTCCCTCTCAACCACCA	HIST1H3A	TTTACGAATAAGCAGTTCAG	OTC	TCTGGGAACACTAGTGATCG	TMEM50A	CTTCACTGTAACTATCACCT
CCDC170	ACTGGATACCACAGAACATG	HIST1H3A	CTCGCACTAAGCAAACTGCT	OTC	GTGTAAAAATGTCCAGTCAG	TMEM50A	AACCACTCATACCATGCCTG

CCDC170	AGCTGAAATGGAGAGCTACA	HIST1H3A	CAAGGCGCCACGCAAACAGT	OTC	GAACACTATAGCTCTCTGAA	TMEM50A	CGAGGTGATAGTTACAGTGA
CCDC170	CTGAACTCTGTCTCTCAAAG	HIST1H3A	TAAACTACCTTTCCAGCGCC	OTC	AAGCGGCTCCAGGCTTTCCA	TMEM50A	GTGGTTGAAATCTTTCATGG
CCDC170	GGCCAGAAACATGATAGAAG	HIST1H3A	CCTGCGCAATCTCGCGCACC	OTC	ACAATCAGATTTGGACACCC	TMEM50A	AGATGCAATCAGAGATCCAA
CCDC34	ACCAGAGATGATGACTTGTG	HIST1H4L	CATCTCAGGCCTTATATACG	OTOP3	GCTCTACCAAGATCCCCACG	TNFRSF14	CCCTCCGGACGTCACCACGG
CCDC34	AAGCCGCCTGACACCATGGG	HIST1H4L	CGCCAAAGCCATACAGGGTG	OTOP3	TCTTGGTAGAGCACGGCGTG	TNFRSF14	TGAGGGTATTGTCTCCTCCA
CCDC34	ACACCTCCCATGGTGTCAGG	HIST1H4L	CCGTGCCAGGCGTCGGATGG	OTOP3	CTGAATGTGGTGTTCCTGGG	TNFRSF14	AGCTCTGCCGTCCTGCAAGG
CCDC34	CCTTTTATAATCCAATTCCG	HIST1H4L	CTCCACGCCGTGCCAGGCGT	OTOP3	GGCTCACATCGTAGCCCACT	TNFRSF14	TACTCGTCCTCCTTGCAGGA
CCDC34	GTATTCTGCACAGAGTTCCA	HIST1H4L	TAACGCCTCCACGCCGTGCC	OTOP3	CTGCCTCAACATCTTCCGAG	TNFRSF14	ACACAGGGTGTCCTGACTCT
CCDC34	TAGCTCTTTGCAGCTGGACG	HIST1H4L	CGGAGTTCTTAAAGTGTTTT	OTOP3	AGCCCACTCGGAAGATGTTG	TNFRSF14	TGGGTACTCGTCCTCCTTGC
CCND2	GTAAATGCACAGCTTCTCCG	HMOX1	TATCACCCTCTGCCTGACTG	PALB2	TGCTTGGCCTGACAAAGAGG	TOP3B	CCAGCGCAACTATGTCACGG
CCND2	CCAGTTGCGATCATCGACGG	HMOX1	CAGAGAAATGCTGAGTTCATG	PALB2	CCCTAAGACGACTCTCAGCG	TOP3B	AAAGTTCTCAGGGTAGTGGG
CCND2	ATGTGCTCAATGAAGTCATG	HMOX1	CATGCCCCAGGATTTGTCAG	PALB2	CTGTGCTTGGCCTGACAAAG	TOP3B	ACGCCATGCAGACGGCTGAG
CCND2	TGAAGGTCTGAGCATGCTTG	HMOX1	TTTGTCAGAGGCCCTGAAGG	PALB2	TCTACGGAACAGGAACCTGA	TOP3B	GGAAAGAAAAGGCCAAGCAG
CCND2	CTTCCAGTTGCGATCATCGA	HMOX1	CCATGCAGCGCTATGTGAAG	PALB2	ACCGGCTCTTTCCCAAAACA	TOP3B	CTGCCAGCGCAACTATGTCA
CCND2	CATGAGGAGTGACAGCTGCC	HMOX1	GTCACCCAGGTAGCGGGTGT	PALB2	AGTGGGAAAAACTTTATACC	TOP3B	CAGGACGATGCCGAGGTTGG
CDC34	CCACTTCCTGTACATCACGG	HNF1A	GCAGAAGAACCCTAGCAAGG	PARP1	GATGTCCACCAGGCCAAGGG	TP53	GCAGTCACAGCACATGACGG
CDC34	TTTCCACTTCCTGTACATCA	HNF1A	GCAGAAGTACCCTCAAGCAG	PARP1	CTACAAGCTGCAGCTTCTGG	TP53	CAAGCAGTCACAGCACATGA
CDC34	CATCTTGGTCAGGAACCGAA	HNF1A	AGACACGCACCTCCGTGACG	PARP1	TTCATAACCGAAGATTGCTG	TP53	TGGGAGAGACCGGCGCACAG
CDC34	TCAGGAGGGAGATCACACTC	HNF1A	GGAGGAGCGAGAGACGCTAG	PARP1	ACATATCAGCAAGTTACCCA	TP53	CCTCGCTTAGTGCTCCCTGG
CDC34	CCGGTGGACGACCCCCAGAG	HNF1A	GGAGCGAGAGACGCTAGTGG	PARP1	CTGTCTGCATTGTTCAGGAG	TP53	TATCTGAGCAGCGCTCATGG
CDC34	TATCTCCATCCTCCACCCGC	HNF1A	GAAGTACCCTCAAGCAGCGG	PARP1	GCGCATGTCCTGGAGAAAGG	TP53	GGTGAGGCTCCCCTTTCTTG
CDCP1	GGTTCCGATCCTGACCACGG	HS2ST1	TGGGCGGCATCATAATCCTG	PBRM1	AAACGGAAAATCAACATGAG	TP73	GCTGGAAAGTGACCTCAAAG
CDCP1	CAAAAAGCAAGGTCTACCTG	HS2ST1	CATAGAAAAAGTTTTGTGCG	PBRM1	TCCATTCTGTCCCCACCAGG	TP73	CATGCCTGTTTACAAGAAAG
CDCP1	CGGCCGAATCGATGCCACCG	HS2ST1	AGTGGGGAGTTTCTTCTCTG	PBRM1	GCTTGTCGCTCTCATTGTAG	TP73	CAGTAGAGTTTCTTCAAGAG
CDCP1	TCTAACTGCAGCCCCACGAG	HS2ST1	CATGCCGTTCGAGAAAAAGA	PBRM1	TTTCAGTTGGCCTGCAGGAG	TP73	TGCGGCCCTCAAAGGACCGG
CDCP1	CACCGTCAGACCCTGCCTGG	HS2ST1	CACCGCCAGCAGCTGCAACT	PBRM1	TCAAGGACTTCCTCTCCTGC	TP73	GGAAAGTGACCTCAAAGTGG
CDCP1	ACTTTCTTTAAGGAGCGGAG	HS2ST1	CGCGGTGGCGATGCTCTTCT	PBRM1	CGAAAGAGTAGTCTGGGTGT	TP73	TGAAGTCCCTCCCGAGCTCG
CDH1	GTGAAGGGAGATGTATTGGG	HTR1F	AGTAAATGGTGGAAACAATG	PDCD1	GCGTGACTTCCACATGAGCG	TRADD	GCGCTGCGAAATCTGAAGTG
CDH1	TCAATGATGTTTATGACCTG	HTR1F	TCCAAATGTTGAGTAAATGG	PDCD1	CGGCCAGTTCCAAACCCTGG	TRADD	TCCGACAGAGAGGGCACCGG
CDH1	ACACACGCTGACCTCTAAGG	HTR1F	TCGCTGCAATTATTGTGACC	PDCD1	CGTGTCACACAACTGCCCAA	TRADD	AAATCTGAAGTGCGGCTCGG
CDH1	TTCACAGCAGAACTAACACA	HTR1F	TGGTGCCTCCAGAATAGAGG	PDCD1	GCAGTTGTGTGACACGGAAG	TRADD	CTTCCTCCGCGCCTACCGCG
CDH1	CAACCCTCATGAGTGTCCCC	HTR1F	ACCACAAGAGACAAGCAAGT	PDCD1	GGACCCAGACTAGCAGCACC	TRADD	TTCTGCGGGCGGCAGCCCTG
CDH1	CAGGGCGGGGAAGATACCGG	HTR1F	CCTCTATTCTGGAGGCACCA	PDCD1	AGCCGGCCAGTTCCAAACCC	TRADD	CGATCAGCTGCGGGTCGCTG
CDK6	AACACTCCAGAGATCCACGG	HTR6	GCAGCACATCACGTCGAAGG	PDGFRA	CTCCCGAGACAGGAGTACCG	TRAF2	TGTCTGCGTATCTACCTGAA
CDK6	ATGATGTTTCAGCTTCTCCG	HTR6	GTTGGACGTGTTGCGCAGCG	PDGFRA	CCGAGACAGGAGTACCGTGG	TRAF2	CGTATCTACCTGAACGGCGA
CDK6	GTCCAGCTACGCCACCCCG	HTR6	GCGAGAGGATGAGCAGGTAG	PDGFRA	TTCAGCCAGGATATCCTGGG	TRAF2	CAGGAAGCGCCAGGAAGCTG
CDK6	GTAACAGATATCGATGAACT	HTR6	CAGGACCCCACGCCCAGGGG	PDGFRA	ATTAAAGCTGATCCGTGCTA	TRAF2	GCCCGAATGACGCCCTGCTG
CDK6	TGGAACTTTATCCAAGTAAG	HTR6	TCACAAAGAACATGCCCAGC	PDGFRA	CACTGAGATCACCACTGATG	TRAF2	GGGAGAAGATGGCGGGTATG
CDK6	ACTCCAGAGATCCACGGGGG	HTR6	GGCCACAAAGAAGGGCAACC	PDGFRA	AACATTTTGTTGTAGAGGTG	TRAF2	AAGCGCCAGGAAGCTGTGGC
CDK8	AATATTTCACTGTCGACAAG	HUS1B	CTGGTGGAAGCAAACCTCAG	PDGFRB	AGGAACGTGCTCATCTGTGA	TREX2	TGCCGAGGCTGTAACCCTGG
CDK8	ATACTTGATAAGGCTGCAGT	HUS1B	ACAGCAAATACATCCTACGA	PDGFRB	GACTCGAATTACATCTCCAA	TREX2	AATCATAATCAAAGCCATTG
CDK8	TCCTTATCACCATGACCAGC	HUS1B	CCTGAGTATAGAGACGGAGG	PDGFRB	GCTAAGCTACATGGACCTCG	TREX2	GGCTGGCTTTGATGGCGCCG
CDK8	GTTTTTCCATATACTTGATA	HUS1B	GACCCTGAGTATAGAGACGG	PDGFRB	ACTCGTTGATCAAAGTTGCT	TREX2	AGGCGAGCAGCTCTGCGGCG
CDK8	GGACAGAATATTCAATGTAA	HUS1B	GCGCCGCCCCTCCCTCACGG	PDGFRB	TGAGCACGTTCCTAGCCGCC	TREX2	GCTTTGATGGCGCCGTGGTG
CDK8	AAGTGGAATGCTTTACTATC	HUS1B	GGCGGAGCACCTGTCCCGGG	PDGFRB	AGGTCCATGTAGCTTAGCAC	TREX2	CAAAGCCATTGTGGGCCACA
CDKN1A	AATGGCGGGCTGCATCCAGG	HYOU1	ACTGAGCCTTTGGAGTTAGG	PIGG	GCCTGCGGAGATGTCCACGG	TRMT11	ATGCATCTAAACCCTCCTGG
CDKN1A	GCCGGCTGATCTTCTCCAAG	HYOU1	CAACACAGGCTTCTCTGTGG	PIGG	CTCCAACAACATTGCCACCG	TRMT11	CTAGTCTTCCACCTAAAACG
CDKN1A	TGTCACCGAGACCACCACTGG	HYOU1	GGCCTGGAAGAATGCAACTC	PIGG	GTCTAAGCCCACGAAGCCTG	TRMT11	AAGAAGAACAGGTTCACAGA
CDKN1A	CAGGCGAAGTCACCCTCCAG	HYOU1	TATGAATGCTTCCAAGCTGT	PIGG	TGCCCGTGAACAGAATGCCA	TRMT11	TTCACAGAAGGAGATACCAA
CDKN1A	ATTTCTACCACTCCAAACGC	HYOU1	GTTCCTGCTTCTCCAGGTCT	PIGG	TCATTAGAGTCTGAATCAAG	TRMT11	AACTCAAGGAAACAGGAACA
CDKN1A	AGATCAGCCGGCGTTTGGAG	HYOU1	GGAAAAAGCTGCCAACAGCT	PIGG	GCACGTCCAACAGACGGATG	TRMT11	CATCTGAAACCAGGACATCA
CDKN1B	GGGCAAGTACGAGTGGCAAG	ICAM4	CGTGACGCAGGTGTTCCCGG	PIK3C2G	TTTGTTGCACAGCCTCAGAG	TRRAP	AAGAGGGGTTGTCCTCCACG
CDKN1B	TTTACGTTTGACGTCTTCTG	ICAM4	TCCAAAATCACGCTGTGGGG	PIK3C2G	ATCCCAGTGAAGTTCGTAGG	TRRAP	CCTCCTTGAGGATGTCGCGG
CDKN1B	CAAGTACGAGTGGCAAGAGG	ICAM4	TTTTTCCTGCGCAGGTCACG	PIK3C2G	ACTTAGCTTTTTCCTCTCTG	TRRAP	GCTGCTTGTAGATCTCCACA
CDKN1B	CCCTAGAGGGCAAGTACGAG	ICAM4	GTGCGGAGGCTGGAATTCTG	PIK3C2G	CATATCCCAGTGAAGTTCGT	TRRAP	TGTTACTCTGAACCTCCTTG
CDKN1B	TCAGACGGTTCCCCAAATGC	ICAM4	AGGTCACGAGGCAGTGCGCG	PIK3C2G	ATGCAAACTGCTTCTGAAGT	TRRAP	GCACACCTTCCCCAATGCCA
CDKN1B	ACAGAAGAAAATGTTTCAGA	ICAM4	TTCCTGCCCTTTAAGACCGG	PIK3C2G	AAAATCTGTTCCAAAATGTA	TRRAP	TTCCCCACAGATGCGCCTCG
CDKN2A	CATCAGCACGAGGGCCACAG	IFNA7	ACATGAATTCAGATTCCCAG	PIK3C3	GTTTATCCAGTCAGTTCCTG	TSC2	AGGTTGCACTCGTAGTCCAG
CDKN2A	ACCACGAAAACCCTCACTCG	IFNA7	TGAATTCAGATTCCCAGAGG	PIK3C3	GCCAAATGGGATTAGTGCTG	TSC2	TGTCTACAATGACTCCGGTG
CDKN2A	ACGCACCGAATAGTTACGGT	IFNA7	TTCTTTACTGATGGTCGTGC	PIK3C3	CTTCAGCCACAGGAACTGAC	TSC2	GGTGGCGCTTCTTGTCGCAG
CDKN2A	TTTTCGTGGTTCACATCCCG	IFNA7	AGACCCACAGCCTGCGTAAT	PIK3C3	ACCTCAGCACTAATCCCATT	TSC2	CCAGCGGGGTGACGATCACG
CDKN2A	CCATGCCCGCATAGATGCCG	IFNA7	AAGAATCACTCTTTATCTAA	PIK3C3	GCTGTTACGGAAAGAAAATC	TSC2	GCCAAGCTTGAAGTCCTCAC
CDKN2A	GGTACCGTGCGACATCGCGA	IFNA7	TTTTCAACAAACTTGAAAAA	PIK3C3	CTGGTGGCTAACACCTTATA	TSC2	CCACGTGATCGTCACCCCGC
CDKN2B	GCAGGTACCCTGCAACGTCG	IGF1R	AGATGAACCTGAAACCAGAG	PIK3CA	ACAGCCACACACTACATCAG	TSHR	GCATTTGGAGGAGTATACAG
CDKN2B	CTCCACTAGTCCCCGCGCCG	IGF1R	GGCCATTAAAACAGTGAACG	PIK3CA	ATGCAAATTCAGTGCAAAGG	TSHR	TCCTGATGGCACTCGCAGGG
CDKN2B	GGTACCCTGCAACGTCGCGG	IGF1R	TCATCATGGAACTGATGACA	PIK3CA	ACAATAAAACAGTTAGCCAG	TSHR	ACCCTGCGAGTGCCATCAGG
CDKN2B	GTTCCAGCCCCGATCCGCCG	IGF1R	TTGCTGGGTGTGGTGTCCCA	PIK3CA	TGAGCCACTGATGTAGTGTG	TSHR	ATTGACAAAGATGCATTTGG
CDKN2B	ACGGAGTCAACCGTTTCGGG	IGF1R	TCCACAGAGACCTTGCTGCC	PIK3CA	GACAATAGGACTCCAAAAGC	TSHR	AGATTAGAAAATGCATGACT
CDKN2B	CCCTGCCACTCTCACCCGAC	IGF1R	CCTTGCTGCCCGGAATTGCA	PIK3CA	TCGTCACAATAGTAACATCA	TSHR	ACGAACACCCCATTCCGCCC
CDKN2C	CAAAGAAGGCCACCTCCGGG	IGFBP1	AGTCGTAGAGAGTTTAGCCA	PIK3CG	CAAAATTCAGCAAAGCACAG	UGT2B28	ATGTTTGGTAAGAATGGATG
CDKN2C	AAGTTGCTCTAGGTCCCCCC	IGFBP1	AGAGAGTTTAGCCAAGGCAC	PIK3CG	GTCGCCTATTTCCAAGAACAA	UGT2B28	TCAGGTTGATCCCAAAACAA
CDKN2C	ACAAACTAGTAAGTTGCTCT	IGFBP1	AGGTACTGATGGCGTCCCAA	PIK3CG	AAATGCAACCATATGGCAGG	UGT2B28	GTACAGAGCTCTGGTGAAAA
CDKN2C	GACGCCAACTCGTTCCCCCA	IGFBP1	CGAGCCATCATAGGTACTGA	PIK3CG	TTGAAATGCAACCATATGGC	UGT2B28	CAAGGGAGCAGCTGTTAGAC
CDKN2C	GGAACTCCACCACCCGGAGG	IGFBP1	CAGTACCTATGATGGCTCGA	PIK3CG	CTGAATTTTGGCAATTGTCG	UGT2B28	TTTCCCCATTGTCTCAAATA
CDKN2C	TGGCAGCCAAGTGCAAGGGC	IGFBP1	TCTGTAGAGTTCTATTCGGC	PIK3CG	AGATTTGTTTATTCCTGTGC	UGT2B28	TGGTAGGCATTCCATTGTTT
CDKN2D	ATGGACTGGACTGGTACCGG	IKZF1	GGCAGGCGTAGTTGCAGAGG	PIK3R1	AACAGTGCCAGACCCAAGAG	USP22	CAGGGGGAAGGACACATACG
CDKN2D	GGGTGTCCAGGAATCCAGTG	IKZF1	CAGTGAGGGCGTCCCTCCGG	PIK3R1	AAAGCTGAAAACCTGTTGCG	USP22	AGCGCCAAGATCAAGTGCAG
CDKN2D	GGACACCCTGAAGGTCCTAG	IKZF1	ATCAGAGAGATCTCTCGTGC	PIK3R1	ATAGAAAAGTTTAAACGTGA	USP22	TGTTAACCATCAAGGGACCT
CDKN2D	CGTCGGGATGCACCAGCTCC	IKZF1	AGGCATAGAGCTCTTACGTT	PIK3R1	GGCAAAAGAAGTTGAACGAG	USP22	CACGTATGTGTCCTTCCCCC
CDKN2D	AGGTGCGCCGCCTTCTGCAC	IKZF1	GCAGAAGACCTGTGCAAGAT	PIK3R1	AGCCCTGTTTACTGCTCTCC	USP22	ATTCACCAGACCAGAGCACT
CDKN2D	CGGCGACCGGCTGAGTGGGG	IKZF1	CCCAGAAGGGCAACCTGCTC	PIK3R1	GAGATGGCACTTTTCTTGTC	USP22	GCAACCGCTGCACTTGATCT
CELF5	CCGTGTCTCCAAACTCCTGG	IL7R	TCAGGCACTTTACCTCCACG	PLS3	AGAGTTCATCCAGTTACGGA	VWC2L	GCGACACCATTCACATGGAG
CELF5	AGCTCGATCCATAAACACCT	IL7R	CAAGTCGTTTCTGGAGAAAG	PLS3	GCATAGAGATGGTTTACGTG	VWC2L	TGTACTAAAGTGGAACACAA
CELF5	GGAGGAAATGATATTGCCGA	IL7R	TGTTTTCATCCTTTTCCTGG	PLS3	CCAACCAGGGAGAATTTAGC	VWC2L	AAAAACTTCTGTGAATATCA
CELF5	GAAGGCAGGATGCAGTGTCT	IL7R	AAAGAGCAATATATGTGTGA	PLS3	GTTTATACAGCCTGGCTGGA	VWC2L	AACACAGTGAACTTCATTGC
CELF5	TGCTGGACTCCGGAGAAGGC	IL7R	CTGAGTGTCGTCTATCGGGA	PLS3	AACTATGACCTTGTGAAGAG	VWC2L	CGGGAAAAATTACAAAATCT
CELF5	GATGGGCGTGATGGCCGCGG	IL7R	CTTCCCGATAGACGACACTC	PLS3	GCATCCTGCTAAATTCTCCC	VWC2L	CATTGTTCTGGTTCATAGAC
CHD8	ACCACATCTCCAGTTCAGCC	INHBA	GGCAAACGTGATGATCTCCG	PMS1	CACTACAAATTGAAGAACTG	WDR27	CTGCTGAGCCCTGACTAGCG
CHD8	GCCGGGCTGAACTGGAGATG	INHBA	AGTGGTTGATGACTGTTGAG	PMS1	GCAGATGACCAAAGATACAG	WDR27	GATACAGTGGAGAGGTCGGT
CHD8	ATCTCCAGTTCAGCCCGGCG	INHBA	CTGTCTCCAGCAGCATCCAG	PMS1	AAACCATTCGCTGTAAGACG	WDR27	AATTCCCAGATACAGTGGAG
CHD8	AGAATTGAACTGTTTGGGAA	INHBA	GTAGTTGGCATGATAGCCAG	PMS1	GGATTTTCTATGAGAAACTG	WDR27	TGGCCGGATCGTGTGTCCCTG
CHD8	CTAGAGTTAGCTGTCTGTAC	INHBA	TGAACTTATGGAGCAGACCT	PMS1	GTGGAAGACATTGAGTGAAG	WDR27	TGCCAAGGAGAAGAGTACCA
CHD8	CAGACAGCTAACTCTAGAAA	INHBA	AGATAGAGGATGACATTGGA	PMS1	AGAGAAGGCTACTAAAGACT	WDR27	AATCTTCCCGCCAAAGAGGG
CHRM4	CACAGAGCTGTCCACCACAG	INPP4A	TTTACAAGAAGTCATCAACG	POGK	GTACGAATCTGCTCTGAGGG	WDR45	GGAAGGAGTACACATAGATG
CHRM4	GCGTTCCTTGGTGTTCTGGG	INPP4A	TCAACGTGGAGAGTTTGGTG	POGK	GGTACCGGCCCTATTTGATG	WDR45	ACTACTACCACCGCCCACCA
CHRM4	TTATCAGCCACGGGGCGCGG	INPP4A	GTTTAAGGAAGTTTTGCCTG	POGK	CAGAGCCGGGAACTAGAGGA	WDR45	CTTGGAAGTATTGCGACCGA
CHRM4	ATTGCGCAGCTCCTCCCGGG	INPP4A	TTGCCCCGGGAGATCCAGAG	POGK	AGTCTCAGAATTCTGACGAG	WDR45	GCCTATGATTGGGCAGTACG
CHRM4	CACAAACTGCCAGAACAAGA	INPP4A	TGAACCGGACCCCATTAAGG	POGK	ACCGGCCCTATTTGATGAGG	WDR45	GATCTGGGACGATGCCCGGG
CHRM4	GATGAGAAGGTTCATGACGG	INPP4A	TAAGGACCGTACAGCCATGT	POGK	CAAAACTTCCCATTCCTCAT	WDR45	GCGCACAGAAAGCACTGGCT
CLDN1	CATACACTTCATGCCAACGG	INPP4B	AGATGAGCACCAGTTACACA	POLD1	GGTGGAGTCTAAGTACACAG	WDR49	CCCGTAACAAGAGTTTGTGG
CLDN1	AGATTGCTATCACTCCCAGG	INPP4B	CGATGAAATTGGAATGCTAG	POLD1	GTGACCTGACACCCAGTCCG	WDR49	TGTTGGGCAAGATGGAGCTG
CLDN1	ATGAGGATGGCTGTCATTGG	INPP4B	CTTTAAATCGGAAATGCCAA	POLD1	TGACCAGGTTGGCCACGAGG	WDR49	GGTAATCAGGGTGAAGAACA
CLDN1	TCTATTGCCATACCATGCTG	INPP4B	AGCTGTACGCAAGTTCCTGA	POLD1	CGGCATTGAGCGTGTAGGAG	WDR49	GTATTTTCTTCTTAAGAATG
CLDN1	CTATTTTAGTTGCCACAGCA	INPP4B	ATGTCAGGGACTGCTTGGCT	POLD1	CAGTGAGGCAGTGACCAGGT	WDR49	ATTTTGACTTTAGCAACCTC
CLDN1	TTAGTTGCCACAGCATGGTA	INPP4B	GAAGGACTGCATGGGAGAAG	POLD1	CAGGGACAACTGCCCCCTCG	WDR49	TTTTCATCCAGCCTGAAGAA
CLDN11	GGATGACACAGCCACCCACG	IQGAP2	CCTTTTCCATCTCAACACCA	POLE	CTGTACAAAGAAGCGCCGTG	WDR70	GGCCGAGTTGGAACCCACGG
CLDN11	GTAGCCAAAGCTCACGATGG	IQGAP2	GATGGAAAAGGAGAACCCAA	POLE	AAGCGATGGCATCTTCCACA	WDR70	TGTTCCGTGAGCCCCGCCAA
CLDN11	GGAGTAGCCAAAGCTCACGA	IQGAP2	GAAGATCATCTATATCTAGC	POLE	CACGGCGCTTCTTTGTACAG	WDR70	TGACGCAAAATGGCTTCCCG

CLDN11	CCGGTGTGGCTAAGTACAGG	IQGAP2	TCAATTAAACTAGATGGAAA	POLE	ATGGATCCATCTAACTATGG	WDR70	ACTGGTACATCTATTCAAAG
CLDN11	GTCAGCAGCAGTAAAATGGC	IQGAP2	GTCTAAACAAGTCTTTATGT	POLE	AGAAATTGTCAGAGAATGGA	WDR70	GGGCTCACGGAACATAGGCA
CLDN11	GATGGGCCAGGAGCCCGGTG	IQGAP2	TAAGCTTCGAAAAGCTGAAT	POLE	TGGATGGATCCATCTAACTA	WDR70	AGGAAGAGAGAGTGCCCCCG
CPN1	ATGTTCCAAGGTTGGAACTG	IRS1	TGTTGAAGCAGCTCTCAAGG	POU3F2	CAAACTGGGATTTACCCAAG	WNT1	GAGCAGTGGGACAGTTCCAG
CPN1	CCGCTGTAACTCCTCTTCGG	IRS1	ACGCTTCTTCGTACTGCGCG	POU3F2	CATCGAGGTGAGCGTCAAGG	WNT1	CCTGCACGTGTGACTACCGG
CPN1	ATGTGCATAGGAGTAGACCT	IRS1	TCTTGCTGGTCAGGCAAAGG	POU3F2	GAACTGCTCCAGGTCGTCCG	WNT1	ACGTGTGACTACCGGCGGCG
CPN1	AATCTCCGCAGTTCCAACCT	IRS1	CTTCGTGAAGCTGAACTCGG	POU3F2	CCAAGCAGTTCAAGCAGCGG	WNT1	AGCTGTTGAGCCGCAAACAG
CPN1	CCCCCGAAGAGGAGTTACAG	IRS1	CCCAGGACCCGCATTCAAAG	POU3F2	TTTGTTGAACAAGTGGTTGG	WNT1	CCACGAACTCCCGGCCGAAG
CPN1	CGACAAGTTTCCCCCCGAAG	IRS1	TGAAGAAGAAGTTTTCCGAG	POU3F2	CTGTAAGCTGTCCGCGAGGG	WNT1	GGTTGACGATCTTGCCGAAG
CPN2	TTGTGACTGCTTCGTCCAGG	IRS2	CAAGGACGAGTACTTCGCCG	PPARD	CACATGCATGAACACCGTAG	WNT3	AGAGCGAGTACTTGGCCCGG
CPN2	GTATATGGCGGGATGTCCAG	IRS2	CCAGAGCAAGAACCTGACGG	PPARD	GCTTCATGCGGATCGTACGA	WNT3	CGTGAACGAAGGCCGACTCG
CPN2	TGGCGGGATGTCCAGTGGGA	IRS2	CCTGATCGCCCTCTACACCA	PPARD	TCTCGTACTCCAGCTTCATG	WNT3	CGAGGCGATGGCGTGAACGA
CPN2	CGGGATGTCCAGTGGGACGG	IRS2	AAGCGCTTCTTCGTGCTGCG	PPARD	CTACGGTGTTCATGCATGTG	WNT3	CTCGCTCTTCAAGCCACCCA
CPN2	GGGTTGTGACTGCTTCGTCC	IRS2	TGACCAGGTCGGTGAGCGCG	PPARD	TCGTACGATCCGCATGAAGC	WNT3	CACGAGGACGGAGAAGCGGA
CPN2	CATCTGAGCAGAACACCTCC	IRS2	GGTTCACCTGCCACACCTCA	PPARD	AACATGGAGTGCCGGGTGTG	WNT3	GCATGATCTCGATGTAATTG
CRABP2	GGTCAGTTCTCTGGTCCACG	ITPRIP	ACACACGCGGAAGAGCCCCA	PPP1R11	AGAATGGACAAGTGACACTG	WT1	ACCAGCTCAAAAGACACCAA
CRABP2	TGCAGCGTCCAAGCCAGCAG	ITPRIP	CGGAGCACCAGAGCTCTGGG	PPP1R11	CGAGACCGTCACTGAGACAA	WT1	ACTTCAAGGACTGTGAACGA
CRABP2	GATTAACTTCAAGGTTGGGG	ITPRIP	GGGCTACGGCCAGATCAAGG	PPP1R11	GGTAACCGTTGTCTCAGTGA	WT1	CACAGTCCTTGAAGTCACAC
CRABP2	CAACTGGAAAATCATCCGAT	ITPRIP	GTGCCTTTAGTGTCGTCCTG	PPP1R11	GGAGCCTTACCATCAAACTT	WT1	ACCCACACCAGGACTCATAC
CRABP2	AGCAGTGGAGATCAAACAGG	ITPRIP	GCAGCAGAACGAGACACGCG	PPP1R11	TTACCATCAAACTTCGGAAA	WT1	TTCGCTGACAAGTTTTACAC
CRABP2	ACCAGAGAACTGACCAACGA	ITPRIP	TCAATGTGTCCCCATCGGCG	PPP1R11	GCTCAGCCCAGCCCCTGCCT	WT1	TGTTTTACCTGTATGAGTCC
CREBBP	GTACAAAAAGATGCTGGACA	JAK1	GGACTCCAAGAACCTGAGTG	PPP1R12C	GACTCTTACAGACCTGAAGG	WTAP	TGTAATGCGACTAGCAACCA
CREBBP	GTATTTTTTGATCAGGTGGG	JAK1	TATTCCTTAAGGCTTCCCGA	PPP1R12C	TGTGACTCTTACAGACCTGA	WTAP	AAAACTAAAGCAACAACAGC
CREBBP	GGAGTGGTACAAAAAGATGC	JAK1	TAAGGAGTATTACACCGTCA	PPP1R12C	GGCAAGAACGCTTCGCTGAG	WTAP	GAAGTGTCGAATGCTTATCC
CREBBP	ATAGGGCAGTTCCTTGGCAC	JAK1	TGGGGTCATAGTTCATGCAG	PPP1R12C	GGCCCCAGAGTCAGAGAAGC	WTAP	TGGTTGCTAGTCGCATTACA
CREBBP	AATGCTCTCTTCTAACACAT	JAK1	TGAGTGTGGCTGCTGACAAG	PPP1R12C	GGAACGCAAGGCCGCAGAGC	WTAP	TGCACAACTTGAAGCAGAGT
CREBBP	TCAAACAAGCAACTGAAGAC	JAK1	GTAGCAGATTTCCCAGAGCG	PPP1R12C	GAGGCCAGCCCTCCTGGAAC	WTAP	CAAGTTGTGCAATACGTCCC
CSF1R	CGTAACGTGCTGTTGACCAA	JAK2	TCTACAGGACAACACTGGGG	PPP3CC	TAGTCTGCTTGCCTCCTGAG	WWTR1	AGGGAGCAGAGCACTGACAG
CSF1R	GCTGTTGACCAATGGTCATG	JAK2	GACAGAGAGCAAGTTTTCTG	PPP3CC	CCTCCTGAGAGGACGCCCAG	WWTR1	CTTCCTAGGGTCTTGCCATG
CSF1R	GAAGGAGCAGATCTGCTGGA	JAK2	TGTCCTGTAGAGGGTCATAC	PPP3CC	GAGCCATTGGGAAGATGGCA	WWTR1	CAGTGTCCCCACAACTCCGG
CSF1R	TACGCGCTGCCACGTCCCGG	JAK2	AGATGTTTGGAGCTTTGGAG	PPP3CC	GCCCAGAGGGAGTGTGCCTG	WWTR1	TCACCACATGGCAAGACCCT
CSF1R	GTGGCTCATGATCTTCAGCT	JAK2	GGCAACGAGAAATATATTGG	PPP3CC	CATAAAGTTTGGAAGCCAGT	WWTR1	ATACTCATGAGCCCTGCGGG
CSF1R	CATGGGTACAGGCTCCCAGA	JAK2	TGACAACATTGTAAAGTACA	PPP3CC	CAGTTCGTAAGGAGATCATC	WWTR1	ACATAGAAAAAATCACCACA
CSF2RB	ACAGGAAAGACACGGCCACG	KAT2A	GTAGCCGATGGCGTACTCGT	PPP6R3	ACCCAGCAGTGCCAACACGG	XIAP	GTGGAGGAGGGCTAACTGAT
CSF2RB	TGTACTGGATCTCAAATGTG	KAT2A	TACGCCGACGAGTACGCCAT	PPP6R3	CAACACGGAGGATAAAATGG	XIAP	TACCATCTTCCAAAATCCTA
CSF2RB	TCGTCTCTGTTCAGCCAAGG	KAT2A	TGATGTGATACTCCTTCAGG	PPP6R3	ACTGAGACAGTGATGAATGG	XIAP	TTGTTCCCAAGGGTCTTCAC
CSF2RB	TCCATCCCTCAACGTGACCA	KAT2A	GCTGCTTCAAGGAGGGCGTG	PPP6R3	TGATGAGGAAGATATATGGG	XIAP	CAAATATCTGTTAGAACAGA
CSF2RB	ACATCGTCTCTGTTCAGCCA	KAT2A	GAATCCCCGCATCCCCTACA	PPP6R3	GGATGCAGAAAGTACAGACA	XIAP	ACGAATGGGGTTCAGTTTCA
CSF2RB	TCTCAGGACGTCCCAGCAAG	KAT2A	GGGGCCTCCGACTTCTTCAC	PPP6R3	CAGAATCCAATGGAGCACCG	XIAP	TACCATAGGATTTTGGAAGA
CSNK1A1	ACATAAAACTTCAACAGGCG	KAT2B	AAAGATGGCCGTGTTATTGG	PRDM1	TGGCGGTACTTCGGTTCAGG	YIPF7	AAAAAAGAATGGGTCCAGTG
CSNK1A1	AGTACAGAGACAACAGGACA	KAT2B	GGCCATCTTTAATTAAAGCA	PRDM1	GAAACACTACCTGGTACACA	YIPF7	CAGGCAGTAACCCAGCACGC
CSNK1A1	ATGTACTTAAACTATTGTCG	KAT2B	TTCCGTATGTTCCCATCTCA	PRDM1	ATTGTCGGGACTTTGCAGAA	YIPF7	TCAGCAAGGCATGAATCACA
CSNK1A1	AGACTACAATGTACTAGTCA	KAT2B	ATTCTTTCAAATGATTCATC	PRDM1	TAAGCCCATCCCTGCCAACC	YIPF7	AGGGGTGTCGTACGGCTGTG
CSNK1A1	AGAGAAGATAAAAACCTCAC	KAT2B	TCAAAGCGCTTGGCCCTTCA	PRDM1	AGGCGGAGGCATCCTTACCA	YIPF7	ATGAATGAAACGGACCTCAC
CSNK1A1	TGTACTAGTCATGGATCTTC	KAT2B	CTTATAACTTCATAATATCC	PRDM1	CAAATGTCAGACTTGCAACA	YIPF7	TGGCAGCATTATGAATGAAA
CTNNB1	ATGATGGTCTGCCAAGTGGG	KCNA1	ACCGAGATAGCTGAGCAGGA	PRDM14	AGAACCAAGAGCTCCTTGTG	YWHAZ	AGGAGCTGAATTATCCAATG
CTNNB1	GGGTTCAGATGATATAAATG	KCNA1	ATGTACCCTGTGACAATTGG	PRDM14	CCTCAAGTACACCCCCTGTG	YWHAZ	GAGCCCGTAGGTCATCTTGG
CTNNB1	GAGCCTCTATACCACCCACT	KCNA1	AATTGTTAGCACACCAGCGA	PRDM14	AGCAGTCTCCATACCACACA	YWHAZ	AAAATGTTGTAGGAGCCCGT
CTNNB1	GAAATAGTTGAAGGTTGTAC	KCNA1	TGAGCAGGAAGGAAACCAGA	PRDM14	GAAGCGGGCACAGTTGACAT	YWHAZ	TACTTGGCTGAGGTTGCCGC
CTNNB1	CACAACCGAATTGTTATCAG	KCNA1	CGAGACGCAGCTCAAGACCC	PRDM14	TCGCATGTGTTTGTTTAGGC	YWHAZ	CCCAGTCTGATAGGATGTGT
CTNNB1	TTAGTCCTCTGATAACAATT	KCNA1	TTCTAAAAACCCTTACCAAG	PRDM14	GGACTCGCATGTGTTTGTTT	YWHAZ	CGGCAACCTCAGCCAAGTAA
CUL3	CCTGTGGTAAACCAACACAG	KCNIP3	CAGTCCACGAGAAGCTCAAG	PREX2	CCAGATGTTTGACAACAGCA	ZFHX3	TTTGAGAACAACCATCACAC
CUL3	TTCTACTTAGCCAAACACAG	KCNIP3	CAATGGTCACTACCCCATCC	PREX2	AAACTTGGGAAGCCAGCAGG	ZFHX3	TGGGAAGGAGATGCGTTTGG
CUL3	GCCCTACAGTCCCTCGCCTG	KCNIP3	TAATCTCTACGACATTAACA	PREX2	GACACAGCTCCGTAGAGACA	ZFHX3	CAACCCGAGTGATAGTGGTG
CUL3	CCGCTGTGTTGGTTTACCAC	KCNIP3	AAAATGGACCGGAACCAGGA	PREX2	CTGTTTGACCTTTTCCAGTG	ZFHX3	AGTCATTAAAGCATGACTTG
CUL3	TGGGATGTTGCACTTTGGTG	KCNIP3	AGTGACCATTGAAGAGTTCC	PREX2	TTACAGAGACAATGTTTCTG	ZFHX3	GAAGCGACCAAAAACAGCTG
CUL3	GCTGGTGGGATGTTGCACTT	KCNIP3	GTTAATGTCGTAGAGATTAA	PREX2	ACGCTGCTGGGAAGATTCCA	ZFHX3	CAGCGTGGCACCTGACTGCG
CUL5	CAATACAGCGAGCTGAAACG	KDM5A	GCACCCCAAGGAAACAACCT	PRF1	CGTAGTTGGAGATAAGCCTG	ZMYM2	GTATTTTGGCCTGAAAACAG
CUL5	TCCCTGATGCTGAACTTAGG	KDM5A	ACTACTAGAGGACTTCACAC	PRF1	ACAACCCCATCTGGTCAGTG	ZMYM2	TTGAAGAAGACTATCTCTGG
CUL5	AGTTGGTCAATATGATTTGG	KDM5A	AGAGATTCCCATCAAATCCG	PRF1	GAACAGCAGGTCGTTAATGG	ZMYM2	TACCAAGTGTCTTCCTTGTG
CUL5	ACTCCTGGTTCACTGAGAAG	KDM5A	ACGAGACTCAACACATATGG	PRF1	CTGTGAAAATGCCCTACAGG	ZMYM2	ATTTTCACAGGACATCTGGA
CUL5	TCTTTGGGTGAGTTGACTTG	KDM5A	GATTCCCATCAAATCCGAGG	PRF1	CCACTGGGAAGGAGCCCGAG	ZMYM2	TTAGGTGTTGGAGAAGGGGG
CUL5	TACCCTCTTCTCAGTGAACC	KDM5A	GCAGTCTGCTTTTAACCGGG	PRF1	ACTCTGAGCGTGCGGCTGTG	ZMYM2	CAAGATTTGGTCTGCATGTG
CXCL16	AACACCTGAGAGCTTACCAT	KDM5C	CATCATGAGCTCCTCCAAGG	PRICKLE1	TGCAGGTGTTCAGTGCTCAG	ZNF319	AGTACGCGTCAGACCTGCAG
CXCL16	TCGTGTAGTATAGACACCGA	KDM5C	CTCGCCTCCTCAGCTCTCCG	PRICKLE1	AAACGGTCCTGGGAGGACAG	ZNF319	AGTGCCAGAAGGCCTTCAAG
CXCL16	TTCATGAACTGAACCGATGG	KDM5C	GATTGGGCCTCGGAGAGCTG	PRICKLE1	TGTGGTTTGAAGATAAATGG	ZNF319	AAAGCCCTTCAAGCACCTGT
CXCL16	GAGCGTGTGTGGGGGCAACA	KDM5C	GTCCACTGTGTATGCGCTCA	PRICKLE1	CTATTTTGCTTGCTTACCAG	ZNF319	CAAGGCCTACAAGCGCGCGT
CXCL16	CTTTCCTGGAGCGTGTGTGG	KDM5C	CGTAGCAGGCCAGGGCTGAC	PRICKLE1	TTGCCAGTCTTTGAGTGAAG	ZNF319	CATGCCGAGAGAGCTCCGAC
CXCL16	ACACGCTCCAGGAAAGGAGC	KDM5C	CCGCAGGTACTGCCGGCTAC	PRICKLE1	ACAGCCCCGGAGAGAAGCAT	ZNF319	AGTACGCACTGATGCGCCAC
CYB561D2	GCAAAGCCCACCTGGTTACG	KDM6A	GATTGTGCACGAAAAACAAG	PRKCI	TAACCCTGACCAGAACACAG	ZNF485	GACACCTGGATGCTGCTCAG
CYB561D2	TAGTGCCTCGGTCATCAGGA	KDM6A	ATTCCAGGAAAGATGAACCA	PRKCI	GCTTTTACAGACAGAGAACG	ZNF485	TGGCCTTTACCCGGATTGAG
CYB561D2	AGAAAACACCAGTAGTGCCT	KDM6A	ATTGGTCATAGACTTGCATC	PRKCI	ATATCAGCAAATCCTGTTTG	ZNF485	GCCCTGGACTGAGGTGCGAG
CYB561D2	AGACATAAGCACCGGGTGCC	KDM6A	ACGAAAAACAAGCGGAAACT	PRKCI	TTGGGTTGTCATCCTCAAAC	ZNF485	CCGGATTGAGTGGAGACACC
CYB561D2	GCACCGGGTGCCAGGAGAAC	KDM6A	GAATATGGCACGAAATATCA	PRKCI	TATTTCTGGGGAATTTGGTT	ZNF485	GAGGTGCGAGAGGCTCCATC
CYB561D2	GCACCCGGTGCTTATGTCTT	KDM6A	AACTGTGTTCATGCCCAATA	PRKCI	TGTGTTCTGGTCAGGGTTAT	ZNF485	CTAATTACTCAGTTGGAGCA
CYP27A1	AAAGGACCCTGAGATCCAGG	KDM6B	GAAACCGAAGATCAACACTG	PSMA4	GACCCTAGTGGAAATTACGG	ZNF501	ATATCACTCAGAATGAAACA
CYP27A1	TAACCCGATGGATCTGACGA	KDM6B	TCCCCGCATTAATCCACACG	PSMA4	CTCTATCAGAGTGACCCTAG	ZNF501	GAGTCCTTTCATGTTCAACA
CYP27A1	AAATGGGTGCTGGATCCTGG	KDM6B	TGGCCCTGGAACGATACGAG	PSMA4	GCTATTATTTCCAATGCATG	ZNF501	CATTCTGAGTGATATTTGGC
CYP27A1	CCTGCAGCGATCCATCCCCG	KDM6B	ACTACTTGACGGGTTCCTGG	PSMA4	CAAAGTACTAAATAAGACCA	ZNF501	AAGAATTGCTTTTGTTTGAA
CYP27A1	CTGCACTTCTTACTGGCCAG	KDM6B	AATGTTGTTGCACCAGCCGG	PSMA4	AGAGAGTTTACTAACATCCA	ZNF501	GTTTCATTCTGAGTGATATT
CYP27A1	GTTCTGGAACATTAACCCGA	KDM6B	CACGTGAATCATGGGCACGA	PSMA4	ATGGAAGCTATTGGACATGC	ZNF501	GAGTAAGATTTGACTGTTTA
CYSLTR2	TCCTGCCCTATCACACACTG	KDR	AGAACAGTAAGCGAAAGAGC	PSMD6	AGAAGCGTTTGGTGTTGGTG	ZNF527	AGGGAAGGAACCGTGGATGG
CYSLTR2	GAAACGCACAACACTCAGCA	KDR	CTCCATACAGGAAACAGGTG	PSMD6	TCTCCCGGCAGCAATAAACC	ZNF527	GTCTAGCGCCACATCTCTGA
CYSLTR2	TCAATAATGCTCCTGGACAG	KDR	ATACAGGAAACAGGTGAGGT	PSMD6	TCATATAGGTCATTAACCCT	ZNF527	ATGGCTGAAGCCATCTCAGA
CYSLTR2	CCAGCAAAGTAATAGAGCAG	KDR	ACCCACGTTTTCAGAGTTGG	PSMD6	ATTGGAAGAAAACAGAGTAA	ZNF527	CTCCAGTAAGGAGATCATGT
CYSLTR2	TCGGGTTCTGTTAAAAGTGG	KDR	ACCATGCTGGACTGCTGGCA	PSMD6	ACGCTTCTGCCATATAGCCA	ZNF527	AGAACTACAGGAACTTGGTA
CYSLTR2	GGACCGTCCACTTGACGACA	KDR	GAGACCCACGTTTTCAGAGT	PSMD6	TATTTTGCAGTGTAGTCTCC	ZNF527	GGTGGAGAGAAAGATGTCAC
DAPL1	ATAATGTAGATCCTTTTCAG	KEAP1	CTGCATCCACCACAACAGTG	PTEN	AGCTGGCAGACCACAAACTG	NTC_01	ACGGAGGCTAAGCGTCGCAA
DAPL1	ATTTCCAGCAACAGTGCACA	KEAP1	CTTGTGGGCCATGAACTGGG	PTEN	TCATCTGGATTATAGACCAG	NTC_02	CGCTTCCGCGGCCCGTTCAA
DAPL1	TGTTGCCAAAATACAGACAC	KEAP1	CTGAGTGTTACTACCCAGAG	PTEN	GAGTAACTATTCCCAGTCAG	NTC_03	ATCGTTTCCGCTTAACGGCG
DAPL1	AAAACAAGAAATTGGCACCT	KEAP1	TCAGGACCAGCTGAACAGCG	PTEN	ACTATTCCAATGTTCAGTGG	NTC_04	GTAGGCGCGCCGCTCTCTAC
DAPL1	TTTTTTGGTATGTCTTTCCA	KEAP1	ACGATGTGGAAACAGAGACG	PTEN	AGAGCGTGCAGATAATGACA	NTC_05	CCATATCGGGGCGAGACATG
DAPL1	TATTTTGGCAACATTTGCAA	KEAP1	CTGTCGGAAGTAGCCGCCCG	PTEN	ATTCTTCATACCAGGACCAG	NTC_06	TACTAACGCCGCTCCTACAG
DAXX	GGAAATGTCCGTCTCCACAG	KIT	CTCCCAAAGAAAAATCCCAT	PTP4A1	TGAACAGCAATACAACAACC	NTC_07	TGAGGATCATGTCGAGCGCC
DAXX	AATGTTGCAAGACAAAAGTG	KIT	TGATCCGACCATGAGTAAGG	PTP4A1	TCAACAATCTGGTTGGATGG	NTC_08	GGGCCCGCATAGGATATCGC
DAXX	GGTTCTTCTGACAGTAACGA	KIT	ATATCCTCCTTACTCATGGT	PTP4A1	GCCCTAGCATTAATTGAAGG	NTC_09	TAGACAACCGCGGAGAATGC
DAXX	TGCTCCATTCTCTAAGACAG	KIT	CAGCCCCTATCCTGGAATGC	PTP4A1	TCATCAACAATCTGGTTGGA	NTC_10	ACGGGCGGCTATCGCTGACT
DAXX	GTCATCTGTCTCAGCTCTGG	KIT	AGAAATATCCTCCTTACTCA	PTP4A1	TTCCACCTTCAATTAATGCT	NTC_100	CGCGGAAATTTTACCGACGA
DAXX	GGAGGCCACAGATTCTGAAG	KIT	ACACGTTTGAAAGTGACGTC	PTP4A1	AATGCTAGGGCAACAAGTAC	NTC_101	CTTACAATCGTCGGTCCAAT
DBNL	TGCCAACTACAGCTTTCACA	KLF8	AGGCAAAGTAGTATACACCA	PTPRD	TAACTTTAATGAGAGCCCAG	NTC_102	GCGTGCGTCCCGGGTTACCC
DBNL	TACAGCTTTCACAAGGAGAG	KLF8	AGGGTCTGGGGAGAAGACTG	PTPRD	AATTCCCTTAGGATATACTG	NTC_103	CGGAGTAACAAGCGGACGGA
DBNL	AGGCTGAGGACTGGAGATGG	KLF8	AGTCTGCCAAATAAGATGGG	PTPRD	ACCAATACTGGCCAGCAGAA	NTC_104	CGAGTGTTATACGCACCGTT
DBNL	TAGAAGGTCTCCTGCTCTGG	KLF8	TGCATCCTGCAAAGTCACAT	PTPRD	CTGCTTCTAACAGTGCATCA	NTC_105	CGACTAACCGGAAACTTTTT
DBNL	TGTGGAGCCTGAGTGCATCA	KLF8	AGCTTTCAGGTGAGAGCTTT	PTPRD	TGGCATGTTGTACTCAGCCA	NTC_106	CAACGGGTTCTCCCGGCTAC
DBNL	GAAAATCTCCCTCGGGTGCA	KLF8	GGATTCTGCGGTGAGCTTTC	PTPRD	AAGAACACAACGACCAGCTA	NTC_107	CAGGAGTCGCCGATACGCGT
DDR2	TACTCTCCCAAGACATCCAG	KLK5	GTTGGGGCCTTAGCAACAGCG	PTPRS	CATACGCCAGAAGTCCCCAA	NTC_108	TTCACGTCGTCTCGCGACCA
DDR2	GGAAAGGTACTTCATGCCAG	KLK5	CGGTGTTGGTGCATCCACAG	PTPRS	GGAGAACAATTCGACGATCG	NTC_109	GTGTCGGATTCCGCCGCTTA
DDR2	TCGCTGGAGGAAGAATTAGG	KLK5	GCTAAGTCAGAAAAGGTGCG	PTPRS	CAGCCGCGTCATCATGACGA	NTC_11	CACGAACTCACACCGCGCGA

DDR2	GACAGTGCGTACATCGCTGG	KLK5	GGTTGTTAGAGTGGCCAGGG	PTPRS	ACAGGGTGTGCCAAAGTCGG	NTC_110	CGCTAGTACGCTCCTCTATA
DDR2	TCGGTGAACAAAATTAAGAG	KLK5	CAACCAGCTCTACTGCGGGG	PTPRS	CGACCATCGTCATGATGACG	NTC_111	TCGCGCTTGGGTTATACGCT
DDR2	AGGAGATAAAGATCATGTCT	KLK5	ACAGGGAGTAGTGGCCGAGA	PTPRS	GTTCCAGTTCACAGACTGGC	NTC_112	CTATCTCGAGTGGTAATGCG
DLC1	CCAACAGGTCTACATCCCAG	KMT2A	GAGATGGTGATTGAGTATGC	PTPRT	GATGAGCACTACAGCAACTG	NTC_113	AATCGACTCGAACTTCGTGT
DLC1	TGCGCGATCGTGATCCACAG	KMT2A	GCTCCATCCAGACTGACAAG	PTPRT	CAGCAACTGTGGTTATAGTG	NTC_114	CCCGATGGACTATACCGAAC
DLC1	TGAGCGAAGGACCCCCTCTG	KMT2A	TTCTCTTACAGAAAAGACCC	PTPRT	ACTCTCCCAACTATAAGCTG	NTC_115	ACGTTCGAGTACGACCAGCT
DLC1	TAAGTCAACTCTGCACATGT	KMT2A	TGAGGAACACAACTGCATCA	PTPRT	ATCGCACCACCACAGGCACG	NTC_116	CGCGACGACTCAACCTAGTC
DLC1	TTAACCCTCACACCCACCAC	KMT2A	ACTGAGAAAAAACCCAAGAA	PTPRT	CTGCTCCCAGGTGAACCCAT	NTC_117	GGTCACCGATCGAGAGCTAG
DLC1	GACCTCCAAAGCCTCAGAGG	KMT2A	GTCATTGACAGATAAAGTCC	PTPRT	CCTCACACGACCAGGTGAGG	NTC_118	CTCAACCGACCGTATGGTCA
DLEU7	CCGAAGTCGAGTCCACCACG	KMT2B	GCAAAGGGGACCGTTCCTGG	RAB8B	AGACAAGTGTCAAAAGAAAG	NTC_119	CGTATTCGACTCTCAACGCG
DLEU7	TGGGGAGTTCGCCCGCGCCG	KMT2B	GAAGACGTCCAAAGAAGCTG	RAB8B	CAGGATCATTCTTTCGACAT	NTC_12	CTAGCCGCCCAGATCGAGCC
DLEU7	GACTTCGGAGCTGGTCAGCG	KMT2B	GGTAACGGAACTTATAGTGC	RAB8B	CATTCTTTCGACATCGGAAG	NTC_120	GAATCGACCGACACTAATGT
DLEU7	TCTGCAGAGCCACCATTTGG	KMT2B	ACTTATAGTGCTGGCAACGC	RAB8B	CCAATTTTTAATATTGTCAA	NTC_13	ACTTCAGTTCGGCGTAGTCA
DLEU7	CTCCATCAGCCACCAAATGG	KMT2B	GTGCTGGCAACGCTGGGCTC	RAB8B	AGTACGCTGTCGTGATTGTT	NTC_14	GTGCGATGTCGCTTCAACGT
DLEU7	GGTAGTGCGAGGCGCTGAGG	KMT2B	GTAGACACCCACAGCTTCTT	RAB8B	TGACTATGGGATTAAATTCT	NTC_15	CGCCTAATTTCCGGATCAAT
DLX3	TAGCTGGAGTAGATCGTACG	KMT2C	TGCGGAACATGTACACACCA	RAC2	CTTGCTGTCCACCATCACAT	NTC_16	CGTGGCCGGAACCGTCATAG
DLX3	GGGCGCTTACTCGCCCAAGT	KMT2C	TCACATGGTCGTTATCCATG	RAC2	TCTGTGGATAGGAGAGCGGC	NTC_17	ACCCTCCGAATCGTAACGGA
DLX3	ATACGCCCCGTATTGCCGGT	KMT2C	AGACCGTGCCAGATACACAT	RAC2	GGCGCGGACGTTCTCATAAG	NTC_18	AAACGGTACGACAGCGTGTG
DLX3	TTGCCGGTAGGAGGCTCCGT	KMT2C	ATTGACGCGACGCTCACAGG	RAC2	CCGGATGGCCTCGTCGAACA	NTC_19	ACATAGTCGACGGCTCGATT
DLX3	GCCGGAAGCAGAGGTGCGCA	KMT2C	AATCCAATGTGTATCTGGCA	RAC2	CATAAGAGGCTGGGCTGACG	NTC_20	GATGGCGCTTCAGTCGTCGG
DLX3	AGTAGATCGTACGCGGCTTT	KMT2C	TTTTTTCTCACACATGCCAC	RAC2	AGGGCACAGCACGGCCCGGA	NTC_21	ATAATCCGGAAACGCTCGAC
DNMT1	AGGTGCACTGATAGCCCATG	KMT2D	ATTGATGCTACGTTGACCGG	RAD50	GCGGAATTATAACTACCGAG	NTC_22	CGCCGGGCTGACAATTAACG
DNMT1	AGTTCCTGACATTCTCCAGG	KMT2D	GGACCTAGAAAAGCACACAA	RAD50	CTGTGGCGAAGTACCTATCG	NTC_23	CGTCGCCATATGCCGGTGGC
DNMT1	ACGGCGTGGCCCAGACTAGG	KMT2D	CCTGGGGCTCTATGCAGCCA	RAD50	GAAACGTTCTGCCTCAACTG	NTC_24	CGGGCCTATAACACCATCGA
DNMT1	GAGGGTGAGCTTCAGGACCA	KMT2D	TGATTCAGCTATGCGAAGCA	RAD50	ATAAAATTATACGTGACCTG	NTC_25	CGCCGTTCCGAGATACTTGA
DNMT1	AAGCTTGATCTCCAAGCCAA	KMT2D	CACCATCATTCGGAACGAGG	RAD50	ATTTGTTGTTGGCTCATCCA	NTC_26	CGGGACGTCGCGAAAATGTA
DNMT1	TATGGAAGGCTCGAGTGGGA	KMT2D	GTTTTGACAGCTCTCCACCC	RAD50	AGCCTCACTCATCATTCGCC	NTC_27	TCGGCATACGGGACACACGC
DNMT3A	AAGTGAGGACCATTACTACG	KNSTRN	ACTGAGTAAGCAAAAATCAG	RASA1	GAGATGATATTGAACATCCG	NTC_28	AGCTCCATCGCCGCGATAAT
DNMT3A	CTCCAGCTTATCATTCACAG	KNSTRN	AACAGCCAAAAAGCAGATGG	RASA1	GAACATCCGTGGATTCAGGA	NTC_29	ATCGTATCATCAGCTAGCGC
DNMT3A	GAGCAGGGTTGACGATGGAG	KNSTRN	TCTGATTTTTGCTTACTCAG	RASA1	ATCCGTGGATTCAGGATGGC	NTC_30	TCGATCGAGGTTGCATTCGG
DNMT3A	CTTGCGAGCAGGGTTGACGA	KNSTRN	AGAATCCACTACTGATCACA	RASA1	GAACATACTTTCAGAGCTTG	NTC_31	CTCGACAGTTCGTCCCGAGC
DNMT3A	TCATGAAGACAGGAAAATGC	KNSTRN	AGAGTCCATGTGATCAGTAG	RASA1	TGCAAGAACACTGATATTAG	NTC_32	CGGTAGTATTAATCGCTGAC
DNMT3A	GGAGTGGGGCCCATTCGATC	KNSTRN	GCTGTTAGAAACTTTGCAAG	RASA1	ATCAGTGTTCTTGCAGCAAT	NTC_33	TGAACGCGTGTTTCCTTGCA
DNMT3B	GAATTACTCACGCCCCAAGG	KRT27	CATCTTCTCCATCTATCAGG	RB1	TAAGGGCTTCGAGGAATGTG	NTC_34	CGACGCTAGGTAACGTAGAG
DNMT3B	GGCGTGAGTAATTCAGCAGG	KRT27	AAGCTCATTCCGGGCTGAGG	RB1	AATGTGAGGTATTGGTGACA	NTC_35	CATTGTTGAGCGGGCGCGCT
DNMT3B	GCTGAATTACTCACGCCCCA	KRT27	TCTAAATCAAAAGGCTATGG	RB1	GGAATCCGTGAAGGGTGAACT	NTC_36	CCGCTATTGAAACCGCCCAC
DNMT3B	CGTCGCTTCTGAAGTGTGTG	KRT27	TGTTCTAAATCAAAAGGCTA	RB1	TTTATAAAACAGTGAAAGAG	NTC_37	AGACACGTCACCGGTCAAAA
DNMT3B	AAAGAGTTGGGCATAAAGGT	KRT27	ATAGCCTTTTGATTTAGAAC	RB1	GAAAGAGAGGTAGATTTCAA	NTC_38	TTTACGATCTAGCGGCGTAG
DNMT3B	TGTTGGAACCGTGAAGCACG	KRT27	TCATCTCGATAAGCTCATTC	RB1	GTCCAAATTTCAGCAGAAAC	NTC_39	TTCGCACGATTGCACCTTGG
DOK3	CGGACACACAGTCAGCCAGG	KRT33B	GAATCAGTATGAGGCCCTGG	RBL1	TGATATAAAAGGCACAAAGG	NTC_40	GGTTAGAGACTAGGCGCGCG
DOK3	ACCAGTCCCATCTACCACAA	KRT33B	GCCGCAGGGACTGCTCCGTC	RBL1	TAAGAGAAGACTCTTTGGAG	NTC_41	CCTCCGTGCTAACGCGGACG
DOK3	GGCCAACGACAGTACCCTGG	KRT33B	CAGGAATCAGTATGAGGCCC	RBL1	TGGTCAAACTCTTCTAACAA	NTC_42	TTATCGCGTAGTGCTGACGT
DOK3	GCACACACAGGTTCTCATAG	KRT33B	CAGGGCCTCATACTGATTCC	RBL1	ATGTTTCAAATGAGTTACGA	NTC_43	TACGCTTGCGTTTAGCGTCC
DOK3	CGTGGTGGTGCAGAGGACTG	KRT33B	CCTCCTTCAGGGACTCCATC	RBL1	GTCCTGATCTAATGAAAGAC	NTC_44	CGCGGCCCACGCGTCATCGC
DOK3	CAGTAGATGGCTTCGCTCGG	KRT33B	CAACAGCCTGCGCAGGATTC	RBL1	CTTTCTGTAAAATAGTGCTA	NTC_45	AGCTCGCCATGTCGGTTCTC
DOT1L	CCTCCCGGAAGCCTCCTCAG	KRTAP25-1	CAGCGACAAAAAATAAAGCT	RBL2	TGGCACAGAGATCCCGAAGG	NTC_46	AACTAGCCCGAGCAGCTTCG
DOT1L	GCTGTGTAAACTCAGGTCCG	KRTAP25-1	CATAAGAGACATGGTTTTGG	RBL2	TGTCACTGTTGGCACCTGTG	NTC_47	CGCAAGGTGTCGGTAACCCT
DOT1L	GACAAGACCCCACTGCTGAG	KRTAP25-1	CCCACAAAATCAGAACAAGC	RBL2	GTTTGGCACAGAGATCCCGA	NTC_48	CTTCGACGCATCGTGCTCA
DOT1L	CTCCCCACTCACCTCAGACG	KRTAP25-1	ATTGACAGCCATAAGAGACA	RBL2	GTGAGGCGAGTAGGTGTGGG	NTC_49	TCCTGGATACCGCGTGGTTA
DOT1L	CCATTTTCCAAGGTTTTCGG	KRTAP25-1	TTGGAAACTGCTGTGCATGA	RBL2	TTGGCACCTGTGAGGCGAGT	NTC_50	ATAGCCGCCGCTCATTACTT
DOT1L	CCCCCGTGCTCAAGAAGGAG	KRTAP25-1	CAAAATCAGAACAAGCTGGT	RBL2	TTGTTATAGGACTCAGCCGC	NTC_51	GTCGTCCGGGATTACAAAAT
DUSP4	ACAGAATTCTGGGTACTCGG	LAMA1	TTTTCCATCACAGAGCACAG	RBPJ	CATTGCCTCAGGAACAAAGG	NTC_52	TAATGCTGCACACGCCGAAT
DUSP4	AACATAGCAGATCGCCCAGG	LAMA1	ACACACCCAGTCTACCTCAG	RBPJ	AGATACTTGCATGTAGAAGG	NTC_53	TATCGCTTCCGATTAGTCCG
DUSP4	CAGCATGGTAGGCACTGCCG	LAMA1	GAGGACGCCATTCTGCGAGG	RBPJ	AGGCTCTCTACCACAGGCAC	NTC_54	GTACCATACCGCGTACCCTT
DUSP4	GGAAGAAAAGTTCACTCCAA	LAMA1	TAACAGCAAACAGCTGGACA	RBPJ	TCACTCCAAATTTACGAGTG	NTC_55	TAAGATCCGCGGGTGGCAAC
DUSP4	GCAGTGCCTACCATGCTGCC	LAMA1	CAGGAGGACGCCATTCTGCG	RBPJ	GTAGCAATGCTTGAACTTAC	NTC_56	GTAGACGTCGTGAGCTTCAC
DUSP4	AAAGTGGTTTGGGCAGTCCG	LAMA1	ATTGGACTAGAGCTTGTGGA	RBPJ	CCAAATTTACGAGTGTGGTT	NTC_57	TCGCGGACATAGGGCTCTAA
DVL2	GGGAGAGTGAAATAGGCCTG	LATS2	GGAGTAGGTGCCAAAAAGGG	RET	GAGGCCAGACAACTGCAGCG	NTC_58	AGCGCAGATAGCGCGTATCA
DVL2	TTGTTGGCCAGAGCAATGAG	LATS2	TCCAAACTACATCGCACCCG	RET	ACATCCTGGTAGCTGAGGGG	NTC_59	GTTCGCTTCGTAACGAGGAA
DVL2	GGCCAACAATGGAGATACCC	LATS2	GAGTGTCCACCTTACAAGCA	RET	ATCCTGGGATTCCTCCTGAG	NTC_60	GACCCCCGATAACTTTTGAC
DVL2	CCCTGGCTCAATGCGCCCGT	LATS2	GACTGGCAGCAGGAGCATCG	RET	AAGAGGATTCCTACGTGAAG	NTC_61	ACGTCCATACTGTCGGCTAC
DVL2	CGGACTTCCAGTCCAGACTC	LATS2	CGAGGCAGACAATGAGTGGG	RET	TCGGATTCCAGTTAAATGGA	NTC_62	GTACCATTGCCGGCTCCCTA
DVL2	GCCATGGCAGCTCCAGAGTC	LATS2	ACACTCAACTCTGTGACTGG	RET	ACCTTCTGAAGACCGGCCAC	NTC_63	TGGTTCCGTAGGTCGGTATA
EGFR	AACCAGCAACAATTCCACCG	LCE1D	CTTAGGGGGACATTTAGGGG	RHOQ	CCGTGTCATAGAGTCCTAGG	NTC_64	TCTGGCTTGACACGACCGTT
EGFR	TCTATCAATGCAAGCCACGG	LCE1D	GCTGCAGCAGCCCCCAGAGT	RHOQ	CCTCCTAGGACTCTATGACA	NTC_65	CGCTAGGTCCGGTAAGTGCG
EGFR	GAATGACAAGGTAGCGCTGG	LCE1D	AGCTCTGGGGTCTGCGACGG	RHOQ	GAGGTACTGCTTGCCCCCCA	NTC_66	AGCACGTAATGTCCGTGGAT
EGFR	ATTTCTATCAATGCAAGCCA	LCE1D	TGACTGCTGCAGCCAGCCCT	RHOQ	CTTCCTTATATGCTTCTCGG	NTC_67	AAGGCGCGCGAATGTGGCAG
EGFR	AGAATTCGATGATCAACTCA	LCE1D	ACATTTAGGGGCGGGGCACT	RHOQ	GGTAAGATAAAGGCCTCAGA	NTC_68	ACTGCGGAGCGCCCAATATC
EGFR	ATGATCAACTCACGGAACTT	LCE1D	GGCGGCTGTGGCTCCAACTC	RHOQ	TGTGAAAGAGGAGTGGGTAC	NTC_69	CGTCGAGTGCTCGAACTCCA
EIF1AY	AAGAGAGTTGGTGTTTAAAG	LDHD	GGTCAACCCTGATGACGCCG	RICTOR	AGCGTATGAGAAGAACCTGG	NTC_70	TCGCAGCGGCGTGGGATCGG
EIF1AY	ACATCAGACATTATATTGGT	LDHD	GACACTGGGGAACGCACACG	RICTOR	ACAACTATGGACACAGACTG	NTC_71	ATCTGTCCTAATTCGGATCG
EIF1AY	AATGTTGGGAAATGGACGAT	LDHD	GATGGGCACACACACATCCG	RICTOR	GGACACCATGGACCGCACTG	NTC_72	TGCGGCGTAATGCTTGAAAG
EIF1AY	TTGGAAGCATTGTGTTTTGA	LDHD	CCCTGCCCCTGAGGCCACAG	RICTOR	AGAGACAGATGGTTAGACTG	NTC_73	CGAACTTAATCCCGTGGCAA
EIF1AY	ACATTATATTGGTTGGTCTA	LDHD	CATCCATCATGACTTCATCC	RICTOR	ATACCACCACATGATGATCG	NTC_74	GCCGTGTTGCTGGATACGCC
EIF1AY	TTCTCAATTTCCCTCTGATA	LDHD	ATGGAACTCCAGGAAGAGTG	RICTOR	TCTTGTATGAACCTCCGACA	NTC_75	TACCCTCCGGATACGGACTG
ELANE	GAGCCCATAACCTCTCGCGG	LGALS9	GCAGGACAGTGCCTGACAGG	RIPK1	GTTTCGTCTGCCTGTCCATG	NTC_76	CCGTTGGACTATGGCGGGTC
ELANE	GAAGTTGGGCGCAATCAGGG	LGALS9	TGGGTACAGCCCTCCCAGAA	RIPK1	GTGTGGCAGTACCTTCAAGC	NTC_77	GTACGGGGCGATCATCCACA
ELANE	TGGGAGCCCATAACCTCTCG	LGALS9	ACTTCGCTCCTCAGACCCCC	RIPK1	ACAGCAGCCCAGACAGAATG	NTC_78	AAGAGTAGTAGACGCCCGGG
ELANE	GCAGGAGCTCAACGTGACGG	LGALS9	AAAACGGGGGTTCAGGTGGA	RIPK1	GCAAACCAGGACTCCTCCAC	NTC_79	AAGAGCGAATCGATTTCGTG
ELANE	GTTTTCGAAGATGCGCTGCA	LGALS9	TCCAAGTCCATCCTCCTGTC	RIPK1	TACAATTATATGGAGATTGG	NTC_80	CGGCTCGTTCTACGCACTGA
ELANE	CTGCGCGGAGGCCACTTCTG	LGALS9	TCTCATCAAAACGGGGGTTC	RIPK1	ATAGCTTGGTACTTAGCAGC	NTC_81	TCCAGCGCGAGCTTACTCGT
ENY2	AGAGCTAAATTAATTGAATG	LMO7	CAGGGACTCGATGATCATGG	RNASE8	TCATCAATAAGTACACAGAA	NTC_82	GGAGTGGTCCCGTACGCAAC
ENY2	CGTTACTGTTGATGACTTGG	LMO7	GATCCTGACTTCAGCTCCTG	RNASE8	CCTGAACACACCTTACATAG	NTC_83	CAAGACCTTATCGTGCAGCG
ENY2	GTGGCTGAAATCACTCCAAA	LMO7	GTTGCCTGTGAGTGTGACCT	RNASE8	GTACTTATTGATGATGCTCA	NTC_84	ACGTCGTTTAGCACCCGGCT
ENY2	ACACGTTACTGTTGATGACT	LMO7	AGTCGTTGCAGTACAGTTGG	RNASE8	ACAACTTTATCCAAGTGCAC	NTC_85	TTTCAGGCTACGGGCGCGGG
ENY2	ATTAATTGAATGTGGCTGGA	LMO7	GCAAATGATAACAAAGACCC	RNASE8	TGGTCAGGGACATGGGCCCG	NTC_86	CAATCGGCGACGTTTTAAAT
ENY2	TGGCTGGAAGGATCAGTTGA	LMO7	TGCAATAACATTCTGGGCAA	RNASE8	CCTCCACAACAGGGTGACCC	NTC_87	GTACCCCTATGGCCGTTCTA
EP300	TCATGCTTCTGACAAAACCG	LYN	CTATAACAACAGTACCAAGG	RNF138	ATCTGGCTAGGATCTCCCCA	NTC_88	TACCCACGCGTATTCCATCT
EP300	GAATCACCCTGAGTCAGGAG	LYN	AGGGAATGGCATACATCGAG	RNF138	CACAGGGGACACTTAAAAGT	NTC_89	CTTGTTGCGTATACGAGACT
EP300	AGATAGATTAACAAGTGCAA	LYN	TTCCTGAAGAGGCGATGAAGG	RNF138	AGTTTCTGTGTTATCAGATG	NTC_90	GAACGCCGCTCAAGTTGATA
EP300	AAAGGAATTGCCTTATTTCG	LYN	CTACGCTGTGGTCACCAGGG	RNF138	CAGATCTCTCAAGATTCAGT	NTC_91	CGCAGTACGTATAGACTTAA
EP300	AAGGTGCCAAGTCTGGTAGA	LYN	TTACTATAACAACAGTACCA	RNF138	GTGATCCAGTAAACGCTGTC	NTC_92	GCGAACCCCGTAGCCAGGCT
EP300	AATGCTTTCTTCCAGAACAT	LYN	TTCGTATAGGAGGATTCCAA	RNF138	CAAGGAAGAGACACACAAAT	NTC_93	CCTCGGGCGTAAATACTCAT
EPHA3	TAAGCCAGTCACCTGTTGTG	MAP2K1	AACATCCTAGTCAACTCCCG	ROS1	TGAGGTTGGCTGTAGCAGCG	NTC_94	AGGGCACCCGGTTCATACGC
EPHA3	CCAGTCGAATGATATTGGGG	MAP2K1	CACAGAGCTTGATCTCCCCA	ROS1	AGAGAACTGCTCAAACATCG	NTC_95	CACGGCCTAACTTGCTGATA
EPHA3	TGTCTGGACAGCACACTGCA	MAP2K1	TAAAAGGCCTGACATATCTG	ROS1	TCTCCAATCTTCACTATCCG	NTC_96	CCGGGAGATTAACGTTAATT
EPHA3	TTCAAAAAAAGAGATTTCAG	MAP2K1	TGGCGAGATCAGTATCTGCA	ROS1	TGAGGTGCACTAATAGAGGG	NTC_97	ATCTCGGGTCGACTGCGGAT
EPHA3	ACACTGCAAGGAAATCTTCA	MAP2K1	TATGGTGCGTTCTACAGCGA	ROS1	TGAAAGACTATACCAGTCCA	NTC_98	CGCCGGGACCGTTAGGGAAT
EPHA3	TATGATTGTCACAGAATACA	MAP2K1	ACGGGAGTTGACTAGGATGT	ROS1	TATAGTCTTTCACGGAAACA	NTC_99	GCAAACCCGAGTGACACGTC

Table 2: FHSC14 GeCKO v2 pilot genome scale CRISPR deletion screen analysis and results
Top 150 genes enriched in the CIS-ETO vs. P0 condition are shown (ranked by positive unadjusted p-value)

	CIS-ETO vs. P0								SAL vs. P0							
Gene	Median Log2(FC)	Pos. RRA	Pos. Unadj. P	Pos. Adj. P	Neg. RRA	Neg. Unadj. P	Neg. Adj. P	Guides Enriched	Median Log2(FC)	Pos. RRA	Pos. Unadj. P	Pos. Adj. P	Neg. RRA	Neg. Unadj. P	Neg. Adj. P	Guides Enriched
USP22	5.6	1.7E-06	8.7E-06	9.8E-02	1.0E+00	1.0E+00	1.0E+00	5	4.4	1.4E-02	5.4E-02	9.8E-01	9.9E-01	9.9E-01	1.0E+00	4
TAF5L	5.8	2.3E-06	1.1E-05	9.8E-02	1.0E+00	1.0E+00	1.0E+00	4	3.5	4.5E-02	1.5E-01	1.0E+00	7.5E-01	8.6E-01	9.9E-01	4
APMAP	4.5	1.3E-05	7.7E-05	4.1E-01	9.4E-01	9.6E-01	1.0E+00	5	-1.5	8.7E-01	9.1E-01	1.0E+00	1.6E-01	3.6E-01	9.5E-01	1
PPP3CC	2.9	1.6E-05	9.2E-05	4.1E-01	6.5E-01	8.3E-01	1.0E+00	3	0.9	4.9E-01	7.1E-01	1.0E+00	1.4E-01	3.3E-01	9.4E-01	2
SUMO1	1.8	2.5E-05	1.5E-04	4.5E-01	6.3E-01	8.3E-01	1.0E+00	2	0.5	2.9E-01	5.2E-01	1.0E+00	1.7E-01	3.7E-01	9.5E-01	3
HFE2	4.3	2.7E-05	1.5E-04	4.5E-01	9.8E-01	9.8E-01	1.0E+00	4	3.4	2.2E-02	7.9E-02	1.0E+00	9.6E-01	9.6E-01	1.0E+00	4
FOXJ1	4.0	4.5E-05	2.5E-04	5.5E-01	1.0E+00	1.0E+00	1.0E+00	5	0.0	6.2E-01	7.8E-01	1.0E+00	4.6E-01	6.8E-01	9.7E-01	2
TADA1	5.2	4.5E-05	2.5E-04	5.5E-01	1.0E+00	1.0E+00	1.0E+00	4	0.8	3.2E-01	5.5E-01	1.0E+00	9.4E-01	9.4E-01	1.0E+00	2
ZNF485	4.7	5.1E-05	2.8E-04	5.5E-01	6.5E-01	8.3E-01	1.0E+00	5	0.9	7.0E-01	8.2E-01	1.0E+00	9.6E-01	9.6E-01	1.0E+00	1
POLD1	3.7	6.0E-05	3.3E-04	5.5E-01	9.9E-01	9.9E-01	1.0E+00	3	-0.2	2.2E-01	4.4E-01	1.0E+00	7.5E-02	2.0E-01	9.3E-01	1
SHC2	3.2	6.3E-05	3.4E-04	5.5E-01	1.0E+00	1.0E+00	1.0E+00	6	0.6	4.6E-01	6.8E-01	1.0E+00	5.6E-01	7.3E-01	9.7E-01	2
NOP10	0.9	7.6E-05	4.1E-04	5.7E-01	8.0E-01	9.0E-01	1.0E+00	1	0.3	6.0E-01	7.7E-01	1.0E+00	5.2E-01	7.1E-01	9.7E-01	2
ZNF319	3.7	7.7E-05	4.1E-04	5.7E-01	9.9E-01	9.9E-01	1.0E+00	5	1.9	1.2E-01	2.9E-01	1.0E+00	9.4E-01	9.4E-01	1.0E+00	3
CYP27A1	4.5	8.6E-05	4.7E-04	6.0E-01	6.0E-01	8.0E-01	1.0E+00	4	1.4	3.1E-01	5.3E-01	1.0E+00	9.7E-01	9.7E-01	1.0E+00	3
FZD3	4.3	1.0E-04	5.6E-04	6.3E-01	2.7E-01	5.3E-01	9.8E-01	5	1.5	1.9E-01	4.1E-01	1.0E+00	1.9E-01	4.0E-01	9.5E-01	3
YIPF7	3.9	1.1E-04	6.0E-04	6.3E-01	1.0E+00	1.0E+00	1.0E+00	5	0.3	6.8E-01	8.1E-01	1.0E+00	4.4E-01	6.6E-01	9.6E-01	1
MAP3K11	4.3	1.1E-04	6.1E-04	6.3E-01	9.7E-01	9.7E-01	1.0E+00	4	-0.2	1.3E-01	3.0E-01	1.0E+00	3.1E-01	5.3E-01	9.6E-01	1
FOLR3	0.6	1.3E-04	6.9E-04	6.9E-01	8.5E-01	9.2E-01	1.0E+00	1	2.3	5.0E-03	2.4E-02	9.8E-01	1.0E+00	1.0E+00	1.0E+00	5
MMP26	4.7	1.5E-04	8.3E-04	7.7E-01	9.9E-01	9.9E-01	1.0E+00	4	0.1	7.3E-01	8.4E-01	1.0E+00	8.5E-01	8.9E-01	9.9E-01	1
FHL3	4.4	2.0E-04	1.1E-03	8.9E-01	7.5E-01	8.8E-01	1.0E+00	4	-1.4	4.7E-01	6.9E-01	1.0E+00	1.4E-01	3.3E-01	9.5E-01	1
CDCP1	2.9	2.1E-04	1.1E-03	8.9E-01	1.0E+00	1.0E+00	1.0E+00	4	-0.5	6.3E-01	7.8E-01	1.0E+00	2.6E-01	4.8E-01	9.5E-01	1
SFXN2	3.7	2.3E-04	1.2E-03	8.9E-01	4.0E-01	6.5E-01	9.9E-01	5	0.7	7.8E-01	8.8E-01	1.0E+00	1.3E-02	4.9E-02	9.3E-01	1
CRABP2	0.3	2.3E-04	1.2E-03	8.9E-01	5.5E-01	7.7E-01	1.0E+00	1	4.0	2.5E-02	9.0E-02	1.0E+00	1.5E-01	3.4E-01	9.5E-01	4
TRMT11	4.3	2.4E-04	1.3E-03	8.9E-01	2.7E-01	5.2E-01	9.8E-01	5	3.9	2.8E-02	9.9E-02	1.0E+00	7.6E-01	8.6E-01	9.9E-01	4
NELL1	3.2	2.5E-04	1.3E-03	8.9E-01	1.0E+00	1.0E+00	1.0E+00	3	-0.9	9.6E-01	9.6E-01	1.0E+00	2.7E-02	9.5E-02	9.3E-01	0
KRTAP25-1	4.7	2.6E-04	1.4E-03	8.9E-01	7.0E-01	8.5E-01	1.0E+00	4	0.4	7.6E-01	8.7E-01	1.0E+00	9.2E-01	9.2E-01	1.0E+00	0
HIST1H4L	4.4	2.6E-04	1.4E-03	8.9E-01	9.5E-01	9.6E-01	1.0E+00	4	0.7	6.0E-02	1.8E-01	1.0E+00	6.6E-01	8.0E-01	9.8E-01	1
ELANE	4.1	2.8E-04	1.5E-03	8.9E-01	7.7E-01	8.8E-01	1.0E+00	4	-1.8	5.4E-01	7.4E-01	1.0E+00	4.5E-01	6.7E-01	9.7E-01	2
PRPF3	-1.3	2.8E-04	1.5E-03	8.9E-01	8.6E-03	3.9E-02	8.8E-01	1	2.8	5.9E-02	1.8E-01	1.0E+00	5.0E-01	7.0E-01	9.7E-01	4
FOXH1	4.3	3.1E-04	1.6E-03	8.9E-01	2.0E-01	4.3E-01	9.6E-01	5	1.1	2.4E-01	4.7E-01	1.0E+00	5.2E-01	7.1E-01	9.7E-01	2
NELFB	2.6	3.1E-04	1.6E-03	8.9E-01	8.4E-01	9.2E-01	1.0E+00	3	-1.7	1.0E+00	1.0E+00	1.0E+00	1.8E-03	8.8E-03	9.0E-01	0
ALDH3A1	2.9	3.2E-04	1.7E-03	8.9E-01	1.0E+00	1.0E+00	1.0E+00	5	-1.4	3.9E-01	6.1E-01	1.0E+00	8.2E-02	2.2E-01	9.3E-01	2
SCML1	4.2	3.3E-04	1.7E-03	8.9E-01	9.7E-01	9.7E-01	1.0E+00	4	2.5	4.1E-02	1.4E-01	1.0E+00	5.6E-01	7.3E-01	9.7E-01	4
KRT27	3.1	3.4E-04	1.8E-03	8.9E-01	9.9E-01	9.9E-01	1.0E+00	3	0.2	7.2E-01	8.4E-01	1.0E+00	9.3E-01	9.4E-01	1.0E+00	1
PIGG	3.3	3.4E-04	1.8E-03	8.9E-01	1.0E+00	1.0E+00	1.0E+00	5	1.5	7.6E-02	2.1E-01	1.0E+00	2.6E-01	4.7E-01	9.5E-01	3
PPP6R3	4.3	3.5E-04	1.9E-03	8.9E-01	6.8E-01	8.5E-01	1.0E+00	4	-1.0	4.5E-01	6.7E-01	1.0E+00	5.0E-03	2.3E-02	9.3E-01	2
CDC34	3.4	3.6E-04	1.9E-03	8.9E-01	6.0E-02	1.9E-01	9.3E-01	5	1.3	1.6E-02	6.0E-02	9.9E-01	1.6E-01	3.5E-01	9.5E-01	3
WDR27	4.1	3.7E-04	2.0E-03	8.9E-01	9.7E-01	9.7E-01	1.0E+00	4	0.9	1.5E-01	3.4E-01	1.0E+00	6.4E-02	1.8E-01	9.3E-01	3
SRSF4	1.3	3.8E-04	2.0E-03	8.9E-01	8.6E-01	9.3E-01	1.0E+00	2	-0.9	1.3E-02	5.1E-02	9.8E-01	5.5E-02	1.6E-01	9.3E-01	2
ETV3	4.1	4.0E-04	2.1E-03	8.9E-01	7.8E-01	8.9E-01	1.0E+00	4	0.3	3.2E-01	5.4E-01	1.0E+00	5.5E-01	7.3E-01	9.7E-01	3
TADA2B	2.4	4.2E-04	2.2E-03	8.9E-01	9.9E-01	9.9E-01	1.0E+00	3	3.1	2.2E-02	7.9E-02	1.0E+00	1.7E-01	3.8E-01	9.5E-01	3
HESX1	3.3	4.3E-04	2.3E-03	8.9E-01	1.0E+00	1.0E+00	1.0E+00	5	1.9	1.2E-01	2.9E-01	1.0E+00	6.7E-01	8.0E-01	9.8E-01	4
DAPL1	3.0	4.4E-04	2.3E-03	8.9E-01	1.0E+00	1.0E+00	1.0E+00	5	-0.4	8.7E-01	9.1E-01	1.0E+00	2.4E-01	4.6E-01	9.5E-01	1
HAGH	2.9	4.5E-04	2.4E-03	8.9E-01	1.0E+00	1.0E+00	1.0E+00	4	0.6	6.6E-01	8.0E-01	1.0E+00	6.7E-01	8.0E-01	9.8E-01	1
DLEU7	3.3	4.6E-04	2.4E-03	8.9E-01	1.0E+00	1.0E+00	1.0E+00	5	0.4	5.6E-01	7.5E-01	1.0E+00	6.6E-01	8.0E-01	9.8E-01	2
ARPC5L	3.2	4.6E-04	2.4E-03	8.9E-01	3.0E-01	5.6E-01	9.8E-01	5	4.4	1.0E-02	4.2E-02	9.8E-01	9.9E-01	9.9E-01	1.0E+00	5
RAB8B	4.1	4.7E-04	2.5E-03	8.9E-01	7.4E-01	8.7E-01	1.0E+00	4	0.6	4.0E-01	6.2E-01	1.0E+00	3.3E-01	5.5E-01	9.6E-01	2
HTR6	2.5	4.8E-04	2.5E-03	8.9E-01	1.0E+00	1.0E+00	1.0E+00	3	0.9	2.4E-01	4.6E-01	1.0E+00	4.0E-01	6.2E-01	9.6E-01	3
GSTM5	4.4	4.8E-04	2.5E-03	8.9E-01	5.5E-01	7.6E-01	1.0E+00	4	0.6	5.1E-02	1.6E-01	1.0E+00	2.8E-01	5.0E-01	9.6E-01	2
KCNA1	2.7	4.8E-04	2.5E-03	8.9E-01	2.1E-01	4.5E-01	9.6E-01	3	2.0	9.3E-02	2.4E-01	1.0E+00	9.8E-01	9.8E-01	1.0E+00	4
CHRM4	4.3	5.0E-04	2.6E-03	9.1E-01	4.7E-01	7.0E-01	9.9E-01	4	1.5	2.4E-01	4.6E-01	1.0E+00	9.8E-01	9.8E-01	1.0E+00	3
FAM90A1	3.7	5.1E-04	2.7E-03	9.1E-01	7.6E-01	8.8E-01	1.0E+00	4	-1.7	8.7E-01	9.1E-01	1.0E+00	1.4E-01	3.2E-01	9.4E-01	1
OTOP3	1.9	5.2E-04	2.7E-03	9.1E-01	8.5E-01	9.3E-01	1.0E+00	2	4.5	1.4E-02	5.3E-02	9.8E-01	9.8E-01	9.8E-01	1.0E+00	4
C2orf62	1.3	5.3E-04	2.8E-03	9.1E-01	6.7E-02	2.0E-01	9.3E-01	2	-1.0	9.6E-01	9.6E-01	1.0E+00	6.7E-03	2.9E-02	9.3E-01	1
TAF6L	1.1	5.3E-04	2.8E-03	9.1E-01	1.3E-01	3.3E-01	9.5E-01	3	0.7	7.7E-01	8.7E-01	1.0E+00	1.5E-01	3.5E-01	9.5E-01	1
SMG9	3.5	5.5E-04	2.9E-03	9.2E-01	1.0E+00	1.0E+00	1.0E+00	5	5.2	4.7E-03	2.2E-02	9.8E-01	7.2E-01	8.3E-01	9.8E-01	4
TOP3B	4.4	5.6E-04	3.0E-03	9.3E-01	7.6E-01	8.8E-01	1.0E+00	5	1.7	1.6E-01	3.5E-01	1.0E+00	6.3E-01	7.7E-01	9.7E-01	3
KEAP1	2.3	5.8E-04	3.0E-03	9.3E-01	6.3E-01	8.2E-01	1.0E+00	3	2.6	7.6E-02	2.1E-01	1.0E+00	7.2E-01	8.3E-01	9.8E-01	3
PRF1	2.4	5.9E-04	3.1E-03	9.3E-01	6.4E-01	8.3E-01	1.0E+00	3	5.0	4.6E-03	2.2E-02	9.8E-01	3.9E-01	6.1E-01	9.6E-01	4
OTC	1.5	6.3E-04	3.3E-03	9.7E-01	7.9E-01	9.0E-01	1.0E+00	2	-1.0	3.9E-01	6.1E-01	1.0E+00	2.6E-01	4.8E-01	9.5E-01	1
RNASE8	4.2	6.4E-04	3.3E-03	9.7E-01	8.5E-01	9.3E-01	1.0E+00	4	0.6	6.9E-01	8.2E-01	1.0E+00	4.0E-01	6.2E-01	9.6E-01	1
GP6	3.7	6.8E-04	3.5E-03	1.0E+00	6.8E-01	8.4E-01	1.0E+00	4	-1.1	8.5E-02	2.3E-01	1.0E+00	5.1E-02	1.6E-01	9.3E-01	2
DLX3	3.2	6.8E-04	3.5E-03	1.0E+00	2.6E-02	9.7E-02	9.2E-01	5	-0.3	6.5E-01	7.9E-01	1.0E+00	1.0E-01	2.6E-01	9.4E-01	2
CCDC34	4.2	6.9E-04	3.6E-03	1.0E+00	9.4E-01	9.6E-01	1.0E+00	5	1.3	9.1E-02	2.4E-01	1.0E+00	9.0E-01	9.1E-01	9.9E-01	3
TCF25	4.2	7.2E-04	3.8E-03	1.0E+00	8.6E-01	9.3E-01	1.0E+00	4	-1.8	8.1E-01	8.9E-01	1.0E+00	8.3E-02	2.2E-01	9.4E-01	2
CBX3	-0.6	7.8E-04	4.0E-03	1.0E+00	1.3E-01	3.3E-01	9.5E-01	2	1.4	2.5E-01	4.7E-01	1.0E+00	4.6E-01	6.8E-01	9.7E-01	3
SLC2A5	2.5	7.8E-04	4.0E-03	1.0E+00	3.2E-01	5.9E-01	9.8E-01	3	-0.6	2.7E-01	5.0E-01	1.0E+00	8.0E-01	8.8E-01	9.9E-01	2
IQGAP2	3.1	8.1E-04	4.2E-03	1.0E+00	9.9E-01	9.9E-01	1.0E+00	3	-1.3	7.0E-01	8.2E-01	1.0E+00	2.0E-02	7.1E-02	9.3E-01	1
P2RX5	1.6	8.1E-04	4.2E-03	1.0E+00	7.8E-01	8.9E-01	1.0E+00	3	-0.6	3.2E-01	5.5E-01	1.0E+00	2.1E-01	4.2E-01	9.5E-01	1
S100G	2.2	8.3E-04	4.3E-03	1.0E+00	9.9E-01	9.9E-01	1.0E+00	3	3.8	3.7E-03	1.8E-02	9.8E-01	1.0E+00	1.0E+00	1.0E+00	5
VWC2L	3.0	8.5E-04	4.4E-03	1.0E+00	1.0E+00	1.0E+00	1.0E+00	3	-0.7	7.3E-01	8.4E-01	1.0E+00	1.5E-01	3.4E-01	9.5E-01	1
CYB561D2	2.1	8.6E-04	4.4E-03	1.0E+00	1.0E+00	1.0E+00	1.0E+00	2	1.0	6.0E-02	1.8E-01	1.0E+00	2.9E-01	5.1E-01	9.6E-01	3
TREX2	4.3	8.6E-04	4.4E-03	1.0E+00	6.4E-01	8.3E-01	1.0E+00	4	1.3	2.0E-01	4.2E-01	1.0E+00	9.5E-01	9.5E-01	1.0E+00	2
ATP6V1G3	2.4	8.8E-04	4.5E-03	1.0E+00	1.0E+00	1.0E+00	1.0E+00	3	-0.2	5.6E-01	7.5E-01	1.0E+00	2.9E-01	5.1E-01	9.6E-01	2
TAL1	-2.7	8.8E-04	4.5E-03	1.0E+00	1.3E-02	5.5E-02	8.8E-01	1	-1.1	6.3E-01	7.8E-01	1.0E+00	1.9E-01	4.0E-01	9.5E-01	2
MED24	3.6	9.2E-04	4.7E-03	1.0E+00	9.6E-01	9.7E-01	1.0E+00	4	-1.9	9.9E-01	9.9E-01	1.0E+00	1.2E-01	2.8E-01	9.4E-01	0
SLC35E1	0.4	9.4E-04	4.8E-03	1.0E+00	4.3E-03	2.1E-02	8.3E-01	2	-0.2	7.8E-01	8.8E-01	1.0E+00	1.2E-01	3.0E-01	9.4E-01	0
MBOAT4	2.0	9.4E-04	4.8E-03	1.0E+00	1.0E+00	1.0E+00	1.0E+00	2	-1.3	8.6E-01	9.0E-01	1.0E+00	3.6E-01	5.8E-01	9.6E-01	1
SLC30A9	-1.4	9.8E-04	5.0E-03	1.0E+00	2.1E-01	4.4E-01	9.6E-01	2	-1.4	3.3E-01	5.5E-01	1.0E+00	1.9E-02	6.9E-02	9.3E-01	1
PNMT	-0.1	9.8E-04	5.0E-03	1.0E+00	8.3E-02	2.4E-01	9.3E-01	1	4.3	2.6E-02	9.1E-02	1.0E+00	2.4E-02	8.6E-02	9.3E-01	4
CPN2	4.2	9.8E-04	5.0E-03	1.0E+00	8.7E-01	9.4E-01	1.0E+00	4	-0.7	9.7E-01	9.7E-01	1.0E+00	1.4E-01	3.2E-01	9.4E-01	0
CELF5	3.3	1.0E-03	5.2E-03	1.0E+00	9.9E-01	9.9E-01	1.0E+00	5	1.8	3.0E-02	1.0E-01	1.0E+00	9.8E-01	9.8E-01	1.0E+00	4
ZNF527	4.0	1.0E-03	5.2E-03	1.0E+00	5.6E-01	7.7E-01	1.0E+00	4	-0.1	8.5E-01	9.0E-01	1.0E+00	7.1E-02	2.0E-01	9.3E-01	1
CPN1	3.2	1.0E-03	5.3E-03	1.0E+00	1.0E+00	1.0E+00	1.0E+00	4	3.1	4.3E-02	1.4E-01	1.0E+00	8.9E-01	9.1E-01	9.9E-01	4
FAH	2.6	1.0E-03	5.3E-03	1.0E+00	1.0E-01	2.8E-01	9.4E-01	3	-1.5	2.5E-01	4.8E-01	1.0E+00	5.7E-02	1.7E-01	9.3E-01	2
WDR49	3.1	1.1E-03	5.4E-03	1.0E+00	1.0E+00	1.0E+00	1.0E+00	5	-1.2	9.7E-01	9.7E-01	1.0E+00	1.1E-02	4.5E-02	9.3E-01	0
IFNA7	3.5	1.1E-03	5.5E-03	1.0E+00	3.8E-02	1.3E-01	9.3E-01	5	-0.1	5.2E-01	7.3E-01	1.0E+00	1.7E-01	3.8E-01	9.5E-01	2
SLC46A2	0.0	1.1E-03	5.5E-03	1.0E+00	1.8E-01	4.0E-01	9.6E-01	2	-0.1	3.4E-01	5.7E-01	1.0E+00	6.7E-01	8.0E-01	9.8E-01	1
SLC25A33	3.8	1.1E-03	5.6E-03	1.0E+00	9.9E-01	9.9E-01	1.0E+00	4	1.0	1.7E-01	3.8E-01	1.0E+00	9.3E-02	2.4E-01	9.4E-01	2
HDGFRP2	2.9	1.1E-03	5.6E-03	1.0E+00	1.8E-01	4.0E-01	9.6E-01	3	1.7	1.7E-01	3.8E-01	1.0E+00	9.3E-01	9.3E-01	1.0E+00	3
MMP14	2.2	1.1E-03	5.7E-03	1.0E+00	6.2E-01	8.1E-01	1.0E+00	2	2.5	1.1E-01	2.8E-01	1.0E+00	9.4E-01	9.4E-01	1.0E+00	3
STIP1	3.3	1.1E-03	5.7E-03	1.0E+00	2.3E-02	8.9E-02	9.1E-01	5	2.7	2.5E-02	9.0E-02	1.0E+00	9.9E-01	9.9E-01	1.0E+00	4
CAMSAP3	2.8	1.2E-03	5.9E-03	1.0E+00	5.6E-01	7.7E-01	1.0E+00	3	1.4	1.4E-01	3.3E-01	1.0E+00	4.9E-01	6.9E-01	9.7E-01	2
ITPRIP	3.2	1.2E-03	5.9E-03	1.0E+00	5.2E-01	7.4E-01	1.0E+00	5	-0.8	4.0E-01	6.3E-01	1.0E+00	1.2E-02	4.8E-02	9.3E-01	3
AKT3	-1.8	1.2E-03	6.0E-03	1.0E+00	1.2E-01	3.1E-01	9.4E-01	2	-0.2	6.5E-01	8.0E-01	1.0E+00	9.0E-01	9.2E-01	9.9E-01	2
C1orf35	1.1	1.2E-03	6.0E-03	1.0E+00	6.8E-01	8.5E-01	1.0E+00	2	-1.0	7.7E-01	8.7E-01	1.0E+00	1.5E-01	3.4E-01	9.5E-01	1
POGK	3.0	1.2E-03	6.1E-03	1.0E+00	1.3E-01	3.3E-01	9.5E-01	5	-0.4	3.9E-01	6.1E-01	1.0E+00	6.2E-01	7.7E-01	9.7E-01	2
ETV1	-1.2	1.2E-03	6.2E-03	1.0E+00	2.1E-01	4.5E-01	9.6E-01	1	-1.8	4.8E-02	1.6E-01	1.0E+00	1.5E-01	3.3E-01	9.5E-01	1
MID1	4.0	1.3E-03	6.4E-03	1.0E+00	9.5E-01	9.6E-01	1.0E+00	4	1.0	1.9E-01	4.1E-01	1.0E+00	1.1E-01	2.7E-01	9.4E-01	3

ZMYM2	3.1	1.3E-03	6.4E-03	1.0E+00	8.9E-01	9.4E-01	1.0E+00	5	-2.0	8.1E-01	8.9E-01	1.0E+00	1.8E-01	3.8E-01	9.5E-01	1
CARM1	3.8	1.3E-03	6.5E-03	1.0E+00	8.8E-01	9.4E-01	1.0E+00	3	0.5	4.1E-01	6.4E-01	1.0E+00	6.0E-01	7.5E-01	9.7E-01	0
CUL5	0.2	1.3E-03	6.6E-03	1.0E+00	4.8E-01	7.1E-01	9.9E-01	2	-2.3	8.9E-01	9.2E-01	1.0E+00	7.0E-01	8.2E-01	9.8E-01	1
SEMA6C	3.8	1.4E-03	6.6E-03	1.0E+00	9.2E-01	9.5E-01	1.0E+00	4	4.2	1.8E-02	6.7E-02	1.0E+00	2.5E-05	1.5E-04	5.2E-01	4
HIST1H3A	4.0	1.4E-03	6.7E-03	1.0E+00	9.8E-01	9.8E-01	1.0E+00	4	0.1	3.3E-01	5.6E-01	1.0E+00	5.4E-01	7.2E-01	9.7E-01	1
MRPL14	2.4	1.4E-03	6.8E-03	1.0E+00	4.7E-01	7.0E-01	9.9E-01	3	0.9	2.3E-01	4.6E-01	1.0E+00	7.1E-01	8.3E-01	9.8E-01	4
PPP1R11	0.6	1.4E-03	7.0E-03	1.0E+00	5.5E-01	7.7E-01	1.0E+00	2	-1.6	4.9E-01	7.1E-01	1.0E+00	1.3E-01	3.1E-01	9.4E-01	1
WDR70	1.4	1.4E-03	7.0E-03	1.0E+00	4.0E-01	6.5E-01	9.9E-01	3	-0.8	4.3E-01	6.5E-01	1.0E+00	5.6E-01	7.3E-01	9.7E-01	1
TMEM50A	3.6	1.5E-03	7.1E-03	1.0E+00	5.1E-01	7.4E-01	1.0E+00	4	-0.8	5.7E-01	7.5E-01	1.0E+00	1.1E-01	2.8E-01	9.4E-01	1
MED23	1.2	1.5E-03	7.1E-03	1.0E+00	6.0E-02	1.9E-01	9.3E-01	3	2.0	1.6E-01	3.6E-01	1.0E+00	5.1E-01	7.1E-01	9.7E-01	3
GSG1L	3.5	1.5E-03	7.1E-03	1.0E+00	4.8E-01	7.1E-01	9.9E-01	5	1.3	3.3E-01	5.6E-01	1.0E+00	4.3E-01	6.5E-01	9.6E-01	2
PTGDR2	2.6	1.5E-03	7.2E-03	1.0E+00	9.7E-01	9.7E-01	1.0E+00	3	-0.4	1.4E-01	3.3E-01	1.0E+00	3.7E-01	5.9E-01	9.6E-01	1
KLF8	2.9	1.5E-03	7.3E-03	1.0E+00	3.3E-01	6.0E-01	9.8E-01	4	-2.2	5.5E-01	7.4E-01	1.0E+00	9.2E-02	2.4E-01	9.4E-01	2
BRD9	4.1	1.5E-03	7.4E-03	1.0E+00	1.3E-01	3.2E-01	9.4E-01	4	1.8	1.1E-01	2.8E-01	1.0E+00	4.6E-01	6.8E-01	9.7E-01	3
SLPI	3.1	1.5E-03	7.4E-03	1.0E+00	9.9E-01	9.9E-01	1.0E+00	3	3.5	6.1E-03	2.8E-02	9.8E-01	9.8E-01	9.8E-01	1.0E+00	5
IGFBP1	4.0	1.6E-03	7.5E-03	1.0E+00	8.4E-01	9.2E-01	1.0E+00	4	-0.3	2.9E-01	5.1E-01	1.0E+00	6.2E-01	7.7E-01	9.7E-01	2
PTGES	-1.7	1.6E-03	7.6E-03	1.0E+00	1.2E-01	3.1E-01	9.4E-01	1	-1.6	4.7E-01	6.9E-01	1.0E+00	3.0E-01	5.1E-01	9.6E-01	2
MED16	3.4	1.6E-03	7.6E-03	1.0E+00	1.8E-01	4.0E-01	9.6E-01	4	1.0	3.7E-01	5.9E-01	1.0E+00	7.3E-01	8.4E-01	9.8E-01	1
HTR1F	3.7	1.6E-03	7.7E-03	1.0E+00	7.6E-01	8.8E-01	1.0E+00	4	1.0	2.6E-01	4.9E-01	1.0E+00	5.0E-01	7.0E-01	9.7E-01	3
PPP1R12C	3.5	1.6E-03	7.7E-03	1.0E+00	1.9E-01	4.2E-01	9.6E-01	3	-0.9	7.6E-01	8.6E-01	1.0E+00	1.3E-01	3.1E-01	9.4E-01	1
LTB4R2	2.8	1.6E-03	7.8E-03	1.0E+00	5.8E-01	7.9E-01	1.0E+00	3	3.4	3.2E-03	1.5E-02	9.8E-01	1.0E+00	1.0E+00	1.0E+00	5
TFAP2B	3.5	1.7E-03	7.9E-03	1.0E+00	1.9E-01	4.2E-01	9.6E-01	3	1.6	1.6E-01	3.5E-01	1.0E+00	9.7E-01	9.7E-01	1.0E+00	3
RPL22L1	1.7	1.7E-03	8.0E-03	1.0E+00	1.2E-01	3.2E-01	9.4E-01	3	-0.3	8.6E-01	9.0E-01	1.0E+00	8.1E-01	8.8E-01	9.9E-01	1
NDUFV3	2.5	1.7E-03	8.0E-03	1.0E+00	6.9E-01	8.5E-01	1.0E+00	3	1.2	5.3E-02	1.7E-01	1.0E+00	7.6E-01	8.6E-01	9.9E-01	3
SSR4	-0.9	1.7E-03	8.0E-03	1.0E+00	3.4E-01	6.1E-01	9.8E-01	2	-0.1	2.0E-01	4.2E-01	1.0E+00	3.3E-01	5.5E-01	9.6E-01	2
HLA-DRB1	3.5	1.7E-03	8.1E-03	1.0E+00	7.7E-01	8.8E-01	1.0E+00	5	-0.1	3.8E-01	6.1E-01	1.0E+00	6.1E-01	7.6E-01	9.7E-01	2
LCNL1	4.0	1.7E-03	8.2E-03	1.0E+00	2.4E-01	4.8E-01	9.7E-01	4	3.1	1.3E-02	5.0E-02	9.8E-01	5.8E-01	7.5E-01	9.7E-01	5
BBS4	0.7	1.7E-03	8.2E-03	1.0E+00	5.6E-01	7.7E-01	1.0E+00	2	0.3	1.1E-02	4.3E-02	9.8E-01	7.0E-01	8.2E-01	9.8E-01	2
HHIPL2	3.3	1.8E-03	8.2E-03	1.0E+00	9.7E-01	9.7E-01	1.0E+00	5	-1.0	3.2E-01	5.5E-01	1.0E+00	5.9E-01	7.5E-01	9.7E-01	3
WDR45	2.4	1.8E-03	8.2E-03	1.0E+00	6.4E-01	8.3E-01	1.0E+00	3	0.9	1.5E-01	3.4E-01	1.0E+00	9.8E-01	9.8E-01	1.0E+00	2
OR8B3	1.7	1.8E-03	8.2E-03	1.0E+00	1.7E-01	3.8E-01	9.6E-01	2	-1.7	7.8E-01	8.8E-01	1.0E+00	3.2E-02	1.1E-01	9.3E-01	1
ZNF501	3.8	1.8E-03	8.3E-03	1.0E+00	9.9E-01	9.9E-01	1.0E+00	4	-0.3	5.8E-01	7.5E-01	1.0E+00	2.6E-01	4.8E-01	9.5E-01	1
C2CD4A	3.5	1.8E-03	8.4E-03	1.0E+00	5.6E-03	2.6E-02	8.5E-01	4	0.4	5.0E-01	7.2E-01	1.0E+00	1.5E-01	3.3E-01	9.5E-01	1
PTP4A1	1.0	1.8E-03	8.5E-03	1.0E+00	1.3E-01	3.3E-01	9.4E-01	2	NA	NA	NA	NA	NA	NA	NA	NA
CCDC170	2.7	1.8E-03	8.5E-03	1.0E+00	3.8E-01	6.3E-01	9.8E-01	3	NA	NA	NA	NA	NA	NA	NA	NA
CXCL16	1.4	1.8E-03	8.5E-03	1.0E+00	1.1E-01	3.0E-01	9.4E-01	3	-0.5	7.0E-01	8.2E-01	1.0E+00	1.4E-01	3.2E-01	9.4E-01	1
ESRP2	3.6	1.9E-03	8.6E-03	1.0E+00	1.5E-01	3.5E-01	9.5E-01	4	-0.4	9.3E-01	9.4E-01	1.0E+00	4.3E-01	6.5E-01	9.6E-01	0
OPN4	3.7	1.9E-03	8.7E-03	1.0E+00	8.2E-01	9.1E-01	1.0E+00	4	0.4	7.8E-01	8.8E-01	1.0E+00	3.0E-01	5.2E-01	9.6E-01	1
FOXF2	1.2	1.9E-03	8.7E-03	1.0E+00	6.0E-02	1.9E-01	9.3E-01	3	-2.5	3.9E-01	6.2E-01	1.0E+00	7.5E-02	2.1E-01	9.3E-01	1
PRICKLE1	2.3	1.9E-03	8.8E-03	1.0E+00	6.9E-01	8.5E-01	1.0E+00	3	-0.7	2.0E-01	4.2E-01	1.0E+00	2.4E-01	4.5E-01	9.5E-01	1
PLS3	0.2	1.9E-03	8.8E-03	1.0E+00	4.0E-01	6.5E-01	9.9E-01	2	2.7	5.7E-02	1.7E-01	1.0E+00	9.9E-02	2.5E-01	9.4E-01	4
SKOR1	3.6	1.9E-03	8.9E-03	1.0E+00	8.1E-01	9.0E-01	1.0E+00	4	3.2	5.9E-03	2.7E-02	9.8E-01	9.7E-01	9.7E-01	1.0E+00	5
TFAP4	2.7	2.0E-03	9.1E-03	1.0E+00	2.1E-01	4.5E-01	9.6E-01	3	-3.1	5.4E-01	7.4E-01	1.0E+00	2.5E-02	8.9E-02	9.3E-01	1
DBNL	3.1	2.0E-03	9.2E-03	1.0E+00	3.8E-01	6.4E-01	9.8E-01	4	1.3	1.5E-01	3.4E-01	1.0E+00	8.6E-01	9.0E-01	9.9E-01	2
RNF138	2.3	2.0E-03	9.2E-03	1.0E+00	6.2E-01	8.1E-01	1.0E+00	3	1.6	1.8E-01	3.9E-01	1.0E+00	2.8E-01	4.9E-01	9.6E-01	3
MRM1	0.9	2.0E-03	9.2E-03	1.0E+00	2.4E-01	4.9E-01	9.7E-01	2	1.7	1.6E-01	3.6E-01	1.0E+00	7.6E-01	8.6E-01	9.9E-01	3
CACNG8	2.8	2.0E-03	9.3E-03	1.0E+00	9.8E-01	9.8E-01	1.0E+00	5	-0.3	2.4E-01	4.7E-01	1.0E+00	5.9E-01	7.5E-01	9.7E-01	1
DOK3	3.3	2.0E-03	9.3E-03	1.0E+00	9.9E-01	9.9E-01	1.0E+00	3	0.0	7.7E-01	8.7E-01	1.0E+00	8.6E-01	9.0E-01	9.9E-01	0
ARNT2	3.1	2.0E-03	9.3E-03	1.0E+00	3.3E-02	1.2E-01	9.3E-01	5	0.1	2.2E-01	4.4E-01	1.0E+00	1.0E-02	4.0E-02	9.3E-01	3
KDM6B	0.2	2.0E-03	9.4E-03	1.0E+00	4.8E-01	7.1E-01	9.9E-01	2	-0.6	4.8E-01	7.0E-01	1.0E+00	6.2E-02	1.8E-01	9.3E-01	2
HS2ST1	3.6	2.1E-03	9.5E-03	1.0E+00	9.7E-01	9.7E-01	1.0E+00	4	-1.5	9.4E-01	9.5E-01	1.0E+00	7.7E-05	4.1E-04	7.1E-01	0

Table 3: NCI109B focused CRISPR deletion gRNA screen gene-level analysis and results
Genes ranked by Pos. RRA in the CIS-ETO vs. P0 condition

	CIS-ETO vs. P0								SAL vs. P0							
Gene	Median Log2(FC)	Pos. RRA	Pos. Unadj. P	Pos. Adj. P	Neg. RRA	Neg. Unadj. P	Neg. Adj. P	Guides Enriched	Median Log2(FC)	Pos. RRA	Pos. Unadj. P	Pos. Adj. P	Neg. RRA	Neg. Unadj. P	Neg. Adj. P	Guides Enriched
TADA2B	4.1	4.6E-06	6.4E-05	2.6E-02	1.0E+00	9.9E-01	9.9E-01	3	0.7	9.1E-04	8.4E-02	1.0E+00	1.0E+00	9.0E-01	9.0E-01	1
SLFN11	3.4	1.1E-05	3.2E-04	4.4E-02	1.0E+00	1.0E+00	1.0E+00	3	0.4	4.3E-03	1.9E-01	1.0E+00	9.9E-01	8.5E-01	8.5E-01	0
USP22	3.4	1.2E-05	3.3E-04	4.4E-02	1.0E+00	8.8E-01	8.9E-01	3	-0.8	3.4E-02	4.6E-01	1.0E+00	6.2E-01	1.3E-01	1.8E-01	1
TAF5L	2.0	1.9E-05	8.8E-04	8.8E-02	1.0E+00	9.3E-01	9.3E-01	3	0.6	5.6E-04	6.9E-02	1.0E+00	7.5E-01	2.8E-01	3.3E-01	0
TAF6L	0.8	7.2E-04	1.9E-02	1.0E+00	9.8E-01	7.2E-01	7.5E-01	2	-0.4	5.7E-01	9.2E-01	1.0E+00	9.4E-01	5.6E-01	5.9E-01	0
TADA1	1.3	1.1E-03	2.7E-02	1.0E+00	9.9E-01	8.6E-01	8.6E-01	2	-0.5	7.9E-01	9.9E-01	1.0E+00	7.0E-01	2.1E-01	2.6E-01	0
DLC1	0.7	2.2E-03	5.0E-02	1.0E+00	9.9E-01	8.6E-01	8.6E-01	1	-0.6	7.7E-01	9.8E-01	1.0E+00	4.5E-01	4.2E-02	7.0E-02	0
NSD1	-0.6	2.9E-03	5.8E-02	1.0E+00	7.5E-01	4.3E-01	5.0E-01	2	-0.8	3.1E-01	8.5E-01	1.0E+00	6.4E-01	1.8E-01	2.4E-01	0
KAT2A	1.0	2.9E-03	5.8E-02	1.0E+00	3.9E-01	1.7E-01	2.8E-01	1	-2.2	9.8E-01	1.0E+00	1.0E+00	8.6E-02	1.0E-03	3.5E-03	0
SLC25A33	-4.2	3.6E-03	6.0E-02	1.0E+00	2.6E-03	1.3E-04	3.5E-03	1	-1.7	5.5E-01	9.2E-01	1.0E+00	7.9E-02	5.3E-04	1.9E-03	0
MBOAT4	0.7	7.7E-03	9.5E-02	1.0E+00	3.8E-01	1.7E-01	2.8E-01	1	-0.4	6.4E-01	9.5E-01	1.0E+00	8.5E-01	3.3E-01	3.7E-01	0
WWTR1	0.6	7.8E-03	9.5E-02	1.0E+00	9.7E-01	6.9E-01	7.3E-01	1	-0.5	7.1E-02	5.8E-01	1.0E+00	6.1E-01	1.3E-01	1.8E-01	0
KDM5A	0.4	8.3E-03	1.0E-01	1.0E+00	8.3E-01	5.3E-01	5.8E-01	2	-1.7	6.5E-01	9.5E-01	1.0E+00	2.2E-01	6.5E-03	1.5E-02	0
ESRP2	-0.3	8.3E-03	1.0E-01	1.0E+00	7.4E-01	4.1E-01	4.8E-01	2	-0.9	5.2E-01	9.1E-01	1.0E+00	6.6E-01	1.9E-01	2.5E-01	0
PTEN	-0.6	1.1E-02	1.3E-01	1.0E+00	6.5E-01	3.3E-01	4.1E-01	1	-0.9	5.6E-01	9.2E-01	1.0E+00	2.9E-01	1.5E-02	3.2E-02	0
BCL2L11	0.6	1.1E-02	1.3E-01	1.0E+00	2.3E-01	1.3E-01	2.4E-01	0	-2.0	2.6E-03	1.4E-01	1.0E+00	8.6E-02	1.0E-03	3.5E-03	0
C2CD4A	-0.3	1.3E-02	1.4E-01	1.0E+00	3.0E-01	1.4E-01	2.4E-01	2	-1.2	8.8E-01	1.0E+00	1.0E+00	3.1E-01	1.7E-02	3.4E-02	0
PIGG	0.2	1.3E-02	1.4E-01	1.0E+00	9.5E-01	6.8E-01	7.1E-01	2	-1.0	4.8E-01	9.0E-01	1.0E+00	3.6E-01	3.7E-02	6.7E-02	0
FLT3	0.4	1.4E-02	1.4E-01	1.0E+00	7.9E-01	4.9E-01	5.5E-01	0	-1.2	7.9E-01	9.9E-01	1.0E+00	3.3E-01	2.2E-02	4.2E-02	0
MAP2K7	0.4	1.4E-02	1.6E-01	1.0E+00	9.9E-01	8.4E-01	8.6E-01	1	-0.3	1.9E-01	7.8E-01	1.0E+00	9.7E-01	6.1E-01	6.2E-01	0
OTC	0.3	1.5E-02	1.6E-01	1.0E+00	9.9E-01	8.6E-01	8.6E-01	1	0.3	2.6E-02	4.0E-01	1.0E+00	8.5E-01	3.3E-01	3.7E-01	1
TFAP4	0.2	1.5E-02	1.6E-01	1.0E+00	7.7E-01	4.9E-01	5.5E-01	2	-1.1	8.4E-01	1.0E+00	1.0E+00	2.7E-01	1.1E-02	2.4E-02	0
STAT5B	0.0	1.5E-02	1.6E-01	1.0E+00	2.2E-01	8.9E-02	1.8E-01	1	-1.5	5.9E-03	2.2E-01	1.0E+00	4.1E-01	4.2E-02	7.0E-02	0
IRS1	0.2	1.6E-02	1.6E-01	1.0E+00	9.8E-01	7.2E-01	7.5E-01	2	-1.4	2.5E-02	4.0E-01	1.0E+00	4.2E-01	4.2E-02	7.0E-02	1
EPHA3	0.4	1.7E-02	1.8E-01	1.0E+00	9.8E-01	7.2E-01	7.5E-01	0	-0.5	3.8E-01	8.7E-01	1.0E+00	7.7E-01	2.9E-01	3.4E-01	0
IKZF1	0.4	1.7E-02	1.8E-01	1.0E+00	7.9E-01	4.9E-01	5.5E-01	0	-0.4	1.8E-01	7.5E-01	1.0E+00	9.6E-01	6.1E-01	6.2E-01	0
KDM6A	0.0	1.7E-02	1.8E-01	1.0E+00	2.1E-01	8.5E-02	1.8E-01	1	-3.0	9.9E-01	1.0E+00	1.0E+00	1.0E-02	3.5E-05	2.4E-04	0
CARM1	-1.0	1.8E-02	1.8E-01	1.0E+00	3.8E-01	1.7E-01	2.8E-01	1	-0.4	7.8E-01	9.9E-01	1.0E+00	9.4E-01	5.6E-01	5.9E-01	0
HEXA	-1.5	2.0E-02	2.0E-01	1.0E+00	1.7E-01	7.0E-02	1.7E-01	1	-0.7	6.7E-01	9.6E-01	1.0E+00	9.6E-01	5.9E-01	6.2E-01	0
NTRK3	0.0	2.0E-02	2.0E-01	1.0E+00	2.1E-01	8.9E-02	1.8E-01	2	-0.6	6.1E-01	9.4E-01	1.0E+00	5.9E-01	1.1E-01	1.5E-01	0
MMP26	0.3	2.1E-02	2.1E-01	1.0E+00	5.4E-01	2.9E-01	4.0E-01	1	0.3	5.2E-03	2.2E-01	1.0E+00	1.0E+00	9.1E-01	9.1E-01	0
PPP1R12C	0.5	2.2E-02	2.2E-01	1.0E+00	9.0E-01	6.3E-01	6.7E-01	1	-1.1	4.4E-01	8.9E-01	1.0E+00	6.3E-01	1.7E-01	2.3E-01	0
KRT33B	0.1	2.2E-02	2.3E-01	1.0E+00	1.4E-01	2.7E-02	7.4E-02	1	-0.8	6.2E-01	9.5E-01	1.0E+00	8.8E-01	4.3E-01	4.7E-01	0
IQGAP2	-2.9	2.3E-02	2.3E-01	1.0E+00	1.1E-01	2.4E-02	7.4E-02	0	-2.0	6.0E-01	9.4E-01	1.0E+00	4.9E-01	5.5E-02	8.2E-02	0
INPP4B	0.0	2.5E-02	2.4E-01	1.0E+00	6.9E-01	3.6E-01	4.3E-01	2	-0.4	2.2E-01	8.1E-01	1.0E+00	6.1E-01	1.3E-01	1.7E-01	0
BAX	-0.2	2.6E-02	2.4E-01	1.0E+00	8.4E-01	5.3E-01	5.8E-01	2	-0.5	1.6E-01	7.2E-01	1.0E+00	7.6E-01	2.8E-01	3.3E-01	0
LGALS9	0.2	2.6E-02	2.4E-01	1.0E+00	3.1E-01	1.4E-01	2.4E-01	2	-0.2	4.4E-03	1.9E-01	1.0E+00	6.4E-01	1.8E-01	2.4E-01	0
PTPRT	0.3	3.0E-02	2.4E-01	1.0E+00	8.8E-01	6.2E-01	6.7E-01	1	0.0	5.9E-03	2.2E-01	1.0E+00	8.8E-01	4.3E-01	4.7E-01	1
METTL14	-4.7	3.4E-02	2.5E-01	1.0E+00	4.5E-02	6.5E-03	3.6E-02	1	-2.3	8.1E-01	9.9E-01	1.0E+00	8.2E-02	6.6E-04	2.4E-03	0
DNMT3A	-1.8	3.5E-02	2.5E-01	1.0E+00	9.8E-02	1.6E-02	5.2E-02	2	-0.9	6.8E-01	9.6E-01	1.0E+00	6.4E-01	1.8E-01	2.4E-01	0
MRPL14	-7.0	3.9E-02	2.5E-01	1.0E+00	1.6E-03	1.1E-04	3.5E-03	1	-3.0	5.8E-01	9.3E-01	1.0E+00	2.4E-03	5.0E-06	7.9E-05	0
ZMYM2	-1.6	4.0E-02	2.6E-01	1.0E+00	9.9E-02	1.6E-02	5.2E-02	1	-0.7	7.3E-01	9.7E-01	1.0E+00	7.6E-01	2.8E-01	3.3E-01	0
CELF5	-0.2	4.0E-02	2.6E-01	1.0E+00	2.8E-01	1.4E-01	2.4E-01	1	-1.3	6.3E-01	9.5E-01	1.0E+00	3.9E-01	3.7E-02	6.7E-02	0
MAP2K4	0.0	4.1E-02	2.6E-01	1.0E+00	4.0E-01	2.1E-01	3.2E-01	1	-0.3	1.4E-01	6.8E-01	1.0E+00	1.0E+00	9.2E-01	9.2E-01	0
MGA	-4.0	4.3E-02	2.7E-01	1.0E+00	1.3E-02	1.7E-03	1.7E-02	1	-2.4	9.7E-01	1.0E+00	1.0E+00	4.4E-03	1.5E-05	1.5E-04	0
MRM1	0.3	4.4E-02	2.7E-01	1.0E+00	9.8E-01	7.4E-01	7.6E-01	0	-1.1	3.5E-01	8.6E-01	1.0E+00	4.5E-01	4.2E-02	7.0E-02	0
ASXL1	-0.8	4.6E-02	2.7E-01	1.0E+00	3.3E-01	1.4E-01	2.4E-01	1	-2.0	8.3E-01	9.9E-01	1.0E+00	9.1E-02	1.2E-03	3.9E-03	0
SHC2	-0.4	4.7E-02	2.8E-01	1.0E+00	4.6E-01	2.5E-01	3.6E-01	1	-0.8	7.8E-01	9.9E-01	1.0E+00	4.7E-01	5.1E-02	8.0E-02	0
CDKN2A	-0.1	4.7E-02	2.8E-01	1.0E+00	2.2E-01	8.9E-02	1.8E-01	1	-0.3	1.9E-01	7.7E-01	1.0E+00	8.6E-01	3.7E-01	4.1E-01	0
NFE2L2	-0.4	4.9E-02	2.9E-01	1.0E+00	1.7E-01	7.5E-02	1.7E-01	0	-1.0	1.2E-01	6.5E-01	1.0E+00	4.6E-01	4.6E-02	7.3E-02	0
APMAP	-0.9	5.5E-02	3.1E-01	1.0E+00	2.9E-01	1.4E-01	2.4E-01	1	-0.6	1.5E-01	6.9E-01	1.0E+00	6.1E-01	1.3E-01	1.8E-01	0
CSF2RB	-0.3	5.6E-02	3.3E-01	1.0E+00	7.7E-01	4.9E-01	5.5E-01	1	-2.3	9.4E-01	1.0E+00	1.0E+00	1.4E-02	4.5E-05	3.1E-04	0
DOK3	-1.3	5.7E-02	3.3E-01	1.0E+00	7.1E-02	9.4E-03	3.8E-02	1	-2.6	9.8E-01	1.0E+00	1.0E+00	2.2E-02	1.0E-04	6.4E-04	0
TLE2	0.0	6.0E-02	3.3E-01	1.0E+00	7.6E-01	4.5E-01	5.3E-01	1	0.2	2.2E-02	3.7E-01	1.0E+00	9.7E-01	6.1E-01	6.2E-01	1
FHL3	0.1	6.0E-02	3.4E-01	1.0E+00	4.6E-01	2.5E-01	3.6E-01	1	-1.7	5.5E-01	9.2E-01	1.0E+00	1.9E-01	5.9E-03	1.5E-02	0
MDM4	-2.3	6.1E-02	3.5E-01	1.0E+00	4.4E-02	6.5E-03	3.6E-02	1	-2.6	9.7E-01	1.0E+00	1.0E+00	2.0E-02	1.0E-04	6.4E-04	0
FOXP1	-1.2	6.4E-02	3.5E-01	1.0E+00	3.6E-03	1.4E-04	3.5E-03	1	0.0	1.2E-03	8.8E-02	1.0E+00	9.8E-01	6.7E-01	6.9E-01	1
HMOX1	0.1	6.6E-02	3.5E-01	1.0E+00	9.6E-01	6.8E-01	7.1E-01	0	0.2	1.3E-02	2.9E-01	1.0E+00	8.0E-01	3.0E-01	3.4E-01	0
RBL1	-2.2	7.0E-02	3.7E-01	1.0E+00	8.3E-02	1.5E-02	5.2E-02	1	-2.0	9.1E-01	1.0E+00	1.0E+00	1.8E-01	5.9E-03	1.5E-02	0
CSNK1A1	-0.2	7.0E-02	3.7E-01	1.0E+00	3.3E-01	1.4E-01	2.4E-01	1	-3.1	6.6E-01	9.6E-01	1.0E+00	3.0E-02	1.6E-04	9.2E-04	0
CLDN11	-0.6	7.2E-02	3.7E-01	1.0E+00	3.0E-01	1.4E-01	2.4E-01	1	-2.0	9.4E-01	1.0E+00	1.0E+00	6.1E-02	4.0E-04	1.7E-03	0
NEGR1	-0.2	7.5E-02	3.8E-01	1.0E+00	6.6E-01	3.6E-01	4.3E-01	1	-1.6	3.1E-01	8.5E-01	1.0E+00	2.2E-01	6.5E-03	1.5E-02	0
SEMA6C	-4.2	8.4E-02	3.9E-01	1.0E+00	4.9E-02	7.0E-03	3.6E-02	1	-2.4	8.8E-01	1.0E+00	1.0E+00	1.7E-02	7.4E-05	5.0E-04	0
KDM5C	-0.8	8.6E-02	4.2E-01	1.0E+00	1.6E-01	2.9E-02	7.4E-02	0	-1.2	1.0E-01	6.2E-01	1.0E+00	4.4E-01	4.2E-02	7.0E-02	0
NDUFV3	-0.8	8.7E-02	4.2E-01	1.0E+00	1.3E-01	2.6E-02	7.4E-02	0	-0.3	6.3E-02	5.7E-01	1.0E+00	9.4E-01	5.6E-01	5.9E-01	0
XIAP	0.1	9.1E-02	4.4E-01	1.0E+00	3.4E-02	5.9E-03	3.6E-02	0	0.3	1.4E-02	2.9E-01	1.0E+00	6.7E-01	2.0E-01	2.5E-01	1
MED16	-0.9	9.3E-02	4.4E-01	1.0E+00	2.6E-01	1.3E-01	2.4E-01	1	-3.0	8.3E-01	9.9E-01	1.0E+00	4.1E-03	1.5E-05	1.5E-04	0
BAP1	-4.4	9.5E-02	4.4E-01	1.0E+00	9.1E-03	6.6E-04	8.1E-03	1	-2.4	8.4E-01	1.0E+00	1.0E+00	1.8E-02	7.4E-05	5.0E-04	0
DDR2	-0.4	9.6E-02	4.4E-01	1.0E+00	5.9E-01	3.3E-01	4.1E-01	1	-0.4	1.4E-01	6.8E-01	1.0E+00	8.8E-02	1.2E-03	3.9E-03	0
MID1	-0.1	9.9E-02	4.6E-01	1.0E+00	6.3E-01	3.3E-01	4.1E-01	1	-0.9	2.5E-01	8.3E-01	1.0E+00	6.0E-01	1.2E-01	1.6E-01	0
CDKN1B	0.0	1.0E-01	4.6E-01	1.0E+00	9.1E-01	6.3E-01	6.7E-01	0	-1.6	3.7E-01	8.7E-01	1.0E+00	4.4E-02	2.9E-04	1.4E-03	0
CREBBP	0.1	1.0E-01	4.7E-01	1.0E+00	4.9E-01	2.6E-01	3.7E-01	0	-0.8	7.1E-01	9.7E-01	1.0E+00	5.5E-01	9.2E-02	1.3E-01	0
RPL22L1	-0.4	1.0E-01	4.7E-01	1.0E+00	4.1E-01	2.1E-01	3.2E-01	0	-1.0	1.3E-02	2.9E-01	1.0E+00	6.1E-01	1.3E-01	1.8E-01	0
HS2ST1	-0.1	1.0E-01	4.7E-01	1.0E+00	6.9E-01	3.8E-01	4.5E-01	1	-1.8	7.2E-01	9.7E-01	1.0E+00	1.5E-01	4.0E-03	1.1E-02	0
CHD8	0.1	1.0E-01	4.8E-01	1.0E+00	9.8E-01	7.4E-01	7.6E-01	1	-1.0	5.8E-01	9.4E-01	1.0E+00	5.9E-01	1.1E-01	1.5E-01	0
GPX3	0.1	1.1E-01	4.8E-01	1.0E+00	8.6E-01	5.9E-01	6.5E-01	0	-0.7	3.6E-01	8.7E-01	1.0E+00	6.9E-01	2.0E-01	2.6E-01	0
DBNL	-1.2	1.1E-01	4.8E-01	1.0E+00	1.5E-01	2.9E-02	7.4E-02	1	-0.4	3.8E-01	8.7E-01	1.0E+00	4.6E-02	2.9E-04	1.4E-03	0
DOT1L	-0.6	1.1E-01	4.8E-01	1.0E+00	3.5E-01	1.5E-01	2.4E-01	1	-1.1	7.2E-01	9.7E-01	1.0E+00	4.6E-01	4.6E-02	7.3E-02	0
SLC35E1	-0.9	1.1E-01	4.8E-01	1.0E+00	5.8E-01	3.3E-01	4.1E-01	1	-0.9	9.1E-01	1.0E+00	1.0E+00	5.5E-01	9.2E-02	1.3E-01	0
HHIPL2	-0.9	1.1E-01	5.0E-01	1.0E+00	3.4E-01	1.5E-01	2.4E-01	0	-0.5	6.0E-01	9.4E-01	1.0E+00	3.1E-01	1.7E-02	3.4E-02	0
NOTCH4	-0.1	1.1E-01	5.1E-01	1.0E+00	6.8E-01	3.6E-01	4.3E-01	1	-0.6	5.0E-01	9.1E-01	1.0E+00	8.0E-01	3.0E-01	3.4E-01	0
NOTCH3	-0.4	1.1E-01	5.1E-01	1.0E+00	3.7E-01	1.6E-01	2.7E-01	0	-1.0	5.2E-01	9.1E-01	1.0E+00	6.5E-01	1.8E-01	2.4E-01	0
STIP1	-0.7	1.1E-01	5.1E-01	1.0E+00	4.0E-01	2.1E-01	3.2E-01	0	-0.4	4.8E-01	8.9E-01	1.0E+00	3.8E-01	3.7E-02	6.7E-02	0
CBX3	-4.4	1.1E-01	5.1E-01	1.0E+00	7.5E-03	3.1E-04	5.0E-03	1	-2.5	7.9E-01	9.9E-01	1.0E+00	6.3E-04	5.0E-06	7.9E-05	0
LAMA1	-0.6	1.1E-01	5.1E-01	1.0E+00	4.9E-01	2.6E-01	3.7E-01	0	-1.4	5.8E-01	9.4E-01	1.0E+00	4.0E-01	4.0E-02	6.8E-02	0
RNF138	-1.0	1.2E-01	5.3E-01	1.0E+00	2.7E-01	1.4E-01	2.4E-01	1	-1.8	4.5E-01	8.9E-01	1.0E+00	6.9E-02	4.3E-04	1.7E-03	0
TP53	-0.6	1.2E-01	5.4E-01	1.0E+00	4.9E-01	2.6E-01	3.7E-01	0	-2.1	8.0E-01	9.9E-01	1.0E+00	5.3E-02	3.8E-04	1.7E-03	0
TP73	-1.1	1.2E-01	5.4E-01	1.0E+00	2.4E-01	1.3E-01	2.4E-01	1	-0.2	7.5E-02	5.9E-01	1.0E+00	6.0E-01	1.2E-01	1.7E-01	0
GLI1	-0.3	1.2E-01	5.4E-01	1.0E+00	4.0E-01	2.1E-01	3.2E-01	1	-2.5	1.0E+00	1.0E+00	1.0E+00	8.7E-04	5.0E-06	7.9E-05	0
PRKCI	-0.3	1.2E-01	5.4E-01	1.0E+00	5.5E-01	3.0E-01	4.1E-01	1	-0.8	7.0E-01	9.7E-01	1.0E+00	3.6E-01	3.7E-02	6.7E-02	0
ARNT2	-0.3	1.2E-01	5.4E-01	1.0E+00	6.1E-01	3.3E-01	4.1E-01	1	-0.7	8.5E-01	1.0E+00	1.0E+00	6.3E-01	1.7E-01	2.3E-01	0
MSH6	-0.3	1.2E-01	5.4E-01	1.0E+00	6.9E-01	3.6E-01	4.3E-01	0	-1.8	6.8E-01	9.6E-01	1.0E+00	2.7E-03	5.0E-06	7.9E-05	0
FOXJ1	-0.3	1.2E-01	5.4E-01	1.0E+00	7.7E-01	4.9E-01	5.5E-01	1	-1.0	9.0E-01	1.0E+00	1.0E+00	5.9E-01	1.1E-01	1.5E-01	0
ARAF	-0.2	1.3E-01	5.5E-01	1.0E+00	1.5E-01	2.9E-02	7.4E-02	0	-1.1	5.8E-01	9.3E-01	1.0E+00	1.5E-01	3.4E-03	1.0E-02	0
MTOR	-2.1	1.3E-01	5.5E-01	1.0E+00	9.2E-02	1.5E-02	5.2E-02	1	-2.6	9.5E-01	1.0E+00	1.0E+00	9.1E-03	2.5E-05	1.9E-04	0
RIPK1	-1.3	1.3E-01	5.5E-01	1.0E+00	1.9E-01	7.8E-02	1.7E-01	0	-1.9	4.7E-01	8.9E-01	1.0E+00	1.1E-01	2.6E-03	8.2E-03	0
ATXN7	-0.6	1.3E-01	5.5E-01	1.0E+00	5.6E-01	3.2E-01	4.1E-01	0	-0.7	2.7E-01	8.3E-01	1.0E+00	5.4E-01	5.5E-02	8.2E-02	0
SLC2A5	-1.3	1.4E-01	5.5E-01	1.0E+00	8.5E-02	1.5E-02	5.2E-02	1	-1.5	4.9E-01	9.0E-01	1.0E+00	1.3E-02	3.5E-05	2.4E-04	0
DVL2	-0.7	1.4E-01	5.6E-01	1.0E+00	4.7E-01	2.5E-01	3.6E-01	0	-1.0	6.4E-01	9.5E-01	1.0E+00	3.7E-01	3.7E-02	6.7E-02	0

AURKB	-1.1	1.4E-01	5.6E-01	1.0E+00	1.9E-01	7.8E-02	1.7E-01	1	-2.8	7.3E-01	9.7E-01	1.0E+00	5.5E-03	1.5E-05	1.5E-04	0
WDR49	-0.2	1.5E-01	5.7E-01	1.0E+00	9.9E-01	8.1E-01	8.3E-01	1	-1.1	6.8E-02	5.8E-01	1.0E+00	4.0E-01	4.0E-02	6.8E-02	0
IGF1R	-4.1	1.5E-01	5.7E-01	1.0E+00	1.1E-01	2.4E-02	7.4E-02	1	-2.1	9.4E-01	1.0E+00	1.0E+00	2.4E-01	9.6E-03	2.2E-02	0
WTAP	-0.8	1.5E-01	5.7E-01	1.0E+00	4.4E-01	2.2E-01	3.2E-01	1	-1.4	9.7E-01	1.0E+00	1.0E+00	4.1E-02	2.5E-04	1.3E-03	0
ZNF527	-0.2	1.5E-01	5.8E-01	1.0E+00	6.4E-01	3.3E-01	4.1E-01	0	-0.1	8.3E-02	6.0E-01	1.0E+00	7.5E-01	2.8E-01	3.3E-01	0
MED12	-0.7	1.5E-01	5.8E-01	1.0E+00	3.8E-01	1.7E-01	2.8E-01	1	-0.8	6.2E-01	9.4E-01	1.0E+00	4.7E-01	5.1E-02	8.0E-02	0
EGFR	-0.8	1.5E-01	5.8E-01	1.0E+00	2.9E-02	5.4E-03	3.6E-02	1	-0.2	4.3E-02	5.4E-01	1.0E+00	2.2E-01	6.5E-03	1.5E-02	0
TMEM50A	-0.5	1.6E-01	5.8E-01	1.0E+00	4.7E-01	2.5E-01	3.6E-01	0	-1.9	2.4E-01	8.2E-01	1.0E+00	1.1E-02	3.5E-05	2.4E-04	0
EPHA7	-0.6	1.6E-01	5.9E-01	1.0E+00	6.1E-01	3.3E-01	4.1E-01	0	0.3	3.1E-02	4.5E-01	1.0E+00	9.5E-01	5.7E-01	6.0E-01	0
INHBA	-0.3	1.6E-01	5.9E-01	1.0E+00	6.9E-01	3.6E-01	4.3E-01	1	-1.5	2.0E-01	7.9E-01	1.0E+00	6.4E-02	4.1E-04	1.7E-03	0
SCML1	0.0	1.7E-01	6.0E-01	1.0E+00	1.0E-01	2.1E-02	6.8E-02	1	-0.8	4.3E-01	8.8E-01	1.0E+00	6.7E-01	2.0E-01	2.5E-01	0
LATS2	-1.2	1.7E-01	6.0E-01	1.0E+00	1.8E-01	7.8E-02	1.7E-01	1	-0.7	1.0E-01	6.2E-01	1.0E+00	1.8E-01	5.3E-03	1.4E-02	0
PPARD	-0.8	1.7E-01	6.0E-01	1.0E+00	4.6E-02	6.5E-03	3.6E-02	1	-0.6	8.0E-01	9.9E-01	1.0E+00	2.2E-02	1.1E-04	6.8E-04	0
ESR1	-0.9	1.8E-01	6.0E-01	1.0E+00	7.0E-02	9.4E-03	3.8E-02	1	-0.9	5.2E-01	9.1E-01	1.0E+00	4.1E-01	4.2E-02	7.0E-02	0
CAMSAP3	-0.6	1.8E-01	6.0E-01	1.0E+00	4.7E-01	2.5E-01	3.6E-01	0	-0.4	1.6E-01	7.2E-01	1.0E+00	7.6E-01	2.8E-01	3.3E-01	0
TJP1	-0.4	1.8E-01	6.0E-01	1.0E+00	7.5E-01	4.5E-01	5.3E-01	0	-2.5	9.1E-01	1.0E+00	1.0E+00	1.0E-01	1.6E-03	5.2E-03	0
LCE1D	-0.3	1.9E-01	6.0E-01	1.0E+00	7.1E-01	3.8E-01	4.5E-01	0	-1.3	8.4E-01	1.0E+00	1.0E+00	3.3E-01	2.2E-02	4.2E-02	0
TGFB1	-0.4	1.9E-01	6.0E-01	1.0E+00	4.4E-01	2.2E-01	3.2E-01	0	-0.7	8.2E-02	6.0E-01	1.0E+00	8.1E-01	3.0E-01	3.4E-01	0
CDKN2C	-0.8	1.9E-01	6.0E-01	1.0E+00	5.5E-01	3.0E-01	4.1E-01	0	-1.1	5.2E-01	9.1E-01	1.0E+00	4.7E-01	4.6E-02	7.3E-02	0
CASP6	-0.7	1.9E-01	6.1E-01	1.0E+00	6.1E-01	3.3E-01	4.1E-01	0	-0.9	3.3E-01	8.6E-01	1.0E+00	6.1E-01	1.3E-01	1.8E-01	0
TCF25	-0.4	2.0E-01	6.1E-01	1.0E+00	6.7E-01	3.6E-01	4.3E-01	1	-1.5	8.8E-01	1.0E+00	1.0E+00	3.0E-01	1.7E-02	3.4E-02	0
SENP2	-0.8	2.0E-01	6.1E-01	1.0E+00	5.0E-01	2.7E-01	3.7E-01	1	-2.7	1.7E-01	7.3E-01	1.0E+00	5.7E-02	3.9E-04	1.7E-03	0
ATRX	-0.2	2.0E-01	6.1E-01	1.0E+00	9.7E-01	6.8E-01	7.1E-01	1	0.5	1.7E-03	1.1E-01	1.0E+00	7.4E-01	2.3E-01	2.8E-01	0
KNSTRN	-0.8	2.1E-01	6.1E-01	1.0E+00	1.9E-01	7.8E-02	1.7E-01	0	-1.7	9.1E-01	1.0E+00	1.0E+00	4.6E-02	2.9E-04	1.4E-03	0
IL7R	-1.3	2.1E-01	6.1E-01	1.0E+00	1.9E-01	7.8E-02	1.7E-01	1	-1.2	1.8E-01	7.5E-01	1.0E+00	2.7E-01	1.1E-02	2.4E-02	0
ERCC4	-2.1	2.1E-01	6.1E-01	1.0E+00	5.1E-02	7.1E-03	3.6E-02	1	-1.2	3.9E-01	8.7E-01	1.0E+00	4.1E-01	4.0E-02	6.8E-02	0
MET	-0.5	2.1E-01	6.1E-01	1.0E+00	6.0E-01	3.3E-01	4.1E-01	0	-0.7	5.2E-01	9.1E-01	1.0E+00	9.2E-01	5.1E-01	5.4E-01	0
RUNX1	-1.3	2.1E-01	6.3E-01	1.0E+00	9.4E-02	1.6E-02	5.2E-02	1	-0.2	3.0E-02	4.4E-01	1.0E+00	5.2E-01	5.5E-02	8.2E-02	0
LMO7	-0.5	2.2E-01	6.3E-01	1.0E+00	7.9E-01	4.9E-01	5.5E-01	1	-1.2	7.6E-01	9.8E-01	1.0E+00	1.7E-01	4.9E-03	1.4E-02	0
FANCA	-0.6	2.2E-01	6.4E-01	1.0E+00	3.3E-01	1.5E-01	2.4E-01	0	-0.5	7.0E-01	9.7E-01	1.0E+00	6.3E-01	1.8E-01	2.3E-01	0
MMP14	-0.7	2.2E-01	6.4E-01	1.0E+00	1.8E-02	2.0E-03	1.8E-02	0	-2.3	9.9E-01	1.0E+00	1.0E+00	5.4E-03	1.5E-05	1.5E-04	0
CDCP1	-0.3	2.2E-01	6.4E-01	1.0E+00	9.8E-01	7.4E-01	7.6E-01	0	-1.8	9.6E-01	1.0E+00	1.0E+00	8.5E-02	1.0E-03	3.5E-03	0
IRS2	-6.8	2.3E-01	6.4E-01	1.0E+00	1.5E-02	1.9E-03	1.7E-02	1	-2.6	7.8E-01	9.9E-01	1.0E+00	7.2E-03	2.5E-05	1.9E-04	0
KIT	-1.1	2.3E-01	6.4E-01	1.0E+00	2.2E-01	8.9E-02	1.8E-01	0	-0.1	2.6E-02	4.0E-01	1.0E+00	1.7E-01	5.3E-03	1.4E-02	0
TCF7	-0.9	2.3E-01	6.4E-01	1.0E+00	1.5E-01	2.9E-02	7.4E-02	1	-1.5	8.8E-01	1.0E+00	1.0E+00	3.1E-02	1.7E-04	9.6E-04	0
VWC2L	-0.4	2.3E-01	6.5E-01	1.0E+00	9.8E-01	7.2E-01	7.5E-01	0	0.0	1.8E-01	7.4E-01	1.0E+00	7.5E-01	2.8E-01	3.3E-01	0
AMER1	-0.8	2.4E-01	6.6E-01	1.0E+00	3.3E-01	1.4E-01	2.4E-01	1	-0.5	1.8E-02	3.3E-01	1.0E+00	9.9E-01	8.5E-01	8.5E-01	1
FZD3	-1.7	2.5E-01	6.7E-01	1.0E+00	3.9E-02	5.9E-03	3.6E-02	1	-2.8	6.1E-01	9.4E-01	1.0E+00	1.4E-01	3.4E-03	1.0E-02	0
RICTOR	-0.4	2.5E-01	6.7E-01	1.0E+00	6.1E-01	3.3E-01	4.1E-01	0	-0.8	2.7E-02	4.0E-01	1.0E+00	3.9E-01	3.7E-02	6.7E-02	1
BBS4	-0.9	2.5E-01	6.7E-01	1.0E+00	6.5E-01	3.3E-01	4.1E-01	0	-0.9	3.5E-01	8.6E-01	1.0E+00	3.3E-01	2.2E-02	4.2E-02	0
SLPI	-0.4	2.5E-01	6.7E-01	1.0E+00	2.0E-01	8.1E-02	1.8E-01	0	-1.0	3.4E-01	8.6E-01	1.0E+00	4.5E-01	4.2E-02	7.0E-02	0
POU3F2	-0.5	2.5E-01	6.7E-01	1.0E+00	8.6E-01	5.9E-01	6.5E-01	1	0.5	3.6E-03	1.7E-01	1.0E+00	3.2E-01	2.2E-02	4.2E-02	1
JAK2	0.0	2.6E-01	6.9E-01	1.0E+00	5.2E-01	2.7E-01	3.7E-01	0	0.0	2.7E-02	4.0E-01	1.0E+00	6.5E-01	1.8E-01	2.4E-01	0
SLC46A2	-1.3	2.7E-01	6.9E-01	1.0E+00	1.0E-01	1.6E-02	5.2E-02	0	-0.4	4.2E-02	5.2E-01	1.0E+00	5.5E-01	9.7E-02	1.4E-01	0
LDHD	-0.3	2.7E-01	6.9E-01	1.0E+00	7.8E-01	4.9E-01	5.5E-01	0	-0.9	6.4E-02	5.8E-01	1.0E+00	7.1E-01	2.1E-01	2.6E-01	0
ERBB4	-0.2	2.8E-01	7.0E-01	1.0E+00	9.4E-01	6.4E-01	6.9E-01	0	-1.7	9.4E-01	1.0E+00	1.0E+00	1.6E-01	4.0E-03	1.1E-02	0
RAB8B	-0.4	2.8E-01	7.0E-01	1.0E+00	8.7E-01	6.2E-01	6.7E-01	0	-0.9	6.7E-02	5.8E-01	1.0E+00	6.0E-01	1.1E-01	1.5E-01	0
ZFHX3	-0.9	2.8E-01	7.1E-01	1.0E+00	4.8E-01	2.6E-01	3.7E-01	0	-0.5	1.7E-01	7.3E-01	1.0E+00	8.4E-01	3.2E-01	3.7E-01	0
CPN1	-0.6	2.8E-01	7.1E-01	1.0E+00	6.4E-01	3.3E-01	4.1E-01	0	-0.6	7.1E-01	9.7E-01	1.0E+00	2.0E-01	6.5E-03	1.5E-02	0
MITF	-0.8	2.9E-01	7.1E-01	1.0E+00	4.2E-01	2.1E-01	3.2E-01	0	-0.7	4.2E-01	8.8E-01	1.0E+00	7.9E-01	3.0E-01	3.4E-01	0
DLX3	-0.5	2.9E-01	7.1E-01	1.0E+00	8.4E-01	5.5E-01	6.1E-01	0	-1.2	3.4E-01	8.6E-01	1.0E+00	6.5E-01	1.9E-01	2.5E-01	0
RHOQ	-2.0	2.9E-01	7.2E-01	1.0E+00	1.5E-01	2.9E-02	7.4E-02	0	-2.8	3.6E-02	4.9E-01	1.0E+00	4.9E-02	3.8E-04	1.7E-03	1
POLD1	-1.6	2.9E-01	7.2E-01	1.0E+00	1.4E-01	2.7E-02	7.4E-02	0	-3.0	4.1E-01	8.8E-01	1.0E+00	3.6E-02	2.2E-04	1.2E-03	0
SFRP5	-0.3	2.9E-01	7.2E-01	1.0E+00	1.9E-01	7.8E-02	1.7E-01	0	-1.2	2.4E-02	4.0E-01	1.0E+00	3.1E-01	1.7E-02	3.4E-02	0
PMS1	-0.2	3.0E-01	7.3E-01	1.0E+00	2.4E-01	1.3E-01	2.4E-01	0	-1.3	7.7E-01	9.8E-01	1.0E+00	2.1E-01	6.5E-03	1.5E-02	0
CXCL16	-1.3	3.0E-01	7.3E-01	1.0E+00	5.9E-02	9.4E-03	3.8E-02	0	-0.9	2.1E-01	8.1E-01	1.0E+00	3.3E-01	2.2E-02	4.2E-02	0
SFXN2	-1.6	3.0E-01	7.3E-01	1.0E+00	8.2E-02	1.5E-02	5.2E-02	0	-0.9	1.7E-01	7.3E-01	1.0E+00	5.4E-01	5.5E-02	8.2E-02	0
FZD7	-1.2	3.1E-01	7.3E-01	1.0E+00	5.7E-02	8.1E-03	3.8E-02	0	-0.8	1.3E-01	6.8E-01	1.0E+00	4.7E-01	5.1E-02	8.0E-02	0
TNFRSF14	-1.3	3.1E-01	7.3E-01	1.0E+00	2.7E-01	1.4E-01	2.4E-01	0	-2.7	5.6E-01	9.2E-01	1.0E+00	4.6E-02	2.9E-04	1.4E-03	0
RB1	-1.5	3.1E-01	7.3E-01	1.0E+00	2.3E-01	9.3E-02	1.9E-01	0	-1.1	8.5E-01	1.0E+00	1.0E+00	2.8E-01	1.2E-02	2.6E-02	0
GAB4	-1.0	3.1E-01	7.3E-01	1.0E+00	5.2E-02	7.6E-03	3.7E-02	0	-1.6	7.3E-01	9.7E-01	1.0E+00	1.7E-01	5.3E-03	1.4E-02	0
NBN	-0.8	3.1E-01	7.3E-01	1.0E+00	1.7E-01	7.5E-02	1.7E-01	0	-1.6	2.7E-01	8.3E-01	1.0E+00	8.5E-02	1.0E-03	3.5E-03	0
FAS	-0.6	3.1E-01	7.3E-01	1.0E+00	3.6E-02	5.9E-03	3.6E-02	0	0.3	3.2E-02	4.5E-01	1.0E+00	9.9E-01	8.5E-01	8.5E-01	1
KAT2B	-1.3	3.1E-01	7.3E-01	1.0E+00	2.2E-01	8.9E-02	1.8E-01	0	-0.1	3.6E-02	4.9E-01	1.0E+00	6.0E-01	1.2E-01	1.7E-01	0
BCAR1	-0.5	3.1E-01	7.3E-01	1.0E+00	6.0E-01	3.3E-01	4.1E-01	0	-1.0	8.8E-01	1.0E+00	1.0E+00	7.2E-01	2.2E-01	2.7E-01	0
KRT27	-1.0	3.2E-01	7.5E-01	1.0E+00	3.4E-01	1.5E-01	2.4E-01	0	-0.4	2.0E-01	8.0E-01	1.0E+00	5.6E-01	9.7E-02	1.4E-01	0
HNF1A	0.0	3.2E-01	7.5E-01	1.0E+00	2.0E-01	8.1E-02	1.8E-01	0	-0.9	7.0E-01	9.7E-01	1.0E+00	5.5E-01	9.2E-02	1.3E-01	0
CHRM4	-0.3	3.2E-01	7.5E-01	1.0E+00	3.2E-01	1.4E-01	2.4E-01	0	-2.2	4.8E-01	8.9E-01	1.0E+00	1.0E-01	1.6E-03	5.2E-03	0
TREX2	-1.3	3.2E-01	7.6E-01	1.0E+00	2.6E-01	1.3E-01	2.4E-01	0	-0.6	5.8E-01	9.3E-01	1.0E+00	8.5E-01	3.3E-01	3.7E-01	0
EIF1AY	-0.5	3.3E-01	7.6E-01	1.0E+00	2.6E-01	1.3E-01	2.4E-01	0	0.5	3.4E-03	1.6E-01	1.0E+00	8.5E-01	3.3E-01	3.7E-01	0
AR	-0.7	3.3E-01	7.6E-01	1.0E+00	6.1E-01	3.3E-01	4.1E-01	0	-0.3	7.1E-03	2.4E-01	1.0E+00	9.7E-01	6.1E-01	6.2E-01	1
KMT2B	-7.0	3.3E-01	7.6E-01	1.0E+00	1.7E-03	1.1E-04	3.5E-03	0	-1.0	7.9E-02	6.0E-01	1.0E+00	1.7E-01	5.3E-03	1.4E-02	0
POGK	-0.3	3.3E-01	7.6E-01	1.0E+00	3.4E-01	1.5E-01	2.4E-01	0	-2.0	8.3E-01	9.9E-01	1.0E+00	1.5E-01	4.0E-03	1.1E-02	0
SSR4	-0.3	3.4E-01	7.6E-01	1.0E+00	5.7E-01	3.3E-01	4.1E-01	0	-1.0	6.8E-01	9.6E-01	1.0E+00	4.4E-01	4.2E-02	7.0E-02	0
SFN	-0.5	3.4E-01	7.6E-01	1.0E+00	8.3E-01	5.1E-01	5.6E-01	0	-1.1	1.2E-01	6.5E-01	1.0E+00	3.1E-01	1.7E-02	3.4E-02	0
IFNA7	-0.5	3.4E-01	7.6E-01	1.0E+00	5.7E-01	3.3E-01	4.1E-01	0	-0.6	5.4E-02	5.5E-01	1.0E+00	8.9E-01	4.4E-01	4.8E-01	0
NME6	-0.4	3.4E-01	7.7E-01	1.0E+00	7.7E-01	4.9E-01	5.5E-01	0	-1.6	7.7E-01	9.8E-01	1.0E+00	2.3E-01	9.0E-03	2.1E-02	0
FZD1	-0.7	3.4E-01	7.8E-01	1.0E+00	7.7E-01	4.9E-01	5.5E-01	0	-0.4	7.7E-01	9.9E-01	1.0E+00	9.7E-01	6.1E-01	6.2E-01	0
PDGFRA	-0.7	3.4E-01	7.8E-01	1.0E+00	6.3E-01	3.3E-01	4.1E-01	0	-0.2	5.4E-01	9.1E-01	1.0E+00	9.4E-01	5.7E-01	6.0E-01	0
UGT2B28	-1.2	3.4E-01	7.8E-01	1.0E+00	1.1E-02	6.7E-04	8.1E-03	0	-0.4	6.0E-01	9.4E-01	1.0E+00	9.3E-01	5.4E-01	5.7E-01	0
MAP3K11	-0.5	3.5E-01	7.8E-01	1.0E+00	4.5E-01	2.5E-01	3.6E-01	0	-2.0	9.2E-01	1.0E+00	1.0E+00	1.5E-01	4.0E-03	1.1E-02	0
ARID2	-1.0	3.5E-01	7.8E-01	1.0E+00	7.0E-02	9.4E-03	3.8E-02	0	-3.0	2.5E-01	8.3E-01	1.0E+00	2.8E-03	5.0E-06	7.9E-05	0
CADM1	-0.2	3.5E-01	7.8E-01	1.0E+00	5.7E-01	3.3E-01	4.1E-01	0	-1.1	8.6E-01	1.0E+00	1.0E+00	3.9E-01	3.7E-02	6.7E-02	0
CAMK2D	-0.1	3.5E-01	7.8E-01	1.0E+00	6.8E-01	3.6E-01	4.3E-01	0	-1.1	3.3E-01	8.6E-01	1.0E+00	7.5E-01	2.8E-01	3.3E-01	0
NCOR1	-0.5	3.5E-01	7.8E-01	1.0E+00	6.4E-01	3.3E-01	4.1E-01	0	-0.5	6.4E-01	9.5E-01	1.0E+00	5.7E-01	1.1E-01	1.5E-01	0
CTNNB1	-0.3	3.5E-01	7.8E-01	1.0E+00	7.8E-01	4.9E-01	5.5E-01	0	0.5	4.7E-03	2.1E-01	1.0E+00	8.9E-01	4.4E-01	4.8E-01	0
ROS1	-1.1	3.5E-01	7.8E-01	1.0E+00	2.3E-01	9.3E-02	1.9E-01	0	-0.9	5.0E-01	9.0E-01	1.0E+00	4.9E-01	5.5E-02	8.2E-02	0
SMG9	-0.4	3.6E-01	7.8E-01	1.0E+00	7.1E-01	3.8E-01	4.5E-01	0	-1.2	9.4E-01	1.0E+00	1.0E+00	5.5E-01	9.2E-02	1.3E-01	0
FLT1	-0.6	3.6E-01	7.8E-01	1.0E+00	9.9E-01	7.7E-01	7.9E-01	0	-0.8	9.0E-01	1.0E+00	1.0E+00	5.1E-01	5.5E-02	8.2E-02	0
TSC2	-1.8	3.6E-01	7.9E-01	1.0E+00	3.6E-02	5.9E-03	3.6E-02	0	-2.5	9.9E-01	1.0E+00	1.0E+00	8.7E-03	2.5E-05	1.9E-04	0
KEAP1	-0.7	3.7E-01	8.1E-01	1.0E+00	3.1E-01	1.4E-01	2.4E-01	0	-1.4	4.8E-01	9.0E-01	1.0E+00	2.1E-01	6.5E-03	1.5E-02	0
PRDM1	-0.1	3.7E-01	8.1E-01	1.0E+00	2.2E-01	8.9E-02	1.8E-01	0	-1.0	6.5E-01	9.6E-01	1.0E+00	6.0E-01	1.2E-01	1.7E-01	0
PREX2	-0.7	3.7E-01	8.1E-01	1.0E+00	1.6E-01	2.9E-02	7.4E-02	0	-0.8	1.1E-01	6.3E-01	1.0E+00	8.7E-01	3.8E-01	4.2E-01	0
CYP27A1	-1.4	3.8E-01	8.2E-01	1.0E+00	5.0E-02	7.1E-03	3.6E-02	0	-2.2	7.4E-01	9.8E-01	1.0E+00	5.2E-02	3.8E-04	1.7E-03	0
ZNF501	-0.4	3.8E-01	8.2E-01	1.0E+00	3.8E-01	1.7E-01	2.8E-01	0	-0.3	5.3E-01	9.1E-01	1.0E+00	7.3E-01	2.3E-01	2.8E-01	0
CBL	-2.0	3.9E-01	8.3E-01	1.0E+00	7.2E-02	9.5E-03	3.8E-02	0	-1.1	4.5E-01	8.9E-01	1.0E+00	3.8E-01	3.7E-02	6.7E-02	0
CCDC170	-0.9	4.0E-01	8.3E-01	1.0E+00	2.2E-01	8.9E-02	1.8E-01	0	-2.0	5.9E-01	9.4E-01	1.0E+00	1.9E-01	5.9E-03	1.5E-02	0
WDR27	-0.7	4.0E-01	8.4E-01	1.0E+00	8.5E-01	5.6E-01	6.1E-01	0	-1.6	6.6E-01	9.6E-01	1.0E+00	4.3E-02	2.8E-04	1.4E-03	0
CDK8	-0.1	4.1E-01	8.4E-01	1.0E+00	9.1E-01	6.3E-01	6.7E-01	0	-0.4	6.9E-01	9.6E-01	1.0E+00	6.8E-01	2.0E-01	2.5E-01	0
HECW1	-1.1	4.2E-01	8.4E-01	1.0E+00	2.6E-01	1.3E-01	2.4E-01	0	-0.8	2.1E-01	8.1E-01	1.0E+00	6.8E-01	2.0E-01	2.5E-01	0
DAXX	-1.5	4.2E-01	8.4E-01	1.0E+00	2.2E-01	8.9E-02	1.8E-01	0	-1.9	9.4E-01	1.0E+00	1.0E+00	7.2E-02	4.4E-04	1.7E-03	0
PPP3CC	-0.8	4.3E-01	8.4E-01	1.0E+00	6.4E-01	3.3E-01	4.1E-01	0	-0.3	4.5E-01	8.9E-01	1.0E+00	8.7E-01	4.0E-01	4.4E-01	0
SMYD3	-2.0	4.3E-01	8.4E-01	1.0E+00	1.2E-01	2.6E-02	7.4E-02	0	-1.1	7.0E-01	9.7E-01	1.0E+00	4.6E-01	4.6E-02	7.3E-02	0
CDH1	-1.1	4.4E-01	8.4E-01	1.0E+00	1.7E-01	7.0E-02	1.7E-01	0	-0.4	4.7E-01	8.9E-01	1.0E+00	2.2E-01	6.5E-03	1.5E-02	0
MAP2K1	-1.3	4.4E-01	8.4E-01	1.0E+00	1.2E-01	2.6E-02	7.4E-02	0	-1.5	5.3E-01	9.1E-01	1.0E+00	1.8E-01	5.9E-03	1.5E-02	0
CACNG8	-1.6	4.4E-01	8.5E-01	1.0E+00	1.5E-01	2.9E-02	7.4E-02	0	-0.4	2.0E-01	7.9E-01	1.0E+00	3.8E-01	3.7E-02	6.7E-02	0
CDKN2B	-0.3	4.5E-01	8.5E-01	1.0E+00	9.9E-01	8.4E-01	8.6E-01	0	-0.7	7.6E-01	9.8E-01	1.0E+00	8.7E-01	3.8E-01	4.2E-01	0
DNMT3B	-2.3	4.5E-01	8.6E-01	1.0E+00	4.0E-02	6.4E-03	3.6E-02	0	-1.7	3.2E-01	8.5E-01	1.0E+00	1.6E-01	4.9E-03	1.4E-02	0

TSHR	-4.2	4.6E-01	8.6E-01	1.0E+00	2.2E-02	2.4E-03	2.0E-02	0	-2.3	8.9E-01	1.0E+00	1.0E+00	6.9E-02	4.3E-04	1.7E-03	0
GRIN2A	-1.3	4.9E-01	8.6E-01	1.0E+00	4.5E-02	6.5E-03	3.6E-02	0	-0.7	6.0E-01	9.4E-01	1.0E+00	8.8E-01	4.4E-01	4.8E-01	0
GSG1L	-2.1	4.9E-01	8.6E-01	1.0E+00	1.4E-01	2.6E-02	7.4E-02	0	-1.2	7.0E-01	9.7E-01	1.0E+00	2.8E-01	1.2E-02	2.6E-02	0
ALDH3A1	-1.3	4.9E-01	8.6E-01	1.0E+00	9.0E-02	1.5E-02	5.2E-02	0	-0.9	8.3E-01	9.9E-01	1.0E+00	2.6E-01	1.0E-02	2.3E-02	0
GSTM5	-1.1	4.9E-01	8.6E-01	1.0E+00	2.9E-01	1.4E-01	2.4E-01	0	-1.0	4.0E-01	8.8E-01	1.0E+00	1.8E-01	5.9E-03	1.5E-02	0
FGFR3	-0.8	5.0E-01	8.6E-01	1.0E+00	6.3E-01	3.3E-01	4.1E-01	0	-0.9	8.9E-01	1.0E+00	1.0E+00	4.2E-01	4.2E-02	7.0E-02	0
BRCA2	-1.2	5.0E-01	8.6E-01	1.0E+00	1.8E-01	7.8E-02	1.7E-01	0	-2.6	7.5E-01	9.8E-01	1.0E+00	2.9E-02	1.6E-04	9.2E-04	0
MAP3K1	-0.5	5.1E-01	8.6E-01	1.0E+00	7.8E-01	4.9E-01	5.5E-01	0	-0.8	7.8E-01	9.9E-01	1.0E+00	2.6E-01	1.0E-02	2.3E-02	0
PIK3R1	-0.3	5.1E-01	8.6E-01	1.0E+00	1.5E-01	2.9E-02	7.4E-02	0	-0.3	6.1E-01	9.4E-01	1.0E+00	9.9E-01	8.5E-01	8.5E-01	0
ALK	-0.6	5.1E-01	8.6E-01	1.0E+00	8.2E-01	5.1E-01	5.6E-01	0	-0.7	8.3E-02	6.0E-01	1.0E+00	5.5E-01	9.2E-02	1.3E-01	0
CRABP2	-1.4	5.2E-01	8.6E-01	1.0E+00	4.4E-02	6.5E-03	3.6E-02	0	-2.6	7.7E-01	9.9E-01	1.0E+00	4.1E-02	2.8E-04	1.4E-03	0
SMAD3	-0.5	5.2E-01	8.7E-01	1.0E+00	1.7E-01	7.0E-02	1.7E-01	0	-1.2	5.0E-02	5.4E-01	1.0E+00	2.6E-01	1.0E-02	2.3E-02	1
HESX1	-0.6	5.3E-01	8.7E-01	1.0E+00	6.4E-01	3.3E-01	4.1E-01	0	-0.4	1.5E-01	7.2E-01	1.0E+00	6.8E-01	2.0E-01	2.5E-01	0
CYSLTR2	-1.1	5.4E-01	8.7E-01	1.0E+00	2.3E-01	9.3E-02	1.9E-01	0	-1.5	7.3E-01	9.7E-01	1.0E+00	1.8E-01	5.9E-03	1.5E-02	0
JAK1	-0.5	5.4E-01	8.7E-01	1.0E+00	1.4E-01	2.9E-02	7.4E-02	0	-1.0	4.0E-01	8.8E-01	1.0E+00	8.4E-01	3.2E-01	3.7E-01	0
FRAT1	-0.4	5.6E-01	8.7E-01	1.0E+00	6.2E-01	3.3E-01	4.1E-01	0	-0.6	1.4E-01	6.9E-01	1.0E+00	8.7E-01	3.8E-01	4.2E-01	0
KCNA1	-0.9	5.6E-01	8.7E-01	1.0E+00	5.0E-01	2.6E-01	3.7E-01	0	-1.0	5.9E-01	9.4E-01	1.0E+00	2.6E-01	1.0E-02	2.3E-02	0
FOXH1	-0.4	5.7E-01	8.7E-01	1.0E+00	6.7E-01	3.6E-01	4.3E-01	0	0.1	2.4E-02	4.0E-01	1.0E+00	6.1E-02	4.0E-04	1.7E-03	0
MSH2	-0.6	5.7E-01	8.7E-01	1.0E+00	4.1E-01	2.1E-01	3.2E-01	0	-0.6	4.1E-01	8.8E-01	1.0E+00	5.5E-02	3.9E-04	1.7E-03	0
KCNIP3	-0.2	5.8E-01	8.7E-01	1.0E+00	2.5E-01	1.3E-01	2.4E-01	0	-1.7	9.5E-01	1.0E+00	1.0E+00	6.4E-02	4.1E-04	1.7E-03	0
CLDN1	-3.7	5.8E-01	8.7E-01	1.0E+00	1.3E-02	1.7E-03	1.7E-02	0	-2.0	8.9E-01	1.0E+00	1.0E+00	2.0E-02	1.0E-04	6.4E-04	0
NQO1	-0.4	5.8E-01	8.7E-01	1.0E+00	6.2E-02	9.4E-03	3.8E-02	0	-1.2	9.3E-02	6.1E-01	1.0E+00	3.3E-01	2.2E-02	4.2E-02	0
TET1	-0.8	5.8E-01	8.7E-01	1.0E+00	5.5E-01	3.0E-01	4.1E-01	0	-1.9	8.9E-01	1.0E+00	1.0E+00	1.7E-01	5.3E-03	1.4E-02	0
ETV3	-1.1	5.9E-01	8.8E-01	1.0E+00	3.8E-01	1.7E-01	2.8E-01	0	-0.4	7.3E-01	9.7E-01	1.0E+00	4.3E-01	4.2E-02	7.0E-02	0
ZNF319	-0.5	5.9E-01	8.8E-01	1.0E+00	2.5E-01	1.3E-01	2.4E-01	0	-1.0	1.3E-01	6.6E-01	1.0E+00	4.6E-01	4.6E-02	7.3E-02	0
RBPJ	-1.7	6.0E-01	8.8E-01	1.0E+00	8.6E-02	1.5E-02	5.2E-02	0	-0.3	9.6E-02	6.1E-01	1.0E+00	9.2E-01	5.1E-01	5.4E-01	0
TRAF2	-1.3	6.0E-01	8.8E-01	1.0E+00	2.6E-01	1.3E-01	2.4E-01	0	-0.8	9.3E-01	1.0E+00	1.0E+00	7.9E-01	3.0E-01	3.4E-01	0
CCND2	-0.9	6.1E-01	8.8E-01	1.0E+00	8.4E-02	1.5E-02	5.2E-02	0	-1.4	2.8E-01	8.4E-01	1.0E+00	1.4E-01	3.1E-03	9.2E-03	0
CDK6	-1.4	6.1E-01	8.8E-01	1.0E+00	5.1E-02	7.1E-03	3.6E-02	0	-0.9	8.6E-01	1.0E+00	1.0E+00	8.7E-01	4.0E-01	4.4E-01	0
RASA1	-1.1	6.1E-01	8.8E-01	1.0E+00	1.6E-01	2.9E-02	7.4E-02	0	-1.4	4.1E-01	8.8E-01	1.0E+00	2.2E-01	6.5E-03	1.5E-02	0
CDKN2D	-0.5	6.2E-01	8.8E-01	1.0E+00	5.9E-01	3.3E-01	4.1E-01	0	-1.8	7.2E-01	9.7E-01	1.0E+00	2.5E-01	1.0E-02	2.3E-02	0
CSF1R	-2.0	6.2E-01	8.9E-01	1.0E+00	8.9E-03	6.6E-04	8.1E-03	0	-2.3	7.0E-01	9.7E-01	1.0E+00	3.3E-02	2.1E-04	1.2E-03	0
CASP3	-1.1	6.3E-01	8.9E-01	1.0E+00	3.0E-01	1.4E-01	2.4E-01	0	0.1	1.1E-01	6.5E-01	1.0E+00	8.3E-01	3.2E-01	3.7E-01	0
PIK3CG	-4.6	6.3E-01	8.9E-01	1.0E+00	4.1E-03	1.5E-04	3.5E-03	0	-1.0	2.1E-01	8.0E-01	1.0E+00	6.9E-01	2.1E-01	2.6E-01	0
BLM	-4.9	6.3E-01	8.9E-01	1.0E+00	1.5E-02	1.9E-03	1.7E-02	0	-3.5	9.6E-01	1.0E+00	1.0E+00	4.3E-03	1.5E-05	1.5E-04	0
GRHL1	-0.5	6.3E-01	9.0E-01	1.0E+00	8.7E-01	6.1E-01	6.7E-01	0	-0.9	6.8E-01	9.6E-01	1.0E+00	8.5E-01	3.3E-01	3.7E-01	0
PIK3C2G	-0.7	6.4E-01	9.0E-01	1.0E+00	4.5E-01	2.2E-01	3.2E-01	0	-0.9	5.3E-01	9.1E-01	1.0E+00	8.5E-01	3.3E-01	3.7E-01	0
PALB2	-1.4	6.4E-01	9.0E-01	1.0E+00	1.6E-01	2.9E-02	7.4E-02	0	-1.6	6.3E-01	9.5E-01	1.0E+00	6.8E-02	4.3E-04	1.7E-03	0
NOTCH2	-0.8	6.4E-01	9.0E-01	1.0E+00	6.3E-01	3.3E-01	4.1E-01	0	-2.6	7.9E-01	9.9E-01	1.0E+00	6.0E-03	1.5E-05	1.5E-04	0
AKT3	-0.5	6.4E-01	9.0E-01	1.0E+00	5.9E-01	3.3E-01	4.1E-01	0	-2.1	7.5E-01	9.8E-01	1.0E+00	7.2E-02	4.4E-04	1.7E-03	0
MGAT5	-1.7	6.4E-01	9.0E-01	1.0E+00	1.2E-01	2.6E-02	7.4E-02	0	-1.7	9.4E-01	1.0E+00	1.0E+00	1.9E-01	5.9E-03	1.5E-02	0
MUC1	-1.1	6.5E-01	9.1E-01	1.0E+00	5.0E-02	7.1E-03	3.6E-02	0	-1.3	4.4E-01	8.9E-01	1.0E+00	1.6E-01	4.9E-03	1.4E-02	0
ARID1B	-1.2	6.5E-01	9.1E-01	1.0E+00	1.7E-01	7.5E-02	1.7E-01	0	-0.9	1.3E-01	6.6E-01	1.0E+00	8.4E-01	3.2E-01	3.7E-01	0
PRDM14	-0.9	6.6E-01	9.1E-01	1.0E+00	4.3E-02	6.5E-03	3.6E-02	0	-2.2	3.2E-02	4.5E-01	1.0E+00	2.9E-03	1.5E-05	1.5E-04	1
ANKS1A	-4.1	6.6E-01	9.1E-01	1.0E+00	1.5E-02	1.9E-03	1.7E-02	0	-0.8	3.2E-01	8.5E-01	1.0E+00	5.2E-01	5.5E-02	8.2E-02	0
RNASE8	-0.5	6.7E-01	9.1E-01	1.0E+00	3.1E-01	1.4E-01	2.4E-01	0	-0.6	1.3E-01	6.7E-01	1.0E+00	8.5E-01	3.3E-01	3.7E-01	0
WDR45	-1.2	6.7E-01	9.1E-01	1.0E+00	2.6E-01	1.3E-01	2.4E-01	0	-1.1	4.6E-01	8.9E-01	1.0E+00	5.0E-01	5.5E-02	8.2E-02	0
CCDC34	-0.4	6.7E-01	9.1E-01	1.0E+00	9.0E-01	6.3E-01	6.7E-01	0	-1.1	2.8E-01	8.3E-01	1.0E+00	5.8E-01	1.1E-01	1.5E-01	0
TBX3	-0.3	6.7E-01	9.1E-01	1.0E+00	4.7E-01	2.5E-01	3.6E-01	0	-0.4	5.5E-01	9.2E-01	1.0E+00	4.8E-01	5.5E-02	8.2E-02	0
TOP3B	-1.4	6.8E-01	9.2E-01	1.0E+00	1.2E-01	2.6E-02	7.4E-02	0	-1.6	8.2E-02	6.0E-01	1.0E+00	8.0E-02	5.3E-04	1.9E-03	0
ATM	-1.3	6.8E-01	9.2E-01	1.0E+00	5.2E-02	7.6E-03	3.7E-02	0	-1.0	8.0E-01	9.9E-01	1.0E+00	6.5E-01	1.8E-01	2.4E-01	0
ELANE	-0.3	6.9E-01	9.2E-01	1.0E+00	7.5E-01	4.3E-01	5.0E-01	0	-1.4	9.1E-01	1.0E+00	1.0E+00	2.6E-01	1.0E-02	2.3E-02	0
MAP3K13	-0.8	6.9E-01	9.2E-01	1.0E+00	1.7E-01	7.0E-02	1.7E-01	0	0.6	1.5E-03	1.0E-01	1.0E+00	8.8E-01	4.3E-01	4.7E-01	0
KLF8	-2.6	7.0E-01	9.2E-01	1.0E+00	1.2E-01	2.6E-02	7.4E-02	0	-1.1	5.7E-01	9.2E-01	1.0E+00	5.0E-01	5.5E-02	8.2E-02	0
FAT1	-0.6	7.0E-01	9.2E-01	1.0E+00	5.9E-01	3.3E-01	4.1E-01	0	-0.2	1.9E-01	7.8E-01	1.0E+00	9.6E-01	6.1E-01	6.2E-01	0
TERT	-1.0	7.0E-01	9.2E-01	1.0E+00	4.4E-01	2.2E-01	3.2E-01	0	-2.5	9.9E-01	1.0E+00	1.0E+00	1.0E-02	2.5E-05	1.9E-04	0
KDM6B	-3.8	7.0E-01	9.2E-01	1.0E+00	3.6E-02	5.9E-03	3.6E-02	0	-0.5	7.3E-01	9.7E-01	1.0E+00	7.4E-01	2.6E-01	3.1E-01	0
HEATR1	-1.7	7.0E-01	9.2E-01	1.0E+00	3.6E-02	5.9E-03	3.6E-02	0	-2.7	9.7E-01	1.0E+00	1.0E+00	6.1E-02	3.9E-04	1.7E-03	0
PRICKLE1	-1.7	7.1E-01	9.2E-01	1.0E+00	1.5E-01	2.9E-02	7.4E-02	0	-1.1	7.6E-01	9.8E-01	1.0E+00	5.6E-01	9.7E-02	1.4E-01	0
HIST1H4L	-0.1	7.1E-01	9.2E-01	1.0E+00	7.1E-01	3.8E-01	4.5E-01	0	0.1	2.2E-02	3.7E-01	1.0E+00	9.5E-01	5.7E-01	6.0E-01	0
ATXN7L3	-0.9	7.1E-01	9.2E-01	1.0E+00	4.1E-01	2.1E-01	3.2E-01	0	-2.2	5.4E-01	9.1E-01	1.0E+00	7.4E-02	5.2E-04	1.9E-03	0
TRMT11	-1.3	7.2E-01	9.3E-01	1.0E+00	2.2E-01	8.9E-02	1.8E-01	0	-2.7	9.5E-01	1.0E+00	1.0E+00	7.5E-02	5.2E-04	1.9E-03	0
YIPF7	-0.7	7.2E-01	9.3E-01	1.0E+00	2.2E-02	2.4E-03	2.0E-02	0	-0.1	6.3E-01	9.5E-01	1.0E+00	9.9E-01	8.5E-01	8.5E-01	0
DAPL1	-1.6	7.3E-01	9.3E-01	1.0E+00	6.7E-02	9.4E-03	3.8E-02	0	-1.3	9.3E-02	6.1E-01	1.0E+00	1.3E-01	3.1E-03	9.2E-03	0
NF1	-0.3	7.3E-01	9.3E-01	1.0E+00	7.9E-01	4.9E-01	5.5E-01	0	-1.3	8.2E-01	9.9E-01	1.0E+00	3.2E-01	2.0E-02	3.9E-02	0
CYB561D2	-1.3	7.3E-01	9.3E-01	1.0E+00	2.9E-01	1.4E-01	2.4E-01	0	-0.5	4.9E-03	2.1E-01	1.0E+00	4.9E-01	5.5E-02	8.2E-02	1
RAD50	-1.9	7.3E-01	9.3E-01	1.0E+00	6.2E-02	9.4E-03	3.8E-02	0	-3.0	8.5E-01	1.0E+00	1.0E+00	4.3E-03	1.5E-05	1.5E-04	0
FOXO1	-0.9	7.4E-01	9.4E-01	1.0E+00	3.9E-01	1.7E-01	2.8E-01	0	-0.4	1.1E-01	6.5E-01	1.0E+00	6.7E-01	2.0E-01	2.5E-01	0
WNT1	-1.3	7.4E-01	9.4E-01	1.0E+00	1.8E-01	7.8E-02	1.7E-01	0	-2.2	9.4E-01	1.0E+00	1.0E+00	8.7E-02	1.2E-03	3.9E-03	0
RBL2	-0.6	7.5E-01	9.4E-01	1.0E+00	7.3E-01	4.1E-01	4.8E-01	0	0.2	3.9E-02	5.0E-01	1.0E+00	8.3E-01	3.2E-01	3.7E-01	0
FAH	-0.8	7.5E-01	9.4E-01	1.0E+00	8.8E-01	6.2E-01	6.7E-01	0	-1.6	6.3E-01	9.5E-01	1.0E+00	2.9E-01	1.5E-02	3.2E-02	0
CACNA1H	-1.4	7.5E-01	9.4E-01	1.0E+00	2.8E-02	5.2E-03	3.6E-02	0	-1.3	1.8E-01	7.4E-01	1.0E+00	2.7E-01	1.1E-02	2.4E-02	0
FGFR4	-1.0	7.5E-01	9.5E-01	1.0E+00	4.3E-01	2.2E-01	3.2E-01	0	-1.5	3.1E-01	8.5E-01	1.0E+00	2.8E-01	1.2E-02	2.6E-02	0
BCOR	-1.1	7.6E-01	9.5E-01	1.0E+00	9.8E-02	1.6E-02	5.2E-02	0	-0.7	1.5E-02	3.0E-01	1.0E+00	4.8E-01	5.1E-02	8.0E-02	0
ARID1A	-1.7	7.6E-01	9.5E-01	1.0E+00	1.1E-01	2.6E-02	7.4E-02	0	-2.4	9.8E-01	1.0E+00	1.0E+00	6.6E-03	2.5E-05	1.9E-04	0
KDR	-0.7	7.7E-01	9.6E-01	1.0E+00	4.5E-01	2.5E-01	3.6E-01	0	0.3	1.5E-02	3.1E-01	1.0E+00	7.1E-01	2.1E-01	2.6E-01	0
FLT4	-1.6	7.7E-01	9.6E-01	1.0E+00	7.9E-02	1.5E-02	5.2E-02	0	-1.4	5.1E-01	9.1E-01	1.0E+00	2.2E-01	6.5E-03	1.5E-02	0
HAGH	-0.6	7.7E-01	9.6E-01	1.0E+00	6.9E-01	3.6E-01	4.3E-01	0	-1.3	6.3E-01	9.5E-01	1.0E+00	4.0E-01	4.0E-02	6.8E-02	0
BBC3	-1.8	7.7E-01	9.6E-01	1.0E+00	5.3E-02	7.6E-03	3.7E-02	0	0.0	1.6E-01	7.2E-01	1.0E+00	5.0E-02	3.8E-04	1.7E-03	0
EP300	-1.3	7.8E-01	9.6E-01	1.0E+00	2.6E-01	1.3E-01	2.4E-01	0	-1.3	8.1E-01	9.9E-01	1.0E+00	2.5E-01	1.0E-02	2.3E-02	0
ARID5B	-3.6	7.8E-01	9.6E-01	1.0E+00	5.8E-02	8.9E-03	3.8E-02	0	-0.6	5.9E-01	9.4E-01	1.0E+00	9.9E-01	8.6E-01	8.6E-01	0
ITPRIP	-0.7	7.8E-01	9.6E-01	1.0E+00	7.0E-01	3.8E-01	4.5E-01	0	-1.2	3.1E-01	8.5E-01	1.0E+00	7.6E-01	2.8E-01	3.3E-01	0
CDKN1A	-1.5	7.8E-01	9.6E-01	1.0E+00	1.1E-01	2.4E-02	7.4E-02	0	-1.8	3.8E-01	8.7E-01	1.0E+00	1.2E-01	2.7E-03	8.2E-03	0
S100G	-0.7	7.8E-01	9.6E-01	1.0E+00	5.8E-01	3.3E-01	4.1E-01	0	-0.9	1.6E-01	7.2E-01	1.0E+00	8.1E-01	3.0E-01	3.4E-01	0
ETV1	-1.5	7.8E-01	9.6E-01	1.0E+00	1.6E-01	7.0E-02	1.7E-01	0	-1.3	6.6E-01	9.6E-01	1.0E+00	3.1E-01	2.0E-02	3.9E-02	0
GOT1	-1.5	7.9E-01	9.7E-01	1.0E+00	3.2E-02	5.9E-03	3.6E-02	0	-1.3	4.1E-01	8.8E-01	1.0E+00	2.2E-01	6.5E-03	1.5E-02	0
NOTCH1	-0.1	7.9E-01	9.7E-01	1.0E+00	3.2E-01	1.4E-01	2.4E-01	0	-0.7	4.3E-01	8.8E-01	1.0E+00	3.7E-01	3.7E-02	6.7E-02	0
ICAM4	-0.3	7.9E-01	9.7E-01	1.0E+00	8.2E-01	5.1E-01	5.6E-01	0	-0.9	2.1E-01	8.0E-01	1.0E+00	5.1E-01	5.5E-02	8.2E-02	0
ENY2	-1.3	7.9E-01	9.7E-01	1.0E+00	2.8E-01	1.4E-01	2.4E-01	0	-2.4	7.4E-01	9.8E-01	1.0E+00	8.4E-03	2.5E-05	1.9E-04	0
DUSP4	-0.5	7.9E-01	9.7E-01	1.0E+00	9.6E-01	6.8E-01	7.1E-01	0	-0.2	1.3E-02	2.9E-01	1.0E+00	6.9E-01	2.1E-01	2.6E-01	1
CPN2	-1.8	7.9E-01	9.7E-01	1.0E+00	1.8E-01	7.8E-02	1.7E-01	0	-1.8	3.8E-01	8.7E-01	1.0E+00	2.0E-01	6.5E-03	1.5E-02	0
SKOR1	-0.8	7.9E-01	9.7E-01	1.0E+00	5.3E-01	2.8E-01	3.9E-01	0	-1.3	2.9E-01	8.4E-01	1.0E+00	3.1E-01	1.7E-02	3.4E-02	0
SUMO1	-1.2	7.9E-01	9.7E-01	1.0E+00	2.1E-01	8.5E-02	1.8E-01	0	-2.6	4.0E-01	8.8E-01	1.0E+00	1.9E-02	9.4E-05	6.1E-04	0
PTPRD	-0.7	7.9E-01	9.7E-01	1.0E+00	4.3E-01	2.2E-01	3.2E-01	0	-0.4	7.2E-01	9.7E-01	1.0E+00	8.8E-01	4.4E-01	4.8E-01	0
NKX3-1	-0.5	8.0E-01	9.7E-01	1.0E+00	9.9E-01	7.8E-01	8.0E-01	0	-0.3	6.3E-01	9.5E-01	1.0E+00	7.7E-01	2.9E-01	3.4E-01	0
NTRK1	-1.0	8.0E-01	9.7E-01	1.0E+00	7.3E-02	9.5E-03	3.8E-02	0	-0.7	2.9E-01	8.4E-01	1.0E+00	4.5E-01	4.2E-02	7.0E-02	0
TRADD	-0.8	8.0E-01	9.7E-01	1.0E+00	2.3E-01	1.3E-01	2.4E-01	0	-1.1	6.1E-01	9.4E-01	1.0E+00	6.4E-01	1.8E-01	2.3E-01	0
HUS1B	-1.6	8.0E-01	9.7E-01	1.0E+00	1.0E-01	1.6E-02	5.2E-02	0	-0.3	2.0E-01	7.9E-01	1.0E+00	8.4E-01	3.2E-01	3.7E-01	0
LYN	-1.2	8.0E-01	9.7E-01	1.0E+00	1.3E-01	2.6E-02	7.4E-02	0	-1.0	1.1E-02	2.7E-01	1.0E+00	5.8E-01	1.1E-01	1.5E-01	1
HIST1H3A	-1.0	8.1E-01	9.7E-01	1.0E+00	4.0E-01	2.1E-01	3.2E-01	0	-0.3	5.9E-02	5.6E-01	1.0E+00	5.5E-01	9.2E-02	1.3E-01	0
GATA3	-0.6	8.2E-01	9.8E-01	1.0E+00	8.0E-01	5.1E-01	5.6E-01	0	0.0	4.0E-02	5.1E-01	1.0E+00	7.2E-01	2.2E-01	2.7E-01	0
MDM2	-4.5	8.2E-01	9.8E-01	1.0E+00	1.5E-02	1.9E-03	1.7E-02	0	-0.4	7.1E-01	9.7E-01	1.0E+00	3.5E-01	2.9E-02	5.4E-02	0
BRAF	-1.0	8.2E-01	9.8E-01	1.0E+00	9.8E-02	1.6E-02	5.2E-02	0	-1.4	2.7E-01	8.3E-01	1.0E+00	2.4E-01	9.6E-03	2.2E-02	0
MED23	-1.8	8.2E-01	9.8E-01	1.0E+00	1.3E-02	1.7E-03	1.7E-02	0	-1.6	3.6E-01	8.7E-01	1.0E+00	6.1E-02	3.9E-04	1.7E-03	0
PSMA4	-1.2	8.2E-01	9.8E-01	1.0E+00	2.9E-01	1.4E-01	2.4E-01	0	-1.7	5.8E-02	5.6E-01	1.0E+00	1.2E-01	2.7E-03	8.2E-03	0
NPM1	-1.3	8.2E-01	9.8E-01	1.0E+00	2.3E-01	1.3E-01	2.4E-01	0	-3.1	8.8E-01	1.0E+00	1.0E+00	1.1E-02	3.5E-05	2.4E-04	0
PPP1R11	-3.5	8.3E-01	9.8E-01	1.0E+00	8.3E-03	6.6E-04	8.1E-03	0	-3.8	1.0E+00	1.0E+00	1.0E+00	4.9E-05	5.0E-06	7.9E-05	0
EPHA5	-0.5	8.3E-01	9.8E-01	1.0E+00	1.5E-02	1.9E-03	1.7E-02	0	-0.6	7.1E-02	5.8E-01	1.0E+00	5.5E-02	3.9E-04	1.7E-03	0

ZNF485	-1.5	8.4E-01	9.8E-01	1.0E+00	1.5E-01	2.9E-02	7.4E-02	0	-1.9	7.0E-02	5.8E-01	1.0E+00	1.0E-01	1.8E-03	5.7E-03	0
KMT2A	-0.9	8.4E-01	9.8E-01	1.0E+00	2.4E-01	1.3E-01	2.4E-01	0	-1.2	8.0E-01	9.9E-01	1.0E+00	2.8E-01	1.2E-02	2.6E-02	0
WNT3	-1.2	8.4E-01	9.8E-01	1.0E+00	1.5E-01	2.9E-02	7.4E-02	0	-1.6	8.9E-01	1.0E+00	1.0E+00	9.7E-02	1.4E-03	4.5E-03	0
PARP1	-0.9	8.5E-01	9.9E-01	1.0E+00	1.3E-01	2.6E-02	7.4E-02	0	-2.8	1.2E-01	6.5E-01	1.0E+00	3.2E-03	1.5E-05	1.5E-04	0
RET	-1.3	8.5E-01	9.9E-01	1.0E+00	9.0E-02	1.5E-02	5.2E-02	0	-2.4	3.5E-01	8.6E-01	1.0E+00	2.7E-02	1.2E-04	7.3E-04	0
IGFBP1	-2.1	8.5E-01	9.9E-01	1.0E+00	4.2E-02	6.5E-03	3.6E-02	0	-1.3	9.5E-01	1.0E+00	1.0E+00	4.3E-01	4.2E-02	7.0E-02	0
PIK3C3	-0.7	8.5E-01	9.9E-01	1.0E+00	1.9E-01	7.8E-02	1.7E-01	0	-0.7	5.2E-02	5.5E-01	1.0E+00	4.1E-01	4.0E-02	6.8E-02	1
DNMT1	-1.2	8.5E-01	9.9E-01	1.0E+00	6.8E-02	9.4E-03	3.8E-02	0	-3.7	1.0E+00	1.0E+00	1.0E+00	4.3E-06	5.0E-06	7.9E-05	0
INPP4A	-1.1	8.6E-01	9.9E-01	1.0E+00	5.5E-02	8.1E-03	3.8E-02	0	-0.9	9.2E-01	1.0E+00	1.0E+00	3.6E-03	1.5E-05	1.5E-04	0
APC	-1.1	8.6E-01	9.9E-01	1.0E+00	1.1E-01	2.4E-02	7.4E-02	0	-0.7	8.5E-01	1.0E+00	1.0E+00	4.0E-01	4.0E-02	6.8E-02	0
TFAP2B	-0.7	8.6E-01	9.9E-01	1.0E+00	4.3E-01	2.2E-01	3.2E-01	0	-1.1	5.3E-01	9.1E-01	1.0E+00	2.9E-01	1.5E-02	3.2E-02	0
MAX	-2.2	8.6E-01	9.9E-01	1.0E+00	7.6E-03	3.9E-04	6.0E-03	0	-1.2	9.1E-01	1.0E+00	1.0E+00	2.8E-01	1.2E-02	2.6E-02	0
KRTAP25-1	-0.8	8.6E-01	9.9E-01	1.0E+00	5.9E-01	3.3E-01	4.1E-01	0	-0.5	6.3E-01	9.5E-01	1.0E+00	9.3E-01	5.4E-01	5.7E-01	0
HTR6	-1.1	8.6E-01	9.9E-01	1.0E+00	4.1E-01	2.1E-01	3.2E-01	0	-1.1	7.1E-01	9.7E-01	1.0E+00	6.1E-01	1.3E-01	1.8E-01	0
PLS3	-1.8	8.7E-01	9.9E-01	1.0E+00	4.1E-02	6.5E-03	3.6E-02	0	-1.9	8.1E-01	9.9E-01	1.0E+00	1.2E-01	2.7E-03	8.2E-03	0
PBRM1	-0.8	8.7E-01	9.9E-01	1.0E+00	5.5E-01	3.0E-01	4.1E-01	0	-1.2	1.3E-01	6.7E-01	1.0E+00	4.0E-01	4.0E-02	6.8E-02	0
SLX4	-7.1	8.7E-01	9.9E-01	1.0E+00	1.1E-03	4.5E-05	3.0E-03	0	-2.6	1.0E+00	1.0E+00	1.0E+00	2.3E-03	5.0E-06	7.9E-05	0
FAM90A1	-1.1	8.8E-01	9.9E-01	1.0E+00	3.3E-01	1.4E-01	2.4E-01	0	-2.9	4.8E-02	5.4E-01	1.0E+00	7.7E-03	2.5E-05	1.9E-04	1
SRSF4	-0.5	8.8E-01	9.9E-01	1.0E+00	9.8E-01	7.1E-01	7.4E-01	0	-2.1	7.5E-01	9.8E-01	1.0E+00	1.7E-01	5.3E-03	1.4E-02	0
TLE3	-0.5	8.8E-01	9.9E-01	1.0E+00	8.4E-02	1.5E-02	5.2E-02	0	-1.1	8.5E-01	1.0E+00	1.0E+00	4.1E-01	4.0E-02	6.8E-02	0
TGFBR2	-0.9	8.8E-01	9.9E-01	1.0E+00	2.8E-01	1.4E-01	2.4E-01	0	-0.4	1.5E-02	3.0E-01	1.0E+00	6.3E-01	1.8E-01	2.3E-01	1
NOP10	-1.7	8.8E-01	9.9E-01	1.0E+00	1.1E-01	2.4E-02	7.4E-02	0	-3.8	9.8E-01	1.0E+00	1.0E+00	4.8E-03	1.5E-05	1.5E-04	0
SETD2	-2.0	8.8E-01	9.9E-01	1.0E+00	1.3E-01	2.6E-02	7.4E-02	0	-1.7	8.8E-01	1.0E+00	1.0E+00	1.2E-01	3.0E-03	9.2E-03	0
AQP9	-0.8	8.9E-01	1.0E+00	1.0E+00	5.2E-01	2.7E-01	3.7E-01	0	-1.0	6.5E-01	9.6E-01	1.0E+00	4.6E-01	4.6E-02	7.3E-02	0
ARPC5L	-1.6	8.9E-01	1.0E+00	1.0E+00	1.0E-01	2.1E-02	6.8E-02	0	-2.1	9.2E-01	1.0E+00	1.0E+00	1.6E-01	4.9E-03	1.4E-02	0
PTPRS	-0.7	8.9E-01	1.0E+00	1.0E+00	2.8E-01	1.4E-01	2.4E-01	0	-1.2	1.7E-01	7.3E-01	1.0E+00	6.4E-01	1.8E-01	2.3E-01	0
SMARCA4	-1.6	9.0E-01	1.0E+00	1.0E+00	7.0E-02	9.4E-03	3.8E-02	0	-1.7	9.9E-01	1.0E+00	1.0E+00	1.2E-02	3.5E-05	2.4E-04	0
FLCN	-1.2	9.0E-01	1.0E+00	1.0E+00	1.9E-01	7.8E-02	1.7E-01	0	-2.7	1.0E+00	1.0E+00	1.0E+00	1.0E-03	5.0E-06	7.9E-05	0
OTOP3	-0.7	9.0E-01	1.0E+00	1.0E+00	5.2E-01	2.7E-01	3.7E-01	0	-0.8	2.8E-01	8.4E-01	1.0E+00	2.1E-01	6.5E-03	1.5E-02	0
STAG2	-0.9	9.1E-01	1.0E+00	1.0E+00	5.3E-01	2.9E-01	4.0E-01	0	-0.8	1.1E-01	6.5E-01	1.0E+00	9.8E-01	6.2E-01	6.4E-01	0
RAC2	-2.1	9.1E-01	1.0E+00	1.0E+00	5.8E-02	8.9E-03	3.8E-02	0	-1.0	6.4E-01	9.5E-01	1.0E+00	5.4E-01	5.5E-02	8.2E-02	0
NELL1	-1.0	9.1E-01	1.0E+00	1.0E+00	1.4E-01	2.7E-02	7.4E-02	0	-2.4	3.3E-01	8.6E-01	1.0E+00	2.8E-02	1.4E-04	8.3E-04	0
HTR1F	-0.8	9.1E-01	1.0E+00	1.0E+00	2.1E-01	8.5E-02	1.8E-01	0	-0.7	7.3E-01	9.7E-01	1.0E+00	1.9E-01	5.9E-03	1.5E-02	0
CASP7	-1.3	9.1E-01	1.0E+00	1.0E+00	2.4E-01	1.3E-01	2.4E-01	0	-1.9	9.9E-01	1.0E+00	1.0E+00	5.4E-03	1.5E-05	1.5E-04	0
TET2	-4.2	9.2E-01	1.0E+00	1.0E+00	5.1E-02	7.1E-03	3.6E-02	0	-1.1	5.6E-01	9.2E-01	1.0E+00	4.5E-01	4.2E-02	7.0E-02	0
WT1	-1.8	9.2E-01	1.0E+00	1.0E+00	1.3E-02	1.7E-03	1.7E-02	0	-1.9	7.3E-01	9.7E-01	1.0E+00	3.4E-03	1.5E-05	1.5E-04	0
PSMD6	-0.9	9.2E-01	1.0E+00	1.0E+00	9.7E-02	1.6E-02	5.2E-02	0	-3.1	9.9E-01	1.0E+00	1.0E+00	9.5E-04	5.0E-06	7.9E-05	0
WDR70	-4.1	9.2E-01	1.0E+00	1.0E+00	4.6E-02	6.5E-03	3.6E-02	0	-3.5	9.3E-01	1.0E+00	1.0E+00	7.9E-03	2.5E-05	1.9E-04	0
EPHB1	-1.0	9.3E-01	1.0E+00	1.0E+00	1.0E-01	2.2E-02	7.1E-02	0	-0.2	2.0E-01	8.0E-01	1.0E+00	5.7E-01	1.1E-01	1.5E-01	0
MST1R	-2.1	9.3E-01	1.0E+00	1.0E+00	4.1E-02	6.5E-03	3.6E-02	0	-1.4	5.6E-01	9.2E-01	1.0E+00	3.5E-01	2.5E-02	4.8E-02	0
GP6	-1.5	9.3E-01	1.0E+00	1.0E+00	3.6E-02	5.9E-03	3.6E-02	0	-1.6	8.6E-01	1.0E+00	1.0E+00	9.3E-02	1.2E-03	3.9E-03	0
METTL3	-1.2	9.3E-01	1.0E+00	1.0E+00	2.7E-01	1.4E-01	2.4E-01	0	-1.7	9.0E-01	1.0E+00	1.0E+00	8.1E-02	6.5E-04	2.4E-03	0
POLE	-6.9	9.3E-01	1.0E+00	1.0E+00	3.6E-03	1.4E-04	3.5E-03	0	-3.0	9.7E-01	1.0E+00	1.0E+00	1.1E-02	3.5E-05	2.4E-04	0
PDCD1	-2.6	9.3E-01	1.0E+00	1.0E+00	3.9E-02	6.0E-03	3.6E-02	0	-2.7	9.0E-01	1.0E+00	1.0E+00	6.3E-03	1.5E-05	1.5E-04	0
CASP14	-0.9	9.4E-01	1.0E+00	1.0E+00	2.5E-01	1.3E-01	2.4E-01	0	-1.0	1.8E-01	7.4E-01	1.0E+00	3.2E-01	2.0E-02	3.9E-02	0
GSK3B	-1.6	9.4E-01	1.0E+00	1.0E+00	3.4E-02	5.9E-03	3.6E-02	0	-0.9	6.7E-01	9.6E-01	1.0E+00	5.6E-01	9.7E-02	1.4E-01	0
PPP6R3	-1.1	9.4E-01	1.0E+00	1.0E+00	8.2E-02	1.5E-02	5.2E-02	0	-3.1	7.5E-01	9.8E-01	1.0E+00	9.1E-04	5.0E-06	7.9E-05	0
ALOX12B	-1.0	9.5E-01	1.0E+00	1.0E+00	2.1E-01	8.5E-02	1.8E-01	0	-2.2	7.8E-01	9.9E-01	1.0E+00	6.8E-02	4.3E-04	1.7E-03	0
SPEN	-1.3	9.5E-01	1.0E+00	1.0E+00	9.9E-02	1.6E-02	5.2E-02	0	-1.7	7.5E-01	9.8E-01	1.0E+00	3.6E-02	2.2E-04	1.2E-03	0
MDC1	-3.8	9.5E-01	1.0E+00	1.0E+00	3.6E-02	5.9E-03	3.6E-02	0	-1.9	8.6E-01	1.0E+00	1.0E+00	1.4E-01	3.4E-03	1.0E-02	0
PDGFRB	-1.1	9.5E-01	1.0E+00	1.0E+00	2.6E-01	1.3E-01	2.4E-01	0	-1.6	8.0E-01	9.9E-01	1.0E+00	1.3E-01	3.1E-03	9.2E-03	0
ANKRD11	-1.1	9.5E-01	1.0E+00	1.0E+00	4.2E-01	2.1E-01	3.2E-01	0	-2.5	9.9E-01	1.0E+00	1.0E+00	5.2E-03	1.5E-05	1.5E-04	0
MED24	-1.3	9.6E-01	1.0E+00	1.0E+00	5.3E-02	7.6E-03	3.7E-02	0	-2.6	6.1E-01	9.4E-01	1.0E+00	2.6E-03	5.0E-06	7.9E-05	0
OPN4	-1.3	9.6E-01	1.0E+00	1.0E+00	1.5E-01	2.9E-02	7.4E-02	0	-0.9	7.4E-01	9.8E-01	1.0E+00	4.7E-01	5.1E-02	8.0E-02	0
NELFB	-2.3	9.6E-01	1.0E+00	1.0E+00	2.4E-02	5.2E-03	3.6E-02	0	-3.0	9.0E-01	1.0E+00	1.0E+00	6.2E-04	5.0E-06	7.9E-05	0
ERBB3	-2.2	9.6E-01	1.0E+00	1.0E+00	5.2E-03	1.9E-04	3.5E-03	0	-1.7	9.7E-01	1.0E+00	1.0E+00	2.4E-02	1.1E-04	6.8E-04	0
CUL3	-4.5	9.7E-01	1.0E+00	1.0E+00	1.5E-02	1.9E-03	1.7E-02	0	-3.3	1.0E+00	1.0E+00	1.0E+00	2.3E-04	5.0E-06	7.9E-05	0
SMC1A	-3.7	9.7E-01	1.0E+00	1.0E+00	6.6E-02	9.4E-03	3.8E-02	0	-2.9	9.5E-01	1.0E+00	1.0E+00	2.0E-02	9.4E-05	6.1E-04	0
FGFR1	-0.8	9.7E-01	1.0E+00	1.0E+00	5.5E-01	3.0E-01	4.1E-01	0	-0.4	4.2E-01	8.8E-01	1.0E+00	7.1E-01	2.1E-01	2.6E-01	0
CBFB	-1.0	9.7E-01	1.0E+00	1.0E+00	1.6E-01	2.9E-02	7.4E-02	0	-1.2	9.7E-01	1.0E+00	1.0E+00	3.6E-01	3.4E-02	6.3E-02	0
PTP4A1	-1.4	9.7E-01	1.0E+00	1.0E+00	8.0E-02	1.5E-02	5.2E-02	0	-1.8	7.8E-01	9.9E-01	1.0E+00	8.3E-02	6.6E-04	2.4E-03	0
KMT2C	-1.0	9.7E-01	1.0E+00	1.0E+00	5.9E-03	2.0E-04	3.5E-03	0	-0.4	5.5E-02	5.5E-01	1.0E+00	2.6E-01	1.0E-02	2.3E-02	0
HGF	-1.3	9.7E-01	1.0E+00	1.0E+00	1.8E-01	7.8E-02	1.7E-01	0	-1.5	8.9E-01	1.0E+00	1.0E+00	2.2E-01	6.5E-03	1.5E-02	0
BRD9	-2.0	9.7E-01	1.0E+00	1.0E+00	7.8E-02	1.5E-02	5.2E-02	0	-2.1	8.8E-01	1.0E+00	1.0E+00	5.4E-02	3.8E-04	1.7E-03	0
ATP6V1G3	-1.3	9.8E-01	1.0E+00	1.0E+00	1.0E-01	2.1E-02	6.8E-02	0	-0.9	7.9E-01	9.9E-01	1.0E+00	6.5E-01	1.8E-01	2.4E-01	0
FBXW7	-3.0	9.8E-01	1.0E+00	1.0E+00	2.8E-03	1.3E-04	3.5E-03	0	-2.8	9.8E-01	1.0E+00	1.0E+00	6.8E-02	4.3E-04	1.7E-03	0
RPTOR	-4.2	9.8E-01	1.0E+00	1.0E+00	1.0E-03	4.5E-05	3.0E-03	0	-2.8	1.0E+00	1.0E+00	1.0E+00	4.1E-04	5.0E-06	7.9E-05	0
KMT2D	-4.9	9.8E-01	1.0E+00	1.0E+00	1.2E-02	1.7E-03	1.7E-02	0	-3.6	1.0E+00	1.0E+00	1.0E+00	4.1E-04	5.0E-06	7.9E-05	0
HYOU1	-1.1	9.8E-01	1.0E+00	1.0E+00	6.8E-02	9.4E-03	3.8E-02	0	-2.4	4.2E-01	8.8E-01	1.0E+00	5.5E-03	1.5E-05	1.5E-04	0
YWHAZ	-7.1	9.9E-01	1.0E+00	1.0E+00	4.1E-04	5.0E-06	6.6E-04	0	-2.0	9.7E-01	1.0E+00	1.0E+00	4.9E-02	3.8E-04	1.7E-03	0
FTSJ3	-3.8	9.9E-01	1.0E+00	1.0E+00	8.9E-03	6.6E-04	8.1E-03	0	-2.1	9.7E-01	1.0E+00	1.0E+00	9.2E-03	2.5E-05	1.9E-04	0
CDC34	-1.7	9.9E-01	1.0E+00	1.0E+00	1.1E-02	6.7E-04	8.1E-03	0	-2.2	7.1E-01	9.7E-01	1.0E+00	4.0E-02	2.5E-04	1.3E-03	0
DLEU7	-6.8	9.9E-01	1.0E+00	1.0E+00	1.3E-03	4.5E-05	3.0E-03	0	-2.0	4.0E-01	8.8E-01	1.0E+00	1.7E-01	5.3E-03	1.4E-02	0
KLK5	-4.2	9.9E-01	1.0E+00	1.0E+00	9.0E-03	6.6E-04	8.1E-03	0	-1.4	9.6E-01	1.0E+00	1.0E+00	3.3E-01	2.2E-02	4.2E-02	0
SLC30A9	-4.6	9.9E-01	1.0E+00	1.0E+00	3.7E-03	1.4E-04	3.5E-03	0	-3.4	2.3E-01	8.2E-01	1.0E+00	1.2E-03	5.0E-06	7.9E-05	0
ALDOA	-5.0	9.9E-01	1.0E+00	1.0E+00	6.8E-03	2.4E-04	4.0E-03	0	-4.0	1.0E+00	1.0E+00	1.0E+00	1.3E-03	5.0E-06	7.9E-05	0
ATR	-1.5	9.9E-01	1.0E+00	1.0E+00	5.6E-03	1.9E-04	3.5E-03	0	-3.7	1.0E+00	1.0E+00	1.0E+00	2.6E-05	5.0E-06	7.9E-05	0
CUL5	-2.0	9.9E-01	1.0E+00	1.0E+00	5.4E-03	1.9E-04	3.5E-03	0	-3.0	7.2E-01	9.7E-01	1.0E+00	1.8E-03	5.0E-06	7.9E-05	0
SF3B1	-2.8	9.9E-01	1.0E+00	1.0E+00	5.3E-03	1.9E-04	3.5E-03	0	-2.9	1.0E+00	1.0E+00	1.0E+00	1.7E-03	5.0E-06	7.9E-05	0
FOXF2	-4.5	9.9E-01	1.0E+00	1.0E+00	5.1E-03	1.9E-04	3.5E-03	0	-1.4	2.6E-01	8.3E-01	1.0E+00	1.2E-01	2.7E-03	8.2E-03	0
PRF1	-1.8	1.0E+00	1.0E+00	1.0E+00	3.0E-03	1.4E-04	3.5E-03	0	-3.4	8.8E-02	6.0E-01	1.0E+00	7.6E-03	2.5E-05	1.9E-04	0
MCM2	-5.4	1.0E+00	1.0E+00	1.0E+00	1.5E-03	1.1E-04	3.5E-03	0	-4.4	1.0E+00	1.0E+00	1.0E+00	3.3E-06	5.0E-06	7.9E-05	0
SHQ1	-4.9	1.0E+00	1.0E+00	1.0E+00	1.7E-03	1.1E-04	3.5E-03	0	-2.9	8.0E-01	9.9E-01	1.0E+00	5.6E-04	5.0E-06	7.9E-05	0
PIK3CA	-4.7	1.0E+00	1.0E+00	1.0E+00	3.9E-04	5.0E-06	6.6E-04	0	-3.3	1.0E+00	1.0E+00	1.0E+00	3.7E-05	5.0E-06	7.9E-05	0
TRRAP	-7.1	1.0E+00	1.0E+00	1.0E+00	8.0E-05	5.0E-06	6.6E-04	0	-3.4	9.9E-01	1.0E+00	1.0E+00	5.4E-04	5.0E-06	7.9E-05	0

Table 4: NCI109B focused CRISPR deletion gRNA screen enriched gRNAs (Log2FC > 2, FDR < 0.05)

		CIS-ETO vs. P0						SAL vs. P0					
Gene	Guide ID	Guide Log2(FC)	Pos. Unadj. P	Pos. Adj. P	Neg. Unadj. P	Neg. Adj. P	Guide Enriched	Guide Log2(FC)	Pos. Unadj. P	Pos. Adj. P	Neg. Unadj. P	Neg. Adj. P	Guide Enriched
TADA2B	EGSC_2108	11.2	0.0E+00	0.0E+00	1.0E+00	1.0E+00	Y	-0.3	7.5E-01	1.0E+00	2.5E-01	5.4E-01	N
TADA2B	EGSC_2107	7.7	0.0E+00	0.0E+00	1.0E+00	1.0E+00	Y	2.2	1.8E-36	1.6E-35	1.0E+00	1.0E+00	Y
TADA2B	EGSC_2109	6.7	0.0E+00	0.0E+00	1.0E+00	1.0E+00	Y	-0.8	9.1E-01	1.0E+00	9.3E-02	3.3E-01	N
TADA2B	EGSC_2110	1.6	2.2E-34	1.9E-33	1.0E+00	1.0E+00	N	0.1	3.9E-01	9.8E-01	6.1E-01	1.0E+00	N
TADA2B	EGSC_2111	0.5	8.0E-03	3.1E-02	9.9E-01	1.0E+00	N	1.9	2.7E-15	1.8E-14	1.0E+00	1.0E+00	N
TADA2B	EGSC_2112	0.0	4.4E-01	1.0E+00	5.6E-01	9.6E-01	N	1.2	5.6E-08	3.0E-07	1.0E+00	1.0E+00	N
SLFN11	EGSC_2014	6.8	0.0E+00	0.0E+00	1.0E+00	1.0E+00	Y	-0.9	9.5E-01	1.0E+00	4.9E-02	2.8E-01	N
SLFN11	EGSC_2013	5.2	0.0E+00	0.0E+00	1.0E+00	1.0E+00	Y	0.5	6.0E-02	2.0E-01	9.4E-01	1.0E+00	N
SLFN11	EGSC_2015	5.0	0.0E+00	0.0E+00	1.0E+00	1.0E+00	Y	0.4	8.7E-02	2.8E-01	9.1E-01	1.0E+00	N
SLFN11	EGSC_2012	1.9	1.2E-60	1.3E-59	1.0E+00	1.0E+00	N	1.8	1.1E-14	7.3E-14	1.0E+00	1.0E+00	N
SLFN11	EGSC_2011	1.5	7.7E-35	6.8E-34	1.0E+00	1.0E+00	N	-0.1	5.6E-01	1.0E+00	4.4E-01	8.1E-01	N
SLFN11	EGSC_2016	0.3	5.5E-02	1.9E-01	9.4E-01	1.0E+00	N	0.3	2.0E-01	5.8E-01	8.0E-01	1.0E+00	N
USP22	EGSC_2281	7.5	0.0E+00	0.0E+00	1.0E+00	1.0E+00	Y	-0.9	9.7E-01	1.0E+00	2.8E-02	2.7E-01	N
USP22	EGSC_2283	6.4	0.0E+00	0.0E+00	1.0E+00	1.0E+00	Y	2.2	2.8E-42	2.7E-41	1.0E+00	1.0E+00	Y
USP22	EGSC_2284	6.0	0.0E+00	0.0E+00	1.0E+00	1.0E+00	Y	-0.7	9.3E-01	1.0E+00	7.3E-02	3.1E-01	N
USP22	EGSC_2282	0.7	1.8E-06	9.1E-06	1.0E+00	1.0E+00	N	-1.6	1.0E+00	1.0E+00	4.9E-03	2.6E-01	N
USP22	EGSC_2285	-0.3	9.1E-01	1.0E+00	8.9E-02	3.3E-01	N	-1.7	1.0E+00	1.0E+00	2.4E-03	1.5E-01	N
USP22	EGSC_2286	-0.5	9.8E-01	1.0E+00	2.2E-02	2.7E-01	N	0.4	1.3E-01	3.8E-01	8.7E-01	1.0E+00	N
TAF5L	EGSC_2114	3.7	0.0E+00	0.0E+00	1.0E+00	1.0E+00	Y	-0.2	7.1E-01	1.0E+00	2.9E-01	6.0E-01	N
TAF5L	EGSC_2113	2.7	0.0E+00	0.0E+00	1.0E+00	1.0E+00	Y	-1.2	9.9E-01	1.0E+00	1.2E-02	2.7E-01	N
TAF5L	EGSC_2117	2.1	4.8E-123	6.5E-122	1.0E+00	1.0E+00	Y	1.5	7.8E-11	4.7E-10	1.0E+00	1.0E+00	N
TAF5L	EGSC_2116	2.0	1.8E-87	2.1E-86	1.0E+00	1.0E+00	N	1.7	2.9E-14	1.9E-13	1.0E+00	1.0E+00	N
TAF5L	EGSC_2115	1.3	3.6E-24	2.8E-23	1.0E+00	1.0E+00	N	1.4	1.3E-09	7.5E-09	1.0E+00	1.0E+00	N
TAF5L	EGSC_2118	-0.4	9.5E-01	1.0E+00	4.5E-02	2.7E-01	N	-2.3	1.0E+00	1.0E+00	2.5E-03	1.5E-01	N

Table 5: FHSC14 focused CRISPR deletion gRNA screen gene-level analysis and results
Genes ranked by Pos. RRA in the CIS-ETO vs. P0 condition

	CIS-ETO vs. P0								SAL vs. P0							
Gene	Median Log2(FC)	Pos. RRA	Pos. Unadj. P	Pos. Adj. P	Neg. RRA	Neg. Unadj. P	Neg. Adj. P	Guides Enriched	Median Log2(FC)	Pos. RRA	Pos. Unadj. P	Pos. Adj. P	Neg. RRA	Neg. Unadj. P	Neg. Adj. P	Guides Enriched
USP22	2.1	5.4E-09	5.0E-06	2.0E-03	1.0E+00	1.0E+00	1.0E+00	4	0.7	7.8E-03	1.3E-01	1.0E+00	9.5E-01	6.8E-01	7.1E-01	2
TADA2B	2.9	2.1E-07	6.4E-05	1.3E-02	9.9E-01	8.5E-01	8.7E-01	3	-0.5	3.5E-02	2.9E-01	1.0E+00	6.9E-01	3.4E-01	4.1E-01	1
TAF6L	1.9	3.2E-06	5.4E-04	7.2E-02	1.0E+00	9.6E-01	9.6E-01	3	-2.4	8.1E-01	9.6E-01	1.0E+00	1.6E-02	3.4E-04	2.7E-03	0
TAF5L	2.0	4.6E-06	7.9E-04	7.9E-02	1.0E+00	1.0E+00	1.0E+00	3	-1.5	2.8E-01	7.5E-01	1.0E+00	1.3E-01	8.7E-03	2.7E-02	0
TADA1	2.3	6.6E-06	1.4E-03	1.1E-01	9.9E-01	8.3E-01	8.6E-01	3	1.4	2.9E-03	6.2E-02	1.0E+00	9.6E-01	6.8E-01	7.1E-01	0
KEAP1	1.8	2.0E-04	2.2E-02	1.0E+00	8.8E-01	5.2E-01	5.8E-01	3	-2.2	5.3E-01	8.8E-01	1.0E+00	1.8E-02	3.5E-04	2.7E-03	0
HEXA	1.2	1.1E-03	6.5E-02	1.0E+00	7.8E-01	3.4E-01	4.3E-01	0	-1.5	1.4E-01	5.9E-01	1.0E+00	2.1E-01	1.6E-02	3.9E-02	1
NSD1	0.9	1.6E-03	7.7E-02	1.0E+00	9.4E-01	6.5E-01	6.9E-01	1	-0.4	8.6E-01	9.6E-01	1.0E+00	7.2E-01	3.6E-01	4.2E-01	0
KAT2A	0.6	3.0E-03	1.3E-01	1.0E+00	1.0E+00	9.0E-01	9.1E-01	2	-2.3	9.1E-01	9.8E-01	1.0E+00	1.3E-02	2.9E-04	2.5E-03	0
MAP2K1	0.6	6.9E-03	1.8E-01	1.0E+00	9.9E-01	8.9E-01	9.1E-01	0	-0.2	1.7E-01	6.4E-01	1.0E+00	1.4E-01	8.7E-03	2.7E-02	0
CREBBP	0.6	8.3E-03	1.9E-01	1.0E+00	8.8E-01	5.2E-01	5.8E-01	0	1.9	1.4E-06	1.6E-04	6.5E-02	4.0E-01	7.6E-02	1.3E-01	3
PTEN	0.0	8.4E-03	1.9E-01	1.0E+00	9.4E-01	6.5E-01	6.9E-01	2	0.9	1.9E-02	2.1E-01	1.0E+00	3.8E-01	7.6E-02	1.3E-01	1
FLCN	0.9	9.1E-03	2.1E-01	1.0E+00	7.4E-01	3.1E-01	4.0E-01	1	-1.2	1.6E-01	6.2E-01	1.0E+00	2.5E-01	2.6E-02	6.0E-02	0
KDM5C	0.3	1.1E-02	2.4E-01	1.0E+00	1.0E+00	9.0E-01	9.1E-01	2	0.0	1.4E-02	1.6E-01	1.0E+00	9.9E-01	9.4E-01	9.4E-01	2
MED12	-0.7	1.1E-02	2.5E-01	1.0E+00	5.9E-01	2.1E-01	3.0E-01	2	-0.1	2.4E-01	7.1E-01	1.0E+00	6.1E-01	2.1E-01	2.7E-01	0
MMP26	-0.7	1.2E-02	2.5E-01	1.0E+00	4.9E-01	1.5E-01	2.6E-01	1	1.0	6.9E-03	1.2E-01	1.0E+00	8.1E-01	4.4E-01	4.9E-01	1
BAX	0.7	1.2E-02	2.5E-01	1.0E+00	9.9E-01	8.5E-01	8.7E-01	0	-0.6	8.4E-01	9.6E-01	1.0E+00	8.8E-01	6.0E-01	6.4E-01	0
CDKN2A	0.3	1.3E-02	2.6E-01	1.0E+00	7.2E-01	3.1E-01	4.0E-01	1	-0.3	4.2E-01	8.5E-01	1.0E+00	5.1E-01	1.1E-01	1.6E-01	0
TET2	0.0	1.4E-02	2.7E-01	1.0E+00	9.2E-01	6.2E-01	6.8E-01	1	-0.9	9.6E-01	1.0E+00	1.0E+00	2.8E-01	4.1E-02	8.5E-02	0
RET	0.5	1.5E-02	2.8E-01	1.0E+00	8.9E-01	5.4E-01	6.0E-01	0	-1.5	7.8E-01	9.6E-01	1.0E+00	1.5E-01	9.6E-03	3.0E-02	0
EIF1AY	0.1	1.5E-02	2.8E-01	1.0E+00	9.2E-01	6.1E-01	6.7E-01	1	-0.2	8.6E-01	9.6E-01	1.0E+00	3.1E-01	4.9E-02	1.0E-01	0
SLFN11	0.4	1.8E-02	2.9E-01	1.0E+00	6.1E-01	2.2E-01	3.2E-01	0	0.2	1.8E-01	6.4E-01	1.0E+00	2.3E-01	2.3E-02	5.5E-02	0
MRM1	-0.1	1.8E-02	2.9E-01	1.0E+00	5.7E-01	1.9E-01	2.9E-01	0	-0.2	2.4E-01	7.0E-01	1.0E+00	4.1E-01	7.6E-02	1.3E-01	0
BBC3	0.3	1.9E-02	2.9E-01	1.0E+00	3.2E-01	8.3E-02	1.7E-01	0	-0.8	3.0E-01	7.6E-01	1.0E+00	4.1E-01	7.6E-02	1.3E-01	0
PIK3R1	0.0	2.0E-02	3.1E-01	1.0E+00	9.4E-01	6.5E-01	6.9E-01	1	-0.5	5.9E-01	9.1E-01	1.0E+00	4.1E-01	7.6E-02	1.3E-01	0
TRADD	-0.4	2.1E-02	3.3E-01	1.0E+00	8.0E-01	3.9E-01	4.8E-01	0	-1.8	8.1E-01	9.6E-01	1.0E+00	1.1E-01	7.1E-03	2.5E-02	0
TP53	0.5	2.2E-02	3.3E-01	1.0E+00	6.5E-01	2.5E-01	3.4E-01	0	-0.6	1.5E-02	1.8E-01	1.0E+00	6.1E-01	2.1E-01	2.7E-01	1
PIK3C2G	0.4	2.1E-02	3.3E-01	1.0E+00	9.5E-01	6.5E-01	6.9E-01	0	-0.2	2.7E-02	2.5E-01	1.0E+00	8.6E-01	5.3E-01	5.8E-01	1
ATXN7	0.2	2.2E-02	3.4E-01	1.0E+00	7.1E-01	3.1E-01	4.0E-01	1	-1.0	9.7E-02	5.2E-01	1.0E+00	3.6E-01	7.3E-02	1.3E-01	1
NOTCH2	-0.4	2.2E-02	3.4E-01	1.0E+00	8.0E-01	3.6E-01	4.4E-01	1	-0.3	3.2E-01	7.7E-01	1.0E+00	4.6E-01	9.8E-02	1.6E-01	0
MAP3K1	0.3	2.3E-02	3.5E-01	1.0E+00	9.8E-01	7.6E-01	7.9E-01	0	0.4	2.9E-02	2.7E-01	1.0E+00	5.5E-01	1.5E-01	2.1E-01	1
AR	-0.6	2.4E-02	3.5E-01	1.0E+00	1.7E-01	1.1E-02	3.3E-02	0	-0.8	5.5E-01	8.8E-01	1.0E+00	5.2E-01	1.1E-01	1.6E-01	0
PTPRT	0.3	2.4E-02	3.5E-01	1.0E+00	1.0E+00	9.0E-01	9.1E-01	1	-0.1	2.4E-01	7.1E-01	1.0E+00	6.6E-01	2.9E-01	3.6E-01	0
CDK6	0.4	2.5E-02	3.6E-01	1.0E+00	6.8E-01	2.7E-01	3.6E-01	0	-0.4	8.8E-01	9.7E-01	1.0E+00	5.3E-01	1.4E-01	2.0E-01	0
FGFR3	-0.5	2.6E-02	3.7E-01	1.0E+00	8.6E-01	5.2E-01	5.8E-01	1	-0.9	8.2E-01	9.6E-01	1.0E+00	3.4E-01	6.1E-02	1.2E-01	0
PLS3	-0.8	2.9E-02	3.9E-01	1.0E+00	3.3E-01	8.3E-02	1.7E-01	1	-1.0	9.4E-01	9.9E-01	1.0E+00	3.2E-01	6.0E-02	1.2E-01	0
WNT3	-0.5	2.9E-02	3.9E-01	1.0E+00	7.2E-01	3.1E-01	4.0E-01	0	-0.8	4.0E-01	8.4E-01	1.0E+00	3.3E-01	6.1E-02	1.2E-01	0
FAH	0.1	3.2E-02	4.0E-01	1.0E+00	5.8E-01	1.9E-01	2.9E-01	1	0.8	1.8E-02	2.0E-01	1.0E+00	9.9E-01	8.8E-01	9.0E-01	1
CPN1	0.3	3.3E-02	4.0E-01	1.0E+00	7.8E-01	3.4E-01	4.3E-01	0	0.9	8.6E-03	1.4E-01	1.0E+00	6.7E-01	3.1E-01	3.9E-01	0
PRICKLE1	0.4	3.3E-02	4.0E-01	1.0E+00	4.7E-01	1.5E-01	2.5E-01	1	-1.3	4.7E-01	8.6E-01	1.0E+00	2.0E-01	1.4E-02	3.5E-02	0
BCL2L11	0.1	3.4E-02	4.1E-01	1.0E+00	5.7E-01	1.9E-01	2.9E-01	1	0.0	5.4E-01	8.8E-01	1.0E+00	7.7E-01	4.0E-01	4.4E-01	0
PRKCI	0.4	3.8E-02	4.3E-01	1.0E+00	3.6E-01	1.3E-01	2.4E-01	1	-1.7	1.0E-01	5.3E-01	1.0E+00	1.2E-01	8.1E-03	2.7E-02	0
FGFR1	0.1	3.9E-02	4.3E-01	1.0E+00	9.4E-01	6.5E-01	6.9E-01	1	-0.8	4.3E-01	8.6E-01	1.0E+00	9.9E-02	7.1E-03	2.5E-02	0
ATRX	-0.2	4.1E-02	4.3E-01	1.0E+00	5.6E-01	1.9E-01	2.9E-01	0	-0.7	7.2E-01	9.3E-01	1.0E+00	5.5E-01	1.5E-01	2.1E-01	0
EPHA3	0.4	4.5E-02	4.5E-01	1.0E+00	8.2E-01	4.1E-01	5.1E-01	0	-0.5	6.6E-01	9.3E-01	1.0E+00	5.4E-01	1.5E-01	2.1E-01	0
JAK2	-0.3	4.6E-02	4.6E-01	1.0E+00	5.6E-01	1.9E-01	2.9E-01	1	0.9	3.2E-03	7.3E-02	1.0E+00	7.8E-01	4.0E-01	4.4E-01	1
TLE3	0.2	4.8E-02	4.6E-01	1.0E+00	8.7E-01	5.2E-01	5.8E-01	1	0.9	5.7E-04	2.1E-02	1.0E+00	1.0E+00	9.9E-01	9.9E-01	0
TBX3	-0.3	4.9E-02	4.7E-01	1.0E+00	9.7E-01	7.3E-01	7.7E-01	1	-1.1	4.7E-01	8.6E-01	1.0E+00	2.8E-01	4.1E-02	8.5E-02	0
MID1	0.4	5.0E-02	4.7E-01	1.0E+00	3.3E-01	8.3E-02	1.7E-01	0	0.0	2.5E-01	7.3E-01	1.0E+00	1.9E-01	1.4E-02	3.5E-02	0
MMP14	-0.2	5.2E-02	4.8E-01	1.0E+00	4.6E-01	1.4E-01	2.5E-01	0	-1.5	7.5E-02	4.7E-01	1.0E+00	4.9E-02	1.1E-03	5.6E-03	1
SLC35E1	-1.3	5.6E-02	4.9E-01	1.0E+00	3.4E-01	1.3E-01	2.4E-01	0	-1.6	2.1E-01	6.8E-01	1.0E+00	1.5E-01	8.7E-03	2.7E-02	1
KDM6A	-1.6	5.7E-02	4.9E-01	1.0E+00	1.3E-01	1.0E-02	3.2E-02	1	-0.6	2.3E-02	2.3E-01	1.0E+00	3.5E-01	7.3E-02	1.3E-01	2
GPX3	0.0	5.9E-02	5.0E-01	1.0E+00	8.8E-01	5.2E-01	5.8E-01	1	-0.2	5.2E-01	8.8E-01	1.0E+00	9.7E-01	7.0E-01	7.2E-01	0
RBL2	-2.5	6.1E-02	5.0E-01	1.0E+00	4.3E-02	1.7E-03	8.0E-03	1	-1.6	1.9E-01	6.6E-01	1.0E+00	1.0E-01	7.1E-03	2.5E-02	0
HIST1H3A	0.2	6.3E-02	5.1E-01	1.0E+00	8.3E-01	4.5E-01	5.4E-01	1	-0.3	7.9E-01	9.6E-01	1.0E+00	4.4E-01	9.0E-02	1.5E-01	0
CDK8	-0.2	6.5E-02	5.2E-01	1.0E+00	6.0E-01	2.1E-01	3.1E-01	0	0.0	8.2E-02	4.7E-01	1.0E+00	5.3E-01	1.4E-01	2.0E-01	0
ATP6V1G3	0.2	6.6E-02	5.2E-01	1.0E+00	7.0E-01	3.0E-01	4.0E-01	1	0.2	2.4E-01	7.1E-01	1.0E+00	3.8E-01	7.6E-02	1.3E-01	0
PRDM14	0.3	7.1E-02	5.5E-01	1.0E+00	7.9E-01	3.4E-01	4.3E-01	0	-0.4	7.0E-01	9.3E-01	1.0E+00	8.1E-01	4.4E-01	4.9E-01	0
GSK3B	0.0	7.3E-02	5.6E-01	1.0E+00	7.5E-01	3.1E-01	4.0E-01	1	-1.4	8.7E-01	9.7E-01	1.0E+00	2.9E-01	4.1E-02	8.5E-02	0
SMG9	0.2	7.3E-02	5.6E-01	1.0E+00	9.9E-01	8.3E-01	8.6E-01	0	-0.3	1.0E-01	5.3E-01	1.0E+00	6.4E-01	2.7E-01	3.4E-01	0
TREX2	-1.2	7.5E-02	5.7E-01	1.0E+00	5.7E-01	1.9E-01	2.9E-01	1	-0.9	2.8E-01	7.5E-01	1.0E+00	5.4E-01	1.4E-01	2.0E-01	0
GLI1	-0.1	7.5E-02	5.7E-01	1.0E+00	6.9E-01	2.7E-01	3.6E-01	0	0.6	1.0E-02	1.4E-01	1.0E+00	9.9E-01	9.3E-01	9.4E-01	1
KLF8	-0.1	7.5E-02	5.7E-01	1.0E+00	7.3E-01	3.1E-01	4.0E-01	0	1.3	3.9E-03	8.7E-02	1.0E+00	3.5E-01	7.3E-02	1.3E-01	2
POU3F2	0.0	7.4E-02	5.7E-01	1.0E+00	9.9E-01	8.5E-01	8.7E-01	0	0.2	2.3E-01	7.0E-01	1.0E+00	9.4E-01	6.6E-01	7.0E-01	0
BRD9	-1.3	7.7E-02	5.7E-01	1.0E+00	3.9E-01	1.4E-01	2.4E-01	1	0.0	1.6E-01	6.2E-01	1.0E+00	4.3E-01	8.4E-02	1.4E-01	1
MGA	0.2	7.7E-02	5.7E-01	1.0E+00	7.0E-01	3.0E-01	4.0E-01	0	-1.3	6.3E-01	9.2E-01	1.0E+00	2.1E-01	1.4E-02	3.5E-02	0
STIP1	-2.1	7.9E-02	5.8E-01	1.0E+00	8.2E-02	6.4E-03	2.4E-02	1	-1.5	5.8E-01	9.1E-01	1.0E+00	1.2E-01	8.7E-03	2.7E-02	0
PREX2	-0.6	7.9E-02	5.8E-01	1.0E+00	3.8E-01	1.3E-01	2.4E-01	0	-1.2	8.3E-02	4.7E-01	1.0E+00	1.4E-01	8.7E-03	2.7E-02	1
ANKS1A	0.1	8.2E-02	5.8E-01	1.0E+00	6.7E-01	2.7E-01	3.6E-01	1	-0.1	2.9E-01	7.6E-01	1.0E+00	2.7E-01	4.1E-02	8.5E-02	0
ZFHX3	-0.9	8.4E-02	5.9E-01	1.0E+00	1.5E-01	1.1E-02	3.3E-02	0	-1.2	7.5E-01	9.4E-01	1.0E+00	2.7E-01	4.1E-02	8.5E-02	0
HTR6	-0.5	8.9E-02	6.0E-01	1.0E+00	7.4E-01	3.1E-01	4.0E-01	1	-1.0	7.4E-01	9.4E-01	1.0E+00	3.4E-01	6.4E-02	1.2E-01	0
PPP3CC	0.3	8.9E-02	6.0E-01	1.0E+00	8.8E-01	5.2E-01	5.8E-01	0	-0.3	2.8E-01	7.5E-01	1.0E+00	9.9E-01	8.9E-01	9.0E-01	0
SRSF4	-0.8	9.5E-02	6.2E-01	1.0E+00	4.6E-01	1.4E-01	2.5E-01	1	0.7	3.0E-02	2.7E-01	1.0E+00	9.8E-01	7.3E-01	7.6E-01	0
SCML1	0.0	9.3E-02	6.2E-01	1.0E+00	8.6E-01	5.2E-01	5.8E-01	1	-0.4	2.6E-02	2.5E-01	1.0E+00	6.5E-01	2.7E-01	3.4E-01	2
ITPRIP	-0.1	1.0E-01	6.2E-01	1.0E+00	9.5E-01	6.5E-01	6.9E-01	0	0.4	9.7E-02	5.2E-01	1.0E+00	3.9E-01	7.6E-02	1.3E-01	0
FHL3	-0.9	1.1E-01	6.2E-01	1.0E+00	1.4E-01	1.1E-02	3.3E-02	1	-0.7	1.1E-01	5.5E-01	1.0E+00	4.3E-01	8.0E-02	1.3E-01	0
PTPRS	-1.4	1.1E-01	6.2E-01	1.0E+00	2.8E-01	7.2E-02	1.6E-01	0	-0.9	6.0E-01	9.1E-01	1.0E+00	4.3E-01	9.0E-02	1.5E-01	0
MSH6	0.2	1.0E-01	6.2E-01	1.0E+00	3.0E-01	7.6E-02	1.6E-01	0	-0.4	3.8E-01	8.2E-01	1.0E+00	5.9E-01	2.0E-01	2.7E-01	0
AMER1	-0.5	1.1E-01	6.2E-01	1.0E+00	5.6E-01	1.9E-01	2.9E-01	0	-0.1	2.0E-01	6.6E-01	1.0E+00	7.4E-01	3.6E-01	4.2E-01	0
DDR2	-0.9	1.1E-01	6.2E-01	1.0E+00	6.3E-01	2.2E-01	3.2E-01	1	-0.5	1.7E-01	6.4E-01	1.0E+00	5.0E-01	1.1E-01	1.6E-01	0
TGFBR2	-0.6	1.0E-01	6.2E-01	1.0E+00	6.7E-01	2.7E-01	3.6E-01	1	0.7	2.5E-02	2.5E-01	1.0E+00	8.1E-01	4.2E-01	4.6E-01	1
DBNL	0.2	1.0E-01	6.2E-01	1.0E+00	7.6E-01	3.1E-01	4.0E-01	1	-0.9	8.4E-01	9.6E-01	1.0E+00	3.4E-02	6.0E-04	3.6E-03	0
RBPJ	0.1	1.1E-01	6.2E-01	1.0E+00	9.8E-01	7.4E-01	7.8E-01	0	0.6	3.1E-02	2.7E-01	1.0E+00	1.7E-01	1.4E-02	3.5E-02	0
KAT2B	0.1	1.2E-01	6.6E-01	1.0E+00	4.4E-01	1.4E-01	2.4E-01	0	-1.2	6.9E-01	9.3E-01	1.0E+00	2.8E-01	4.1E-02	8.5E-02	0
CHD8	0.0	1.2E-01	6.6E-01	1.0E+00	7.7E-01	3.4E-01	4.3E-01	0	-0.5	1.4E-01	6.0E-01	1.0E+00	3.8E-01	7.6E-02	1.3E-01	0
FOXP1	0.2	1.2E-01	6.7E-01	1.0E+00	1.0E+00	9.7E-01	9.7E-01	0	-0.8	5.7E-01	9.0E-01	1.0E+00	3.4E-01	6.7E-02	1.3E-01	0
FOXJ1	-1.9	1.2E-01	6.8E-01	1.0E+00	1.2E-01	9.4E-03	3.0E-02	0	-1.3	6.8E-01	9.3E-01	1.0E+00	2.8E-01	4.1E-02	8.5E-02	0
INPP4A	0.2	1.2E-01	6.8E-01	1.0E+00	9.1E-01	6.1E-01	6.7E-01	0	0.4	1.1E-01	5.5E-01	1.0E+00	8.1E-01	4.4E-01	4.9E-01	0
HUS1B	-0.1	1.3E-01	6.8E-01	1.0E+00	9.8E-01	7.6E-01	7.9E-01	0	-0.9	2.0E-01	6.6E-01	1.0E+00	2.2E-02	4.1E-04	2.8E-03	1
YIPF7	-0.6	1.3E-01	6.8E-01	1.0E+00	5.1E-01	1.7E-01	2.8E-01	0	0.3	1.9E-01	6.6E-01	1.0E+00	7.5E-01	4.0E-01	4.4E-01	1
RNASE8	-1.6	1.3E-01	6.9E-01	1.0E+00	2.0E-01	1.5E-02	3.9E-02	1	-0.3	3.2E-01	7.7E-01	1.0E+00	7.6E-01	4.0E-01	4.4E-01	0
ESRP2	-0.2	1.3E-01	6.9E-01	1.0E+00	3.2E-01	8.0E-02	1.7E-01	0	-0.6	5.1E-01	8.7E-01	1.0E+00	7.7E-01	4.0E-01	4.4E-01	0
LATS2	-0.3	1.3E-01	6.9E-01	1.0E+00	8.6E-01	4.9E-01	5.7E-01	0	-0.7	3.5E-01	8.0E-01	1.0E+00	6.2E-01	2.3E-01	3.0E-01	0
GP6	-0.3	1.3E-01	6.9E-01	1.0E+00	9.7E-01	7.3E-01	7.7E-01	1	-0.6	5.1E-01	8.7E-01	1.0E+00	3.7E-01	7.6E-02	1.3E-01	0
CASP7	-0.1	1.4E-01	6.9E-01	1.0E+00	1.3E-01	9.4E-03	3.0E-02	1	-0.3	8.3E-01	9.6E-01	1.0E+00	6.4E-01	2.7E-01	3.4E-01	0
ERBB4	-0.9	1.4E-01	6.9E-01	1.0E+00	8.8E-01	5.2E-01	5.8E-01	1	0.6	5.4E-03	1.0E-01	1.0E+00	9.4E-01	6.6E-01	7.0E-01	0
UGT2B28	-0.7	1.5E-01	7.0E-01	1.0E+00	8.1E-01	4.1E-01	5.1E-01	1	0.8	1.5E-02	1.8E-01	1.0E+00	9.3E-01	6.6E-01	7.0E-01	0
KRTAP25-1	-0.5	1.6E-01	7.1E-01	1.0E+00	4.0E-01	1.4E-01	2.4E-01	0	-0.4	1.3E-02	1.6E-01	1.0E+00	5.2E-01	1.2E-01	1.7E-01	1
EPHA5	-0.5	1.6E-01	7.1E-01	1.0E+00	5.1E-01	1.7E-01	2.8E-01	0	0.4	5.8E-02	4.0E-01	1.0E+00	7.8E-01	4.0E-01	4.4E-01	1

CAMSAP3	-0.6	1.6E-01	7.1E-01	1.0E+00	8.1E-01	4.1E-01	5.1E-01	1	-0.5	3.2E-01	7.7E-01	1.0E+00	4.3E-01	7.6E-02	1.3E-01	0
MED16	-0.2	1.6E-01	7.1E-01	1.0E+00	8.5E-01	4.6E-01	5.5E-01	1	-2.1	1.5E-01	6.1E-01	1.0E+00	4.5E-02	1.1E-03	5.6E-03	0
TLE2	-0.8	1.7E-01	7.1E-01	1.0E+00	5.0E-01	1.6E-01	2.7E-01	0	-1.4	1.2E-01	5.5E-01	1.0E+00	1.7E-01	1.4E-02	3.5E-02	1
TCF25	-0.7	1.7E-01	7.1E-01	1.0E+00	5.2E-01	1.8E-01	2.9E-01	0	-0.1	1.0E-01	5.2E-01	1.0E+00	6.8E-01	3.3E-01	4.1E-01	1
GOT1	-0.5	1.6E-01	7.1E-01	1.0E+00	5.5E-01	1.9E-01	2.9E-01	0	-0.4	2.3E-01	7.0E-01	1.0E+00	6.0E-01	2.1E-01	2.7E-01	0
RUNX1	-1.2	1.7E-01	7.2E-01	1.0E+00	5.4E-01	1.9E-01	2.9E-01	0	-0.4	5.5E-01	8.8E-01	1.0E+00	6.2E-01	2.3E-01	3.0E-01	0
CCDC34	-0.2	1.7E-01	7.2E-01	1.0E+00	7.4E-01	3.1E-01	4.0E-01	0	0.0	4.2E-01	8.5E-01	1.0E+00	5.7E-01	1.5E-01	2.1E-01	0
SFRP5	-0.4	1.7E-01	7.2E-01	1.0E+00	9.8E-01	7.6E-01	7.9E-01	0	0.6	3.5E-02	2.8E-01	1.0E+00	8.7E-01	5.8E-01	6.2E-01	0
ALDH3A1	-0.3	1.7E-01	7.2E-01	1.0E+00	9.9E-01	8.1E-01	8.4E-01	1	-0.5	7.0E-02	4.6E-01	1.0E+00	9.5E-01	6.8E-01	7.1E-01	1
GRHL1	-0.8	1.8E-01	7.3E-01	1.0E+00	3.4E-01	1.3E-01	2.4E-01	0	0.1	1.6E-01	6.2E-01	1.0E+00	5.6E-01	1.5E-01	2.1E-01	0
APMAP	-0.6	1.8E-01	7.3E-01	1.0E+00	9.1E-01	5.8E-01	6.4E-01	0	-0.3	4.9E-01	8.7E-01	1.0E+00	8.1E-01	4.5E-01	5.0E-01	0
WWTR1	-1.5	1.9E-01	7.3E-01	1.0E+00	1.7E-01	1.1E-02	3.3E-02	0	0.7	3.6E-02	2.9E-01	1.0E+00	1.4E-01	8.7E-03	2.7E-02	1
MBOAT4	-0.6	1.9E-01	7.3E-01	1.0E+00	5.4E-01	1.9E-01	2.9E-01	0	2.0	1.4E-05	1.1E-03	2.2E-01	5.7E-01	1.5E-01	2.1E-01	3
FAS	-0.2	1.9E-01	7.3E-01	1.0E+00	8.4E-01	4.5E-01	5.4E-01	0	0.8	4.7E-03	9.1E-02	1.0E+00	9.8E-01	7.6E-01	7.8E-01	0
SMAD3	-0.1	2.0E-01	7.5E-01	1.0E+00	4.5E-01	1.4E-01	2.5E-01	0	-0.6	3.4E-02	2.8E-01	1.0E+00	5.7E-01	1.5E-01	2.1E-01	1
ALK	-1.4	2.0E-01	7.5E-01	1.0E+00	2.9E-01	7.2E-02	1.6E-01	0	-1.2	5.4E-01	8.8E-01	1.0E+00	2.8E-02	4.6E-04	2.9E-03	0
CYSLTR2	-1.0	2.0E-01	7.5E-01	1.0E+00	3.7E-01	1.3E-01	2.4E-01	1	-0.8	2.3E-01	7.0E-01	1.0E+00	3.4E-01	6.4E-02	1.2E-01	1
GATA3	-0.3	2.0E-01	7.5E-01	1.0E+00	8.0E-01	3.9E-01	4.8E-01	0	-0.4	5.1E-01	8.7E-01	1.0E+00	7.8E-01	4.0E-01	4.4E-01	0
DVL2	-0.9	2.0E-01	7.5E-01	1.0E+00	8.3E-01	4.5E-01	5.4E-01	0	-0.3	6.0E-02	4.0E-01	1.0E+00	3.0E-01	4.4E-02	9.0E-02	0
MDM2	-1.6	2.1E-01	7.5E-01	1.0E+00	2.1E-01	1.6E-02	4.2E-02	0	-1.3	3.3E-01	7.9E-01	1.0E+00	2.1E-01	1.4E-02	3.5E-02	0
CCDC170	-0.8	2.1E-01	7.5E-01	1.0E+00	6.0E-01	2.2E-01	3.2E-01	0	-0.7	6.9E-01	9.3E-01	1.0E+00	3.7E-01	7.6E-02	1.3E-01	0
HEATR1	-3.1	2.2E-01	7.5E-01	1.0E+00	2.0E-02	4.7E-04	3.0E-03	0	-1.5	8.4E-01	9.6E-01	1.0E+00	1.6E-01	1.1E-02	3.2E-02	0
TRAF2	-1.6	2.2E-01	7.5E-01	1.0E+00	2.0E-01	1.5E-02	3.9E-02	0	-0.9	8.6E-01	9.6E-01	1.0E+00	2.3E-01	2.6E-02	6.0E-02	0
HESX1	-1.1	2.1E-01	7.5E-01	1.0E+00	4.3E-01	1.4E-01	2.4E-01	0	-0.1	1.2E-01	5.5E-01	1.0E+00	6.1E-01	2.1E-01	2.7E-01	1
KLK5	-0.4	2.1E-01	7.5E-01	1.0E+00	8.5E-01	4.6E-01	5.5E-01	0	-0.3	2.4E-01	7.2E-01	1.0E+00	4.2E-01	7.6E-02	1.3E-01	1
BCAR1	-1.5	2.2E-01	7.6E-01	1.0E+00	1.7E-01	1.1E-02	3.3E-02	0	-0.3	1.6E-01	6.2E-01	1.0E+00	9.7E-01	7.3E-01	7.6E-01	0
ZNF319	-1.0	2.2E-01	7.6E-01	1.0E+00	2.0E-01	1.5E-02	3.9E-02	0	-0.8	6.1E-01	9.1E-01	1.0E+00	2.9E-01	4.2E-02	8.7E-02	0
NOTCH3	-0.7	2.2E-01	7.6E-01	1.0E+00	8.5E-01	4.6E-01	5.5E-01	0	-0.9	5.7E-01	9.0E-01	1.0E+00	3.3E-01	6.0E-02	1.2E-01	0
HHIPL2	-0.6	2.2E-01	7.6E-01	1.0E+00	5.2E-01	1.8E-01	2.9E-01	0	-0.3	2.5E-01	7.3E-01	1.0E+00	1.7E-01	1.4E-02	3.5E-02	0
GAB4	-0.6	2.3E-01	7.6E-01	1.0E+00	6.3E-01	2.3E-01	3.3E-01	0	0.1	1.7E-01	6.2E-01	1.0E+00	6.8E-01	3.3E-01	4.1E-01	0
FLT1	-0.2	2.3E-01	7.6E-01	1.0E+00	8.7E-01	5.2E-01	5.8E-01	0	-0.4	1.3E-01	5.7E-01	1.0E+00	3.4E-01	6.4E-02	1.2E-01	1
SFN	-0.8	2.3E-01	7.8E-01	1.0E+00	1.5E-01	1.1E-02	3.3E-02	0	-0.8	9.0E-01	9.7E-01	1.0E+00	3.0E-01	4.2E-02	8.7E-02	0
SPEN	-2.3	2.4E-01	7.8E-01	1.0E+00	1.8E-02	4.1E-04	2.7E-03	0	-1.3	2.4E-01	7.1E-01	1.0E+00	1.6E-01	1.1E-02	3.2E-02	1
PRF1	-0.6	2.4E-01	7.9E-01	1.0E+00	6.6E-01	2.6E-01	3.5E-01	0	-0.6	8.5E-01	9.6E-01	1.0E+00	4.7E-01	1.1E-01	1.6E-01	0
ALDOA	-3.1	2.5E-01	8.0E-01	1.0E+00	3.1E-03	2.5E-05	2.8E-04	0	-1.0	5.4E-01	8.8E-01	1.0E+00	2.6E-01	3.2E-02	7.2E-02	0
CLDN11	-1.8	2.5E-01	8.0E-01	1.0E+00	1.9E-01	1.5E-02	3.9E-02	0	-1.6	5.2E-01	8.8E-01	1.0E+00	1.5E-01	9.6E-03	3.0E-02	0
DOT1L	-1.2	2.5E-01	8.0E-01	1.0E+00	3.7E-01	1.3E-01	2.4E-01	0	-0.3	1.6E-02	1.9E-01	1.0E+00	1.9E-01	1.4E-02	3.5E-02	1
INHBA	-0.3	2.5E-01	8.0E-01	1.0E+00	8.8E-01	5.2E-01	5.8E-01	0	1.4	2.0E-03	4.8E-02	1.0E+00	9.8E-01	8.1E-01	8.3E-01	0
HTR1F	-0.6	2.6E-01	8.0E-01	1.0E+00	7.4E-01	3.1E-01	4.0E-01	0	-0.5	2.9E-01	7.6E-01	1.0E+00	6.0E-01	2.1E-01	2.7E-01	0
MED23	-0.2	2.6E-01	8.0E-01	1.0E+00	7.7E-01	3.4E-01	4.3E-01	0	-1.6	3.6E-02	2.9E-01	1.0E+00	3.4E-02	6.0E-04	3.6E-03	1
FAT1	0.0	2.6E-01	8.0E-01	1.0E+00	7.9E-01	3.4E-01	4.3E-01	0	-0.5	1.5E-01	6.1E-01	1.0E+00	2.6E-01	3.2E-02	7.2E-02	1
INPP4B	-0.6	2.6E-01	8.0E-01	1.0E+00	8.7E-01	5.2E-01	5.8E-01	0	-1.0	8.9E-01	9.7E-01	1.0E+00	2.0E-01	1.4E-02	3.5E-02	0
HECW1	-1.1	2.7E-01	8.2E-01	1.0E+00	5.5E-01	1.9E-01	2.9E-01	0	-0.4	2.9E-02	2.6E-01	1.0E+00	3.4E-01	6.1E-02	1.2E-01	2
SLPI	-0.3	2.7E-01	8.3E-01	1.0E+00	5.8E-01	2.0E-01	3.0E-01	0	0.2	1.6E-01	6.2E-01	1.0E+00	3.8E-01	7.6E-02	1.3E-01	0
PRDM1	-0.9	2.7E-01	8.3E-01	1.0E+00	1.9E-01	1.5E-02	3.9E-02	0	0.7	1.8E-02	2.0E-01	1.0E+00	7.3E-01	3.6E-01	4.2E-01	2
IKZF1	-0.9	2.8E-01	8.4E-01	1.0E+00	6.6E-01	2.6E-01	3.5E-01	0	0.3	1.6E-01	6.2E-01	1.0E+00	9.8E-01	8.3E-01	8.5E-01	0
WDR49	-0.6	2.8E-01	8.4E-01	1.0E+00	6.6E-01	2.6E-01	3.5E-01	0	-0.7	1.2E-01	5.5E-01	1.0E+00	4.8E-01	1.1E-01	1.6E-01	1
AKT3	-1.1	2.8E-01	8.4E-01	1.0E+00	3.2E-01	8.0E-02	1.7E-01	0	-0.6	6.9E-01	9.3E-01	1.0E+00	7.8E-01	4.0E-01	4.4E-01	0
TET1	-0.4	2.9E-01	8.4E-01	1.0E+00	9.9E-01	8.9E-01	9.1E-01	0	-0.5	2.1E-02	2.1E-01	1.0E+00	7.9E-02	3.9E-03	1.6E-02	2
BCOR	-1.3	2.9E-01	8.5E-01	1.0E+00	2.6E-01	6.9E-02	1.6E-01	0	-0.6	8.2E-01	9.6E-01	1.0E+00	4.3E-01	8.0E-02	1.3E-01	0
LAMA1	-0.8	3.0E-01	8.5E-01	1.0E+00	8.6E-01	4.8E-01	5.6E-01	0	-0.1	1.5E-01	6.1E-01	1.0E+00	1.7E-01	1.4E-02	3.5E-02	1
IRS1	-0.6	3.0E-01	8.5E-01	1.0E+00	7.5E-01	3.1E-01	4.0E-01	0	-0.4	1.0E-01	5.3E-01	1.0E+00	2.4E-01	2.6E-02	6.0E-02	1
SKOR1	-0.6	3.0E-01	8.5E-01	1.0E+00	8.4E-01	4.6E-01	5.5E-01	0	-0.8	8.5E-02	4.9E-01	1.0E+00	1.8E-01	1.4E-02	3.5E-02	0
NOP10	-2.5	3.1E-01	8.6E-01	1.0E+00	8.5E-02	6.8E-03	2.4E-02	0	-4.2	5.0E-01	8.7E-01	1.0E+00	3.7E-03	1.5E-05	2.5E-04	0
TRMT11	-2.7	3.1E-01	8.6E-01	1.0E+00	2.8E-02	6.2E-04	3.6E-03	0	-1.6	6.1E-02	4.1E-01	1.0E+00	7.1E-02	3.1E-03	1.4E-02	1
ARNT2	-0.5	3.1E-01	8.6E-01	1.0E+00	7.3E-01	3.1E-01	4.0E-01	0	1.1	5.1E-03	1.0E-01	1.0E+00	9.8E-01	7.7E-01	7.7E-01	2
PPP6R3	-2.1	3.1E-01	8.6E-01	1.0E+00	4.0E-02	1.6E-03	8.0E-03	0	-2.5	5.6E-01	8.8E-01	1.0E+00	1.5E-02	3.3E-04	2.7E-03	0
MAP3K13	-2.0	3.2E-01	8.6E-01	1.0E+00	5.8E-02	5.7E-03	2.3E-02	0	-2.1	9.5E-01	1.0E+00	1.0E+00	2.4E-02	4.1E-04	2.8E-03	0
ALOX12B	-0.8	3.2E-01	8.7E-01	1.0E+00	3.2E-01	8.0E-02	1.7E-01	0	0.0	2.1E-01	6.9E-01	1.0E+00	8.9E-01	6.2E-01	6.6E-01	0
FZD7	-0.5	3.2E-01	8.7E-01	1.0E+00	2.6E-01	2.4E-02	5.7E-02	0	-0.6	3.6E-01	8.0E-01	1.0E+00	5.6E-01	1.5E-01	2.1E-01	0
S100G	0.1	3.2E-01	8.7E-01	1.0E+00	8.6E-01	5.2E-01	5.8E-01	0	-0.6	3.4E-01	7.9E-01	1.0E+00	8.2E-01	4.5E-01	5.0E-01	0
RB1	-0.8	3.3E-01	8.7E-01	1.0E+00	5.4E-01	1.9E-01	2.9E-01	0	0.1	2.2E-01	7.0E-01	1.0E+00	7.7E-01	4.0E-01	4.4E-01	0
CSF1R	-0.6	3.3E-01	8.7E-01	1.0E+00	6.6E-01	2.6E-01	3.5E-01	0	-0.5	6.0E-01	9.1E-01	1.0E+00	3.3E-01	6.1E-02	1.2E-01	0
KCNIP3	-1.2	3.3E-01	8.7E-01	1.0E+00	2.6E-01	6.9E-02	1.6E-01	0	0.8	2.4E-02	2.3E-01	1.0E+00	9.9E-01	9.0E-01	9.1E-01	0
GSTM5	-0.4	3.3E-01	8.7E-01	1.0E+00	5.9E-01	2.1E-01	3.0E-01	0	-0.6	9.3E-01	9.9E-01	1.0E+00	3.2E-01	6.0E-02	1.2E-01	0
CDKN1A	-2.4	3.4E-01	8.8E-01	1.0E+00	3.6E-02	1.5E-03	7.8E-03	0	-1.9	4.3E-01	8.6E-01	1.0E+00	8.0E-02	3.9E-03	1.6E-02	0
OTC	-1.4	3.4E-01	8.8E-01	1.0E+00	2.5E-01	2.4E-02	5.7E-02	0	-0.7	4.2E-01	8.5E-01	1.0E+00	5.2E-01	1.2E-01	1.7E-01	0
MUC1	-0.9	3.5E-01	8.8E-01	1.0E+00	4.2E-01	1.4E-01	2.4E-01	0	-1.2	6.2E-01	9.2E-01	1.0E+00	2.0E-02	3.6E-04	2.7E-03	0
CLDN1	-0.9	3.3E-01	8.8E-01	1.0E+00	4.8E-01	1.5E-01	2.5E-01	0	-0.6	2.4E-01	7.0E-01	1.0E+00	2.3E-01	2.3E-02	5.5E-02	0
KRT33B	-0.7	3.4E-01	8.8E-01	1.0E+00	5.3E-01	1.8E-01	2.9E-01	0	-0.7	3.7E-01	8.2E-01	1.0E+00	4.6E-01	9.8E-02	1.6E-01	0
IQGAP2	-0.4	3.4E-01	8.8E-01	1.0E+00	8.4E-01	4.6E-01	5.5E-01	0	-1.8	6.6E-02	4.5E-01	1.0E+00	1.5E-01	8.7E-03	2.7E-02	1
BBS4	-0.4	3.3E-01	8.8E-01	1.0E+00	9.1E-01	6.1E-01	6.7E-01	0	0.7	2.4E-02	2.3E-01	1.0E+00	6.3E-01	2.4E-01	3.0E-01	0
STAG2	-1.8	3.5E-01	8.8E-01	1.0E+00	1.1E-02	1.9E-04	1.5E-03	0	-1.5	9.4E-01	9.9E-01	1.0E+00	5.2E-02	1.1E-03	5.7E-03	0
KMT2A	-1.6	3.5E-01	8.8E-01	1.0E+00	3.5E-02	1.5E-03	7.8E-03	0	-3.5	9.2E-01	9.9E-01	1.0E+00	5.9E-03	2.5E-05	3.3E-04	0
EP300	-2.1	3.6E-01	8.8E-01	1.0E+00	7.0E-02	5.7E-03	2.3E-02	0	0.0	1.5E-01	6.1E-01	1.0E+00	4.0E-01	7.6E-02	1.3E-01	0
SFXN2	-1.1	3.7E-01	8.8E-01	1.0E+00	3.4E-01	1.3E-01	2.4E-01	0	0.5	6.1E-02	4.0E-01	1.0E+00	7.1E-01	3.6E-01	4.2E-01	1
PDGFRB	-0.7	3.5E-01	8.8E-01	1.0E+00	3.9E-01	1.4E-01	2.4E-01	0	-1.3	9.4E-01	9.9E-01	1.0E+00	2.6E-01	4.1E-02	8.5E-02	0
LMO7	-1.0	3.7E-01	8.9E-01	1.0E+00	4.3E-01	1.4E-01	2.4E-01	0	0.9	7.4E-03	1.3E-01	1.0E+00	9.7E-01	7.2E-01	7.5E-01	1
WTAP	-1.4	3.7E-01	8.9E-01	1.0E+00	3.4E-02	1.5E-03	7.8E-03	0	-1.2	6.7E-01	9.3E-01	1.0E+00	7.8E-02	3.9E-03	1.6E-02	0
CDKN2B	-1.0	3.7E-01	9.0E-01	1.0E+00	3.2E-01	8.0E-02	1.7E-01	0	-0.8	5.0E-01	8.7E-01	1.0E+00	4.5E-01	9.8E-02	1.6E-01	0
MITF	-0.5	3.7E-01	9.0E-01	1.0E+00	5.8E-01	2.0E-01	3.0E-01	0	0.2	5.1E-02	3.7E-01	1.0E+00	4.3E-01	8.0E-02	1.3E-01	1
CBL	-0.4	3.8E-01	9.0E-01	1.0E+00	6.7E-01	2.7E-01	3.6E-01	0	0.0	1.2E-01	5.5E-01	1.0E+00	7.5E-01	4.0E-01	4.4E-01	0
ROS1	-0.6	3.8E-01	9.0E-01	1.0E+00	8.8E-01	5.2E-01	5.8E-01	0	-1.3	3.0E-02	2.7E-01	1.0E+00	1.9E-01	1.4E-02	3.5E-02	1
PTP4A1	-0.7	3.8E-01	9.0E-01	1.0E+00	4.3E-01	1.4E-01	2.4E-01	0	1.0	3.2E-03	7.3E-02	1.0E+00	9.9E-01	9.2E-01	9.3E-01	1
CDCP1	-0.7	3.8E-01	9.0E-01	1.0E+00	8.8E-01	5.2E-01	5.8E-01	0	0.1	2.1E-01	6.8E-01	1.0E+00	9.0E-01	6.2E-01	6.6E-01	0
SLC2A5	-0.7	3.8E-01	9.0E-01	1.0E+00	9.3E-01	6.4E-01	6.9E-01	0	-0.8	9.2E-01	9.9E-01	1.0E+00	4.7E-01	1.1E-01	1.6E-01	0
HIST1H4L	-0.2	3.8E-01	9.0E-01	1.0E+00	9.4E-01	6.5E-01	6.9E-01	0	0.3	3.2E-02	2.8E-01	1.0E+00	7.3E-01	3.6E-01	4.2E-01	1
OTOP3	0.1	3.9E-01	9.1E-01	1.0E+00	9.4E-01	6.5E-01	6.9E-01	0	1.8	5.8E-04	2.1E-02	1.0E+00	9.5E-01	6.8E-01	7.1E-01	3
NCOR1	-0.2	3.9E-01	9.1E-01	1.0E+00	7.1E-01	3.1E-01	4.0E-01	0	-1.1	3.9E-01	8.3E-01	1.0E+00	2.6E-01	4.1E-02	8.5E-02	0
TFAP2B	-0.4	4.0E-01	9.1E-01	1.0E+00	8.6E-01	4.8E-01	5.6E-01	0	-0.2	8.3E-02	4.7E-01	1.0E+00	6.9E-01	3.4E-01	4.1E-01	1
SLC25A33	-2.7	4.0E-01	9.2E-01	1.0E+00	8.3E-03	1.8E-04	1.5E-03	0	-0.7	7.3E-02	4.7E-01	1.0E+00	4.3E-01	8.4E-02	1.4E-01	1
IL7R	-1.2	4.1E-01	9.2E-01	1.0E+00	2.9E-01	7.2E-02	1.6E-01	0	-0.4	6.2E-01	9.2E-01	1.0E+00	7.9E-01	4.0E-01	4.4E-01	0
DLC1	-0.9	4.1E-01	9.2E-01	1.0E+00	6.1E-01	2.2E-01	3.2E-01	0	-0.8	7.9E-01	9.6E-01	1.0E+00	3.3E-01	6.1E-02	1.2E-01	0
KDM6B	-0.6	4.1E-01	9.2E-01	1.0E+00	6.4E-01	2.4E-01	3.4E-01	0	0.6	3.0E-02	2.7E-01	1.0E+00	7.3E-01	3.6E-01	4.2E-01	0
ERCC4	-3.7	4.2E-01	9.2E-01	1.0E+00	2.9E-03	2.5E-05	2.8E-04	0	-3.6	9.9E-01	1.0E+00	1.0E+00	7.3E-04	5.0E-06	1.0E-04	0
CDKN2C	-1.3	4.1E-01	9.2E-01	1.0E+00	4.6E-01	1.4E-01	2.5E-01	0	-1.5	1.2E-03	3.3E-02	1.0E+00	2.0E-01	1.4E-02	3.5E-02	1
TGFB1	-2.0	4.3E-01	9.2E-01	1.0E+00	8.0E-02	6.4E-03	2.4E-02	0	-0.4	8.2E-01	9.6E-01	1.0E+00	8.2E-01	4.6E-01	5.0E-01	0
CACNG8	-1.8	4.4E-01	9.2E-01	1.0E+00	1.3E-01	1.0E-02	3.2E-02	0	-1.0	8.2E-01	9.6E-01	1.0E+00	2.5E-01	2.6E-02	6.0E-02	0
EPHB1	-1.3	4.3E-01	9.2E-01	1.0E+00	2.1E-01	1.7E-02	4.5E-02	0	-1.7	8.0E-01	9.6E-01	1.0E+00	9.6E-02	5.9E-03	2.2E-02	0
NOTCH1	-2.6	4.8E-01	9.2E-01	1.0E+00	8.7E-03	1.8E-04	1.5E-03	0	-1.2	9.4E-01	9.9E-01	1.0E+00	1.9E-01	1.4E-02	3.5E-02	0
CRABP2	-1.6	4.8E-01	9.2E-01	1.0E+00	7.0E-02	5.7E-03	2.3E-02	0	-2.2	9.5E-01	1.0E+00	1.0E+00	2.1E-02	4.0E-04	2.8E-03	0
TOP3B	-1.6	4.7E-01	9.2E-01	1.0E+00	1.7E-01	1.1E-02	3.3E-02	0	-2.7	8.3E-03	1.3E-01	1.0E+00	2.9E-02	4.6E-04	2.9E-03	1
PMS1	-1.6	4.6E-01	9.2E-01	1.0E+00	1.9E-01	1.4E-02	3.9E-02	0	-0.8	1.8E-01	6.4E-01	1.0E+00	2.0E-01	1.4E-02	3.5E-02	0
ZNF501	-1.5	4.6E-01	9.2E-01	1.0E+00	2.0E-01	1.5E-02	3.9E-02	0	-0.5	1.5E-01	6.1E-01	1.0E+00	2.1E-01	1.4E-02	3.5E-02	0
RAC2	-1.1	4.7E-01	9.2E-01	1.0E+00	4.8E-01	1.5E-01	2.6E-01	0	-2.4	9.5E-01	1.0E+00	1.0E+00	3.4E-02	5.9E-04	3.6E-03	0
RIPK1	-0.4	4.8E-01	9.2E-01	1.0E+00	7.9E-01	3.4E-01	4.3E-01	0	-1.0	2.0E-02	2.1E-01	1.0E+00	3.1E-01	4.9E-02	1.0E-01	1
HNF1A	-2.5	4.9E-01	9.2E-01	1.0E+00	1.8E-02	3.9E-04	2.6E-03	0	-1.9	5.0E-01	8.7E-01	1.0E+00	8.0E-02	3.9E-03	1.6E-02	0
VWC2L	-1.1	5.0E-01	9.2E-01	1.0E+00	2.0E-01	1.5E-02	3.9E-02	0	-2.3	8.3E-01	9.6E-01	1.0E+00	4.3E-02	1.0E-03	5.6E-03	0

ARPC5L	-1.8	5.0E-01	9.2E-01	1.0E+00	2.4E-01	2.4E-02	5.7E-02	0	-1.5	5.7E-01	9.0E-01	1.0E+00	5.5E-02	1.5E-03	7.6E-03	0
NQO1	-1.2	5.1E-01	9.2E-01	1.0E+00	3.3E-01	8.3E-02	1.7E-01	0	1.0	1.3E-02	1.5E-01	1.0E+00	8.0E-01	4.0E-01	4.4E-01	0
CARM1	-1.1	5.1E-01	9.2E-01	1.0E+00	3.6E-01	1.3E-01	2.4E-01	0	-1.4	9.0E-01	9.8E-01	1.0E+00	7.0E-02	2.7E-03	1.2E-02	0
NKX3-1	0.0	5.0E-01	9.2E-01	1.0E+00	5.8E-01	2.0E-01	3.0E-01	0	-0.2	1.6E-01	6.2E-01	1.0E+00	3.5E-01	7.3E-02	1.3E-01	1
FZD1	-1.8	5.3E-01	9.2E-01	1.0E+00	5.7E-02	5.7E-03	2.3E-02	0	-0.7	4.1E-02	3.0E-01	1.0E+00	6.3E-01	2.4E-01	3.0E-01	1
NF1	-2.0	5.1E-01	9.2E-01	1.0E+00	6.7E-02	5.7E-03	2.3E-02	0	0.0	2.5E-01	7.3E-01	1.0E+00	7.7E-01	4.0E-01	4.4E-01	0
RASA1	-1.2	5.1E-01	9.2E-01	1.0E+00	2.8E-01	7.0E-02	1.6E-01	0	-0.6	3.4E-02	2.8E-01	1.0E+00	5.5E-01	1.5E-01	2.1E-01	2
LGALS9	-1.0	5.2E-01	9.2E-01	1.0E+00	5.4E-01	1.9E-01	2.9E-01	0	-0.2	1.3E-01	5.9E-01	1.0E+00	4.9E-01	1.1E-01	1.6E-01	0
TRRAP	-2.3	5.5E-01	9.3E-01	1.0E+00	4.2E-02	1.7E-03	8.0E-03	0	-1.4	9.4E-01	9.9E-01	1.0E+00	1.6E-01	1.1E-02	3.2E-02	0
ICAM4	-1.7	5.6E-01	9.3E-01	1.0E+00	9.5E-02	7.1E-03	2.5E-02	0	0.2	1.8E-02	2.0E-01	1.0E+00	5.7E-01	1.5E-01	2.1E-01	2
RNF138	-1.3	5.7E-01	9.3E-01	1.0E+00	2.6E-01	2.4E-02	5.7E-02	0	-1.9	9.9E-01	1.0E+00	1.0E+00	6.3E-03	2.5E-05	3.3E-04	0
CAMK2D	-2.4	5.8E-01	9.3E-01	1.0E+00	4.7E-02	1.8E-03	8.0E-03	0	-1.1	4.0E-01	8.5E-01	1.0E+00	2.8E-01	4.1E-02	8.5E-02	0
CDKN1B	-1.8	5.8E-01	9.3E-01	1.0E+00	5.2E-02	2.1E-03	9.6E-03	0	-2.6	9.8E-01	1.0E+00	1.0E+00	6.0E-03	2.5E-05	3.3E-04	0
HS2ST1	-1.2	5.8E-01	9.3E-01	1.0E+00	2.7E-01	6.9E-02	1.6E-01	0	-0.9	8.8E-01	9.7E-01	1.0E+00	4.7E-01	1.1E-01	1.6E-01	0
PTPRD	-0.8	5.8E-01	9.3E-01	1.0E+00	5.0E-01	1.7E-01	2.8E-01	0	-0.5	1.2E-01	5.6E-01	1.0E+00	6.3E-01	2.4E-01	3.0E-01	1
EGFR	-1.2	6.0E-01	9.3E-01	1.0E+00	3.1E-01	7.8E-02	1.7E-01	0	-0.4	5.5E-02	3.9E-01	1.0E+00	2.5E-01	2.6E-02	6.0E-02	1
MRPL14	-3.8	6.1E-01	9.3E-01	1.0E+00	6.1E-04	5.0E-06	7.1E-05	0	-2.7	9.8E-01	1.0E+00	1.0E+00	7.1E-03	4.5E-05	5.6E-04	0
FAM90A1	-2.3	6.2E-01	9.3E-01	1.0E+00	4.2E-02	1.7E-03	8.0E-03	0	-2.4	6.3E-01	9.2E-01	1.0E+00	1.4E-02	3.3E-04	2.7E-03	0
TMEM50A	-2.3	6.1E-01	9.3E-01	1.0E+00	6.8E-02	5.7E-03	2.3E-02	0	-0.4	2.1E-01	6.9E-01	1.0E+00	5.4E-01	1.5E-01	2.1E-01	0
ZNF485	-0.2	6.1E-01	9.3E-01	1.0E+00	1.0E+00	9.0E-01	9.1E-01	0	-0.2	4.1E-01	8.5E-01	1.0E+00	8.7E-01	5.9E-01	6.3E-01	0
PDGFRA	-1.2	6.2E-01	9.4E-01	1.0E+00	2.9E-01	7.4E-02	1.6E-01	0	-1.0	4.9E-01	8.7E-01	1.0E+00	3.7E-01	7.6E-02	1.3E-01	0
LCE1D	-0.1	6.2E-01	9.4E-01	1.0E+00	8.5E-01	4.6E-01	5.5E-01	0	0.0	8.6E-02	4.9E-01	1.0E+00	5.9E-01	2.0E-01	2.7E-01	0
CYP27A1	-0.6	6.2E-01	9.4E-01	1.0E+00	6.2E-01	2.2E-01	3.2E-01	0	-1.9	4.1E-01	8.5E-01	1.0E+00	1.3E-01	8.7E-03	2.7E-02	0
YWHAZ	-1.2	6.3E-01	9.4E-01	1.0E+00	2.8E-01	7.2E-02	1.6E-01	0	-2.2	9.5E-01	1.0E+00	1.0E+00	4.7E-02	1.1E-03	5.6E-03	0
KMT2B	-2.6	6.4E-01	9.4E-01	1.0E+00	3.2E-02	1.5E-03	7.8E-03	0	-3.8	8.5E-01	9.6E-01	1.0E+00	1.1E-02	1.3E-04	1.3E-03	0
DNMT3A	-2.2	6.5E-01	9.4E-01	1.0E+00	1.1E-02	2.3E-04	1.8E-03	0	-2.0	9.9E-01	1.0E+00	1.0E+00	8.6E-03	1.1E-04	1.3E-03	0
PIK3CG	-2.3	6.6E-01	9.4E-01	1.0E+00	7.6E-02	5.9E-03	2.3E-02	0	-1.1	8.8E-01	9.7E-01	1.0E+00	2.2E-01	1.9E-02	4.7E-02	0
FGFR4	-0.4	6.5E-01	9.4E-01	1.0E+00	9.7E-01	7.3E-01	7.7E-01	0	-0.1	1.9E-01	6.6E-01	1.0E+00	9.5E-01	6.8E-01	7.1E-01	0
FANCA	-2.3	6.6E-01	9.4E-01	1.0E+00	2.7E-02	6.2E-04	3.6E-03	0	-0.9	4.5E-01	8.6E-01	1.0E+00	2.4E-01	2.6E-02	6.0E-02	0
ZMYM2	-1.0	6.7E-01	9.5E-01	1.0E+00	2.9E-01	7.2E-02	1.6E-01	0	-0.6	1.5E-01	6.1E-01	1.0E+00	6.1E-02	2.7E-03	1.2E-02	1
EPHA7	-0.7	6.6E-01	9.5E-01	1.0E+00	5.8E-01	1.9E-01	2.9E-01	0	-1.2	3.1E-01	7.7E-01	1.0E+00	8.9E-02	4.5E-03	1.7E-02	0
FOXO1	-0.4	6.7E-01	9.5E-01	1.0E+00	4.1E-01	1.4E-01	2.4E-01	0	0.7	2.3E-02	2.2E-01	1.0E+00	4.2E-01	7.6E-02	1.3E-01	0
IGFBP1	-1.9	6.7E-01	9.5E-01	1.0E+00	1.2E-01	9.4E-03	3.0E-02	0	-1.4	3.5E-01	8.0E-01	1.0E+00	2.1E-01	1.4E-02	3.5E-02	0
ARID1B	-1.5	6.7E-01	9.5E-01	1.0E+00	2.0E-01	1.5E-02	3.9E-02	0	-0.2	1.7E-01	6.2E-01	1.0E+00	3.0E-01	4.2E-02	8.7E-02	0
RPL22L1	-1.9	6.8E-01	9.6E-01	1.0E+00	1.0E-01	8.1E-03	2.7E-02	0	0.4	5.6E-02	4.0E-01	1.0E+00	6.3E-01	2.4E-01	3.0E-01	1
PARP1	-2.4	6.8E-01	9.6E-01	1.0E+00	3.6E-02	1.5E-03	7.8E-03	0	-3.3	1.0E+00	1.0E+00	1.0E+00	1.0E-03	5.0E-06	1.0E-04	0
C2CD4A	-0.6	6.9E-01	9.6E-01	1.0E+00	9.0E-01	5.6E-01	6.3E-01	0	-1.2	7.0E-01	9.3E-01	1.0E+00	8.3E-02	4.3E-03	1.7E-02	0
AQP9	-1.1	6.9E-01	9.6E-01	1.0E+00	4.5E-01	1.4E-01	2.4E-01	0	-2.6	1.5E-01	6.1E-01	1.0E+00	2.2E-02	4.0E-04	2.8E-03	1
FOXH1	-1.9	7.1E-01	9.6E-01	1.0E+00	1.1E-01	8.1E-03	2.7E-02	0	0.7	4.5E-02	3.3E-01	1.0E+00	3.1E-01	5.5E-02	1.1E-01	1
OPN4	-0.5	7.1E-01	9.6E-01	1.0E+00	3.3E-01	8.3E-02	1.7E-01	0	-0.1	4.6E-01	8.6E-01	1.0E+00	8.1E-01	4.2E-01	4.6E-01	0
ETV1	-1.4	7.1E-01	9.6E-01	1.0E+00	3.4E-01	1.3E-01	2.4E-01	0	-0.7	8.0E-01	9.6E-01	1.0E+00	3.8E-01	7.6E-02	1.3E-01	0
CACNA1H	-0.3	7.1E-01	9.6E-01	1.0E+00	4.3E-01	1.4E-01	2.4E-01	0	-0.3	5.1E-01	8.7E-01	1.0E+00	2.1E-01	1.4E-02	3.5E-02	0
WDR27	-0.8	7.1E-01	9.6E-01	1.0E+00	5.5E-01	1.9E-01	2.9E-01	0	-0.3	3.7E-01	8.2E-01	1.0E+00	4.5E-01	9.8E-02	1.6E-01	0
RICTOR	-0.9	7.1E-01	9.6E-01	1.0E+00	2.8E-01	7.2E-02	1.6E-01	0	-1.7	6.2E-01	9.2E-01	1.0E+00	7.9E-02	3.9E-03	1.6E-02	0
NELL1	-0.8	7.1E-01	9.6E-01	1.0E+00	5.6E-01	1.9E-01	2.9E-01	0	-0.5	5.2E-01	8.8E-01	1.0E+00	7.5E-01	4.0E-01	4.4E-01	0
FBXW7	-4.7	7.2E-01	9.7E-01	1.0E+00	8.6E-05	5.0E-06	7.1E-05	0	-4.9	1.0E+00	1.0E+00	1.0E+00	1.1E-04	5.0E-06	1.0E-04	0
NBN	-1.2	7.2E-01	9.7E-01	1.0E+00	1.8E-01	1.4E-02	3.9E-02	0	-2.0	2.0E-01	6.7E-01	1.0E+00	5.1E-02	1.1E-03	5.7E-03	0
TP73	-0.4	7.2E-01	9.7E-01	1.0E+00	5.0E-01	1.5E-01	2.6E-01	0	-0.9	1.1E-01	5.5E-01	1.0E+00	5.6E-01	1.5E-01	2.1E-01	1
TCF7	-0.8	7.4E-01	9.7E-01	1.0E+00	1.2E-01	9.4E-03	3.0E-02	0	-1.7	8.3E-01	9.6E-01	1.0E+00	3.7E-02	8.3E-04	4.9E-03	0
LDHD	-1.5	7.4E-01	9.7E-01	1.0E+00	2.7E-01	6.9E-02	1.6E-01	0	-0.3	3.2E-01	7.7E-01	1.0E+00	8.0E-01	4.0E-01	4.4E-01	0
DOK3	-1.1	7.3E-01	9.7E-01	1.0E+00	4.9E-01	1.5E-01	2.6E-01	0	-1.6	3.5E-01	8.0E-01	1.0E+00	1.3E-01	8.7E-03	2.7E-02	0
DLEU7	-1.1	7.3E-01	9.7E-01	1.0E+00	5.2E-01	1.8E-01	2.9E-01	0	0.0	8.9E-01	9.7E-01	1.0E+00	3.7E-01	7.6E-02	1.3E-01	0
NEGR1	-0.5	7.4E-01	9.7E-01	1.0E+00	6.1E-01	2.2E-01	3.2E-01	0	-0.1	3.0E-01	7.6E-01	1.0E+00	7.9E-01	4.0E-01	4.4E-01	0
CBFB	-0.7	7.3E-01	9.7E-01	1.0E+00	9.5E-01	6.5E-01	6.9E-01	0	-2.2	8.6E-01	9.6E-01	1.0E+00	4.3E-02	1.0E-03	5.6E-03	0
XIAP	-1.8	7.5E-01	9.7E-01	1.0E+00	9.9E-02	7.5E-03	2.6E-02	0	-0.2	4.6E-01	8.6E-01	1.0E+00	4.7E-01	1.1E-01	1.6E-01	0
TERT	-0.7	7.4E-01	9.7E-01	1.0E+00	8.4E-01	4.6E-01	5.5E-01	0	-1.9	9.9E-01	1.0E+00	1.0E+00	7.9E-03	8.4E-05	1.0E-03	0
ZNF527	-0.5	7.4E-01	9.7E-01	1.0E+00	9.5E-01	6.5E-01	6.9E-01	0	-0.7	2.9E-01	7.6E-01	1.0E+00	3.6E-01	7.3E-02	1.3E-01	0
MET	-0.5	7.5E-01	9.7E-01	1.0E+00	9.8E-01	7.6E-01	7.9E-01	0	0.2	2.8E-02	2.6E-01	1.0E+00	5.5E-01	1.5E-01	2.1E-01	0
DUSP4	-0.8	7.6E-01	9.7E-01	1.0E+00	3.6E-01	1.3E-01	2.4E-01	0	-0.1	6.9E-01	9.3E-01	1.0E+00	7.3E-01	3.6E-01	4.2E-01	0
DAPL1	-1.5	7.6E-01	9.7E-01	1.0E+00	1.5E-01	1.1E-02	3.3E-02	0	-0.5	3.4E-01	8.0E-01	1.0E+00	9.3E-02	5.4E-03	2.0E-02	0
HYOU1	-2.0	7.6E-01	9.7E-01	1.0E+00	7.9E-02	6.2E-03	2.4E-02	0	-2.7	9.9E-01	1.0E+00	1.0E+00	9.0E-03	1.2E-04	1.3E-03	0
POGK	-0.6	7.6E-01	9.7E-01	1.0E+00	3.7E-01	1.3E-01	2.4E-01	0	-0.3	6.3E-01	9.2E-01	1.0E+00	7.8E-01	4.0E-01	4.4E-01	0
CXCL16	-0.6	7.7E-01	9.8E-01	1.0E+00	2.2E-02	4.7E-04	3.0E-03	0	-0.7	5.4E-01	8.8E-01	1.0E+00	4.8E-01	1.1E-01	1.6E-01	0
CBX3	-1.9	7.7E-01	9.8E-01	1.0E+00	5.9E-02	5.7E-03	2.3E-02	0	-0.8	4.9E-01	8.7E-01	1.0E+00	6.4E-02	2.7E-03	1.2E-02	0
ESR1	-2.0	7.8E-01	9.8E-01	1.0E+00	9.6E-02	7.1E-03	2.5E-02	0	-0.5	9.0E-02	4.9E-01	1.0E+00	6.2E-01	2.3E-01	3.0E-01	1
PPP1R12C	-1.5	7.8E-01	9.8E-01	1.0E+00	2.3E-01	2.4E-02	5.7E-02	0	-0.9	4.3E-01	8.6E-01	1.0E+00	2.0E-01	1.4E-02	3.5E-02	0
CASP14	-0.6	7.7E-01	9.8E-01	1.0E+00	3.6E-01	1.3E-01	2.4E-01	0	-0.3	5.7E-01	9.0E-01	1.0E+00	7.8E-01	4.0E-01	4.4E-01	0
SLC46A2	-0.8	7.8E-01	9.8E-01	1.0E+00	6.5E-01	2.5E-01	3.4E-01	0	-1.6	2.9E-01	7.5E-01	1.0E+00	1.8E-01	1.4E-02	3.5E-02	0
MAP3K11	-0.4	7.8E-01	9.8E-01	1.0E+00	2.5E-01	2.4E-02	5.7E-02	0	-0.7	2.2E-01	7.0E-01	1.0E+00	6.3E-01	2.4E-01	3.0E-01	1
CYB561D2	-0.6	7.8E-01	9.8E-01	1.0E+00	7.3E-01	3.1E-01	4.0E-01	0	-0.3	2.2E-01	7.0E-01	1.0E+00	6.5E-01	2.7E-01	3.4E-01	0
SSR4	-0.9	7.8E-01	9.8E-01	1.0E+00	5.5E-01	1.9E-01	2.9E-01	0	-0.4	8.5E-01	9.6E-01	1.0E+00	6.0E-01	2.1E-01	2.7E-01	0
ARAF	-1.3	7.9E-01	9.8E-01	1.0E+00	2.2E-01	1.9E-02	4.8E-02	0	-0.2	1.9E-01	6.5E-01	1.0E+00	5.8E-01	2.0E-01	2.7E-01	0
WDR45	-0.9	8.0E-01	9.8E-01	1.0E+00	5.8E-01	2.0E-01	3.0E-01	0	-0.8	5.5E-01	8.8E-01	1.0E+00	5.2E-01	1.1E-01	1.6E-01	0
TJP1	-0.9	8.0E-01	9.9E-01	1.0E+00	2.3E-01	2.4E-02	5.7E-02	0	-0.9	4.4E-01	8.6E-01	1.0E+00	3.8E-01	7.6E-02	1.3E-01	0
ETV3	-1.5	8.1E-01	9.9E-01	1.0E+00	2.8E-01	7.0E-02	1.6E-01	0	-0.3	1.3E-01	5.9E-01	1.0E+00	5.0E-01	1.1E-01	1.6E-01	1
DLX3	-0.5	8.1E-01	9.9E-01	1.0E+00	6.5E-01	2.6E-01	3.5E-01	0	-0.5	1.9E-01	6.5E-01	1.0E+00	5.5E-01	1.5E-01	2.1E-01	1
STAT5B	-1.5	8.1E-01	9.9E-01	1.0E+00	5.3E-01	1.9E-01	2.9E-01	0	-1.6	1.1E-01	5.5E-01	1.0E+00	1.8E-01	1.4E-02	3.5E-02	1
PPARD	-1.1	8.2E-01	9.9E-01	1.0E+00	9.0E-02	6.8E-03	2.4E-02	0	-0.6	5.7E-02	4.0E-01	1.0E+00	1.1E-01	7.1E-03	2.5E-02	1
MAP2K7	-1.5	8.3E-01	9.9E-01	1.0E+00	9.2E-02	6.8E-03	2.4E-02	0	0.0	4.6E-02	3.3E-01	1.0E+00	7.0E-01	3.4E-01	4.1E-01	1
NME6	-0.8	8.3E-01	9.9E-01	1.0E+00	5.5E-01	1.9E-01	2.9E-01	0	0.3	6.6E-02	4.5E-01	1.0E+00	7.2E-01	3.6E-01	4.2E-01	1
FOXF2	-0.9	8.3E-01	9.9E-01	1.0E+00	6.1E-01	2.2E-01	3.2E-01	0	-0.3	4.7E-01	8.6E-01	1.0E+00	6.3E-01	2.4E-01	3.0E-01	0
HAGH	-0.9	8.3E-01	9.9E-01	1.0E+00	7.0E-01	3.0E-01	4.0E-01	0	-1.8	9.1E-02	4.9E-01	1.0E+00	7.0E-02	2.7E-03	1.2E-02	1
CDKN2D	-1.0	8.3E-01	9.9E-01	1.0E+00	8.5E-01	4.6E-01	5.5E-01	0	0.0	3.7E-01	8.2E-01	1.0E+00	8.9E-01	6.2E-01	6.6E-01	0
NOTCH4	-1.4	8.3E-01	9.9E-01	1.0E+00	2.5E-01	2.4E-02	5.7E-02	0	0.4	6.1E-02	4.0E-01	1.0E+00	8.1E-01	4.4E-01	4.8E-01	0
SHC2	-1.9	8.4E-01	9.9E-01	1.0E+00	1.2E-01	9.4E-03	3.0E-02	0	-1.0	8.3E-01	9.6E-01	1.0E+00	4.7E-01	1.1E-01	1.6E-01	0
CCND2	-1.2	8.4E-01	9.9E-01	1.0E+00	2.3E-01	2.4E-02	5.7E-02	0	-0.7	4.9E-01	8.7E-01	1.0E+00	2.5E-02	4.5E-04	2.9E-03	0
ASXL1	-2.4	8.4E-01	9.9E-01	1.0E+00	2.5E-02	4.8E-04	3.0E-03	0	0.2	2.6E-01	7.3E-01	1.0E+00	4.0E-01	7.6E-02	1.3E-01	0
RBL1	-2.6	8.4E-01	9.9E-01	1.0E+00	3.0E-02	6.3E-04	3.6E-03	0	-3.2	8.0E-01	9.6E-01	1.0E+00	6.6E-03	4.5E-05	5.6E-04	0
CELF5	-1.3	8.4E-01	9.9E-01	1.0E+00	3.0E-01	7.6E-02	1.6E-01	0	-0.6	6.5E-01	9.3E-01	1.0E+00	4.0E-01	7.6E-02	1.3E-01	0
HMOX1	-1.8	8.4E-01	9.9E-01	1.0E+00	1.4E-01	1.1E-02	3.3E-02	0	1.2	9.4E-03	1.4E-01	1.0E+00	5.4E-01	1.4E-01	2.0E-01	1
CASP3	-1.9	8.5E-01	9.9E-01	1.0E+00	1.4E-01	1.1E-02	3.3E-02	0	-0.5	8.7E-01	9.6E-01	1.0E+00	5.0E-01	1.1E-01	1.6E-01	0
CHRM4	-0.4	8.5E-01	9.9E-01	1.0E+00	4.9E-01	1.5E-01	2.6E-01	0	-1.0	5.1E-01	8.7E-01	1.0E+00	1.1E-01	7.1E-03	2.5E-02	0
ARID5B	-0.8	8.5E-01	9.9E-01	1.0E+00	8.3E-01	4.5E-01	5.4E-01	0	1.2	8.4E-03	1.3E-01	1.0E+00	5.7E-01	1.5E-01	2.1E-01	1
GRIN2A	-1.7	8.5E-01	9.9E-01	1.0E+00	1.8E-01	1.4E-02	3.9E-02	0	0.0	1.9E-01	6.6E-01	1.0E+00	7.1E-01	3.6E-01	4.2E-01	0
KDR	-1.2	8.5E-01	9.9E-01	1.0E+00	2.1E-01	1.6E-02	4.2E-02	0	-1.5	3.4E-01	7.9E-01	1.0E+00	1.4E-01	8.7E-03	2.7E-02	0
PSMA4	-3.0	8.5E-01	9.9E-01	1.0E+00	5.8E-03	1.6E-04	1.5E-03	0	-2.5	3.3E-01	7.7E-01	1.0E+00	1.8E-03	1.5E-05	2.5E-04	0
IGF1R	-0.3	8.6E-01	9.9E-01	1.0E+00	8.4E-01	4.5E-01	5.4E-01	0	0.2	3.9E-02	2.9E-01	1.0E+00	9.4E-01	6.6E-01	7.0E-01	2
MGAT5	-1.9	8.7E-01	1.0E+00	1.0E+00	8.1E-02	6.4E-03	2.4E-02	0	-0.2	1.6E-01	6.2E-01	1.0E+00	6.8E-01	3.3E-01	4.1E-01	1
KMT2C	-1.5	8.7E-01	1.0E+00	1.0E+00	9.4E-02	7.1E-03	2.5E-02	0	-2.6	1.0E+00	1.0E+00	1.0E+00	1.0E-04	5.0E-06	1.0E-04	0
CASP6	-1.0	8.7E-01	1.0E+00	1.0E+00	4.5E-01	1.4E-01	2.4E-01	0	-0.5	4.5E-02	3.3E-01	1.0E+00	9.6E-01	6.8E-01	7.1E-01	1
SHQ1	-3.8	8.8E-01	1.0E+00	1.0E+00	5.3E-04	5.0E-06	7.1E-05	0	-2.6	1.0E+00	1.0E+00	1.0E+00	6.8E-04	5.0E-06	1.0E-04	0
SENP2	-3.5	8.8E-01	1.0E+00	1.0E+00	7.7E-03	1.8E-04	1.5E-03	0	-1.9	8.5E-01	9.6E-01	1.0E+00	7.3E-02	3.9E-03	1.6E-02	0
KNSTRN	-2.2	8.9E-01	1.0E+00	1.0E+00	1.3E-02	2.6E-04	1.9E-03	0	-0.7	5.9E-03	1.1E-01	1.0E+00	4.3E-01	8.4E-02	1.4E-01	1
PSMD6	-0.4	8.7E-01	1.0E+00	1.0E+00	2.5E-01	2.4E-02	5.7E-02	0	0.2	2.0E-01	6.7E-01	1.0E+00	5.4E-01	1.4E-01	2.0E-01	0
NFE2L2	-1.5	8.7E-01	1.0E+00	1.0E+00	3.9E-01	1.4E-01	2.4E-01	0	-2.0	4.7E-01	8.6E-01	1.0E+00	6.3E-02	2.7E-03	1.2E-02	0
PIGG	-1.1	8.8E-01	1.0E+00	1.0E+00	6.2E-01	2.2E-01	3.2E-01	0	0.3	1.4E-01	5.9E-01	1.0E+00	6.0E-01	2.0E-01	2.7E-01	0
RAB8B	-1.3	8.9E-01	1.0E+00	1.0E+00	2.0E-01	1.5E-02	3.9E-02	0	-0.7	1.4E-01	5.9E-01	1.0E+00	6.5E-01	2.7E-01	3.4E-01	0
NTRK3	-1.2	8.9E-01	1.0E+00	1.0E+00	3.3E-01	8.3E-02	1.7E-01	0	0.5	4.5E-02	3.2E-01	1.0E+00	7.4E-01	3.6E-01	4.2E-01	0

TNFRSF14	-1.0	8.9E-01	1.0E+00	1.0E+00	4.3E-01	1.4E-01	2.4E-01	0	-0.7	1.9E-01	6.5E-01	1.0E+00	8.4E-01	4.8E-01	5.2E-01	0
DAXX	-2.8	9.0E-01	1.0E+00	1.0E+00	2.9E-02	6.3E-04	3.6E-03	0	-1.2	7.5E-01	9.5E-01	1.0E+00	9.2E-02	5.4E-03	2.0E-02	0
SETD2	-4.8	9.0E-01	1.0E+00	1.0E+00	6.4E-04	5.0E-06	7.1E-05	0	-2.9	8.8E-01	9.7E-01	1.0E+00	1.2E-03	5.0E-06	1.0E-04	0
BRAF	-1.4	9.0E-01	1.0E+00	1.0E+00	3.5E-01	1.3E-01	2.4E-01	0	-1.6	9.6E-01	1.0E+00	1.0E+00	1.1E-01	7.1E-03	2.5E-02	0
CADM1	-1.9	9.0E-01	1.0E+00	1.0E+00	8.1E-02	6.4E-03	2.4E-02	0	-0.3	6.0E-01	9.1E-01	1.0E+00	4.7E-01	1.1E-01	1.6E-01	0
FLT4	-0.9	9.0E-01	1.0E+00	1.0E+00	6.5E-01	2.4E-01	3.4E-01	0	-0.2	1.4E-01	5.9E-01	1.0E+00	5.3E-01	1.4E-01	2.0E-01	1
APC	-2.1	9.0E-01	1.0E+00	1.0E+00	1.0E-01	8.1E-03	2.7E-02	0	-1.2	2.9E-01	7.6E-01	1.0E+00	2.8E-01	4.1E-02	8.5E-02	0
MAX	-2.0	9.1E-01	1.0E+00	1.0E+00	5.4E-02	5.2E-03	2.3E-02	0	-1.7	8.7E-01	9.6E-01	1.0E+00	1.1E-01	7.1E-03	2.5E-02	0
MSH2	-0.8	9.1E-01	1.0E+00	1.0E+00	1.8E-01	1.4E-02	3.9E-02	0	-0.5	8.7E-01	9.6E-01	1.0E+00	7.0E-01	3.4E-01	4.1E-01	0
SUMO1	-2.3	9.1E-01	1.0E+00	1.0E+00	4.2E-02	1.7E-03	8.0E-03	0	-1.3	7.0E-01	9.3E-01	1.0E+00	2.4E-01	2.6E-02	6.0E-02	0
SLX4	-2.5	9.1E-01	1.0E+00	1.0E+00	1.3E-03	5.0E-06	7.1E-05	0	-3.0	9.6E-01	1.0E+00	1.0E+00	1.0E-02	1.3E-04	1.3E-03	0
NDUFV3	-1.6	9.1E-01	1.0E+00	1.0E+00	9.0E-02	6.8E-03	2.4E-02	0	-0.1	2.5E-01	7.3E-01	1.0E+00	2.4E-01	2.6E-02	6.0E-02	0
NTRK1	-1.5	9.2E-01	1.0E+00	1.0E+00	2.9E-01	7.4E-02	1.6E-01	0	-0.2	1.1E-01	5.4E-01	1.0E+00	5.1E-01	1.1E-01	1.6E-01	0
CDC34	-2.6	9.2E-01	1.0E+00	1.0E+00	3.2E-03	2.5E-05	2.8E-04	0	-2.0	3.0E-01	7.6E-01	1.0E+00	8.8E-03	1.2E-04	1.3E-03	1
SEMA6C	-1.2	9.2E-01	1.0E+00	1.0E+00	3.0E-01	7.6E-02	1.6E-01	0	-0.3	5.2E-02	3.8E-01	1.0E+00	2.8E-01	4.1E-02	8.5E-02	1
METTL3	-3.3	9.2E-01	1.0E+00	1.0E+00	1.8E-02	3.8E-04	2.6E-03	0	-3.1	8.5E-01	9.6E-01	1.0E+00	1.5E-03	5.0E-06	1.0E-04	0
BLM	-3.1	9.4E-01	1.0E+00	1.0E+00	1.6E-02	3.4E-04	2.4E-03	0	-0.6	8.8E-01	9.7E-01	1.0E+00	1.9E-01	1.4E-02	3.5E-02	0
GSG1L	-2.2	9.3E-01	1.0E+00	1.0E+00	4.5E-02	1.8E-03	8.0E-03	0	-0.9	4.4E-01	8.6E-01	1.0E+00	5.7E-02	1.6E-03	7.9E-03	0
PIK3CA	-2.3	9.3E-01	1.0E+00	1.0E+00	4.7E-02	1.8E-03	8.0E-03	0	-0.9	9.3E-01	9.9E-01	1.0E+00	7.3E-02	3.9E-03	1.6E-02	0
ELANE	-2.1	9.3E-01	1.0E+00	1.0E+00	1.9E-01	1.5E-02	3.9E-02	0	-2.1	8.5E-01	9.6E-01	1.0E+00	1.2E-02	2.5E-04	2.2E-03	0
HGF	-1.2	9.3E-01	1.0E+00	1.0E+00	3.3E-01	8.3E-02	1.7E-01	0	-0.8	8.5E-02	4.9E-01	1.0E+00	6.0E-01	2.0E-01	2.7E-01	0
TFAP4	-2.5	9.5E-01	1.0E+00	1.0E+00	8.3E-03	1.8E-04	1.5E-03	0	-2.4	9.7E-01	1.0E+00	1.0E+00	2.4E-02	4.5E-04	2.9E-03	0
MED24	-1.7	9.4E-01	1.0E+00	1.0E+00	1.5E-02	3.2E-04	2.3E-03	0	-1.6	9.4E-01	9.9E-01	1.0E+00	1.0E-01	7.1E-03	2.5E-02	0
MDM4	-2.4	9.5E-01	1.0E+00	1.0E+00	2.6E-02	5.6E-04	3.4E-03	0	-2.6	4.2E-01	8.5E-01	1.0E+00	2.1E-02	4.0E-04	2.8E-03	0
ERBB3	-1.8	9.4E-01	1.0E+00	1.0E+00	3.6E-02	1.5E-03	7.8E-03	0	-1.7	5.6E-01	8.9E-01	1.0E+00	2.2E-02	4.0E-04	2.8E-03	0
MST1R	-1.9	9.5E-01	1.0E+00	1.0E+00	5.4E-02	5.2E-03	2.3E-02	0	-1.2	4.7E-01	8.6E-01	1.0E+00	2.6E-01	3.2E-02	7.2E-02	0
KCNA1	-2.0	9.5E-01	1.0E+00	1.0E+00	7.6E-02	5.9E-03	2.3E-02	0	-0.1	5.9E-02	4.0E-01	1.0E+00	4.1E-01	7.6E-02	1.3E-01	1
WNT1	-1.7	9.5E-01	1.0E+00	1.0E+00	1.0E-01	8.1E-03	2.7E-02	0	-2.2	6.7E-01	9.3E-01	1.0E+00	9.6E-03	1.2E-04	1.3E-03	0
KRT27	-1.6	9.5E-01	1.0E+00	1.0E+00	2.6E-01	2.4E-02	5.7E-02	0	-3.3	9.0E-01	9.8E-01	1.0E+00	1.0E-02	1.3E-04	1.3E-03	0
TSHR	-1.2	9.4E-01	1.0E+00	1.0E+00	2.9E-01	7.2E-02	1.6E-01	0	-0.9	4.2E-01	8.5E-01	1.0E+00	1.7E-01	1.2E-02	3.5E-02	0
WT1	-1.1	9.5E-01	1.0E+00	1.0E+00	3.6E-01	1.3E-01	2.4E-01	0	-0.8	1.1E-01	5.5E-01	1.0E+00	1.7E-01	1.4E-02	3.5E-02	1
MAP2K4	-1.1	9.5E-01	1.0E+00	1.0E+00	4.4E-01	1.4E-01	2.4E-01	0	-1.1	5.9E-01	9.1E-01	1.0E+00	3.1E-01	5.7E-02	1.2E-01	0
ENY2	-3.1	9.6E-01	1.0E+00	1.0E+00	3.7E-03	3.5E-05	3.5E-04	0	-1.5	7.9E-01	9.6E-01	1.0E+00	8.0E-02	3.9E-03	1.6E-02	0
KIT	-2.5	9.6E-01	1.0E+00	1.0E+00	4.1E-03	3.5E-05	3.5E-04	0	-0.5	1.6E-01	6.2E-01	1.0E+00	8.9E-01	6.2E-01	6.6E-01	1
TSC2	-2.5	9.5E-01	1.0E+00	1.0E+00	3.0E-02	6.3E-04	3.6E-03	0	-0.3	2.0E-01	6.6E-01	1.0E+00	4.7E-01	1.1E-01	1.6E-01	0
BAP1	-2.4	9.6E-01	1.0E+00	1.0E+00	3.8E-02	1.5E-03	7.8E-03	0	-1.0	4.3E-01	8.6E-01	1.0E+00	1.7E-01	1.4E-02	3.5E-02	0
PDCD1	-2.1	9.5E-01	1.0E+00	1.0E+00	6.1E-02	5.7E-03	2.3E-02	0	-1.6	8.8E-01	9.7E-01	1.0E+00	6.5E-02	2.7E-03	1.2E-02	0
ANKRD11	-1.3	9.6E-01	1.0E+00	1.0E+00	2.2E-01	2.4E-02	5.7E-02	0	-2.0	7.9E-01	9.6E-01	1.0E+00	5.8E-02	2.0E-03	9.9E-03	0
MTOR	-3.7	9.6E-01	1.0E+00	1.0E+00	7.8E-04	5.0E-06	7.1E-05	0	-3.5	6.7E-01	9.3E-01	1.0E+00	6.5E-04	5.0E-06	1.0E-04	0
CDH1	-2.4	9.7E-01	1.0E+00	1.0E+00	2.8E-03	2.5E-05	2.8E-04	0	-1.3	9.9E-01	1.0E+00	1.0E+00	1.5E-02	3.3E-04	2.7E-03	0
RHOQ	-3.4	9.6E-01	1.0E+00	1.0E+00	3.2E-03	2.5E-05	2.8E-04	0	-4.1	1.0E+00	1.0E+00	1.0E+00	2.4E-03	1.5E-05	2.5E-04	0
DNMT3B	-1.6	9.6E-01	1.0E+00	1.0E+00	5.9E-02	5.7E-03	2.3E-02	0	-0.6	3.9E-02	2.9E-01	1.0E+00	1.2E-01	8.1E-03	2.7E-02	1
IFNA7	-2.2	9.6E-01	1.0E+00	1.0E+00	1.1E-01	9.2E-03	3.0E-02	0	-1.4	6.3E-01	9.2E-01	1.0E+00	7.5E-02	3.9E-03	1.6E-02	0
FRAT1	-0.9	9.6E-01	1.0E+00	1.0E+00	8.6E-01	4.8E-01	5.6E-01	0	0.2	2.3E-01	7.0E-01	1.0E+00	6.5E-01	2.7E-01	3.4E-01	1
CTNNB1	-1.6	9.7E-01	1.0E+00	1.0E+00	2.5E-01	2.4E-02	5.7E-02	0	-0.5	9.0E-01	9.7E-01	1.0E+00	4.9E-01	1.1E-01	1.6E-01	0
POLD1	-3.6	9.7E-01	1.0E+00	1.0E+00	4.8E-04	5.0E-06	7.1E-05	0	-1.0	4.8E-01	8.7E-01	1.0E+00	2.9E-01	4.2E-02	8.7E-02	0
CSF2RB	-1.2	9.7E-01	1.0E+00	1.0E+00	4.1E-01	1.4E-01	2.4E-01	0	-1.4	6.3E-01	9.2E-01	1.0E+00	1.1E-01	7.1E-03	2.5E-02	0
IRS2	-2.9	9.8E-01	1.0E+00	1.0E+00	1.8E-02	3.9E-04	2.6E-03	0	-1.3	5.9E-01	9.1E-01	1.0E+00	8.1E-02	3.9E-03	1.6E-02	0
FZD3	-2.1	9.8E-01	1.0E+00	1.0E+00	4.1E-02	1.7E-03	8.0E-03	0	-0.7	5.9E-01	9.1E-01	1.0E+00	6.4E-01	2.7E-01	3.4E-01	0
PIK3C3	-2.0	9.8E-01	1.0E+00	1.0E+00	4.6E-02	1.8E-03	8.0E-03	0	-0.8	3.1E-01	7.7E-01	1.0E+00	3.9E-01	7.6E-02	1.3E-01	0
ATM	-1.4	9.8E-01	1.0E+00	1.0E+00	3.0E-01	7.8E-02	1.7E-01	0	-1.6	1.7E-01	6.4E-01	1.0E+00	5.0E-02	1.1E-03	5.7E-03	0
RAD50	-3.5	9.8E-01	1.0E+00	1.0E+00	2.4E-03	2.5E-05	2.8E-04	0	-2.0	9.9E-01	1.0E+00	1.0E+00	1.1E-02	2.1E-04	1.9E-03	0
JAK1	-1.7	9.8E-01	1.0E+00	1.0E+00	4.0E-02	1.6E-03	8.0E-03	0	-0.3	1.1E-01	5.3E-01	1.0E+00	5.2E-01	1.1E-01	1.6E-01	1
FLT3	-1.7	9.9E-01	1.0E+00	1.0E+00	1.3E-02	2.6E-04	1.9E-03	0	-1.1	1.9E-01	6.6E-01	1.0E+00	2.0E-01	1.4E-02	3.5E-02	1
WDR70	-2.5	9.9E-01	1.0E+00	1.0E+00	1.2E-02	2.4E-04	1.8E-03	0	-2.0	9.8E-01	1.0E+00	1.0E+00	6.1E-02	2.7E-03	1.2E-02	0
ARID2	-2.4	9.9E-01	1.0E+00	1.0E+00	1.3E-02	2.4E-04	1.8E-03	0	-4.9	3.1E-01	7.6E-01	1.0E+00	1.1E-04	5.0E-06	1.0E-04	0
ARID1A	-4.6	9.9E-01	1.0E+00	1.0E+00	8.8E-05	5.0E-06	7.1E-05	0	-4.0	7.7E-01	9.5E-01	1.0E+00	3.1E-03	1.5E-05	2.5E-04	0
ATR	-3.5	9.9E-01	1.0E+00	1.0E+00	2.6E-04	5.0E-06	7.1E-05	0	-3.9	3.7E-01	8.2E-01	1.0E+00	1.5E-04	5.0E-06	1.0E-04	0
SMARCA4	-3.2	9.9E-01	1.0E+00	1.0E+00	5.0E-03	1.5E-04	1.5E-03	0	-2.0	5.0E-01	8.7E-01	1.0E+00	5.2E-02	1.1E-03	5.7E-03	0
CPN2	-2.1	9.9E-01	1.0E+00	1.0E+00	5.9E-03	1.7E-04	1.5E-03	0	-2.2	9.9E-01	1.0E+00	1.0E+00	8.7E-03	1.1E-04	1.3E-03	0
KDM5A	-2.8	9.9E-01	1.0E+00	1.0E+00	7.4E-03	1.8E-04	1.5E-03	0	0.3	5.5E-02	3.9E-01	1.0E+00	1.9E-01	1.4E-02	3.5E-02	1
SMYD3	-1.7	9.9E-01	1.0E+00	1.0E+00	7.6E-03	1.8E-04	1.5E-03	0	-1.9	2.0E-01	6.6E-01	1.0E+00	6.1E-02	2.7E-03	1.2E-02	1
FTSJ3	-4.2	1.0E+00	1.0E+00	1.0E+00	5.0E-04	5.0E-06	7.1E-05	0	-4.8	9.7E-01	1.0E+00	1.0E+00	2.2E-04	5.0E-06	1.0E-04	0
LYN	-2.4	1.0E+00	1.0E+00	1.0E+00	4.1E-03	3.5E-05	3.5E-04	0	-2.3	9.6E-01	1.0E+00	1.0E+00	4.9E-02	1.1E-03	5.6E-03	0
MCM2	-3.0	9.9E-01	1.0E+00	1.0E+00	4.6E-03	3.5E-05	3.5E-04	0	-2.1	7.2E-01	9.3E-01	1.0E+00	1.1E-02	1.4E-04	1.3E-03	0
NELFB	-5.0	1.0E+00	1.0E+00	1.0E+00	3.2E-06	5.0E-06	7.1E-05	0	-3.7	9.6E-01	1.0E+00	1.0E+00	1.5E-03	5.0E-06	1.0E-04	0
KMT2D	-4.3	1.0E+00	1.0E+00	1.0E+00	4.7E-05	5.0E-06	7.1E-05	0	-2.7	1.0E+00	1.0E+00	1.0E+00	1.9E-03	1.5E-05	2.5E-04	0
SMC1A	-3.4	1.0E+00	1.0E+00	1.0E+00	2.7E-03	2.5E-05	2.8E-04	0	-3.7	9.3E-01	9.9E-01	1.0E+00	5.6E-03	2.5E-05	3.3E-04	0
SLC30A9	-2.8	1.0E+00	1.0E+00	1.0E+00	3.5E-03	2.5E-05	2.8E-04	0	-1.7	8.9E-01	9.7E-01	1.0E+00	2.9E-02	4.6E-04	2.9E-03	0
RPTOR	-5.3	1.0E+00	1.0E+00	1.0E+00	3.3E-09	5.0E-06	7.1E-05	0	-5.1	1.0E+00	1.0E+00	1.0E+00	7.9E-07	5.0E-06	1.0E-04	0
BRCA2	-4.4	1.0E+00	1.0E+00	1.0E+00	7.0E-07	5.0E-06	7.1E-05	0	-0.9	2.4E-01	7.0E-01	1.0E+00	1.7E-01	1.4E-02	3.5E-02	0
SF3B1	-4.7	1.0E+00	1.0E+00	1.0E+00	2.5E-06	5.0E-06	7.1E-05	0	-5.1	9.9E-01	1.0E+00	1.0E+00	7.1E-07	5.0E-06	1.0E-04	0
CUL3	-4.8	1.0E+00	1.0E+00	1.0E+00	1.0E-05	5.0E-06	7.1E-05	0	-3.8	8.6E-01	9.6E-01	1.0E+00	7.1E-04	5.0E-06	1.0E-04	0
PALB2	-4.6	1.0E+00	1.0E+00	1.0E+00	4.9E-05	5.0E-06	7.1E-05	0	-2.8	9.5E-01	1.0E+00	1.0E+00	1.3E-02	2.6E-04	2.3E-03	0
CSNK1A1	-2.6	1.0E+00	1.0E+00	1.0E+00	8.3E-05	5.0E-06	7.1E-05	0	0.0	2.8E-01	7.5E-01	1.0E+00	2.7E-01	4.1E-02	8.5E-02	0
CUL5	-3.2	1.0E+00	1.0E+00	1.0E+00	8.5E-05	5.0E-06	7.1E-05	0	-1.5	5.8E-01	9.0E-01	1.0E+00	1.9E-01	1.4E-02	3.5E-02	0
AURKB	-3.5	1.0E+00	1.0E+00	1.0E+00	2.0E-04	5.0E-06	7.1E-05	0	-3.5	8.1E-01	9.6E-01	1.0E+00	1.1E-04	5.0E-06	1.0E-04	0
DNMT1	-4.1	1.0E+00	1.0E+00	1.0E+00	2.2E-04	5.0E-06	7.1E-05	0	-3.3	9.4E-01	9.9E-01	1.0E+00	2.9E-04	5.0E-06	1.0E-04	0
PPP1R11	-4.0	1.0E+00	1.0E+00	1.0E+00	2.8E-04	5.0E-06	7.1E-05	0	-3.3	1.0E+00	1.0E+00	1.0E+00	3.6E-04	5.0E-06	1.0E-04	0
METTL14	-4.5	1.0E+00	1.0E+00	1.0E+00	3.6E-04	5.0E-06	7.1E-05	0	-2.7	1.0E+00	1.0E+00	1.0E+00	1.4E-03	5.0E-06	1.0E-04	0
POLE	-3.9	1.0E+00	1.0E+00	1.0E+00	4.3E-04	5.0E-06	7.1E-05	0	-3.7	9.9E-01	1.0E+00	1.0E+00	5.3E-03	2.5E-05	3.3E-04	0
PBRM1	-3.1	1.0E+00	1.0E+00	1.0E+00	4.3E-04	5.0E-06	7.1E-05	0	-1.7	4.7E-01	8.6E-01	1.0E+00	4.8E-02	1.1E-03	5.6E-03	0
ATXN7L3	-4.6	1.0E+00	1.0E+00	1.0E+00	6.1E-04	5.0E-06	7.1E-05	0	-3.2	9.9E-01	1.0E+00	1.0E+00	9.3E-03	1.2E-04	1.3E-03	0
MDC1	-3.0	1.0E+00	1.0E+00	1.0E+00	1.3E-03	5.0E-06	7.1E-05	0	-1.2	9.5E-01	9.9E-01	1.0E+00	1.6E-01	1.1E-02	3.2E-02	0
NPM1	-3.8	1.0E+00	1.0E+00	1.0E+00	1.6E-03	5.0E-06	7.1E-05	0	-3.6	9.9E-01	1.0E+00	1.0E+00	5.2E-03	2.5E-05	3.3E-04	0

Table 6: FHSC14 focused CRISPR deletion gRNA screen enriched gRNAs (Log2FC > 2, FDR < 0.05)

		CIS-ETO vs. P0						SAL vs. P0					
Gene	Guide ID	Guide Log2(FC)	Pos. Unadj. P	Pos. Adj. P	Neg. Unadj. P	Neg. Adj. P	Guide Enriched	Guide Log2(FC)	Pos. Unadj. P	Pos. Adj. P	Neg. Unadj. P	Neg. Adj. P	Guide Enriched
USP22	EGSC_2281	2.7	1.1E-189	1.8E-188	1.0E+00	1.0E+00	Y	0.3	1.3E-01	4.1E-01	8.7E-01	1.0E+00	N
USP22	EGSC_2285	2.6	3.9E-154	5.6E-153	1.0E+00	1.0E+00	Y	1.1	2.2E-10	1.3E-09	1.0E+00	1.0E+00	N
USP22	EGSC_2283	2.1	2.9E-74	3.2E-73	1.0E+00	1.0E+00	Y	3.1	0.0E+00	0.0E+00	1.0E+00	1.0E+00	Y
USP22	EGSC_2286	2.1	3.4E-65	3.6E-64	1.0E+00	1.0E+00	Y	-1.1	1.0E+00	1.0E+00	3.5E-03	2.0E-01	N
USP22	EGSC_2282	1.8	1.9E-41	1.7E-40	1.0E+00	1.0E+00	N	2.4	7.4E-108	9.5E-107	1.0E+00	1.0E+00	Y
USP22	EGSC_2284	1.7	6.4E-35	5.6E-34	1.0E+00	1.0E+00	N	-0.6	9.5E-01	1.0E+00	5.0E-02	2.8E-01	N
TADA2B	EGSC_2109	6.1	0.0E+00	0.0E+00	1.0E+00	1.0E+00	Y	-1.7	1.0E+00	1.0E+00	9.8E-04	6.9E-02	N
TADA2B	EGSC_2107	4.9	0.0E+00	0.0E+00	1.0E+00	1.0E+00	Y	2.1	1.5E-53	1.5E-52	1.0E+00	1.0E+00	Y
TADA2B	EGSC_2111	4.5	0.0E+00	0.0E+00	1.0E+00	1.0E+00	Y	-1.8	1.0E+00	1.0E+00	9.2E-04	6.5E-02	N
TADA2B	EGSC_2108	1.2	1.4E-11	8.4E-11	1.0E+00	1.0E+00	N	2.0	2.4E-47	2.3E-46	1.0E+00	1.0E+00	N
TADA2B	EGSC_2110	1.2	1.5E-10	8.7E-10	1.0E+00	1.0E+00	N	-0.5	9.3E-01	1.0E+00	7.5E-02	3.1E-01	N
TADA2B	EGSC_2112	-0.8	9.8E-01	1.0E+00	1.5E-02	2.6E-01	N	-0.6	9.5E-01	1.0E+00	4.9E-02	2.8E-01	N
TAF6L	EGSC_2123	4.5	0.0E+00	0.0E+00	1.0E+00	1.0E+00	Y	-2.3	1.0E+00	1.0E+00	3.0E-05	3.7E-03	N
TAF6L	EGSC_2122	2.3	1.1E-94	1.3E-93	1.0E+00	1.0E+00	Y	-2.5	1.0E+00	1.0E+00	8.1E-06	1.3E-03	N
TAF6L	EGSC_2124	2.3	1.2E-79	1.4E-78	1.0E+00	1.0E+00	Y	0.5	2.2E-02	8.0E-02	9.8E-01	1.0E+00	N
TAF6L	EGSC_2121	1.6	6.5E-23	4.9E-22	1.0E+00	1.0E+00	N	-0.4	9.0E-01	1.0E+00	9.8E-02	3.4E-01	N
TAF6L	EGSC_2119	1.5	3.9E-21	2.9E-20	1.0E+00	1.0E+00	N	-4.7	1.0E+00	1.0E+00	9.2E-07	2.3E-04	N
TAF6L	EGSC_2120	-0.1	6.7E-01	1.0E+00	3.3E-01	6.6E-01	N	-3.8	1.0E+00	1.0E+00	1.5E-06	3.3E-04	N
TAF5L	EGSC_2113	4.9	0.0E+00	0.0E+00	1.0E+00	1.0E+00	Y	1.9	2.5E-46	2.4E-45	1.0E+00	1.0E+00	N
TAF5L	EGSC_2115	3.3	0.0E+00	0.0E+00	1.0E+00	1.0E+00	Y	-2.1	1.0E+00	1.0E+00	5.1E-05	5.8E-03	N
TAF5L	EGSC_2116	3.2	0.0E+00	0.0E+00	1.0E+00	1.0E+00	Y	-1.5	1.0E+00	1.0E+00	1.2E-03	8.1E-02	N
TAF5L	EGSC_2117	0.7	4.4E-04	1.9E-03	1.0E+00	1.0E+00	N	-1.5	1.0E+00	1.0E+00	5.8E-04	4.4E-02	N
TAF5L	EGSC_2114	0.6	2.8E-03	1.1E-02	1.0E+00	1.0E+00	N	-1.7	1.0E+00	1.0E+00	2.1E-04	1.9E-02	N
TAF5L	EGSC_2118	0.6	8.0E-03	3.1E-02	9.9E-01	1.0E+00	N	0.0	5.0E-01	1.0E+00	5.0E-01	8.9E-01	N
TADA1	EGSC_2105	5.0	0.0E+00	0.0E+00	1.0E+00	1.0E+00	Y	-0.6	9.6E-01	1.0E+00	3.8E-02	2.7E-01	N
TADA1	EGSC_2101	4.0	0.0E+00	0.0E+00	1.0E+00	1.0E+00	Y	-0.9	9.9E-01	1.0E+00	5.6E-03	2.6E-01	N
TADA1	EGSC_2102	2.9	8.2E-275	1.5E-273	1.0E+00	1.0E+00	Y	1.6	4.3E-28	3.5E-27	1.0E+00	1.0E+00	N
TADA1	EGSC_2106	1.6	2.1E-26	1.6E-25	1.0E+00	1.0E+00	N	1.2	1.4E-10	8.3E-10	1.0E+00	1.0E+00	N
TADA1	EGSC_2103	-0.4	8.6E-01	1.0E+00	1.4E-01	4.0E-01	N	1.9	2.1E-37	1.9E-36	1.0E+00	1.0E+00	N
TADA1	EGSC_2104	-0.7	9.9E-01	1.0E+00	1.3E-02	2.6E-01	N	1.9	1.2E-47	1.1E-46	1.0E+00	1.0E+00	N
KEAP1	EGSC_1146	2.4	4.6E-93	5.6E-92	1.0E+00	1.0E+00	Y	-1.1	9.9E-01	1.0E+00	6.5E-03	2.6E-01	N
KEAP1	EGSC_1144	2.2	5.4E-82	6.3E-81	1.0E+00	1.0E+00	Y	-3.4	1.0E+00	1.0E+00	1.5E-06	3.3E-04	N
KEAP1	EGSC_1143	2.2	2.6E-65	2.8E-64	1.0E+00	1.0E+00	Y	0.3	1.2E-01	3.6E-01	8.8E-01	1.0E+00	N
KEAP1	EGSC_1141	1.4	4.0E-19	2.9E-18	1.0E+00	1.0E+00	N	0.5	1.3E-02	4.6E-02	9.9E-01	1.0E+00	N
KEAP1	EGSC_1142	0.3	1.7E-01	5.1E-01	8.3E-01	1.0E+00	N	-4.5	1.0E+00	1.0E+00	3.8E-06	6.9E-04	N
KEAP1	EGSC_1145	-1.9	1.0E+00	1.0E+00	1.1E-04	1.1E-02	N	-6.6	1.0E+00	1.0E+00	1.4E-07	4.8E-05	N
CREBBP	EGSC_0446	1.9	5.9E-33	5.1E-32	1.0E+00	1.0E+00	N	0.1	4.2E-01	1.0E+00	5.8E-01	9.8E-01	N
CREBBP	EGSC_0448	1.5	5.9E-22	4.4E-21	1.0E+00	1.0E+00	N	0.1	3.4E-01	8.7E-01	6.6E-01	1.0E+00	N
CREBBP	EGSC_0445	1.2	4.1E-12	2.5E-11	1.0E+00	1.0E+00	N	3.8	0.0E+00	0.0E+00	1.0E+00	1.0E+00	Y
CREBBP	EGSC_0449	0.0	4.6E-01	1.0E+00	5.4E-01	9.3E-01	N	-4.1	1.0E+00	1.0E+00	2.0E-06	4.2E-04	N
CREBBP	EGSC_0450	-0.2	7.0E-01	1.0E+00	3.0E-01	6.2E-01	N	3.6	0.0E+00	0.0E+00	1.0E+00	1.0E+00	Y
CREBBP	EGSC_0447	-2.1	1.0E+00	1.0E+00	1.1E-04	1.1E-02	N	5.7	0.0E+00	0.0E+00	1.0E+00	1.0E+00	Y
MBOAT4	EGSC_1297	1.9	2.2E-46	2.1E-45	1.0E+00	1.0E+00	N	3.3	0.0E+00	0.0E+00	1.0E+00	1.0E+00	Y
MBOAT4	EGSC_1298	0.6	1.7E-03	7.0E-03	1.0E+00	1.0E+00	N	1.9	7.3E-46	6.9E-45	1.0E+00	1.0E+00	N
MBOAT4	EGSC_1301	0.0	5.4E-01	1.0E+00	4.6E-01	8.4E-01	N	2.1	1.7E-33	1.5E-32	1.0E+00	1.0E+00	Y
MBOAT4	EGSC_1302	-1.2	1.0E+00	1.0E+00	1.7E-03	1.1E-01	N	1.6	5.3E-28	4.3E-27	1.0E+00	1.0E+00	N
MBOAT4	EGSC_1300	-1.4	1.0E+00	1.0E+00	1.0E-03	7.3E-02	N	2.1	5.4E-59	5.6E-58	1.0E+00	1.0E+00	Y
MBOAT4	EGSC_1299	-2.0	1.0E+00	1.0E+00	2.8E-05	3.5E-03	N	-2.4	1.0E+00	1.0E+00	7.6E-06	1.2E-03	N
OTOP3	EGSC_1581	0.3	1.5E-01	4.4E-01	8.5E-01	1.0E+00	N	2.2	2.5E-70	2.7E-69	1.0E+00	1.0E+00	Y
OTOP3	EGSC_1583	0.2	2.2E-01	6.1E-01	7.8E-01	1.0E+00	N	-0.6	9.6E-01	1.0E+00	4.4E-02	2.7E-01	N
OTOP3	EGSC_1584	0.1	3.1E-01	8.1E-01	6.9E-01	1.0E+00	N	-1.2	1.0E+00	1.0E+00	2.8E-03	1.7E-01	N
OTOP3	EGSC_1582	0.0	4.5E-01	1.0E+00	5.5E-01	9.5E-01	N	2.1	1.4E-49	1.4E-48	1.0E+00	1.0E+00	Y
OTOP3	EGSC_1580	-0.6	9.5E-01	1.0E+00	4.7E-02	2.8E-01	N	1.6	1.5E-24	1.1E-23	1.0E+00	1.0E+00	N
OTOP3	EGSC_1579	-1.7	1.0E+00	1.0E+00	3.9E-04	3.2E-02	N	2.1	2.5E-56	2.5E-55	1.0E+00	1.0E+00	Y

Table 7: sgRNA sequences used for isogenic model generation in this study

Name	sgRNA sequence (5'->3')
CRISPR Ctrl-sg1 FWD	GAGACGGTTGTAAATGAGCA
CRISPR Ctrl-sg1 REV	TGCTCATTTACAACCGTCTC
CRISPR Ctrl-sg2 FWD	GTAGCGAACGTGTCCGGCGT
CRISPR Ctrl-sg2 REV	ACGCCGGACACGTTCGCTAC
CRISPR USP22-sg1 FWD	CAGGGGGAAGGACACATACG
CRISPR USP22-sg1 REV	CGTATGTGTCCTTCCCCCTG
CRISPR USP22-sg2 FWD	TGTTAACCATCAAGGGACCT
CRISPR USP22-sg2 REV	AGGTCCCTTGATGGTTAACA

Table 8: RNA-seq Enrichr pathways analyses: MSigDB Hallmark 2020

FHSC14: sgUSP22 vs sgCtrl (Enriched = UP in sgUSP22; Depleted = DOWN in sgUSP22)

SAL				CIS-ETO			
Enriched Pathway	Enriched Adj. P	Depleted Pathway	Depleted Adj. P	Enriched Pathway	Enriched Adj. P	Depleted Pathway	Depleted Adj. P
Interferon Alpha Response	3.01E-21	Estrogen Response Early	7.39E-05	Interferon Alpha Response	5.02E-21	Pancreas Beta Cells	1.42E-02
Interferon Gamma Response	1.73E-16	UV Response Dn	6.03E-03	Hypoxia	3.93E-18	UV Response Dn	1.42E-02
IL-2/STAT5 Signaling	3.35E-05	TNF-alpha Signaling via NF-kB	6.03E-03	Interferon Gamma Response	3.65E-16		
Hypoxia	5.12E-05	Pancreas Beta Cells	6.29E-03	Glycolysis	4.36E-11		
Myogenesis	5.12E-05	Hedgehog Signaling	9.52E-03	p53 Pathway	8.26E-08		
KRAS Signaling Up	5.12E-05	Hypoxia	1.40E-02	IL-2/STAT5 Signaling	5.55E-06		
UV Response Up	1.56E-04	Cholesterol Homeostasis	1.96E-02	TNF-alpha Signaling via NF-kB	5.55E-06		
p53 Pathway	2.55E-04	Estrogen Response Late	2.14E-02	mTORC1 Signaling	1.23E-05		
mTORC1 Signaling	5.54E-04	Apical Junction	3.72E-02	KRAS Signaling Up	1.23E-05		
Allograft Rejection	1.17E-03			Epithelial Mesenchymal Transition	8.17E-05		
Estrogen Response Late	2.21E-03			Apoptosis	1.70E-04		
Glycolysis	2.21E-03			Estrogen Response Late	3.71E-04		
Apical Junction	4.44E-03			Complement	3.71E-04		
Estrogen Response Early	8.64E-03			Inflammatory Response	3.71E-04		
PI3K/AKT/mTOR Signaling	1.11E-02			Allograft Rejection	8.24E-04		
Apical Surface	1.12E-02			UV Response Up	1.53E-03		
TNF-alpha Signaling via NF-kB	1.28E-02			Apical Junction	1.66E-03		
Complement	1.28E-02			UV Response Dn	2.28E-03		
Epithelial Mesenchymal Transition	1.28E-02			Mitotic Spindle	2.83E-03		
Apoptosis	1.44E-02			Estrogen Response Early	2.83E-03		
Notch Signaling	1.59E-02			Myogenesis	2.83E-03		
Inflammatory Response	2.13E-02			KRAS Signaling Dn	2.83E-03		
Pperoxisome	3.65E-02			Apical Surface	5.64E-03		
				Notch Signaling	1.08E-02		
				Androgen Response	3.79E-02		

NCI109B: sgUSP22 vs sgCtrl (Enriched = UP in sgUSP22; Depleted = DOWN in sgUSP22)

SAL				CIS-ETO			
Enriched Pathway	Enriched Adj. P	Depleted Pathway	Depleted Adj. P	Enriched Pathway	Enriched Adj. P	Depleted Pathway	Depleted Adj. P
Protein Secretion	4.42E-05	E2F Targets	5.61E-13	mTORC1 Signaling	3.07E-03	E2F Targets	4.83E-05
Glycolysis	5.03E-04	Myc Targets V1	9.14E-13	Oxidative Phosphorylation	3.07E-03	Mitotic Spindle	1.98E-03
UV Response Dn	5.03E-04	mTORC1 Signaling	6.09E-12	Myogenesis	4.57E-03	G2-M Checkpoint	7.92E-03
Myogenesis	1.12E-03	Unfolded Protein Response	1.04E-08	Glycolysis	4.57E-03	p53 Pathway	7.92E-03
		G2-M Checkpoint	1.57E-08	Protein Secretion	4.57E-03	UV Response Dn	1.11E-02
		Myc Targets V2	1.87E-07	Notch Signaling	4.57E-03		
		Mitotic Spindle	4.49E-06	TNF-alpha Signaling via NF-kB	4.57E-03		
		Hypoxia	2.00E-04	Estrogen Response Early	4.57E-03		
		Cholesterol Homeostasis	2.00E-04	Estrogen Response Late	4.57E-03		
		UV Response Dn	6.45E-04	Myc Targets V1	7.37E-03		
		Apical Junction	1.97E-03	heme Metabolism	1.17E-02		
		Glycolysis	3.25E-03	Reactive Oxygen Species Pathway	2.69E-02		
		Epithelial Mesenchymal Transition	8.77E-03	Hedgehog Signaling	2.69E-02		
		DNA Repair	8.77E-03	Adipogenesis	3.92E-02		
		Oxidative Phosphorylation	1.32E-02	Interferon Gamma Response	3.92E-02		
		IL-2/STAT5 Signaling	2.93E-02				
		p53 Pathway	3.04E-02				
		Wnt-beta Catenin Signaling	3.15E-02				
		Estrogen Response Early	4.23E-02				

JHU-LX33: USP22oe vs Empty (Enriched = UP in USP22oe; Depleted = DOWN in USP22oe)

SAL				CIS-ETO			
Enriched Pathway	Enriched Adj. P	Depleted Pathway	Depleted Adj. P	Enriched Pathway	Enriched Adj. P	Depleted Pathway	Depleted Adj. P
Myogenesis	4.00E-18	G2-M Checkpoint	2.67E-02	Myogenesis	1.38E-09	Hypoxia	2.02E-20
Hypoxia	2.09E-17			Epithelial Mesenchymal Transition	8.30E-04	Glycolysis	2.97E-08
Glycolysis	1.77E-05			Apical Junction	1.29E-03	UV Response Dn	8.21E-08
Estrogen Response Early	2.27E-04			Oxidative Phosphorylation	1.29E-03	mTORC1 Signaling	8.21E-08
Epithelial Mesenchymal Transition	2.27E-04			TNF-alpha Signaling via NF-kB	8.42E-03	Mitotic Spindle	7.45E-06
Apical Junction	6.72E-04			Estrogen Response Late	1.57E-02	Epithelial Mesenchymal Transition	1.22E-04
p53 Pathway	6.72E-04			p53 Pathway	1.57E-02	Cholesterol Homeostasis	1.94E-03
Apoptosis	5.22E-03			Estrogen Response Early	3.38E-02	Estrogen Response Early	4.34E-03
Angiogenesis	2.05E-02			DNA Repair	4.11E-02	Hedgehog Signaling	6.91E-03
mTORC1 Signaling	2.05E-02					Androgen Response	1.00E-02
						Angiogenesis	3.93E-02

Table 9: RNA-seq Enrichr pathways analyses: Gene Ontology Biological Process 2023

FHSC14: sgUSP22 vs sgCtrl (Enriched = UP in sgUSP22; Depleted = DOWN in sgUSP22)

SAL				CIS-ETO			
Enriched Pathway	Enriched Adj. P	Depleted Pathway	Depleted Adj. P	Enriched Pathway	Enriched Adj. P	Depleted Pathway	Depleted Adj. P
Antigen Processing And Presentation Of	1.15E-05	Nervous System Development	1.81E-10	Cytoplasmic Translation	4.85E-21	Nervous System Development	4.74E-06
Defense Response To Virus (GO:0051607)	8.44E-04	Axon Guidance (GO:0007411)	6.82E-08	Peptide Biosynthetic Process	2.53E-14	Synapse Organization	3.78E-05
Defense Response To Symbiont (GO:0140546)	8.44E-04	Central Nervous System Development	2.56E-06	Macromolecule Biosynthetic	3.37E-13	Synapse Assembly (GO:0007416)	7.37E-05
Interleukin-27-Mediated Signaling Pathway	1.89E-03	Regulation Of Cell Migration	2.56E-06	Translation (GO:0006412)	1.45E-09	Axon Guidance (GO:0007411)	7.52E-05
Negative Regulation Of Viral Process	3.40E-03	Cell-Cell Adhesion Via Plasma-	7.41E-06	Gene Expression (GO:0010467)	2.28E-08	Cell-Cell Adhesion Via Plasma-	1.03E-04
Positive Regulation Of Intracellular Signal	4.11E-03	Synapse Organization (GO:0050808)	1.21E-05	Negative Regulation Of Viral	2.28E-08	Cell Junction Assembly	1.91E-04
Antigen Processing And Presentation Of	4.11E-03	Axonogenesis (GO:0007409)	1.85E-05	Defense Response To Symbiont	1.63E-07	Axonogenesis (GO:0007409)	1.56E-03
Antigen Processing And Presentation Of	4.11E-03	Modulation Of Chemical Synaptic	3.05E-05	Defense Response To Virus	2.17E-07	Positive Regulation Of	2.42E-03
Antigen Processing And Presentation Of	4.11E-03	Neuron Projection Guidance	1.22E-04	Negative Regulation Of Viral	3.73E-07	DNA-templated DNA Replication	2.42E-03
Antigen Processing And Presentation Of	4.11E-03	Synapse Assembly (GO:0007416)	2.25E-04	Ribonucleoprotein Complex	5.00E-04	Chordate Embryonic Development	7.52E-03
Antigen Processing And Presentation Of Peptide	4.11E-03	Chordate Embryonic Development	2.43E-04	Interleukin-27-Mediated Signaling	5.39E-04	Neuron Projection Guidance	7.52E-03
Epithelial Cell Migration (GO:0010631)	4.51E-03	Chemical Synaptic Transmission	2.43E-04	Regulation Of Viral Genome	6.13E-04	Type B Pancreatic Cell	8.20E-03
Negative Regulation Of Mitotic Cell Cycle Phase	4.51E-03	Cell Junction Assembly (GO:0034329)	3.46E-04	Response To Cytokine	1.12E-03	Calcium-Dependent Cell-Cell	9.57E-03
Antigen Processing And Presentation Of Peptide	4.51E-03	Generation Of Neurons (GO:0048699)	8.34E-04	Antigen Processing And	1.27E-03	Positive Regulation Of Cell	9.57E-03
Regulation Of Dendritic Cell Differentiation	5.89E-03	Regulation Of Transcription By RNA	1.62E-03	Proteolysis (GO:0006508)	2.05E-03	Regulation Of Cell Migration	9.74E-03
Response To Cytokine (GO:0034097)	6.45E-03	Positive Regulation Of Axonogenesis	2.63E-03	Epithelial Cell Migration	2.06E-03	Regulation Of Nucleic Acid-	1.22E-02
Peptide Metabolic Process (GO:0006518)	7.12E-03	Regulation Of JNK Cascade	3.35E-03	Extracellular Matrix Organization	2.06E-03	Regulation Of Axonogenesis	1.96E-02
Antigen Processing And Presentation Of	8.61E-03	Negative Regulation Of DNA-templated	3.36E-03	Endothelial Cell Migration	2.06E-03	Glandular Epithelial Cell	2.43E-02
Negative Regulation Of Protein Serine/Threonine	9.12E-03	Brain Development (GO:0007420)	3.36E-03	Regulation Of T Cell Receptor	2.06E-03	Parallel Actin Filament Bundle	2.43E-02
Cellular Response To Thyroid Hormone Stimulus	9.12E-03	Negative Regulation Of Transcription By	3.61E-03	Negative Regulation Of Apoptotic	2.06E-03	Type B Pancreatic Cell	2.43E-02
Regulation Of G1/S Transition Of Mitotic Cell	1.10E-02	Regulation Of Axonogenesis	6.21E-03	Regulation Of Cell Population	2.32E-03	Central Nervous System	3.04E-02
Peptide Catabolic Process (GO:0043171)	1.10E-02	Positive Regulation Of Cell Projection	8.08E-03	Regulation Of T Cell Activation	2.50E-03	Chemical Synaptic Transmission	3.37E-02
Negative Regulation Of Viral Genome Replication	1.24E-02	Regulation Of DNA-templated	9.29E-03	Protein Catabolic Process	2.89E-03	Spinal Cord Development	4.80E-02
Response To Thyroid Hormone (GO:0097066)	1.43E-02	Transmembrane Receptor Protein	9.29E-03	Negative Regulation Of Protein	3.95E-03	Respiratory System Development	4.80E-02
Regulation Of T Cell Activation (GO:0050863)	1.61E-02	SMAD Protein Signal Transduction	9.29E-03	Antigen Processing And	4.07E-03		
Negative Regulation Of Neuron Death	2.34E-02	Calcium-Dependent Cell-Cell Adhesion	9.29E-03	Regulation Of Angiogenesis	4.07E-03		
Negative Regulation Of Cell Population	2.64E-02	Respiratory System Development	9.33E-03	Positive Regulation Of Intracellular	5.33E-03		
Protein Localization To Membrane (GO:0072657)	3.60E-02	Regulation Of Signal Transduction	1.12E-02	Positive Regulation Of Cell	5.93E-03		
Regulation Of Cell Population Proliferation	3.60E-02	Lung Development (GO:0030324)	1.16E-02	Positive Regulation Of	5.98E-03		
Central Nervous System Development	3.60E-02	Type B Pancreatic Cell Differentiation	1.27E-02	Ribosome Biogenesis	7.04E-03		
Negative Regulation Of G1/S Transition Of Mitotic	3.60E-02	Positive Regulation Of JNK Cascade	1.59E-02	Regulation Of Ubiquitin Protein	9.40E-03		
Protein Catabolic Process (GO:0030163)	3.60E-02	Kidney Morphogenesis (GO:0060993)	1.59E-02	Contact Inhibition (GO:0060242)	1.28E-02		
Regulation Of Interleukin-10 Production	3.60E-02	Retinal Ganglion Cell Axon Guidance	1.59E-02	Positive Regulation Of Cell Motility	1.31E-02		
Positive Regulation Of Protein Processing	3.60E-02	Neuron Projection Morphogenesis	1.92E-02	Positive Regulation Of T Cell	1.31E-02		
Regulation Of Immune Response (GO:0050776)	3.60E-02	Positive Regulation Of Transmembrane	1.95E-02	Negative Regulation Of Cell	1.31E-02		
Antigen Processing And Presentation Of	3.60E-02	Regulation Of Trans-Synaptic Signaling	2.10E-02	Regulation Of Epithelial Cell	1.46E-02		
Positive Regulation Of Cholesterol Metabolic	3.60E-02	Transmembrane Receptor Protein	2.12E-02	Regulation Of Viral Entry Into Host	1.50E-02		
Regulation Of Coagulation (GO:0050818)	3.60E-02	Positive Regulation Of Developmental	2.17E-02	Extracellular Structure Organization	1.50E-02		
Negative Regulation Of Cardiocyte Differentiation	3.60E-02	Positive Regulation Of Stress-Activated	2.19E-02	Response To Type I Interferon	1.52E-02		
Receptor Catabolic Process (GO:0032801)	3.84E-02	Negative Regulation Of Chemotaxis	2.67E-02	rRNA Processing (GO:0006364)	1.57E-02		
Positive Regulation Of T Cell Mediated	3.84E-02	Negative Regulation Of Cell Motility	2.67E-02	External Encapsulating Structure	1.57E-02		
Endothelial Cell Migration (GO:0043542)	3.89E-02	Anterograde Trans-Synaptic Signaling	3.02E-02	Regulation Of Myelination	1.69E-02		
		Homophilic Cell Adhesion Via Plasma	3.15E-02	Positive Regulation Of Cellular	1.99E-02		
		Negative Regulation Of Cell Migration	3.15E-02	Negative Regulation Of Gene	2.06E-02		
		Glandular Epithelial Cell Development	3.15E-02	Antigen Processing And	2.06E-02		
		Parallel Actin Filament Bundle	3.15E-02	Positive Regulation Of Antigen	2.06E-02		
		Type B Pancreatic Cell Development	3.15E-02	Positive Regulation Of Protein	2.06E-02		
		Neuron Differentiation (GO:0030182)	3.24E-02	Negative Regulation Of	2.10E-02		
		Regulation Of Neuron Projection	3.48E-02	Regulation Of Coagulation	2.28E-02		
		Negative Regulation Of Apoptotic	3.79E-02	Antigen Processing And	2.33E-02		
		Neuron Migration (GO:0001764)	4.14E-02	Response To Type II Interferon	2.40E-02		
		Negative Regulation Of Cell Population	4.37E-02	Cellular Response To Cytokine	2.41E-02		
		Semaphorin-Plexin Signaling Pathway	4.37E-02	Cellular Response To Hypoxia	2.45E-02		
		Regulation Of Microtubule-Based	4.40E-02	Peptide Catabolic Process	2.53E-02		
		Stabilization Of Membrane Potential	4.60E-02	Positive Regulation Of DNA-	2.70E-02		
		Negative Regulation Of Programmed	4.61E-02	Cellular Response To Decreased	2.70E-02		
				rRNA Metabolic Process	2.87E-02		
				Antigen Processing And	2.87E-02		
				Potassium Ion Import Across	2.87E-02		
				Regulation Of Apoptotic Process	2.87E-02		
				Positive Regulation Of Mitotic	2.87E-02		
				Regulation Of Plasminogen	2.87E-02		
				Cellular Response To Thyroid	2.97E-02		
				Positive Regulation Of	2.97E-02		
				Positive Regulation Of Mitotic	2.97E-02		
				Ribosomal Small Subunit	3.19E-02		
				Positive Regulation Of Peptidyl-	3.19E-02		
				Positive Regulation Of Proteolysis	3.27E-02		
				Integrin-Mediated Signaling	3.49E-02		
				Potassium Ion Homeostasis	3.58E-02		
				Negative Regulation Of RNA	3.58E-02		
				Regulation Of Viral Transcription	3.58E-02		
				Positive Regulation Of	3.58E-02		
				Lamellipodium Organization	3.82E-02		
				Proteolysis Involved In Protein	4.00E-02		
				Defense Response To Bacterium	4.00E-02		
				Response To Thyroid Hormone	4.06E-02		
				Mononuclear Cell Differentiation	4.35E-02		
				Regulation Of Cyclin-Dependent	4.38E-02		
				Negative Regulation Of Neuron	4.38E-02		
				Regulation Of Nervous System	4.47E-02		
				Antigen Processing And	4.47E-02		

NCI109B: sgUSP22 vs sgCtrl (Enriched = UP in sgUSP22; Depleted = DOWN in sgUSP22)

SAL				CIS-ETO			
Enriched Pathway	Enriched Adj. P	Depleted Pathway	Depleted Adj. P	Enriched Pathway	Enriched Adj. P	Depleted Pathway	Depleted Adj. P
Response To Calcium Ion (GO:0051592)	7.79E-03	Regulation Of DNA-templated	4.49E-14	Cytoplasmic Translation	3.69E-03	Regulation Of DNA-templated	1.03E-19
Nervous System Development (GO:0007399)	3.26E-02	DNA Metabolic Process (GO:0006259)	8.97E-12	Macromolecule Biosynthetic	4.29E-03	Regulation Of Transcription By	4.53E-14
Synapse Organization (GO:0050808)	4.76E-02	Regulation Of Transcription By RNA	2.35E-10	Peptide Biosynthetic Process	7.71E-03	DNA Damage Response	2.56E-08
		Negative Regulation Of DNA-templated	7.75E-10	Axon Guidance (GO:0007411)	7.71E-03	Negative Regulation Of DNA-	9.23E-08
		DNA Damage Response (GO:0006974)	3.38E-08	TORC1 Signaling (GO:0038202)	1.19E-02	DNA Metabolic Process	1.19E-06
		Positive Regulation Of DNA-templated	6.03E-08	Translation (GO:0006412)	4.76E-02	Positive Regulation Of DNA-	5.35E-06
		mRNA Processing (GO:0006397)	2.84E-07			Negative Regulation Of Nucleic	3.08E-05
		Regulation Of Translation	1.54E-06			Negative Regulation Of	3.14E-05
		RNA Splicing, Via Transesterification	1.85E-06			Positive Regulation Of Nucleic	1.24E-04
		mRNA Splicing, Via Spliceosome	4.05E-06			DNA Repair (GO:0006281)	2.41E-04
		DNA-templated DNA Replication	4.47E-06			DNA-templated DNA Replication	6.72E-04
		DNA Replication (GO:0006260)	5.75E-06			DNA-templated DNA Replication	6.72E-04
		Mitotic Sister Chromatid Segregation	5.90E-06			Protein Modification Process	6.72E-04
		Negative Regulation Of Transcription By	6.66E-06			Double-Strand Break Repair Via	7.98E-04
		DNA Unwinding Involved In DNA	1.13E-05			Mitotic Sister Chromatid	7.98E-04
		Positive Regulation Of Nucleic Acid-	2.03E-05			Regulation Of Nucleic Acid-	9.96E-04
		Metaphase Plate Congression	2.03E-05			Double-Strand Break Repair	1.49E-03
		Negative Regulation Of Nucleic Acid-	2.83E-05			Regulation Of DNA-templated	1.63E-03
		Regulation Of Canonical Wnt Signaling	2.93E-05			Regulation Of Gene Expression	1.63E-03
		DNA Repair (GO:0006281)	3.18E-05			DNA Unwinding Involved In DNA	1.69E-03
		Double-Strand Break Repair Via	3.55E-05			Protein Phosphorylation	2.36E-03
		Response To Unfolded Protein	4.93E-05			Neuron Differentiation	2.79E-03
		Double-Strand Break Repair	7.38E-05			Regulation Of Canonical Wnt	2.99E-03

Protein Ubiquitination (GO:0016567)	7.38E-05
Regulation Of Cell Cycle Process	9.01E-05
Negative Regulation Of Amide	9.48E-05
Proteasome-Mediated Ubiquitin-	1.31E-04
Mitotic Metaphase Plate Congression	1.63E-04
Response To Endoplasmic Reticulum	1.74E-04
'De Novo' Post-Translational Protein	1.77E-04
Mitochondrial Gene Expression	1.77E-04
DNA Duplex Unwinding (GO:0032508)	1.77E-04
Ubiquitin-Dependent Protein Catabolic	1.79E-04
Mitotic Spindle Organization	1.79E-04
Ribosome Biogenesis (GO:0042254)	2.28E-04
Regulation Of Gene Expression	2.28E-04
Chaperone Cofactor-Dependent Protein	2.28E-04
Translation (GO:0006412)	2.29E-04
Positive Regulation Of Transcription By	2.61E-04
Regulation Of DNA-templated DNA	3.06E-04
Regulation Of Cell Population	3.12E-04
Ribonucleoprotein Complex Biogenesis	3.41E-04
Positive Regulation Of Developmental	3.48E-04
Neuron Development (GO:0048666)	3.48E-04
protein-RNA Complex Assembly	3.48E-04
Negative Regulation Of Translation	3.55E-04
RNA Processing (GO:0006396)	3.55E-04
protein-DNA Complex Disassembly	3.92E-04
Negative Regulation Of Cell Projection	3.92E-04
Protein Polyubiquitination	3.92E-04
Regulation Of Nucleic Acid-Templated	5.37E-04
Negative Regulation Of Macromolecule	6.03E-04
Double-Strand Break Repair Via Break-	6.30E-04
Microtubule Cytoskeleton Organization	8.45E-04
Positive Regulation Of Cell Cycle G2/M	8.94E-04
Regulation Of Mitotic	9.04E-04
Neuron Differentiation (GO:0030182)	1.02E-03
Chromatin Organization (GO:0006325)	1.04E-03
Regulation Of Proteasomal Ubiquitin-	1.22E-03
Regulation Of DNA Repair	1.22E-03
Protein Modification By Small Protein	1.22E-03
Protein-Containing Complex Assembly	1.26E-03
Modification-Dependent Protein	1.35E-03
Negative Regulation Of Canonical Wnt	1.43E-03
Protein Localization To Nucleus	1.43E-03
Positive Regulation Of DNA	1.59E-03
Positive Regulation Of Transferase	1.59E-03
Chromatin Remodeling (GO:0006338)	1.59E-03
Regulation Of DNA-templated DNA	1.63E-03
Regulation Of Apoptotic Process	1.69E-03
Nervous System Development	1.70E-03
Adherens Junction Organization	2.02E-03
Regulation Of Neuron Projection	2.04E-03
Mitotic Cytokinesis (GO:0000281)	2.10E-03
Positive Regulation Of Mitotic Cell Cycle	2.35E-03
Axonogenesis (GO:0007409)	2.40E-03
Positive Regulation Of DNA-templated	2.41E-03
Regulation Of Stem Cell Population	2.41E-03
Regulation Of Cell Differentiation	2.58E-03
Cell-Cell Junction Assembly	2.67E-03
Mitochondrial Translation (GO:0032543)	2.74E-03
Proteasomal Protein Catabolic Process	2.85E-03
Nucleosome Disassembly	3.02E-03
Regulation Of Protein Phosphorylation	3.02E-03
DNA-templated DNA Replication	3.10E-03
Recombinational Repair (GO:0000725)	3.19E-03
Protein Stabilization (GO:0050821)	3.19E-03
Chaperone-Mediated Protein Complex	3.21E-03
Positive Regulation Of G2/M Transition	3.21E-03
Regulation Of Mitotic Cell Cycle	4.51E-03
Gene Expression (GO:0010467)	4.54E-03
Negative Regulation Of Cell Cycle	4.60E-03
Cellular Response To Growth Factor	4.93E-03
Ganglion Development (GO:0061548)	5.02E-03
Protein Localization To Kinetochore	5.02E-03
Positive Regulation Of Proteasomal	5.71E-03
Positive Regulation Of Cellular Process	6.44E-03
Negative Regulation Of Wnt Signaling	6.59E-03
Axon Development (GO:0061564)	6.96E-03
Histone Lysine Methylation	7.01E-03
Regulation Of Metaphase/Anaphase	7.01E-03
Regulation Of Mitotic Spindle	7.77E-03
Ribosomal Small Subunit Biogenesis	8.34E-03
Positive Regulation Of Neuron	8.34E-03
Regulation Of Cell Cycle (GO:0051726)	8.56E-03
protein-RNA Complex Disassembly	8.56E-03
Axon Extension (GO:0048675)	8.62E-03
Regulation Of Protein Ubiquitination	9.15E-03
Golgi Organization (GO:0007030)	9.56E-03
Regulation Of Transcription Elongation	9.62E-03
mRNA Metabolic Process	9.69E-03
Positive Regulation Of DNA Repair	9.69E-03
Transcription By RNA Polymerase II	1.13E-02
Intracellular Protein Transport	1.19E-02
Positive Regulation Of Apoptotic	1.28E-02
Mitotic Cell Cycle Phase Transition	1.29E-02
Positive Regulation Of Chromosome	1.41E-02
Nucleosome Organization	1.42E-02
Cell Cycle G1/S Phase Transition	1.42E-02
Positive Regulation Of Proteasomal	1.42E-02
Mitotic DNA Replication (GO:1902969)	1.61E-02
Protein Localization To Condensed	1.61E-02
Negative Regulation Of Protein	1.71E-02
DNA Recombination (GO:0006310)	1.86E-02
Intrinsic Apoptotic Signaling Pathway	1.87E-02
Post-Transcriptional Regulation Of	1.91E-02
Protein Modification Process	1.91E-02
Positive Regulation Of Cell Projection	1.96E-02
Intracellular Protein Transmembrane	1.97E-02
Protein Sumoylation (GO:0016925)	1.97E-02
Replication Fork Processing	1.97E-02
Regulation Of Translational Initiation	1.97E-02
Positive Regulation Of Telomere	2.13E-02
Negative Regulation Of Protein	2.14E-02
Positive Regulation Of Axon Extension	2.14E-02
Regulation Of Centriole Replication	2.14E-02
Positive Regulation By Host Of Viral	2.14E-02
RNA Splicing (GO:0008380)	2.19E-02
Sympathetic Ganglion Development	2.22E-02
Regulation Of mRNA Splicing, Via	2.22E-02

Regulation Of DNA Metabolic	3.38E-03
Regulation Of Centrosome	3.38E-03
Regulation Of DNA Repair	3.46E-03
Axon Development (GO:0061564)	4.17E-03
Organelle Assembly	4.98E-03
Positive Regulation Of	5.51E-03
Regulation Of DNA Replication	5.52E-03
Regulation Of RNA Splicing	7.05E-03
DNA Duplex Unwinding	8.86E-03
DNA Replication (GO:0006260)	8.86E-03
Recombinational Repair	9.38E-03
Sister Chromatid Segregation	9.38E-03
Protein Localization (GO:0008104)	9.53E-03
Plasma Membrane Bounded Cell	1.10E-02
Regulation Of DNA-templated	1.12E-02
Replication Fork Processing	1.12E-02
Protein Dephosphorylation	1.17E-02
Mitotic Cytokinesis (GO:0000281)	1.44E-02
Regulation Of Cellular Response	1.44E-02
Peptidyl-Lysine Modification	1.57E-02
Regulation Of Protein	1.79E-02
Phosphorylation (GO:0016310)	1.79E-02
Dephosphorylation (GO:0016311)	2.02E-02
Positive Regulation Of RNA	2.02E-02
DNA Repair-Dependent	2.06E-02
Generation Of Neurons	2.13E-02
Protein Localization To Membrane	2.15E-02
Nervous System Development	2.23E-02
Protein Modification By Small	2.34E-02
Protein Ubiquitination	2.34E-02
Regulation Of Neuron Projection	2.47E-02
Golgi Ribbon Formation	2.47E-02
Somatic Recombination Of	2.47E-02
Negative Regulation Of Cell	2.63E-02
G1/S Transition Of Mitotic Cell	2.90E-02
Positive Regulation Of DNA	2.91E-02
Response To Ionizing Radiation	3.03E-02
Mitotic Recombination	3.19E-02
Metaphase Plate Congression	3.19E-02
Negative Regulation Of	3.19E-02
mRNA Transcription	3.19E-02
Regulation Of Chromosome	3.19E-02
Chromatin Remodeling	3.19E-02
Cilium Organization (GO:0044782)	3.19E-02
Response To UV (GO:0009411)	3.19E-02
Cellular Response To Reactive	3.29E-02
Regulation Of Cell Population	3.33E-02
Regulation Of DNA Damage	3.35E-02
Regulation Of Chromosome	3.35E-02
Positive Regulation Of RNA	3.81E-02
Positive Regulation Of	4.06E-02
Regulation Of DNA Damage	4.06E-02
Ureteric Bud Development	4.06E-02
Regulation Of Cyclin-Dependent	4.06E-02
Negative Regulation Of Amide	4.22E-02
Positive Regulation Of Protein	4.33E-02
Negative Regulation Of	4.33E-02
Muscle Cell Migration	4.38E-02
Regulation Of Protein Acetylation	4.38E-02
Mitotic Chromosome	4.38E-02
Regulation Of Cellular Component	4.57E-02
Positive Regulation Of Cell Cycle	4.81E-02
Negative Regulation Of Cell Cycle	4.81E-02
Proteasome-Mediated Ubiquitin-	4.96E-02

		Spliceosomal Complex Assembly	2.28E-02				
		Regulation Of Mitotic Cell Cycle Phase	2.28E-02				
		Regulation Of Transforming Growth	2.28E-02				
		Positive Regulation Of Microtubule	2.30E-02				
		Regulation Of Spindle Assembly	2.30E-02				
		Negative Regulation Of Protein	2.30E-02				
		Neuron Projection Guidance	2.30E-02				
		Positive Regulation Of RNA Splicing	2.31E-02				
		RNA Modification (GO:0009451)	2.52E-02				
		Positive Regulation Of Erythrocyte	2.57E-02				
		Regulation Of Nucleotide-Excision	2.57E-02				
		Protein Localization To Chromosome	2.58E-02				
		Negative Regulation Of Gene	2.66E-02				
		Positive Regulation Of Telomerase	2.66E-02				
		Regulation Of G0 To G1 Transition	2.66E-02				
		Negative Regulation Of Cellular	2.67E-02				
		Macromolecule Biosynthetic Process	2.73E-02				
		Mitotic Spindle Assembly (GO:0090307)	2.73E-02				
		Regulation Of DNA-templated	2.73E-02				
		Regulation Of Axon Guidance	2.75E-02				
		Negative Regulation Of calcineurin-	2.83E-02				
		Negative Regulation Of Calcineurin-	2.83E-02				
		Regulation Of Cell Migration	2.92E-02				
		Endoplasmic Reticulum Calcium Ion	2.98E-02				
		Regulation Of Spindle Organization	2.98E-02				
		Regulation Of Protein Catabolic Process	2.99E-02				
		Formation Of Cytoplasmic Translation	3.03E-02				
		Histone H2A Monoubiquitination	3.03E-02				
		Positive Regulation Of Telomerase RNA	3.03E-02				
		Positive Regulation Of Cell Cycle	3.03E-02				
		Central Nervous System Neuron	3.03E-02				
		Regulation Of Mitotic Cell Cycle Spindle	3.03E-02				
		Regulation Of Telomerase RNA	3.03E-02				
		Positive Regulation Of Protein	3.03E-02				
		rRNA Processing (GO:0006364)	3.03E-02				
		Axon Guidance (GO:0007411)	3.14E-02				
		Positive Regulation Of Programmed	3.24E-02				
		Regulation Of Telomerase Activity	3.26E-02				
		Regulation Of Chromatin Organization	3.26E-02				
		Negative Regulation Of Ras Protein	3.26E-02				
		Sensory Perception Of Mechanical	3.28E-02				
		Cytoskeleton-Dependent Cytokinesis	3.46E-02				
		Regulation Of RNA Splicing	3.46E-02				
		Membrane Fission (GO:0090148)	3.56E-02				
		Positive Regulation Of Axonogenesis	3.56E-02				
		Establishment Of Protein Localization	3.56E-02				
		Protein Localization To Organelle	3.56E-02				
		RNA Export From Nucleus	3.56E-02				
		Protein Exit From Endoplasmic	3.62E-02				
		Regulation Of Endoplasmic Reticulum	3.62E-02				
		Phosphorylation (GO:0016310)	3.66E-02				
		Negative Regulation Of Cell Motility	3.67E-02				
		Positive Regulation Of Protein Metabolic	3.67E-02				
		Substantia Nigra Development	3.74E-02				
		Neuron Projection Development	3.90E-02				
		Dephosphorylation (GO:0016311)	3.96E-02				
		Golgi Inheritance (GO:0048313)	3.96E-02				
		Adherens Junction Assembly	3.96E-02				
		Intrinsic Apoptotic Signaling Pathway By	4.08E-02				
		Positive Regulation Of Telomere	4.08E-02				
		Regulation Of G2/M Transition Of	4.08E-02				
		Protein K48-linked Ubiquitination	4.09E-02				
		Protein Depolymerization (GO:0051261)	4.24E-02				
		Neuron Fate Commitment	4.31E-02				
		Regulation Of DNA Damage Checkpoint	4.31E-02				
		Neuron Projection Extension	4.36E-02				
		Positive Regulation Of Lymphocyte	4.36E-02				
		Histone Monoubiquitination	4.43E-02				
		Positive Regulation Of Ubiquitin-	4.43E-02				
		Endoplasmic Reticulum To Cytosol	4.43E-02				
		Phagosome Maturation (GO:0090382)	4.43E-02				
		Regulation Of Cellular Response To	4.43E-02				
		Sympathetic Nervous System	4.43E-02				
		Protein Autophosphorylation	4.49E-02				
		Negative Regulation Of Cellular Process	4.49E-02				
		DNA-templated Transcription	4.68E-02				
		RNA Polyadenylation (GO:0043631)	4.70E-02				
		Negative Regulation Of Response To	4.70E-02				
		Regulation Of Chondrocyte	4.70E-02				
		Sensory Perception Of Sound	4.70E-02				
		Negative Regulation Of Programmed	4.99E-02				

JHU-LX33: USP22oe vs Empty (Enriched = UP in USP22oe; Depleted = DOWN in USP22oe)

SAL				CIS-ETO			
Enriched Pathway	Enriched Adj. P	Depleted Pathway	Depleted Adj. P	Enriched Pathway	Enriched Adj. P	Depleted Pathway	Depleted Adj. P
Muscle Contraction (GO:0006936)	3.82E-08	Nervous System Development	2.89E-02	Skeletal Muscle Contraction	1.17E-05	Regulation Of Cold-Induced	1.00E-04
Striated Muscle Contraction (GO:0006941)	5.00E-07			Striated Muscle Contraction	1.17E-05	Negative Regulation Of Inclusion	1.11E-03
Myofibril Assembly (GO:0030239)	6.87E-06			Regulation Of Muscle Contraction	4.10E-04	Positive Regulation Of DNA-	1.11E-03
Muscle Cell Development (GO:0055001)	4.33E-05			Axon Guidance (GO:0007411)	1.03E-03	Positive Regulation Of	1.11E-03
Muscle Organ Development (GO:0007517)	4.33E-05			Muscle Filament Sliding	6.43E-03	Positive Regulation Of Cold-	1.11E-03
Sarcomere Organization (GO:0045214)	2.52E-04			Myofibril Assembly (GO:0030239)	1.31E-02	Regulation Of Transcription By	1.11E-03
Cellular Response To Hypoxia (GO:0071456)	2.52E-04			Actin-Myosin Filament Sliding	1.36E-02	Establishment Of Mitotic Sister	1.36E-03
Cellular Response To Decreased Oxygen Levels	2.52E-04			Axonogenesis (GO:0007409)	1.50E-02	Positive Regulation Of Metabolic	2.04E-03
Regulation Of Filopodium Assembly	2.53E-04			Sarcomere Organization	1.62E-02	Cellular Response To Metal Ion	3.66E-03
Heart Morphogenesis (GO:0003007)	2.77E-04			Actomyosin Structure Organization	2.26E-02	Cellular Response To Zinc Ion	3.71E-03
Eye Photoreceptor Cell Differentiation	2.77E-04			Muscle Contraction (GO:0006936)	3.03E-02	Response To Zinc Ion	3.75E-03
Actomyosin Structure Organization	2.77E-04			Neuron Projection Guidance	3.03E-02	Kidney Development	6.76E-03
Eye Photoreceptor Cell Development	3.97E-04					Cellular Response To Hypoxia	6.83E-03
Axon Guidance (GO:0007411)	6.61E-04					Cellular Response To Decreased	6.83E-03
Myotube Differentiation (GO:0014902)	7.28E-04					Maintenance Of Blood-Brain	6.83E-03
Cellular Response To Zinc Ion (GO:0071294)	7.29E-04					Regulation Of Inclusion Body	7.77E-03
Regulation Of Myoblast Differentiation	8.05E-04					Cellular Response To Copper Ion	1.03E-02
Regulation Of Angiogenesis (GO:0045765)	8.47E-04					Phosphate-Containing Compound	1.14E-02
Regulation Of Muscle Contraction (GO:0006937)	1.45E-03					Insulin Receptor Signaling	1.14E-02
Skeletal Muscle Contraction (GO:0003009)	1.98E-03					Negative Regulation Of Cell	1.18E-02
Negative Regulation Of Growth (GO:0045926)	1.98E-03					Cellular Heat Acclimation	1.18E-02
Positive Regulation Of Blood Vessel Endothelial	1.98E-03					Heat Acclimation (GO:0010286)	1.18E-02
Muscle Filament Sliding (GO:0030049)	2.02E-03					Regulation Of Basement	1.18E-02
Skeletal System Development (GO:0001501)	2.02E-03					Positive Regulation Of Integrin-	1.18E-02
Cellular Response To Copper Ion (GO:0071280)	2.23E-03					Regulation Of Extracellular Matrix	1.43E-02
Cellular Response To Vascular Endothelial	2.67E-03					Response To Copper Ion	1.70E-02
Response To Cadmium Ion (GO:0046686)	2.67E-03					Cellular Response To Steroid	2.01E-02
Cellular Response To Cadmium Ion	3.28E-03					Cellular Response To Heat	2.38E-02
Cellular Response To Metal Ion (GO:0071248)	3.28E-03					Negative Regulation Of	2.38E-02
Actin-Myosin Filament Sliding (GO:0033275)	3.61E-03					Positive Regulation Of Cell	2.38E-02
Regulation Of Myotube Differentiation	3.73E-03					Positive Regulation Of Muscle Cell	2.38E-02
Regulation Of Endothelial Cell Proliferation	3.82E-03					Histone Lysine Demethylation	2.98E-02

Cellular Heat Acclimation (GO:0070370)	3.82E-03			Cellular Response To Insulin	3.26E-02
Heat Acclimation (GO:0010286)	3.82E-03			Glycolytic Process (GO:0006096)	3.32E-02
Positive Regulation Of Myoblast Differentiation	3.96E-03			Brain Development (GO:0007420)	3.65E-02
Response To Copper Ion (GO:0046688)	4.00E-03			Neuron Projection Morphogenesis	3.66E-02
Regulation Of Myoblast Fusion (GO:1901739)	4.16E-03			Positive Regulation Of	4.15E-02
Response To Zinc Ion (GO:0010043)	4.66E-03			Neuron Development	4.31E-02
Cellular Response To Heat (GO:0034605)	4.79E-03			Negative Regulation Of DNA-	4.31E-02
Vascular Endothelial Growth Factor Signaling	5.06E-03			Negative Regulation Of	4.43E-02
Photoreceptor Cell Development (GO:0042461)	5.06E-03			Extracellular Matrix Organization	4.43E-02
Positive Regulation Of Endothelial Cell	5.06E-03			Regulation Of Integrin-Mediated	4.43E-02
Neuron Projection Guidance (GO:0097485)	5.32E-03			Eye Morphogenesis	4.43E-02
Extracellular Matrix Organization (GO:0030198)	5.50E-03			Mitotic Sister Chromatid Cohesion	4.43E-02
Skeletal Muscle Tissue Development	5.50E-03			Regulation Of Wnt Signaling	4.70E-02
Regulation Of Axon Guidance (GO:1902667)	5.56E-03			Negative Regulation Of Cell-Cell	4.70E-02
Positive Regulation Of Vasculature Development	6.25E-03			Negative Regulation Of Sodium	4.70E-02
Positive Regulation Of Chemotaxis	6.73E-03				
Regulation Of Blood Vessel Endothelial Cell	7.53E-03				
Regulation Of Kinase Activity (GO:0043549)	7.53E-03				
Positive Regulation Of Endothelial Cell Migration	7.53E-03				
Extracellular Structure Organization	8.03E-03				
Regulation Of Chemokine-Mediated Signaling	8.03E-03				
Regulation Of Skeletal Muscle Fiber	8.03E-03				
Positive Regulation Of Myotube Differentiation	8.03E-03				
External Encapsulating Structure Organization	8.04E-03				
Detection Of Visible Light (GO:0009584)	8.48E-03				
Positive Regulation Of Cell Differentiation	1.04E-02				
Myoblast Fusion (GO:0007520)	1.04E-02				
Endochondral Ossification (GO:0001958)	1.14E-02				
Positive Regulation Of Blood Vessel Endothelial	1.14E-02				
Positive Regulation Of Multicellular Organismal	1.21E-02				
Heart Development (GO:0007507)	1.21E-02				
Regulation Of Cell Adhesion (GO:0030155)	1.21E-02				
Semaphorin-Plexin Signaling Pathway	1.21E-02				
Positive Regulation Of Angiogenesis	1.21E-02				
Generation Of Neurons (GO:0048699)	1.21E-02				
Skeletal Muscle Organ Development	1.37E-02				
Regulation Of Blood Vessel Endothelial Cell	1.45E-02				
Positive Regulation Of Neurogenesis	1.45E-02				
Positive Regulation Of Myoblast Fusion	1.45E-02				
Neuron Migration (GO:0001764)	1.55E-02				
Positive Regulation Of Endothelial Cell	1.64E-02				
Muscle Cell Differentiation (GO:0042692)	1.64E-02				
Cellular Response To Growth Factor Stimulus	1.85E-02				
Regulation Of Inclusion Body Assembly	1.89E-02				
Negative Regulation Of Inclusion Body Assembly	1.89E-02				
Synapse Organization (GO:0050808)	2.09E-02				
Regulation Of Axon Extension Involved In Axon	2.09E-02				
Regulation Of Phosphorylation (GO:0042325)	2.19E-02				
Detection Of Light Stimulus Involved In Sensory	2.40E-02				
Detection Of Light Stimulus Involved In Visual	2.40E-02				
Cell-Matrix Adhesion (GO:0007160)	2.49E-02				
Positive Regulation Of Striated Muscle Cell	2.72E-02				
Endochondral Bone Morphogenesis	3.05E-02				
Cardiac Muscle Cell Development (GO:0055013)	3.09E-02				
Response To Unfolded Protein (GO:0006986)	3.12E-02				
Positive Regulation Of Phosphorylation	3.23E-02				
Regulation Of Extrinsic Apoptotic Signaling	3.31E-02				
Cardiac Muscle Cell Differentiation (GO:0055007)	3.31E-02				
Chaperone Cofactor-Dependent Protein	3.31E-02				
Peptide Cross-Linking (GO:0018149)	3.31E-02				
Positive Regulation Of Filopodium Assembly	3.31E-02				
Neuron Differentiation (GO:0030182)	3.40E-02				
Response To Chemokine (GO:1990868)	3.50E-02				
Skin Development (GO:0043588)	3.59E-02				
Vascular Endothelial Growth Factor Receptor	3.65E-02				
Epithelial To Mesenchymal Transition	3.73E-02				
Regulation Of Endothelial Cell Chemotaxis	4.13E-02				
Cardiac Cell Development (GO:0055006)	4.13E-02				
Myotube Cell Development (GO:0014904)	4.13E-02				
Regulation Of Cell Migration Involved In	4.51E-02				
Negative Regulation Of Nucleic Acid-Templated	4.78E-02				
Regulation Of Cell Population Proliferation	4.90E-02				
Positive Regulation Of Syncytium Formation By	4.90E-02				
Supramolecular Fiber Organization	4.96E-02				

Table 10: RNA-seq Enrichr pathways analyses: WikiPathways 2024

FHSC14: sgUSP22 vs sgCtrl (Enriched = UP in sgUSP22; Depleted = DOWN in sgUSP22)

SAL				CIS-ETO			
Enriched Pathway	Enriched Adj. P	Depleted Pathway	Depleted Adj. P	Enriched Pathway	Enriched Adj. P	Depleted Pathway	Depleted Adj. P
Ebola Virus Infection In Host WP4217	1.95E-05	Development Of Ureteric Collection	3.09E-03	Cytoplasmic Ribosomal Proteins WP477	3.94E-24	Development Of Ureteric	5.37E-04
Type II Interferon Signaling WP619	2.16E-03	Ectoderm Differentiation WP2858	2.00E-02	Type II Interferon Signaling WP619	2.15E-05	DNA Replication WP466	4.62E-03
Primary Focal Segmental Glomerulosclerosis	2.35E-03			Immune Response To Tuberculosis	1.48E-04	Retinoblastoma Gene In Cancer	5.47E-03
Small Cell Lung Cancer WP4658	6.78E-03			Primary Focal Segmental	1.96E-04	Cell Cycle WP179	6.87E-03
Non Genomic Actions Of 1 25	9.65E-03			Focal Adhesion WP306	2.35E-04	DNA IR Damage And Cellular	2.02E-02
Immune Response To Tuberculosis WP4197	1.04E-02			Network Map Of SARS CoV 2 Signaling	2.35E-04	G1 To S Cell Cycle Control	2.18E-02
P53 Transcriptional Gene Network WP4963	2.13E-02			Focal Adhesion PI3K Akt mTOR Signaling	3.40E-04	Breast Cancer Pathway WP4262	3.97E-02
TROP2 Regulatory Signaling WP5300	2.13E-02			Aerobic Glycolysis WP4629	3.40E-04		
2Q13 Copy Number Variation Syndrome	2.13E-02			PI3K Akt Signaling Pathway WP4172	4.83E-04		
Alpha 6 Beta 4 Signaling Pathway WP244	2.61E-02			VEGFA VEGFR2 Signaling WP3888	1.59E-03		
Pleural Mesothelioma WP5087	2.61E-02			Non Genomic Actions Of 1 25	2.38E-03		
Wnt Signaling WP428	2.61E-02			Alpha 6 Beta 4 Signaling Pathway WP244	2.65E-03		
Focal Adhesion WP306	2.61E-02			Nuclear Receptors Meta Pathway WP2882	2.74E-03		
Arrhythmogenic Right Ventricular	3.52E-02			Ebola Virus Infection In Host WP4217	2.98E-03		
				Small Cell Lung Cancer WP4658	3.07E-03		
				Cori Cycle WP1946	3.07E-03		
				Nephrotic Syndrome WP4758	6.84E-03		
				TYROBP Causal Network In Microglia	7.63E-03		
				Pleural Mesothelioma WP5087	9.02E-03		
				IL 24 Signaling Pathway WP5413	9.20E-03		
				P53 Transcriptional Gene Network WP4963	1.34E-02		
				miR 509 3P Alteration Of YAP1 ECM Axis	1.98E-02		
				Photodynamic Therapy Induced HIF 1	1.98E-02		
				Inflammatory Response Pathway WP453	1.98E-02		
				Glycolysis And Gluconeogenesis WP534	2.06E-02		
				Metabolic Pathways Of Fibroblasts WP5312	2.91E-02		
				Glucose Metabolism In Triple Negative	3.03E-02		
				Hippo Merlin Signaling Dysregulation	3.22E-02		
				NRF2 Pathway WP2884	3.50E-02		
				Clear Cell Renal Cell Carcinoma Pathways	4.05E-02		

NCI109B: sgUSP22 vs sgCtrl (Enriched = UP in sgUSP22; Depleted = DOWN in sgUSP22)

SAL				CIS-ETO			
Enriched Pathway	Enriched Adj. P	Depleted Pathway	Depleted Adj. P	Enriched Pathway	Enriched Adj. P	Depleted Pathway	Depleted Adj. P
1P36 Copy Number Variation Syndrome	9.71E-03	VEGFA VEGFR2 Signaling WP3888	3.62E-06	Cytoplasmic Ribosomal Proteins WP477	4.38E-04	DNA IR Double Strand Breaks	4.18E-06
		DNA Replication WP466	3.18E-04	1P36 Copy Number Variation Syndrome	2.67E-02	Androgen Receptor Signaling	3.82E-04
		DNA IR Double Strand Breaks And	3.18E-04	16P11 2 Proximal Deletion Syndrome	4.71E-02	MAPK Signaling Pathway	4.17E-04
		Retinoblastoma Gene In Cancer	3.18E-04	VEGFA VEGFR2 Signaling WP3888	4.71E-02	DNA Repair Pathways Full	5.06E-04
		mRNA Processing WP411	3.18E-04	Purine Metabolism And Related Disorders	4.71E-02	G1 To S Cell Cycle Control	6.46E-04
		Regulation Of Wnt B Catenin	3.18E-04	Neuroinflammation And Glutamatergic	4.78E-02	DNA IR Damage And Cellular	7.47E-04
		Translation Factors WP107	4.29E-04	Clear Cell Renal Cell Carcinoma Pathways	4.78E-02	Breast Cancer Pathway WP4262	1.25E-03
		Cell Cycle WP179	4.56E-04			DNA Replication WP466	1.96E-03
		DNA IR Damage And Cellular	8.95E-04			Glioblastoma Signaling Pathways	1.97E-03
		Neural Crest Differentiation WP2064	1.07E-03			Insulin Signaling WP481	5.46E-03
		Hippo Merlin Signaling	2.04E-03			Cell Cycle WP179	6.73E-03
		Wnt Beta Catenin Signaling	2.20E-03			Hippo Merlin Signaling	6.73E-03
		Androgen Receptor Signaling	2.91E-03			Brain Derived Neurotrophic	1.03E-02
		Photodynamic Therapy Induced	2.91E-03			Retinoblastoma Gene In Cancer	1.11E-02
		Pleural Mesothelioma WP5087	2.91E-03			Alzheimer 39 S Disease And	1.25E-02
		Endoderm Differentiation WP2853	2.91E-03			Alzheimer 39 S Disease WP5124	1.25E-02
		Nsp1 From SARS CoV 2 Inhibits	3.78E-03			Cohesin Complex Cornelia De	1.25E-02
		CKAP4 Signaling Pathway Map	3.78E-03			Pleural Mesothelioma WP5087	1.36E-02
		SMC1 SMC3 Role In DNA Damage	3.92E-03			Gastrin Signaling Pathway	1.95E-02
		G1 To S Cell Cycle Control WP45	5.60E-03			EGF EGFR Signaling Pathway	1.95E-02
		Pathways Affected In Adenoid	7.05E-03			Nucleotide Excision Repair	1.95E-02
		Androgen Receptor Network In	7.16E-03			Genes Controlling	1.95E-02
		Wnt Signaling Pathway And	7.16E-03			Embryonic Stem Cell	1.96E-02
		Brain Derived Neurotrophic Factor	1.09E-02			Bardet Biedl Syndrome WP5234	1.96E-02
		Serine Metabolism WP4688	1.88E-02			Physico Chemical Features And	2.08E-02
		Gastrin Signaling Pathway WP4659	1.88E-02			ErbB Signaling Pathway WP673	2.62E-02
		Glioblastoma Signaling Pathways	1.91E-02			IL 4 Signaling Pathway WP395	2.63E-02
		Pathogenic Escherichia Coli	2.20E-02			4P16 3 Copy Number Variation	2.77E-02
		Development Of Ureteric Collection	2.80E-02			Interactome Of Polycomb	3.18E-02
		TROP2 Regulatory Signaling	2.80E-02			Development Of Ureteric	3.18E-02
		Cohesin Complex Cornelia De	2.80E-02			miRNA Regulation Of DNA	3.18E-02
		Mesodermal Commitment Pathway	2.80E-02			P38 MAPK Signaling Pathway	3.42E-02
		Alzheimer 39 S Disease And miRNA	2.80E-02			Hippo Signaling Regulation	3.63E-02
		Alzheimer 39 S Disease WP5124	2.80E-02			Interleukin 11 Signaling Pathway	3.94E-02
		Hippo Signaling Regulation	2.80E-02			MAP3K1 Role In Promoting And	4.49E-02
		miRNA Regulation Of DNA Damage	2.80E-02			ATM Signaling In Development	4.67E-02
		DNA Damage Response WP707	2.80E-02			Regulation Of Actin Cytoskeleton	4.67E-02
		DNA Repair Pathways Full Network	2.96E-02				
		Physico Chemical Features And	3.35E-02				
		Focal Adhesion PI3K Akt mTOR	3.61E-02				
		5Q35 Copy Number Variation	3.61E-02				
		Prion Disease Pathway WP3995	3.61E-02				
		Metabolic Pathways Of Fibroblasts	3.61E-02				
		Parkin Ubiquitin Proteasomal	3.61E-02				
		Endometrial Cancer WP4155	3.65E-02				
		ATM Signaling Pathway WP2516	4.09E-02				
		Integrated Cancer Pathway WP1971	4.09E-02				
		mRNA Protein And Metabolite	4.09E-02				
		Exercise Induced Circadian	4.09E-02				
		Rett Syndrome Causing Genes	4.09E-02				
		Head And Neck Squamous Cell	4.65E-02				
		ATM Signaling In Development And	4.96E-02				
		Ciliary Landscape WP4352	4.97E-02				
		IL 24 Signaling Pathway WP5413	4.97E-02				

JHU-LX33: USP22oe vs Empty (Enriched = UP in USP22oe; Depleted = DOWN in USP22oe)

SAL				CIS-ETO			
Enriched Pathway	Enriched Adj. P	Depleted Pathway	Depleted Adj. P	Enriched Pathway	Enriched Adj. P	Depleted Pathway	Depleted Adj. P
Striated Muscle Contraction Pathway WP383	3.99E-11			Clear Cell Renal Cell Carcinoma Pathways	2.99E-05	Striated Muscle Contraction	2.16E-06
Arrhythmogenic Right Ventricular	2.11E-07			Endoderm Differentiation WP2853	3.12E-05		
Focal Adhesion PI3K Akt mTOR Signaling	8.50E-06			Sterol Regulatory Element Binding Proteins	6.72E-05		
PI3K Akt Signaling Pathway WP4172	6.44E-04			Cholesterol Metabolism With Bloch And	1.17E-03		
Copper Homeostasis WP3286	3.61E-03			A Network Map Of Macrophage Stimulating	1.18E-03		
Small Cell Lung Cancer WP4658	5.02E-03			Glucose Metabolism In Triple Negative	1.18E-03		
Focal Adhesion WP306	5.88E-03			Photodynamic Therapy Induced HIF 1	1.18E-03		
Inflammatory Response Pathway WP453	1.14E-02			Warburg Effect Modulated By	1.26E-03		
Non Small Cell Lung Cancer WP4255	1.83E-02			Mesodermal Commitment Pathway	1.51E-03		
Burn Wound Healing WP5055	1.93E-02			MECP2 And Associated Rett Syndrome	1.94E-03		
Zinc Homeostasis WP3529	1.93E-02			Glycolysis And Gluconeogenesis WP534	2.78E-03		
Overlap Between Signal Transduction	1.93E-02			Hereditary Leiomyomatosis And Renal Cell	2.78E-03		
Pathophysiological Roles Of DUX4 In FSHD1	2.20E-02			Glycolysis In Senescence WP5049	2.83E-03		
MAPK Signaling Pathway WP382	2.30E-02			Aerobic Glycolysis WP4629	3.86E-03		
Glycolysis In Senescence WP5049	2.30E-02			Zinc Homeostasis WP3529	4.41E-03		
2Q37 Copy Number Variation Syndrome	2.30E-02			Copper Homeostasis WP3286	4.41E-03		
Vitamins A And D Action Mechanisms	2.30E-02			Lactate Shuttle In Glial Cells WP5314	4.51E-03		

Lung Fibrosis WP3624	2.30E-02		Omega 9 Fatty Acid Synthesis WP4724	5.86E-03	
Endochondral Ossification WP474	2.30E-02		Metabolic Epileptic Disorders WP5355	6.26E-03	
Endochondral Ossification With Skeletal	2.30E-02		Transcriptional Activation By NRF2 In	7.07E-03	
Fas Ligand Pathway And Stress Induction Of	2.30E-02		SREBF And miR33 In Cholesterol And Lipid	8.81E-03	
Vitamin A And Carotenoid Metabolism	2.30E-02		Cori Cycle WP1946	1.08E-02	
Heart Development WP1591	2.44E-02		TGF Beta Signaling Pathway WP366	1.86E-02	
IL 24 Signaling Pathway WP5413	2.45E-02		PI3K AKT mTOR Vitamin D3 Signaling	2.67E-02	
Physico Chemical Features And Toxicity	2.45E-02		PKC Gamma Calcium Signaling Pathway In	2.67E-02	
Pleural Mesothelioma WP5087	2.47E-02		NRF2 ARE Regulation WP4357	3.05E-02	
Abnormal Calcium Handling And Its Effects	3.20E-02		Glycogen Synthesis And Degradation	3.61E-02	
Dopaminergic Neurogenesis WP2855	3.40E-02		Neural Crest Differentiation WP2064	3.63E-02	
GPCRs Class C Metabotropic Glutamate	3.67E-02		Resolvin E1 And Resolvin D1 Signaling	3.63E-02	
Disturbed Pathways In Duchenne Muscular	3.67E-02		Metabolic Reprogramming In Colon Cancer	4.04E-02	
Neural Crest Differentiation WP2064	3.91E-02		Mevalonate Arm Of Cholesterol	4.21E-02	
Quercetin And Nf kB AP 1 Induced Apoptosis	3.91E-02		Cholesterol Biosynthesis Pathway In	4.21E-02	
Galanin Receptor Pathway WP4970	3.91E-02		Canonical And Non Canonical Notch	4.38E-02	
Epithelial To Mesenchymal Transition In	3.91E-02				
Adipogenesis WP236	3.91E-02				
Amplification And Expansion Of Oncogenic	4.30E-02				

Table 11: RNA-seq Enrichr pathways analyses: KEGG 2021

FHSC14: sgUSP22 vs sgCtrl (Enriched = UP in sgUSP22; Depleted = DOWN in sgUSP22)

SAL				CIS-ETO			
Enriched Pathway	Enriched Adj. P	Depleted Pathway	Depleted Adj. P	Enriched Pathway	Enriched Adj. P	Depleted Pathway	Depleted Adj. P
Human papillomavirus infection	2.37E-05	Herpes simplex virus 1 infection	1.98E-10	Coronavirus disease	1.17E-18	Herpes simplex virus 1 infection	1.08E-11
Epstein-Barr virus infection	3.33E-04	Axon guidance	2.06E-06	Ribosome	3.34E-13	Cell cycle	3.49E-03
ECM-receptor interaction	3.33E-04	Wnt signaling pathway	2.09E-02	ECM-receptor interaction	5.90E-08	Axon guidance	4.10E-03
Small cell lung cancer	1.88E-03			Human papillomavirus infection	8.42E-06	Cushing syndrome	5.27E-03
Influenza A	2.38E-03			HIF-1 signaling pathway	1.68E-05	Breast cancer	4.20E-02
Phosphatidylinositol signaling system	2.61E-03			Focal adhesion	4.46E-05		
Pathways in cancer	2.61E-03			Influenza A	8.62E-05		
Human cytomegalovirus infection	2.76E-03			Antigen processing and presentation	6.46E-04		
Arrhythmogenic right ventricular	3.31E-03			PI3K-Akt signaling pathway	7.42E-04		
Thyroid hormone signaling pathway	4.23E-03			Oxytocin signaling pathway	1.41E-03		
Phagosome	6.06E-03			Pathways in cancer	1.41E-03		
Oxytocin signaling pathway	6.80E-03			Amoebiasis	1.45E-03		
Cellular senescence	7.44E-03			Toxoplasmosis	1.62E-03		
Protein digestion and absorption	7.44E-03			Human T-cell leukemia virus 1 infection	2.10E-03		
Fluid shear stress and atherosclerosis	7.44E-03			Mucin type O-glycan biosynthesis	2.21E-03		
Antigen processing and presentation	7.44E-03			Small cell lung cancer	2.92E-03		
Focal adhesion	1.02E-02			Arrhythmogenic right ventricular	3.51E-03		
Human immunodeficiency virus 1	1.02E-02			Protein digestion and absorption	3.51E-03		
Hypertrophic cardiomyopathy	1.02E-02			Fluid shear stress and atherosclerosis	8.24E-03		
AGE-RAGE signaling pathway in diabetic	1.13E-02			Central carbon metabolism in cancer	1.29E-02		
Mucin type O-glycan biosynthesis	1.17E-02			Lysosome	1.67E-02		
Coronavirus disease	1.79E-02			AGE-RAGE signaling pathway in	1.71E-02		
Inflammatory mediator regulation of TRP	2.16E-02			Human immunodeficiency virus 1	1.83E-02		
Human T-cell leukemia virus 1 infection	2.74E-02			Epstein-Barr virus infection	1.83E-02		
Melanogenesis	2.74E-02			Salivary secretion	1.94E-02		
Amoebiasis	2.83E-02			Phagosome	1.94E-02		
Glioma	2.83E-02			Arginine and proline metabolism	2.07E-02		
Gastric acid secretion	2.87E-02			Regulation of actin cytoskeleton	2.20E-02		
VEGF signaling pathway	2.87E-02			Leishmaniasis	2.20E-02		
Viral carcinogenesis	2.87E-02			Viral myocarditis	2.33E-02		
PI3K-Akt signaling pathway	2.87E-02			Amphetamine addiction	2.33E-02		
Kaposi sarcoma-associated herpesvirus	2.87E-02			Rap1 signaling pathway	2.39E-02		
Fc epsilon RI signaling pathway	2.87E-02			Relaxin signaling pathway	2.84E-02		
Viral myocarditis	2.90E-02			Hypertrophic cardiomyopathy	2.84E-02		
Proteoglycans in cancer	2.90E-02			B cell receptor signaling pathway	2.89E-02		
Dilated cardiomyopathy	2.90E-02			Proteoglycans in cancer	3.10E-02		
Adipocytokine signaling pathway	2.90E-02			Apoptosis	3.19E-02		
Regulation of actin cytoskeleton	3.19E-02			Other types of O-glycan biosynthesis	3.34E-02		
Endocrine and other factor-regulated	3.19E-02			Dilated cardiomyopathy	4.47E-02		
Adherens junction	3.41E-02			Estrogen signaling pathway	4.47E-02		
Phospholipase D signaling pathway	3.51E-02			Cell adhesion molecules	4.52E-02		
HIF-1 signaling pathway	3.55E-02			Notch signaling pathway	4.55E-02		
Sphingolipid signaling pathway	3.56E-02			VEGF signaling pathway	4.55E-02		
Adrenergic signaling in cardiomyocytes	3.80E-02			Adrenergic signaling in cardiomyocytes	4.74E-02		
Toxoplasmosis	4.24E-02			Oocyte meiosis	4.74E-02		
Apoptosis	4.24E-02			cAMP signaling pathway	4.74E-02		
Salivary secretion	4.24E-02						

NCI109B: sgUSP22 vs sgCtrl (Enriched = UP in sgUSP22; Depleted = DOWN in sgUSP22)

SAL				CIS-ETO			
Enriched Pathway	Enriched Adj. P	Depleted Pathway	Depleted Adj. P	Enriched Pathway	Enriched Adj. P	Depleted Pathway	Depleted Adj. P
Apelin signaling pathway	2.84E-03	Herpes simplex virus 1 infection	2.76E-06	Purine metabolism	3.00E-02	Herpes simplex virus 1 infection	1.18E-09
Thyroid hormone signaling pathway	2.84E-03	Protein processing in endoplasmic	2.76E-06	Ribosome	3.00E-02	Breast cancer	1.18E-03
Circadian entrainment	2.84E-03	Spliceosome	1.41E-04	Toxoplasmosis	3.00E-02	MAPK signaling pathway	1.19E-03
Insulin secretion	7.54E-03	RNA transport	2.18E-04	Proteoglycans in cancer	3.00E-02	Cell cycle	7.64E-03
Cholinergic synapse	7.54E-03	Cell cycle	7.76E-04	Coronavirus disease	3.00E-02	Dopaminergic synapse	1.09E-02
Small cell lung cancer	7.54E-03	Hippo signaling pathway	1.02E-03	Kaposi sarcoma-associated herpesvirus	3.00E-02	DNA replication	2.66E-02
Pancreatic cancer	7.54E-03	mRNA surveillance pathway	5.16E-03	Circadian entrainment	3.00E-02	mRNA surveillance pathway	2.66E-02
Pathways in cancer	1.01E-02	Amyotrophic lateral sclerosis	7.95E-03	Thyroid hormone signaling pathway	3.00E-02	Autophagy	2.66E-02
Morphine addiction	1.01E-02	Salmonella infection	1.34E-02	Human papillomavirus infection	3.00E-02	ErbB signaling pathway	2.66E-02
AGE-RAGE signaling pathway in diabetic	1.01E-02	Endocytosis	1.63E-02	GABAergic synapse	3.00E-02	Chronic myeloid leukemia	2.66E-02
Growth hormone synthesis, secretion and	1.15E-02	Ubiquitin mediated proteolysis	1.63E-02	HIF-1 signaling pathway	3.06E-02	Signaling pathways regulating	2.66E-02
GABAergic synapse	1.15E-02	DNA replication	1.86E-02	Pathways in cancer	3.06E-02	Focal adhesion	3.12E-02
Cellular senescence	1.15E-02	Prostate cancer	2.77E-02	Notch signaling pathway	3.06E-02	Nucleotide excision repair	3.12E-02
Renin secretion	1.34E-02	Hepatocellular carcinoma	2.90E-02	Pyruvate metabolism	3.19E-02	Longevity regulating pathway	3.12E-02
Purine metabolism	1.91E-02	Autophagy	2.90E-02	Renal cell carcinoma	3.19E-02	Axon guidance	3.12E-02
Other types of O-glycan biosynthesis	1.91E-02	Pathways of neurodegeneration	3.21E-02	Small cell lung cancer	3.19E-02	Endocytosis	3.60E-02
Proteoglycans in cancer	1.91E-02	Signaling pathways regulating	3.21E-02	Glutathione metabolism	3.64E-02	Gastric cancer	3.80E-02
Retrograde endocannabinoid signaling	1.91E-02	Chronic myeloid leukemia	4.18E-02	Legionellosis	3.64E-02	Colorectal cancer	4.10E-02
Non-small cell lung cancer	1.91E-02	Neurotrophin signaling pathway	4.18E-02	Cholinergic synapse	3.64E-02	Basal cell carcinoma	4.10E-02
Human papillomavirus infection	2.17E-02	Tight junction	4.28E-02	Retrograde endocannabinoid signaling	3.67E-02	Prostate cancer	4.64E-02
Serotonergic synapse	2.19E-02			Pancreatic cancer	3.69E-02		
Dopaminergic synapse	2.30E-02			Growth hormone synthesis, secretion	3.69E-02		
Human T-cell leukemia virus 1 infection	2.45E-02			Thermogenesis	3.80E-02		
Notch signaling pathway	3.54E-02			Ferroptosis	3.82E-02		
Insulin signaling pathway	3.85E-02			Fructose and mannose metabolism	3.88E-02		
p53 signaling pathway	3.85E-02			Vibrio cholerae infection	3.88E-02		
Calcium signaling pathway	3.85E-02			Axon guidance	4.04E-02		
Glutamatergic synapse	3.85E-02			Amoebiasis	4.08E-02		
Renal cell carcinoma	3.89E-02			TNF signaling pathway	4.08E-02		
Cortisol synthesis and secretion	4.03E-02			Adipocytokine signaling pathway	4.08E-02		
Vasopressin-regulated water	4.07E-02			Epithelial cell signaling in Helicobacter	4.72E-02		
Hepatocellular carcinoma	4.10E-02						
Oxytocin signaling pathway	4.20E-02						
Longevity regulating pathway	4.20E-02						
Insulin resistance	4.91E-02						
Long-term potentiation	4.91E-02						

JHU-LX33: USP22oe vs Empty (Enriched = UP in USP22oe; Depleted = DOWN in USP22oe)

SAL				CIS-ETO			
Enriched Pathway	Enriched Adj. P	Depleted Pathway	Depleted Adj. P	Enriched Pathway	Enriched Adj. P	Depleted Pathway	Depleted Adj. P
Arrhythmogenic right ventricular	3.91E-07			Cardiac muscle contraction	3.39E-03	HIF-1 signaling pathway	3.26E-04
Hypertrophic cardiomyopathy	1.29E-05			Oxidative phosphorylation	1.13E-02	Mineral absorption	1.09E-03
Dilated cardiomyopathy	1.77E-05			Dilated cardiomyopathy	1.44E-02		
PI3K-Akt signaling pathway	5.45E-05			Adrenergic signaling in cardiomyocytes	2.17E-02		
ECM-receptor interaction	2.31E-04			Thermogenesis	3.55E-02		
Focal adhesion	2.31E-04			cGMP-PKG signaling pathway	3.55E-02		
MAPK signaling pathway	1.37E-03			Diabetic cardiomyopathy	3.55E-02		
Human papillomavirus infection	1.59E-03			Pancreatic secretion	3.55E-02		
Mineral absorption	3.22E-03			Hypertrophic cardiomyopathy	4.19E-02		
Pathways in cancer	4.04E-03						
HIF-1 signaling pathway	4.40E-03						
Toxoplasmosis	4.95E-03						
Small cell lung cancer	5.89E-03						
Calcium signaling pathway	1.02E-02						
Legionellosis	1.02E-02						
Protein digestion and absorption	1.02E-02						
Proteoglycans in cancer	2.34E-02						
Adrenergic signaling in cardiomyocytes	2.70E-02						

Axon guidance	2.82E-02			

Table 12: FHSC14 CUT&Tag and RNA-seq integrated analysis – H2AK119ub
Genes with enriched H2AK119ub peaks (Log2FC >0, FDR < 0.05) with concurrent downregulated RNA (Log2FC < 0, FDR < 0.05) in sgUSP22 vs sgCtrl in the SAL and CIS-ETO conditions.

sgUSP22 vs sgCtrl in SAL		sgUSP22 vs sgCtrl in CIS-ETO	
Enriched.Peak Depleted.RNA	Pathway	Enriched.Peak Depleted.RNA	Pathway
ABCA2	GO_Central_Nervous_System_Development	ADAM15	NaN
ADGRB1	GO_Nervous_System_Development	ADCY5	NaN
AMOTL2	NaN	AJAP1	NaN
ARHGAP39	NaN	AMOTL2	NaN
ARHGAP45	NaN	ARHGAP39	NaN
BOP1	NaN	ARHGAP45	NaN
BSX	NaN	ASTN2	NaN
C8orf82	NaN	BCL6	NaN
CBX8	NaN	BOP1	NaN
CENPX	NaN	BSX	NaN
CILP2	NaN	C2CD4C	NaN
CLDN10	NaN	C8orf82	NaN
DNAAF5	NaN	CALCA	NaN
DSP	NaN	CCDC8	NaN
EPS8L2	NaN	CENPX	NaN
FNDC3B	NaN	CILP2	NaN
GLI4	NaN	CLDN10	NaN
GPSM1	NaN	CROCC	NaN
GPT	NaN	DACH1	NaN
GRIN3B	NaN	DLGAP1	NaN
HSPA1A	NaN	DNAAF5	NaN
KIF26A	NaN	EEF1A2	NaN
MYO15B	NaN	FJX1	NaN
NKX2-1	GO_Central_Nervous_System_Development	FNDC3B	NaN
NKX2-2	GO_Nervous_System_Development; GO_Central_Nervous_System_Development	GDNF	GO_Nervous_System_Development; GO_Central_Nervous_System_Development
PLXNA1	GO_Central_Nervous_System_Development	GLDC	NaN
RDH10	NaN	GLI4	NaN
SEMA6A	GO_Nervous_System_Development	GOLGA3	NaN
SLC22A23	NaN	GPSM1	NaN
SOGA1	NaN	GRIN3B	NaN
THEG	NaN	HMCN1	NaN
TONSL	NaN	IMPA1	NaN
TTYH3	NaN	INTS7	NaN
ZIC5	GO_Nervous_System_Development; GO_Central_Nervous_System_Development	ITPR2	NaN
ZNF517	NaN	KIF26A	GO_Central_Nervous_System_Development
		KIFC3	NaN
		KLC3	NaN
		KSR2	NaN
		MADCAM1	NaN
		MAMDC4	NaN
		MET	GO_Nervous_System_Development
		MYO10	NaN
		NKX2-2	GO_Nervous_System_Development; GO_Central_Nervous_System_Development
		NRP2	GO_Nervous_System_Development; GO_Central_Nervous_System_Development
		OSR2	NaN
		PDE10A	NaN
		PHLDA1	NaN
		PKD1	GO_Nervous_System_Development; GO_Central_Nervous_System_Development
		PLEC	NaN
		POLE	NaN
		PPDPF	NaN
		PPFIA3	NaN
		RADIL	NaN
		RALYL	NaN
		RHOU	NaN
		ROR1	GO_Central_Nervous_System_Development
		SCX	NaN
		SEMA6A	GO_Nervous_System_Development
		SH2D5	NaN
		SIX1	GO_Central_Nervous_System_Development
		SLC22A23	NaN
		TAFA5	NaN
		TEDC1	NaN
		THBD	NaN
		TONSL	NaN
		TOP1MT	NaN
		UBASH3B	NaN
		ZEB2	GO_Nervous_System_Development; GO_Central_Nervous_System_Development
		ZMIZ1	GO_Central_Nervous_System_Development
		ZNF704	NaN